

**PROBABILISTIC MODELLING OF
DEBRIS FLOW TRAVEL DISTANCE
USING EMPIRICAL VOLUMETRIC RELATIONSHIPS**

by

MICHAEL PAUL WISE

B.A.Sc. University of British Columbia, 1989

**A THESIS SUBMITTED IN PARTIAL FULFILLMENT OF
THE REQUIREMENTS FOR THE DEGREE OF
MASTER OF APPLIED SCIENCE
DEPARTMENT OF CIVIL ENGINEERING**

in

THE FACULTY OF GRADUATE STUDIES

We accept this thesis as conforming
to the required standard

UNIVERSITY OF BRITISH COLUMBIA

April 1997

© Michael Paul Wise, 1997

In presenting this thesis in partial fulfilment of the requirements for an advanced degree at the University of British Columbia, I agree that the Library shall make it freely available for reference and study. I further agree that permission for extensive copying of this thesis for scholarly purposes may be granted by the head of my department or by his or her representatives. It is understood that copying or publication of this thesis for financial gain shall not be allowed without my written permission.

Department of Civil Engineering, Faculty of Applied Science.
The University of British Columbia
Vancouver, Canada

Date April 14/97.

ABSTRACT

Debris flows can occur on both forested (natural) and clearcut (logged) hillslopes in coastal British Columbia. Prediction of the travel distance of a potential debris flow event prior to clearcut harvesting is important to accurately assess the risk to downslope environmental resources. The travel distance is the distance from the point of initiation of a debris flow to the point of terminal deposition at the end of the flow path.

Forensic data from 449 debris flow events in the Queen Charlotte Islands are used to characterize debris flow events in terrain where clearcut logging has been carried out. From these data, a subset of 131 events are used for the development of regression equations to calculate entrainment volume and deposition volume along distinct reaches of a debris flow event path. Slope morphology and geometry along the path, as well as the flow volume entering the reach, are used as input parameters for the regression equations.

The regression equations are applied in an empirical-statistical model which uses the cumulative debris flow volume along the event path as a basis for determining the travel distance of debris flow events. The cumulative flow volume is defined as the volume of the flow as the event travels down the path, with the entrainment of debris material increasing the flow volume and the deposition of material decreasing the flow volume.

Back-analyses of debris flow events were carried out for 20 independent events in the Queen Charlotte Islands and 17 events in other areas of coastal British Columbia. The model showed reasonable agreement with the peak cumulative flow volume, and the travel distance, of debris flow events reported from observations and surveys in the field.

An observed variability in the forensic data was incorporated to create the empirical-statistical model *UBCDFLOW*. Variations in initial volume, as well as flow width, are used repeatedly to simulate the cumulative debris flow volume along a potential travel path. The probability of an event reaching a point along the path is determined based from the travel distances of these simulated flows. A comparative study of different the scenarios using *UBCDFLOW* illustrates that for confined flow events in gully channels, the initiation location is an important factor in determining travel distance, whereas the size of the initial volume is an important factor for unconfined flows on open slopes.

TABLE OF CONTENTS

ABSTRACT	ii
LIST OF TABLES	ix
LIST OF FIGURES	x
ACKNOWLEDGEMENTS	xv
1.0 INTRODUCTION	
1.1 Characterization of Debris Flows	2
1.2 Risk Assessment of Debris Flows	3
1.3 Objectives of Research	5
1.4 Organization of Thesis	6
2.0 DEBRIS FLOW PROCESSES: LITERATURE REVIEW	
2.1 Classification of Debris Flows	8
2.2 Initiation of Debris Flows	11
2.2.1 Initiation on Open Slopes	12
2.2.2 Initiation in Gully Channels	14
2.3 Rheological Models of Debris Flows	15
2.3.1 Dilatant Grain Flow Model	15
2.3.2 Bingham (Newtonian Viscous) Model	16
2.3.3 Practical Aspects	17
2.4 Volumetric Behaviour of Debris Flows	18
2.4.1 Equilibrium Solids Concentration and Slope Angle	19
2.4.2 Entrainment During Debris Flow Movement	19
2.4.3 Deposition During Debris Flow Movement	22
2.5 Travel Distance and Runout Prediction of Debris Flows	25

2.5.1	Empirical and Semi-Empirical Models	25
2.5.2	Analytical Methods	29
2.6	Concluding Remarks	30
3.0	DEBRIS FLOW SURVEYING	
3.1	Forensic Observations	36
3.2	Reach Attributes of Event Path	39
3.3	Survey Methodology	41
3.4	Remarks on Survey Methodology	42
4.0	DATA CHARACTERIZATION	
4.1	Debris Flow Study Areas	48
4.1.1	Skidegate Plateau (Queen Charlotte Islands)	49
4.1.2	Mamquam Watershed (Squamish)	50
4.1.3	Eve River River (Tsitika Valley)	51
4.1.4	Nootka Island (Kyuquot Sound)	51
4.2	Formation of the Q.C.I. (Selected) Data Set	52
4.3	Debris Flow Event Characterization	53
4.3.1	Types of Event	54
4.3.2	Peak Flow Volume of Events	55
4.3.3	Travel Distances of Events	56
4.4	Reach Characterization	57
4.4.1	Unconfined Flow Geometry and Morphology	59
4.4.2	Confined Flow Geometry and Morphology	60
4.4.3	Transition Flow Geometry and Morphology	61
4.5	Summary	62

5.0	DATA ANALYSIS AND MODEL DEVELOPMENT	
5.1	Volumetric Model	79
5.2	Volumetric Corrections for Q.C.I. (Selected) Events	80
5.3	Response and Predictor Variables for Regression Analyses	82
5.3.1	Response Variables	84
5.3.2	Choice of Predictor Variables	84
5.3.2.1.	Unconfined Flow	85
5.3.2.2.	Confined Flow	87
5.3.2.3.	Transition Flow	88
5.3.2.4.	Derived Variables	89
5.3.3	Partitioning of the Q.C.I. (Selected) Data Based on Slope Angle	91
5.3.4	Transformations of Variables	94
5.3.4.1.	Unconfined Flow	95
5.3.4.2.	Confined Flow	96
5.3.4.3.	Transition Flow	96
5.3.4.4.	Derived Variables	97
5.4	Regression Analyses	98
5.4.1	Unconfined Flow	99
5.4.2	Confined Flow	102
5.4.3	Transition Flow	102
5.5	Cross Validation of Regression Equations	103
5.5.1	Unconfined Flow	104
5.5.2	Confined Flow	106
5.5.3	Transition Flow	106
5.6	Summary	106

6.0	BACK-ANALYSES OF DEBRIS FLOW EVENTS	
6.1	Model Validation Using the Q.C.I. (Original) Events	140
6.1.1	Event 2294	142
6.1.2	Event 22101	144
6.1.3	Event 2290	145
6.1.4	Event 2296	145
6.2	Model Validation Using the Supplementary Events	146
6.2.1	Event 4001	148
6.2.2	Event 3202	149
6.2.3	Event 5501	150
6.2.4	Event 3006	151
6.3	Summary	152
7.0	PROBABILISTIC MODELLING USING <i>UBCDFLOW</i>	
7.1	General	159
7.1.1	Assumptions for the Application of <i>UBCDFLOW</i>	161
7.2	Probabilistic Modelling	163
7.2.1	Prediction of Initial Volume, V_{init}	164
7.2.2	Prediction of Reach Flow Width, W_f	165
7.2.3	Prediction of Deposition Width, W_d	166
	<u>7.2.3.1</u> Unconfined Flow	166
	<u>7.2.3.2</u> Confined Flow	170
	<u>7.2.3.3</u> Transition Flow	170
7.2.4	Prediction of Travel Distance	171
7.3	Example Scenarios	173
7.3.1	Scenario A1: Gully Headwall Failure	174
7.3.2	Scenario A2: Variable Gully Headwall Failure	175

7.3.3	Scenario A3: Gully Sidewall Failure	176
7.3.4	Calculation of P(Ex) for Scenarios A1 to A3	177
7.3.5	Scenario B1: Open Slope Failure	177
7.3.6	Scenario B2: Small Open Slope Failure	178
7.3.7	Scenario B3: Large Open Slope Failure	179
7.3.8	Calculation of P(Ex) for Scenarios B1 to B3	180
7.4	Summary	180
8.0	CONCLUSIONS	
8.1	Volumetric Model	208
8.1.1	Debris Flow Data	209
8.1.2	Regression Equations	210
8.1.3	Testing of Volumetric Model	212
8.2	Incorporation of Probability	213
8.3	Recommendations for Future Research	214
9.0	REFERENCES	217
Appendix A:	Selected (Q.C.I.) Data	221
Appendix B:	Field form and Supplementary Data	235
Appendix C:	Correlation Tables for Regression Analyses	241
Appendix D:	Back-Analyses of Type 7 Events and Supplementary Events ...	255

LIST OF TABLES

2.1(a)	Abbreviated classification of slope movements (after Varnes, 1978)	9
2.1(b)	Classification of debris flow types (after VanDine, 1985)	9
2.2	Classification of debris flow types (after Fannin and Rollerson, 1993)	11
4.1	Characteristics for surveyed debris flow events	54
4.2	Reach characteristics for Q.C.I. (Selected) Data and Supplementary Data	59
5.1	Partitioning of Q.C.I. (Selected) Data based on slope angle and flow mode	94
5.2	Summary of regression equations	100
5.3	Summary of subset regression equations (used in Cross-Validation Testing)	105
6.1	Summary of regression equations used in deterministic model	139
6.2	Paired <i>t</i> -tests on Type 7 Events, Q.C.I. (Original) Data	143
6.3	Paired <i>t</i> -tests on Supplementary Events	147
7.1	Summary of regression equations used in <i>UBCDFLOW</i>	161
7.2	Input parameters for <i>UBCDFLOW</i>	162
7.3	Summary of Test Parameters for <i>UBCFLOW</i> Examples	173

LIST OF FIGURES

1.1	Schematic view of portions of debris flow event (from Chatwin <i>et al</i> , 1994)	7
1.2	Schematic view of debris flow snout or surge (after Pierson, 1986)	7
2.1	Schematic view of debris flow types (from Chatwin <i>et al</i> , 1994)	34
2.2(a)	Flow curves for Bingham, dilatant grain flow, and idealized flow models (after Jordan, 1994)	35
2.2(b)	Dimensionless velocity profiles for a wide channel (after Jordan, 1994)	35
3.1(a)	Attributes of a typical reach along debris flow event path	44
3.1(b)	Attributes of reach relative to upslope reach	45
3.2	Example reaches along debris flow travel path	46
3.3	Example data card for reaches of Event 1206, Q.C.I. Data	47
4.1	Study areas for debris flow research	64
4.2	Sample area locations on the Queen Charlotte Islands, B.C. (after Rollerson, 1992)	65
4.3	Sample area locations in the Mamquam River watershed, Squamish, B.C.	66
4.4	Sample area locations in the Eve River watershed, Vancouver Island, B.C.	67
4.5	Sample area locations on Nootka Island, Kyuquot Sound, B.C.	68
4.6	Flow chart showing criteria for extraction of events	69
4.7	Event types for surveyed debris flow events (event types after Fannin and Rollerson, 1993)	70
4.8	Peak flow volume of debris flow events	71
4.9	Travel distance of debris flow events	72

4.10(a)	Reach characteristics - Unconfined flow reaches, Q.C.I. (Selected) Data	73
4.10(b)	Reach characteristics - Unconfined flow reaches, Supplementary Data	74
4.11(a)	Reach characteristics - Confined flow reaches, Q.C.I. (Selected) Data	75
4.11(b)	Reach characteristics - Confined flow reaches, Supplementary Data	76
4.12(a)	Reach characteristics - Transition flow reaches, Q.C.I. (Selected) Data	77
4.12(b)	Reach characteristics - Transition flow reaches, Supplementary Data	78
5.1	Flow chart of Volumetric Model	109
5.2	Schematic plot of cumulative flow volume and volumetric error	110
5.3(a)	Scatterplots of reach entrainment volume +dV vs predictor variables - Unconfined Flow Reaches; Q.C.I.(Selected) Data	111
5.3(b)	Scatterplots of reach deposition volume -dV vs predictor variables - Unconfined Flow Reaches; Q.C.I.(Selected) Data	112
5.4(a)	Scatterplots of reach entrainment volume +dV vs predictor variables - Confined Flow Reaches; Q.C.I.(Selected) Data	113
5.4(b)	Scatterplots of reach deposition volume -dV vs predictor variables - Confined Flow Reaches; Q.C.I.(Selected) Data	114
5.5(a)	Scatterplots of reach entrainment volume +dV vs predictor variables - Transition Reaches; Q.C.I.(Selected) Data	115
5.5(b)	Scatterplots of reach deposition volume -dV vs predictor variables - Transition Reaches; Q.C.I.(Selected) Data	116
5.6(a)	Scatterplots of reach entrainment volume +dV vs derived predictor variables - Unconfined Reaches; Q.C.I.(Selected) Data	117
5.6(b)	Scatterplots of reach deposition volume -dV vs derived predictor variables - Unconfined Reaches; Q.C.I.(Selected) Data	118

5.6(c)	Scatterplots of reach entrainment volume +dV vs derived predictor variables - Confined Reaches; Q.C.I.(Selected) Data	119
5.6(d)	Scatterplots of reach deposition volume -dV vs derived predictor variables - Confined Reaches; Q.C.I.(Selected) Data	120
5.6(e)	Scatterplots of reach entrainment volume +dV vs derived predictor variables - Transition Reaches; Q.C.I.(Selected) Data	121
5.6(f)	Scatterplots of reach deposition volume -dV vs derived predictor variables - Transition Reaches; Q.C.I.(Selected) Data	122
5.7	Filtered volume change behaviour for the Q.C.I.(Original) Data	123
5.8(a)	Scatterplots of transformed entrainment volume +dV vs transformed predictor variables for Unconfined Flow reaches, $19^{\circ} \leq TH \leq 29^{\circ}$, Q.C.I.(Selected) Data	124
5.8(b)	Scatterplots of transformed entrainment volume +dV vs transformed predictor variables for Unconfined Flow reaches, $30^{\circ} \leq TH \leq 55^{\circ}$, Q.C.I.(Selected) Data	125
5.8(c)	Scatterplots of transformed deposition volume -dV vs transformed predictor variables for Unconfined Flow reaches, $0^{\circ} \leq TH \leq 24^{\circ}$, Q.C.I.(Selected) Data	126
5.9	Scatterplots of transformed entrainment volume +dV vs transformed predictor variables for Confined Flow reaches, $10^{\circ} \leq TH \leq 55^{\circ}$, Q.C.I.(Selected) Data	127
5.10	Scatterplots of transformed deposition volume -dV vs transformed predictor variables for Transition Flow reaches, $0^{\circ} \leq TH \leq 22^{\circ}$, Q.C.I.(Selected) Data	128
5.11(a)	Scatterplots of transformed entrainment volume +dV vs transformed derived variables - Unconfined Flow Reaches, $19^{\circ} \leq TH \leq 29^{\circ}$; Q.C.I.(Selected) Data	129
5.11(b)	Scatterplots of transformed entrainment volume +dV vs transformed derived variables - Unconfined Flow Reaches, $30^{\circ} \leq TH \leq 55^{\circ}$; Q.C.I.(Selected) Data	130
5.11(c)	Scatterplots of transformed deposition volume -dV vs transformed derived variables - Unconfined Flow Reaches, $0^{\circ} \leq TH \leq 24^{\circ}$; Q.C.I.(Selected) Data	131

5.12	Scatterplots of transformed entrainment volume +dV vs transformed derived variables - Confined Flow Reaches, $10^{\circ} \leq TH \leq 55^{\circ}$; Q.C.I.(Selected) Data	132
5.13	Scatterplots of transformed deposition volume -dV vs transformed derived variables - Transition Flow Reaches, $0^{\circ} \leq TH \leq 20^{\circ}$; Q.C.I.(Selected) Data	133
5.14	Test of subset model regression equations, deposition Unconfined Flow Reaches, $0^{\circ} \leq TH \leq 24^{\circ}$, Q.C.I.(Selected) Data	134
5.15	Test of subset model regression equations, entrainment Unconfined Flow Reaches, $19^{\circ} \leq TH \leq 55^{\circ}$, Q.C.I.(Selected) Data	135
5.16	Test of subset model regression equations, entrainment Confined Flow Reaches, $10^{\circ} \leq TH \leq 55^{\circ}$, Q.C.I.(Selected) Data	136
5.17	Test of subset model regression equations, deposition Transition Flow Reaches, $0^{\circ} \leq TH \leq 20^{\circ}$, Q.C.I.(Selected) Data	137
6.1	Test of regression equations using Type 7 Q.C.I. (Original) Data and Supplementary Data	154
6.2(a)	Back-analysis of Event 2294, Q.C.I. (Original) Data	155
6.2(b)	Back-analysis of Event 22101, Q.C.I. (Original) Data	155
6.3(a)	Back-analysis of Event 2290, Q.C.I. (Original) Data	156
6.3(b)	Back-analysis of Event 2296, Q.C.I. (Original) Data	156
6.4(a)	Back-analysis of Event 4001, Eve River Data	157
6.4(b)	Back-analysis of Event 3202, Mamquam River Data	157
6.5(a)	Back-analysis of Event 5001, Nootka Island Data	158
6.5(b)	Back-analysis of Event 3006 Q.C.I. (Additional) Data	158
7.1(a)	Flow chart showing probabilistic modelling for a single simulation	183
7.1(b)	Flow chart showing probabilistic modelling for scenarios	184
7.2(a)	Determination of initial volume for a potential open slope failure	185
7.2(b)	Initial volumes for various slope morphologies in the Q.C.I. (Original) Data	186

7.2(c)	Determination of initial volume for a potential roadfill failure	187
7.3	Schematic triangular distributions for flow width, W_f	188
7.4	Unfiltered volume change behaviour for Q.C.I. (Original) Data, $14^\circ < TH < 34^\circ$	189
7.5(a)	W_d / W_f functions for reach slope angles of 16° to 21°	190
7.5(b)	W_d / W_f functions for reach slope angles of 22° to 27°	191
7.6(a)	Schematic plan view of potential debris flow path	192
7.6(b)	Histogram of simulated flow terminations along flow path	193
7.6(c)	Probability of impact along debris flow path	193
7.7(a)	Input data and cumulative flow volumes for Scenario A1	194
7.7(b)	Flow volumes at selected reaches, Scenario A1	195
7.8(a)	Input data and cumulative flow volumes for Scenario A2	196
7.8(b)	Flow volumes at selected reaches, Scenario A2	197
7.9(a)	Input data and cumulative flow volumes for Scenario A3	198
7.9(b)	Flow volumes at selected reaches, Scenario A3	199
7.10	Tabulated results and $P(Ex)$ along flow path for Scenarios A1, A2, and A3	200
7.11(a)	Input data and cumulative flow volumes for Scenario B1	201
7.11(b)	Flow volumes at selected reaches, Scenario B1	202
7.12(a)	Input data and cumulative flow volumes for Scenario B2	203
7.12(b)	Flow volumes at selected reaches, Scenario B2	204
7.13(a)	Input data and cumulative flow volumes for Scenario B3	205
7.13(b)	Flow volumes at selected reaches, Scenario B3	206
7.14	Tabulated results and $P(Ex)$ along flow path for Scenarios B1, B2, and B3	207

AKNOWLEDGEMENTS

Firstly, I would like to thank my thesis advisor, Dr. R. Jonathan Fannin, P.Eng. for his guidance as well as his academic and logistical support during the thesis research. His enthusiastic approach and keen research skills provided the impetus for much of this project work.

I would also very much like to thank Mr. Terry Rollerson, P.Geo. at the Ministry of Forests for the use of the landslide data from the Queen Charlotte Islands. This data was obtained by Terry Rollerson, Gray Switzer, Dave Dunkley, Steve Chatwin, and other personnel from MacMillan Bloedel's Land Use Advisory Team (LUPAT) in the mid 1980's. Their insight into the development of an extensive landslide database to study forestry-related landslide events and perseverance in the field must be commended.

This research project was funded by the Science Council of British Columbia, under a G.R.E.A.T. grant. Collaborators on the project were, in addition to Dr. Fannin and Terry Rollerson, were Tony Rice of Golder Associates (now with Bruce Geotechnical Consultants). All the collaborators provided valuable insight and guidance during the project. With the G.R.E.A.T. grant, Golder Associates provided funding during the research project. Steve Chatwin at the Ministry of Forests provided funding for the field work required in surveying the supplementary debris flow events.

Special thanks are also extended to Terry Rollerson, Tom Millard, Frank Baumann, John Wilkinson, and Doug VanDine for hours of discussion regarding landslide behaviour. It's reassuring to know that others also find this stuff interesting.

Lastly, I would like to thank all the members of my family for their never-ending understanding and support.

Chapter 1 INTRODUCTION

Debris flows, or flowslides, are natural landslide hazards involving water, soil, rocks, and pieces of organic debris which move rapidly downslope in a fluid-like manner. They occur on both unconfined open hillslopes and confined gully channels. In gully channels, debris flows differ from fluvial transport: debris flows move as a slurry, with coarse rock and soil particles moving at the same speed as the interstitial fluid, while fluvial transport is characterized by the slower movement of coarse particles relative to the interstitial fluid.

Debris flows can pose a risk to downslope resources. These resources may include infrastructure corridors (highways, railways, and pipelines), urban development, fish habitat or community watersheds. The risk of debris flow impact on these resources must be assessed if rational decisions are to be made regarding the siting of projects, construction of debris flow defenses, or zoning of downslope areas. In these situations, assessment of the debris flow impacts must be carried out to ensure the best use of limited funds to protect the important downslope resources most at risk.

Risk assessments are also required in some areas downslope of proposed forestry activities, as forestry activities can change the stability and debris supply conditions on the hillslope areas and subsequently increase the risk to fish habitat and other downslope resources (B.C. Ministry of Forests, 1995a). The quantification of risk from debris flows can greatly assist the integrated management of both timber and fisheries resources in the steep, mountainous terrain of coastal British Columbia.

1.1 Characterization of Debris Flows

A schematic illustration of a debris flow event is shown in Figure 1.1. Debris flow events on open slopes are termed "debris slides" or "debris avalanches" (Varnes, 1978). Debris flow events confined for part of the path length in gully channels are termed "debris torrents" or "channelized debris flows". Each debris flow event has an initiation point where the flow originates, a travel path along which the flow moves, and a termination point where the flow stops (Figure 1.1). Several surges or "roll waves" may occur within the context of a single debris torrent event, as channel material is mobilized minutes or hours after the debris flow snout has reached the termination point (Jordan, 1994).

The travel path of a debris flow can be divided into distinct reaches, with each reach having a relatively consistent geometry (width, slope angle, and azimuth angle), slope morphology, and in the case of forensic surveying of events, volume change behaviour. Entrainment of debris within steeper reaches of the travel path increases the flow volume, while deposition on flatter reaches decreases the flow volume. Depending on the slope morphology of the reaches along the event path, the debris flow event is either confined within a gully channel, or unconfined on gully headwalls and sidewalls, debris fans, open slopes, or forestry roads. Figure 1.1 shows typical cross-section geometries for confined flow in gully channels and unconfined flow on open slopes and gully fans.

The potential for impact damage from debris flows is a result of the momentum (velocity and mass) of the flow. Debris flows have been reported to move at velocities of up to 20 m/s, with flow depths ranging from 1.5 to 4 m (Hung *et al*, 1984). Where boulders are present in the flow, these are moved to the front of the flow to form a "snout" by means of "kinetic sorting" (Takahashi *et al*, 1992). The direct impact of this snout can pose significant risk to bridges,

infrastructure corridors, and urban development. If the debris flow contains fine-grained sands and silts, or a significant amount of large woody debris (LWD) such as logs or stumps, then the flow may present a significant risk to fish habitat. Deposition of large amounts of silt or fine sand can alter the gradation of stream gravel used for salmonid egg incubation. The deposition of LWD within stream channels may create logjams within streams which can prove impassable to spawning salmon and retard the movement of sediment through the stream system.

Forestry activities can increase the probability of initiation of debris flows, and may change the types of debris entrained along the travel path. Marginally stable logging roads and steep clearcut slopes, subjected to extreme rainfall events, can lead to the initiation of a debris slide or debris avalanche on open slopes, or the initiation of debris torrents in gully channels. Clearcut logging of a hillslope may leave significant amounts of LWD in gully channels, leading to higher sediment accumulation rates and debris torrents which carry a disproportionately large amount of LWD to stream channels. The increase in probability of initiation of debris flows, and the increase in LWD carried by flows from logged areas, can greatly increase the risk to fish habitat.

1.2 Risk Assessment of Debris Flows

Frameworks to assess the risk of impact/damage by debris flows have been developed for both qualitative and quantitative analyses. The Gully Assessment Procedure (B.C. Ministry of Forests, 1995a) presents a framework for qualitatively assessing the risks of debris flow initiation and runout (travel distance) within gully systems following logging activities. Morgan *et al* (1992) present a quantitative framework which can be used to evaluate the risk of

debris flows to points of interest along a potential debris flow event path. The risk due to a debris flow hazard is calculated as:

$$Risk = P(H) P(S:H) Severity \quad [1.1]$$

$$P.D.I. = P(H) P(S:H) P(L:T) \quad [1.2]$$

$$Risk Cost = P(H) P(S:H) \{Severity\} \quad [1.3]$$

where *Risk* is the risk due to debris flow impact, $P(H)$ is the annual probability of debris flow occurrence/initiation, $P(S:H)$ is the probability of spatial impact given initiation of the flow, and *Severity* is a quantitative estimate of the damage due to a debris flow event. The *P.D.I.*, Probability of Death to an Individual, can be found as the product of *Risk* and $P(L:T)$, where $P(L:T)$ is the probability of loss of life due to direct temporal and spatial impact of the hazard. Similarly, the *Risk Cost* can be determined by multiplying *Risk* and the dollar cost of the consequences of the debris flow occurrence. Thus, the assessment of debris flow risk at a specific location requires not only the probability of initiation, but also the probability of impact and some measure of the severity of impact.

While the determination of *P.D.I.* and *Risk Cost* is often used to assess the risk to infrastructure corridors in mountainous regions, a determination of risk to fish habitat is required to successfully integrate the management of resources in coastal British Columbia. Although this risk is usually not needed in terms of a dollar value, it is important to determine the probability of impact and expected severity of impact on fisheries and water resources. The minimum requirements for terrain stability assessments for forestry activities on steep slopes include a description of potential downslope damage, such as estimated travel distances and an order of magnitude estimate of the amount of landslide debris that might enter a stream or impact other downslope resources. The Gully Assessment Procedure (B.C. Ministry of Forests, 1995)

requires that an assessment by a Professional Geoscientist or Engineer be carried out in situations where potential debris torrents may impact dwellings, infrastructure corridors, community watersheds/watercourses, or high-value fish habitat. For these situations, an evaluation of the probability of debris flow travel to a sensitive area and the volume of debris likely to be deposited are key parameters required for the risk assessment of debris flow hazards.

1.3 Objectives of Research

The quantitative risk assessment of debris flow hazards requires a determination of the probability of impact along the debris flow path, and the likely severity of potential impacts. These results are required for risk assessment to points of concern downslope of potential debris flow initiation sites.

The specific objectives of this research are:

1. to develop empirical relationships between debris flow volume change along the event travel path and the reach characteristics of the debris flow path, using data from the Queen Charlotte Islands, B.C.;
2. to use these relationships within a Volumetric Model framework to calculate debris flow volume changes and travel distance along the debris flow path;
3. to test the Volumetric Model through back-analyses of other debris flow events surveyed from four geographic areas of coastal B.C.;
4. to modify the Volumetric Model, by incorporating observed flow variability, to determine the probability of impact and severity of debris flow events along a potential debris flow path.

1.4 Organization of the Thesis

The presentation of material is as follows:

- Chapter 2 presents a review of theories on debris flow processes reported in the literature, and identifies several key points regarding the behaviour of debris flows;
- Chapter 3 outlines the field methodology used to survey the debris flow events, and discusses the forensic nature of the survey parameters;
- Chapter 4 characterizes the debris flow event data for events from the Queen Charlotte Islands and three other geographic areas in coastal British Columbia;
- Chapter 5 describes a deterministic Volumetric Model to calculate debris flow volume and travel distance, as well as the development of regression equations used to calculate volume changes along the event path;
- Chapter 6 uses the regression equations and deterministic Volumetric Model to back-analyze debris flow volumes and the travel distance of selected events surveyed from the Queen Charlotte Islands and three other geographic areas of coastal B.C.;
- Chapter 7 presents the use of the deterministic Volumetric Model for the prediction of debris flow events using repeated (Monte Carlo type) simulations, to account for the variability in flow behaviour, and examines the influence of the location of the initiation point and initial volume on the volume change behaviour, prediction of event path length, and probability of spacial impact along the flow path;
- Chapter 8 concludes with a summary of the study findings and recommendations for future research.

For all chapters, the figures are presented at the end of the chapter and tables are integrated into the text. Data for the debris flow events, results of statistical analyses, and results of the back-analyses of debris flow events are presented in the Appendices.

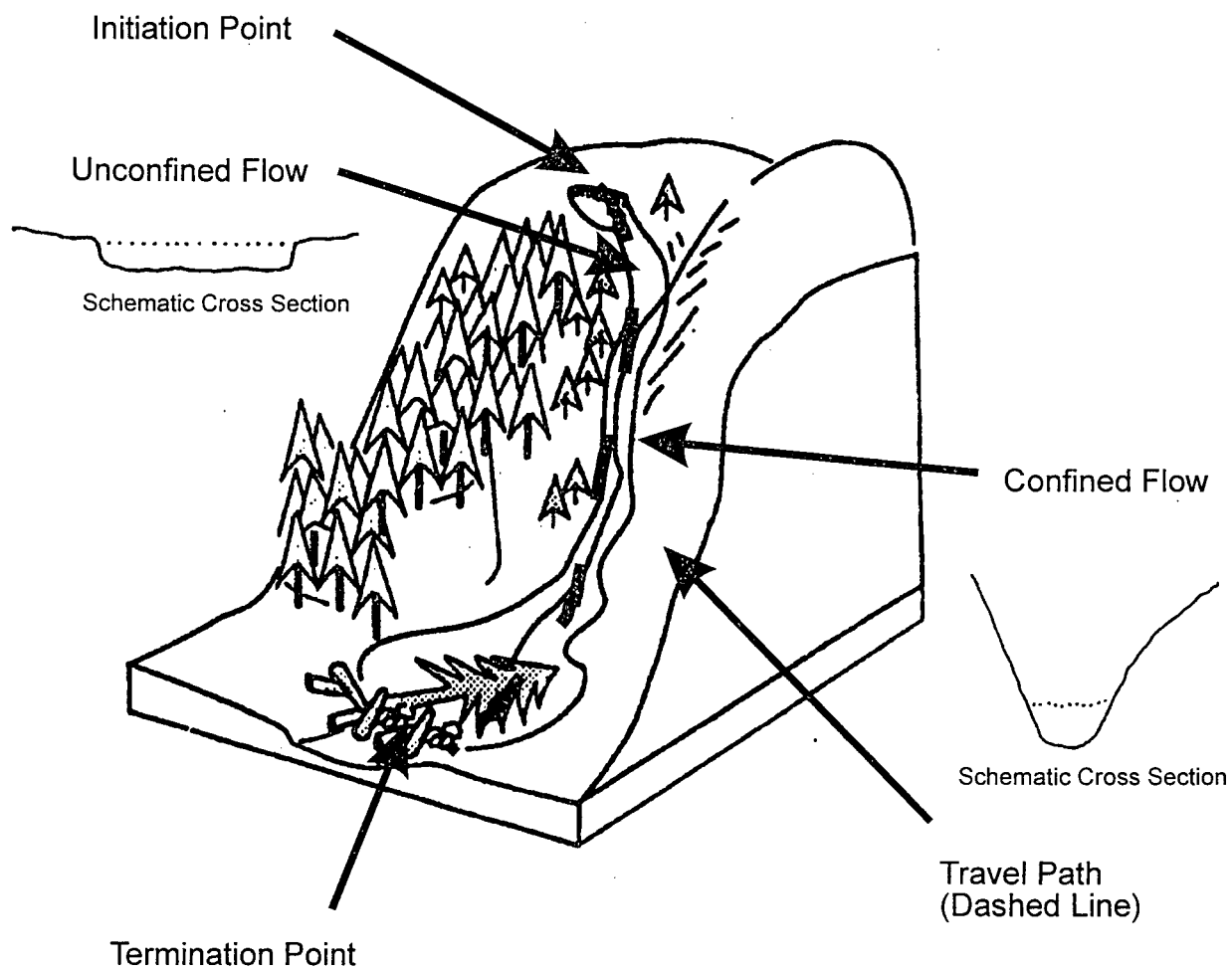


Figure 1.1: Schematic view of portions of debris flow event (modified from Chatwin et al, 1994)

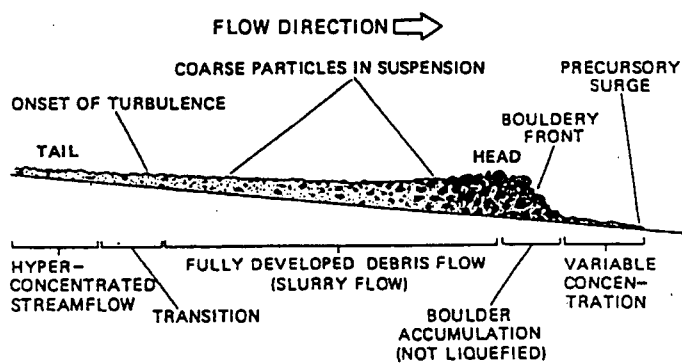


Figure 1.2: Schematic view of debris flow snout (after Pierson, 1986)

Chapter 2 DEBRIS FLOW PROCESSES: LITERATURE REVIEW

Research on debris flows addresses two major issues: the factors controlling debris flow initiation, to determine the probability of debris flow occurrence; and the movement of debris flows, to determine the mobility (flow velocity, terminal deposition angle, and travel distance) of a debris flow event. This chapter briefly explains current theories involving debris flow initiation, and then summarizes several current theories for modelling debris flow mobility in terms of flow rheology, volume change, and travel distance prediction.

2.1 Classification of Debris Flows

Debris flows, as defined by Varnes (1978), are differentiated from other types of mass movement based on the material incorporated in the flow and the presence of flow as a transportation mechanism. Debris is classified by Varnes as a "high percentage of coarse fragments" with over 50% of the particles being sand size or greater. Flow is described as a "fluid-like movement" and "usually involves relatively large displacements and the body of material takes the appearance of a flow." The abbreviated classification of slope movements by Varnes (1978) is presented in Table 2.1(a).

Different types of debris flow are recognized based on the morphology of the debris flow path and the amount of moisture present in the flow. Specific types include translational (planar) debris slides, debris avalanches, and debris torrents. Debris slides and avalanches occur on open hillslopes, while debris torrents occur in pre-existing drainage courses. Table 2.1(b) provides the characteristics of the specific types of debris flow as well as the related

Table 2.1(a) Abbreviated Classification of Slope Movements
(after Varnes, 1978)

TYPE OF MOVEMENT			TYPE OF MATERIAL		
			BEDROCK	ENGINEERING SOILS	
				Predominantly Coarse	Predominantly Fine
FALLS			Rock fall	Debris fall	Earth fall
TOPPLES			Rock topple	Debris topple	Earth topple
SLIDES	ROTATIONAL	few units	Rock slump	Debris slump	Earth slump
	TRANSLATIONAL		Rock block slide	Debris block slide	Earth block slide
			many units	Rock slide	Debris slide
LATERAL SPREADS			Rock spread	Debris spread	Earth spread
FLOWS			Rock flow (deep creep)	Debris flow (soil creep)	Earth flow
COMPLEX			Combination of two or more principal types of movement		

Table 2.1(b) Classification of Debris Flow Types (after VanDine, 1985).

		DEBRIS FLOW TYPE	Mudflow	Debris Flow		Debris Slide	Debris Avalanche
				Debris Torrent	Planar Debris Flow		
CHARACTERISTICS							
Materials Involved	Predominantly fine-grained, inorganic						
	Predominantly coarse-grained, inorganic & organic						
Mechanics of movement	Flow						
	Translation						
Where movement occurs	Pre-existing Channel						
	Planar Slope						
Water Content	Saturated						
	Under-saturated	Wet					
		Dry					

phenomena of mudflow and waterflood as reported by VanDine (1985) for events in the Canadian Cordillera. VanDine states that the distinguishing characteristics of debris avalanches and debris slides are translational movements of unsaturated material on planar (open) slopes, with a spectrum grading from dry material for the debris avalanches to the wet material involved in a debris slide. Debris torrents, and debris flows on open slopes, involve the flow of saturated material. Figure 2.1 shows open slope and confined channelized debris flow types.

Debris flows occur in both unlogged (natural) terrain and clearcut logged (harvested) terrain. Although both situations have the same processes of debris flow initiation and movement along the event path, possible impacts of forest harvesting activities can increase the probability of debris flow initiation and the peak volume of events. It is believed such impacts may include changes in the hillslope hydrology, a reduction of root strength (cohesion) due to the removal of forest cover, and the large amount of organic debris left on the hillslope and in gullies after logging activities.

A classification system developed for debris flows from logged terrain has been developed by Fannin and Rollerson (1993). Based on data from logged terrain in the Queen Charlotte Islands, seven types of debris flow event were identified based on the morphology of the travel path, the characteristic slope angle in the deposition zone, and whether the observed debris flow path joins with the path(s) from other events to form a multiple event in a spatial sense (but not a temporal sense). Table 2.2 summarizes the classification system, with corresponding debris flow types from VanDine, 1985.

Table 2.2: Classification of Debris Flow Event Types (after Fannin and Rollerson, 1993).

Event Type	Event Name ¹	Event Path	Path Morphology ²	Characteristic Reach Slope Angle, i (deg)
1	DS / DA	Single	OS	n/a
2	DT	Single	OS=>G; G	$i > 15^\circ$
3	DT	Single	OS=>G; G	$15^\circ > i > 5^\circ$
4	DS/DT	Single	G	n/a
5	DT	Multiple	OS=>G; G	$i > 15^\circ$
6	DT	Multiple	OS=>G; G	$15^\circ > i > 5^\circ$
7	DT	Multiple	OS=>G; G	n/a

¹DS debris slide; DA debris avalanche; DT debris torrent (after VanDine, 1985)

²OS open slope; G gully

The terminology describing a debris flow event has evolved since the early work on mass movement classification by Varnes (1978). Recently completed research and guidelines on debris flow assessment by Jordan (1994), Millard (1993) and Fannin and Rollerson (1993), as well as the Gully Assessment Procedure (B.C. Ministry of Forests, 1995b) have slightly modified the original terms developed by Varnes (1978). Examples include the current reference to the "headscarp" of an event instead of the "crown", the "failure plane" of an event rather than the "plane of separation", and the "deposition zone" of an event rather than the "zone of accumulation". For this research, the former, more recent terms have been used to better integrate with current concepts, research, and application.

2.2 Initiation of Debris Flows

The initiation of debris flows typically occurs when the imposed shear stresses exceed the available shear strength along a plane at some depth below ground surface. Movement along this failure plane may be as either a translational slide or a slurry flow. Generally, the initiation of debris flows occurs in two types of morphology: unconfined (open) slopes and confined (gully) channels. Discussions regarding debris flow initiation are contained in O'Loughlin

(1972), Hammond *et al* (1992), Sidle (1992), and others for open, unconfined hillslopes following logging activities. Takahashi *et al* (1992), Hungr *et al* (1984), and Millard (1993) describe theories of debris flow initiation within confined gully channels.

2.2.1 Initiation on Open Hillslopes

Debris slides, debris avalanches, and planar debris flows initiate on steep hillslopes, and typically begin as translational slides along a failure plane which often corresponds to an interface between a relatively loose soil layer and more competent stratum at depth. Examples of such an interface include a soil/bedrock boundary, colluvium/till boundary, and a roadfill/native soil boundary.

Several criteria are important to determine the slope stability or probability of debris flow initiation of a soil mass at a particular location (Hammond *et al*, 1990). These include the position of the groundwater table in relation to the thickness of the soil mass, the slope angle of the hillslope, the angle of shearing resistance of material along the failure plane, and the saturated and unsaturated unit weights of the soil. Integrated root systems of trees and other vegetation on the hillslope may also contribute strength to the upper soil strata, often quantified as an apparent cohesion in the Mohr-Coloumb model. The infinite slope model can be used to calculate the Factor of Safety against sliding, or stability, of a soil layer where the sides and the toe of the soil layer above the failure plane are assumed to contribute a negligible amount of shear strength over a given slope area. The reduction in root strength is modelled as a reduction in soil cohesion in the strength of the soil. Previous studies of debris flow initiation sites by Fannin and Rollerson (1993), Hammond *et al* (1992) and O'Loughlin (1972) have shown the infinite slope model can be used to determine the stability of debris flow initiation sites on hillslopes following logging activities.

Considerable evidence suggests that some logging practices can affect the stability of forested hillslopes. Aside from the construction of potentially unstable roadfills on hillslopes, the reduction of soil cohesion due to the deterioration of root strength, and the exposure of soil due to yarding activities can affect hillslope groundwater hydrology and stability. Groundwater table fluctuations and any loss of tree root strength must be considered in the time following logging, until new roots grow to replace those lost due to harvesting. A discussion of the infinite slope model by Hammond *et al* (1992) states that a high groundwater level, due to an extreme rainfall event, can create pore water pressures at the failure plane which reduce the Factor of Safety against sliding by approximately one half when compared to completely dry soil conditions. This phenomenon is also discussed in terms of classical soil mechanics in Craig (1992). The deterioration of tree root systems following clearcut logging can significantly reduce the available cohesion in the soil layer and lead to increased probability of debris flow initiation. The use of skyline or helicopter based yarding systems during logging can minimize road construction and yarding disturbance on steep hillslopes.

Once a debris slide, debris avalanche, or planar debris flow has initiated, the moving soil mass breaks up and liquefies as it moves downslope and may display properties of both a slide and a flow. Takahashi (1992) concludes, based on field and laboratory data, that a soil mass will liquefy into a flow if the translational displacements of the mass reach over ten times the thickness of the moving soil layer and sufficient water is supplied to create a slurry from the soil mass. Varnes (1978) notes "as deformation and disintegration continue, and especially as water content or velocity or both increase, the broken or disrupted slide mass may change into a flow; however all gradations (between slide and flow) exist".

2.2.2 Initiation in Gully Channels

Debris torrents in gully channels initiate in pre-existing gully channels on steep hillslopes.

Takahashi (1991) reports that debris torrents can be initiated by impulsive loading, natural dam collapse, and high waterflows along the surface of the gully bed. Impulsive loading occurs as a debris slide, debris avalanche, or planar debris flow enters the gully from the hillslope above and mobilizes saturated debris material resident on the gully floor. Rockslides and rockfalls may also cause debris torrents as documented by Bovis and Dagg (1992). A natural dam in a gully channel may occur as material slides into the gully channel and remains in place on the gully floor, or when material has accumulated behind large organic debris blocking the channel. This dam can collapse due to overtopping during excessive streamflows in the gully channel, sliding along the base of the channel, progressive failure starting at the toe of the dam, or "structural" failure of the large woody debris retaining sediment. Sudden, excessive streamflows in the gully channel can also cause debris torrents as the soil materials on the gully floor surface are rapidly eroded.

Logging activities can increase the sediment storage capacity of gully channels (Millard, 1993).

Woody debris which remains in gully channels following logging can trap sediment within the channel, increasing the probability of initiation and likely magnitude of a debris torrent.

Logging activities can also disturb vegetation on the sidewalls of a gully, causing increased rates of sediment transfer into the gully channel. Buffer strips, and other logging strategies as outlined in the Gully Assessment Procedure (B.C. Ministry of Forests, 1995a), can be used to minimize the effects of logging activities on gully channels.

2.3 Rheological Models of Debris Flows

Much attention has focused on the constitutive relations describing debris flow behaviour. Chen (1987) presents a summary of many models which have been developed, and concludes that theoretically-based rheologic models have limited practical applications, and semi-empirical models are generally accepted for engineering purposes. These semi-empirical models fall into two categories: a dilatant grain flow model, based on Bagnold's concept of dispersive pressure, and a Newtonian viscous model (Bingham model) based on the concept of a yield strength for the flowing debris. Jordan (1994) has evaluated these rheological models in relation to actual debris flow events in the Coast Mountains of southwest British Columbia. This section discusses briefly the assumptions of each of these models and their practical application to debris flows in logged terrain within coastal British Columbia. Figure 2.2(a) and 2.2(b) show the flow curves and dimensionless velocity profiles for the dilatant grain rheology and Bingham rheology, as well as the rheology of an idealized Newtonian fluid.

2.3.1 Dilatant Grain Flow Model

Research by Bagnold (1956) and later refinements by Takahashi (1991) have shown that the intergranular collisions within a debris flow generate a "dispersive pressure". To measure this dispersive pressure, Bagnold suspended neutrally buoyant wax beads in the annulus between a rotating cylinder and a stationary cylinder. The grain shear stress, τ (the shear stress in addition to the shear stress due to momentum transfer within the interstitial fluid), and grain normal stress, P (additional normal stress exerted by the interstitial fluid), were equated

$$\tau = -PN \quad [2.1]$$

where N is the Bagnold Number, dependent on a number of parameters. Later, N was equated to $\tan \alpha$, where α is the "dynamic friction angle".

Takahashi (1991) has stated that the use of a dilatant grain flow rheological model is applicable to debris flow events when the particles in the flow are predominantly coarse-grained. The use of this rheological model also conceptually predicts the migration of larger particles to the top and front of the debris flow through a process of kinetic sieving (Takahashi *et al*, 1993), even though the original experiments of Bagnold were carried out using spheres of identical size.

Jordan (1994) showed that dilatant grain flow model rheology was more applicable where the coarse-grained debris was derived from granitic and metasedimentary bedrock sources. In these cases, the dynamic behaviour was determined to be a result of the dynamic friction of the flowing debris, which is in turn the result of the dispersive pressure from intergranular collisions. Observations of debris flow events as "clast-supported, matrix deficient boulder accumulations" (Takahashi, 1991) and "a layer of coarse clasts over homogenous flow deposits" (Jordan, 1994) provide field evidence in support of a grain-dispersive rheology.

2.3.2 Bingham (Newtonian Viscous) Model

A Bingham rheological flow model based on a Newtonian fluid with a finite yield strength has been used to describe the rheology of fine-grained debris flows (Pierson and Costa, 1987).

Algebraically, the Bingham Model can expressed as

$$\tau = k + \mu \frac{du}{dz} \quad [2.2]$$

where τ is the shear stress, k is the yield strength of the fine-grained slurry, μ is a flow resistance (viscosity) term, and $\frac{du}{dz}$ is the strain rate. Figure 2.2(a) compares the constitutive relationships of the Bingham model and the dilatant grain flow model. The relationship for a Newtonian fluid is included for comparative purposes, even though it is not applicable to the rheology of debris flows (Jordan, 1994). Dimensionless velocity profiles from Jordan (1994) for the three rheological models are plotted in Figure 2.2(b). The yield strength of the

Bingham fluid leads to the vertical portion of the velocity of the profile above depth 0.5, whereas the dilatant fluid has the greatest velocity at the surface of the flow. Observational data such as the existence of a "rigid" plug at the center of the debris flow front, and deposition of debris as "sheets" of uniform thickness, provide field evidence of a debris flow behaviour as a Bingham fluid with finite yield strength.

Jordan (1994) examined the dynamic behaviour of debris flow events in the Southern Coast Mountains. Some of these flows contained approximately 9% or greater clay content, and were designated as "fine-grained" flow events; events with less than about 9% clay were termed "coarse-grained" events. In some cases, matrix-supported deposits were observed "where topography permitted". However, for debris flow events where the fine-textured flows contained coarse clasts, these clasts were moved to the front and sides of the flow and consequently the dynamic debris flow behaviour of these events was not indicative of a Bingham fluid. Jordan (1994) concludes that a flow with a clay content larger than about 10% and with few clasts in the flow will likely behave as a Bingham fluid, but that the travel distance on the fan for a debris flow event is influenced more by the volume of the event than the rheology of the flow.

2.3.3 Practical Aspects

Selecting a rheological model to predict debris flow behaviour can be difficult in practical terms. Jordan (1994) also makes the important point that "no single model adequately describes the diverse behaviour of debris flows, which include a wide range of materials, initiating mechanisms, and scales." In addition, the dilatant grain flow and Bingham flow rheologic models are only applicable to steady state uniform flow, whereas actual debris flow events are typically unsteady and non-uniform. Although Hungr *et al* (1984) and Takahashi

(1991) advocate the use of viscous Newtonian flow and grain-dispersive rheological flow models, these are semi-empirical relationships which appear to simplify actual flow behaviour in a limited range of debris flow (Jordan, 1994). More theoretical models have been developed to describe debris flow behaviour, but are often difficult to apply in a practical sense due to the need to measure a large number of parameters (Chen, 1987).

Jordan (1994) also points out that the permeability of the debris material plays an important role in the determination of the rheological behaviour of a flow event. Coarse-grained flows drain very quickly as a result of their low permeability and consequently these events terminate on slopes of 8° to 14° . Fine-grained flows take more time to drain than coarse-grained flows, and thus are able to flow as a slurry on slopes as gentle as 5° . Most rheological models do not explicitly account for permeability of the debris within the flow, so the permeability of the material in the flow must be assumed before a rheological model can be applied with confidence. Moreover, for debris flows in logged terrain, the high proportion of woody debris is likely to cause rheological behaviour different than those predicted by previously developed constitutive relationships.

2.4 Volumetric Behaviour of Debris Flows

The volume of a debris flow event changes as the flow moves down the event path. Debris flow events begin with an initial volume, and increase in volume as material is entrained (or decrease in volume as material is deposited) along the event path. At any point along the path, the volume of the flow is a result of the cumulative changes in volume which have occurred through the upslope portions of the travel path. Two important factors in determining the volumetric behaviour (entrainment and/or deposition) of a debris flow event are the

equilibrium solids concentration and equilibrium slope angle for debris flow events.

Determination of the volumetric behaviour is important for modelling debris flows since volume changes along the path are used in many empirical models to determine the travel distance of debris flow events, discussed in Section 2.5.1.

2.4.1 Equilibrium Solids Concentration and Slope Angle

Research by Takahashi (1978) has shown that a debris flow travelling on a reach with a slope angle greater than the equilibrium slope angle q_e will continuously entrain material. Slope angles below q_e and above the threshold angles for deposition result in a "quasi-steady state" as long as the discharge (supply of flowing debris) is constant. This quasi-steady state is characterized by a equilibrium volumetric solids concentration, c_∞ , of approximately 0.7 (Takahashi, 1978). The equilibrium slope angle θ_e is given by Takahashi:

$$\tan \theta_e = \frac{c(\sigma - \rho) \tan \phi}{c(\sigma - \rho) + \rho} \quad [2.3]$$

where c is the volume concentration of solids in the flow (which varies between 0.2 to 0.9 times the maximum possible concentration, c^*), s is the density of the solids in the flow, r is the bulk density of the flow, and f is the dynamic friction angle for the flowing debris. The value for $\tan \theta_e$ is essentially the same as the friction slope S_f used in the runout equations of Takahashi and Yoshida (Hung *et al*, 1984), discussed in Section 2.5.1. The equilibrium slope angle θ_e is also the upper bound for the deposition angles measured by for events less than 60,000 m³ Jordan (1994), specifically about 5° for fine-grained flows and 10° to 13° for coarse-grained flows.

2.4.2 Entrainment During Debris Flow Movement

Entrainment of debris material during a flow event takes place in the transportation zone and may occur on either unconfined or confined slope morphologies. For an unconfined

morphology, such as open slopes, entrainment of material is the result of large-strain failures of colluvial material and organics above a competent stratum. A conservative method to determine the amount of material available for entrainment is to estimate the depth of the organics and colluvial material above the likely failure plane and multiply by the event width to determine the potential entrainment volume per unit length of the event flow path. More analytical methods to determine the entrainment volumes, such as Takahashi (1978), have not been applied to unconfined flow conditions.

Debris flows in a confined morphology, such as gully channels, can entrain material by fluvial scour due to rapid rises in streamflow, liquefaction of a debris slide mass which has moved down to block water flow in the gully channel, or the collapse of a "natural dam" which formed at some earlier time. An empirical method to determine the amount of material available for entrainment in a gully is to use a "channel yield rate" and multiply by the length of channel and tributaries along the path of a torrent. The channel yield rate is the amount of material available for entrainment averaged along the length of the channel and its tributaries. Fannin and Rollerson (1993) provide examples and discuss its application to debris flows in the Queen Charlotte Islands, while Hungr *et al*, (1984) discuss several examples for natural debris flows in coastal B.C. The channel yield rate was also used by Benda and Cundy (1990) to determine the debris flow volume for numerous events in the Pacific Northwest.

However, the selection of a single channel yield at a given debris flow site is not straightforward. Fannin and Rollerson (1993) calculated the channel debris yield for 449 debris flow events in the Queen Charlotte Islands and they determined that there was a large variation in this parameter. The variation was calculated to be almost 100% between flows of different event types, and for each event type the standard deviation in channel yield rate is

greater than the average value, indicating a large coefficient of variation in channel yield rates for a single event type. Moreover, the use of a channel yield implies that the entrainment of material is uniform over the entire channel length (or channel reach, as for Benda and Cundy, 1990). This is likely not a valid assumption, since to achieve this the material would have to be uniformly distributed over the length of the channel or reach and the entrainment capability of the flow would have to be the constant over its length, which is unlikely given the unsteady flow characteristics of debris flow events. The concept of a channel yield is also independent of incoming flow volume and flow moisture content, two factors which will affect the depth of entrainment along the base of the flow (Takahashi, *et al*, 1994; see equation 2.6, below).

An analytical method to determine the entrainment depth along gully channels of a debris flow path, and thus the entrainment volume, has been developed by Takahashi *et al* (1994). For saturated channel bed materials the channel bed material is scoured to a depth where the shear stress of the overlying debris flow exceeds the shear strength of the channel bed materials. In this case, the solids concentration of the flowing debris is determined and compared to the equilibrium solids concentration:

$$c_{\infty} = \frac{\rho \tan \theta}{(\sigma - \rho)(\tan \phi - \tan \theta)} \quad [2.4]$$

where c_{∞} is the equilibrium solids concentration, and q is the slope angle of the channel bed, and r , s , and f are as defined previously in [2.3]. If the solids concentration at a point in the path is less than c_{∞} , and the velocity of the flow is greater than the equilibrium velocity U_e , the flow is able to entrain material from the channel. The equilibrium velocity is given by

$$U_e = \frac{2}{5d} \left[\frac{g \sin \theta_e}{0.02} \frac{\rho_T}{\sigma} \right]^{\frac{1}{2}} \lambda^{-1} h^{\frac{3}{2}} \quad [2.5]$$

where r_T is the bulk density of the debris flow, l is the linear concentration of solids in the flow, h is the flow depth, d is the mean particle diameter in a vertical cross-section through the flow. Takahashi *et al* (1992) gives the depth of entrainment as

$$a_L = \frac{c_\infty - c}{c_* - c_\infty} h \quad [2.6]$$

where a_L is the depth of entrainment, c is the volume concentration of solids in the flow, c_∞ is the volume concentration of bed materials in the channel bed, and h is the height of the debris flow. For the case of unsaturated channel bed materials, Takahashi (1991) postulates that entrainment occurs as a result of the dynamic shearing action of the interstitial fluid in the flowing debris.

It should be noted that recent research has quantified entrainment of material in gully channels as removal of all material available, usually down to bedrock or dense stratum (Millard, 1993). Although it is possible to measure the amount of material resident in the gully channel prior to logging, clearcut logging will have some effect on the sediment transfer rate and thus the amount, gradation, and composition of material in the channel after logging cannot easily be determined.

2.4.3 Deposition During Debris Flow Movement

Deposition of debris usually occurs on unconfined slope morphologies such as open slopes, debris fans, and forestry roads. Deposition can occur in confined gully channels, but only significant proportions of the flow volume are deposited if the event encounters a logjam (or other obstruction) in the channel, or a distinct change in path azimuth occurs. Most of the volume of a debris torrent is deposited on unconfined debris fans, as lobes or levees below the mouth of the gully channel.

Both empirical and analytical methods have been developed to determine the amount of deposition on unconfined slopes. Empirical methods for deposition are based on forensic debris flow event deposition data and laboratory experiments on flowing debris. Hungr *et al* (1984) and VanDine (1985) report that typical slope angles to cause deposition are 10° to 12° for unconfined slopes, for flows which were predominantly coarse-grained. Benda and Cundy (1990) assumed a deposition angle of 3.5° for their debris flow routing model, and above 3.5° no deposition was assumed to occur unless a junction angle (change in path orientation) in excess of 70° was encountered along the travel path. The assumption of 3.5° is generally consistent with the observations of Jordan (1994) for predominantly fine-grained flows. Jordan also concludes that the difference in deposition behaviour is a result of the low permeability maintaining pore pressures within the flow for a longer duration in fine-grained flows as compared to coarse-grained flows.

Fannin and Rollerson (1993) indicate that many debris flow events studied in the Queen Charlotte Islands (Q.C.I.) deposit on angles greater than 15° , although some events were observed to deposit on slope angles flatter than 5° . The steeper slope angles for deposition in these events have a greater slope angle than the events documented by Hungr *et al* (1984) and VanDine (1985). This is likely due to the smaller volume (size) of the Q.C.I. events, as well as other factors such as the amount of water and woody debris incorporated in the event. The momentum flux, which transfers momentum from the body of the flow to the snout, is of longer duration for larger events (Hungr *et al*, 1984). Thus, the smaller debris flow events associated with logged terrain tend to terminate on steeper slopes, and consequently have shorter travel distances, than larger natural debris flows. Events with less water and more woody debris are more likely to terminate on steeper slopes, due to increases in friction within the flow.

Analytical methods to predict debris flow deposition have been developed by Takahashi (1978) based on laboratory data and some field observations of debris flows in Japan. Deposition occurs when the slope angle of the channel or fan is less than the equilibrium slope angle θ_e , or the flow velocity falls below the equilibrium flow velocity U_e (equation 2.5). Either of these criteria will lead to a solids concentration in the flow which is greater than the equilibrium value, and the deposition of excess debris material from the flow. Further research into this debris flow behaviour has been carried out, and an implicit finite difference model has been developed to model debris flow deposition with particle segregation (Takahashi *et al*, 1992). However, this research is not easily applicable in a practical sense, particularly for the analysis of debris flows from logged terrain. The detailed topographic information required to use such a numerical modelling scheme requires extensive mapping of the deposition area, and often such information is not available. Furthermore, the constitutive relations developed by Takahashi rely on empirical coefficients which have been developed from laboratory testing of a two-phase system (sediment and water). Full-scale flows which incorporate significant amounts of large woody debris will behave differently due to the difference in scale and the addition of woody debris into a two-phase system, which will affect the loss of flow momentum due to dilatant grain flow.

Deposition of debris flows which are confined in gully morphologies is estimated to occur on slope angles of 8° to 10° (Hung *et al*, 1984 and VanDine, 1985). Slope angles flatter than 8° have been observed to transport debris flows (Fannin and Rollerson, 1993; Benda and Cundy, 1990). Based on these studies, it is conservative to assume that debris flows will not deposit in a confined slope morphology such as a gully channel, even though limited deposition may occur on smaller, flatter portions of the gully channel.

Thus, substantial deposition of debris flows in gully channels seldom occurs, with the exception of the formation of a natural dam from a debris slide entering the gully channel. A dam such as this may subsequently fail to cause a debris flow, as discussed in Section 2.2.2. If a small flow does terminate in the gully channel, the material may be easily incorporated into a debris flow during a subsequent rise in water flow within the gully channel. Fluvial activity subsequent to a debris flow event will also transport any deposited debris flow material, resident in the channel, down to the gully fan.

2.5 Travel Distance and Runout Prediction of Debris Flows

Prediction of the travel distance of debris flows is important to accurately assess the debris flow risk at locations downslope of the potential initiation site. Prediction of the runout distance, defined by Takahashi and Yoshida (1979) as the distance from the onset of continuous deposition until the event terminates, has been the focus of previous studies. Since the methods for runout prediction have been used to determine the termination point for debris flows, methods for calculating both runout distance and travel distance are included in this review. These methods can be grouped into empirical/semi-empirical methods, and analytical methods.

2.5.1 Empirical and Semi-Empirical Methods

Empirical methods for determining the path length of a debris flow event include the volumetric modelling of debris flows and the examination of slope angles in the deposition zone. Volumetric modelling has been used by Cannon (1993) to determine the travel distance of debris flows based on empirical relationships for volumetric change. Based on computer

topographic surveys of debris flow events on the islands of Hawaii, a regression equation to determine the volume change per unit length of the debris flow travel path was developed:

$$\log\left(\frac{V_i - V_f}{D}\right) = 0.14 \log R - 1.40\theta + 2.16 \quad [2.7]$$

where V_i and V_f are the initial and final debris flow volumes in a reach; D is the path length of the channel reach under consideration; R is the event width of the travel path and θ is the average slope angle of the reach. Limited field checking was carried out to determine the applicability of this equation to actual debris flow behaviour. The procedure uses an initial volume at the point of initiation of the debris flow event and for reaches along the debris flow path, the change in volume is calculated using the above equation. Positive values for the changes indicate entrainment of material and an increase in debris flow volume; negative values indicate deposition and a decrease in flow volume. When the calculated flow volume reaches zero, the flow is assumed to have terminated and the individual reach lengths can be summed to determine the event path length.

A similar method was developed to determine debris flow event path length by Benda and Cundy (1990). Based on about 50 debris flow events in the Oregon Cascades, channel yield values were determined using regression techniques. Using selected values for deposition slope angle and the regression equations for channel yield (in m^3 per meter of channel length) the event path length of debris torrents was determined using volumetric changes along the travel path. In testing of the model against actual debris flow events, Benda and Cundy noted the model was not successful in predicting what they termed as "premature" deposition on relatively steep slope angles of 15° .

While the methods of both Cannon (1993) and Benda and Cundy (1990) can be used to successfully calculate debris flow event path length, limitations are evident. The equation

developed by Cannon contains the implicit assumption that the predictor variables and regression coefficients in the equation are identical for both entrainment and deposition, which is likely not the case based on more analytical studies of debris flow behaviour by Takahashi *et al* (1992). For the model developed by Benda and Cundy (1990), the inability of the model to accurately predict deposition on slopes of greater than 15° in three test cases suggests that the model is valid only for fine-grained flows, rather than the coarse-grained flows associated with areas in coastal British Columbia.

A semi-empirical method of predicting debris flow runout distance is presented in Takahashi and Yoshida (1979, in Japanese; summarized in Hungr *et al*, 1984). By integrating momentum losses of the flow through only the deposition zone of the debris flow (for a unit width of the flow), the following equations were derived:

$$X_L = \frac{V^2}{G} \quad [2.8]$$

$$V = v_u \cos(\theta_u - \theta) \left[1 + \frac{gh_u \cos \theta_u}{2v_u^2} \right] \quad [2.9]$$

$$G = g(S_f \cos \theta - \sin \theta) \quad [2.10]$$

where X_L is the runout length of the debris flow measured from the onset of deposition; v_u and h_u are the velocity and height of the incoming flow at the top of the deposition zone, respectively; θ_u and θ are the upslope and deposition slope angles, respectively; S_f is the friction slope of the flowing debris; and g is the acceleration due to gravity. One drawback of this formulation was pointed out by Jordan (1994) in that if the value of S_f is within about one degree of q , then the equation is mathematically unstable and X_L cannot be accurately calculated. Unfortunately, since debris flow events are often depositing over previous flow deposits, the slope angle of these deposits is likely close to S_f . In fact, Jordan (1994) found that

the formulations of Takahashi and Yoshida (1979) were not successful in predicting the runout distance of debris flow events in the Coast Mountains of British Columbia.

The use of equations 2.8 through 2.10 is restricted to the deposition zone since it cannot account for the momentum used by the flow to entrain material. Hungr *et al* (1984) discuss several practical aspects of the application of these equations. One observed limitation of the equations is a tendency to underestimate the runout distance of "smaller" volume debris flows due to the short duration of the momentum influx from the main body of the flow to the snout. Other aspects which limit the use of these equations are the need to empirically determine a design discharge to obtain the v_u and h_u of the surge front of the debris flow, and the assumption of a constant friction angle S_f of the debris flow snout (since usually it cannot be calculated). Values of S_f are dependent on the rheology of the debris flow (Jordan, 1994), and are likely to vary substantially through the deposition zone as the velocity and water content of the flow decrease while the flow terminates.

Empirical and semi-empirical methods have been used to predict debris flow event path length. Empirical methods attempt to account for volume changes along the debris flow path, and identify where the debris flow volume drops to zero indicating that all entrained material has been deposited. The semi-empirical method of Takahashi and Yoshida (1979) provides an analytical solution for the deposition zone of the debris flow path, but most of the input parameters for the model must be developed using empirical estimates of debris flow event discharge and are not easily obtained with confidence.

2.5.2 Analytical Methods

The use of momentum and continuity relationships has been extended into analytical methods to determine debris flow event path length. Examples of such analytical methods include the implicit finite difference model of Takahashi *et al* (1992), and the dynamic analysis method of Hungr (1995).

An implicit finite difference method has been developed by Takahashi *et al* (1992) to predict debris torrent flow volume and travel distance based on changes in solids concentration and mean particle-size distribution (through a vertical plane of the flow snout). Inputs into the model include detailed topography, gradation of debris material stored in the gully channel, and the hydrograph for the storm which triggers the flow. The numerical model was verified using laboratory flume experiments. However, most of the constitutive relationships used as a basis for the finite difference model are developed from laboratory experiments, thus the model requires more calibration to existing full-scale events. The laboratory relationships are developed without including the effects of woody debris which is a large component of debris flow events from logged terrain.

An extension of the lumped mass approach for modelling flowslides (snow avalanches, rock avalanches, and large landslides) has been developed by Hungr (1995). The two-dimensional model DAN (Dynamic Analysis) models blocks of fixed volume in contact as they move down the slope as a flowslide. Time steps are used to balance the equations of momentum and continuity along the flow path to determine the stopping position of the flowslide/debris flow. Deformations within the blocks are used to simulate changes in flow height as the event progresses downslope. The rheological behaviour of the flow can be varied according to several accepted constitutive models. For dilatant grain flow rheology, the lateral stress can be

altered to change the internal pressure and strain within each of the blocks. Several examples of the model calibration on existing flowslides are presented in Hungr (1995): the movement of dry sand down a laboratory flume, the dam break problem using viscous oil instead of water, and the movement of a rock avalanche into Avalanche Lake in the Northwest Territories (as documented by Evans *et al*, 1993). It must be noted that these types of flow differ from most debris flows in logged terrain, as the flows in logged terrain entrain significant amounts of material as the event moves down the path (Fannin and Rollerson, 1993). However, DAN cannot model the entrainment of material along the flow path. Natural debris torrents also entrain significant amounts of material during the flow down the gully channel and the amount of material entrained in the flow can be many times greater than the initial volume (VanDine, 1985).

In summary, numerical modelling approaches are being developed to predict the travel distance of potential debris flows. Although these numerical models can determine debris flow discharge, height, and velocity on impact for a point in the deposition zone, often these models cannot determine the amount of debris delivered to the deposition zone and the probability of such an impact, two important parameters required for risk assessment of potential debris flow impact. Application of the lumped mass approach to modelling debris flows is inappropriate unless the amount of entrained material is negligible compared to the initial volume or further development permits the entrainment of material along the flow path.

2.6 Concluding Remarks

Debris flow is a type of landslide or mass movement which is used to describe the related phenomena of debris slides, debris avalanches and debris torrents. These types of flow are

identified by the slope morphology along the event path. The slope morphology along the event path also influences the water content and materials entrained in the flow: debris torrents generally have a higher water content as topography concentrates surface water flows and fluvial erosion leaves coarser sediments in the gully channels, while debris slides and debris avalanches on open slope morphologies can have significantly less water than debris torrents and may have finer sediments.

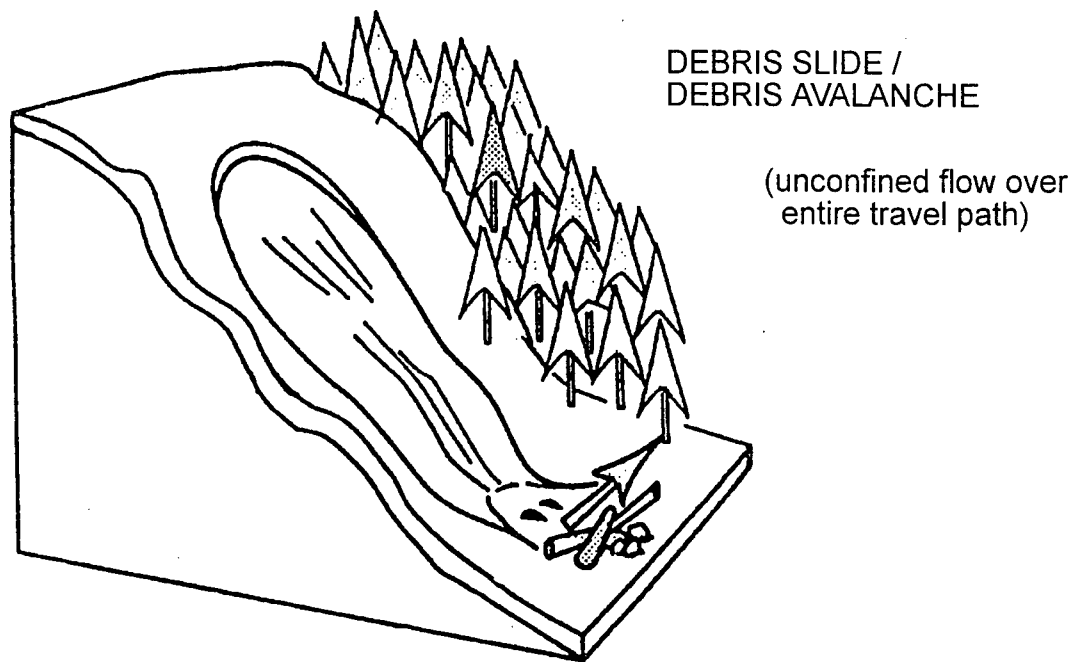
Debris slides and debris avalanches may initiate on open slopes in logged terrain due to high pore pressures, the loss of root cohesion after the decay of stump roots and instability due to roadfills on forestry roads. In gully channels, logging activities which result in woody debris accumulations can trap sediment and increase the probability of initiation due to gully sidewall instability or high streamflow in the channel. Blocked culverts at locations where forestry roads cross gully channels may also lead to the initiation of a debris torrent during high streamflow.

Rheological models of varying complexity are used to characterize debris flow movement. Simple models are more practical than complex models, since the number of parameters required to use the complex models often makes them impractical. Generally two types of flow are recognized: dilatant grain flow characteristic of coarse-grained flows, and viscoplastic Bingham flow characteristic of fine-grained flows. Coarse-grained flows are found to originate within most types of geologic terrain, while fine-grained flows are found to occur in relatively young volcanic terrain. Jordan (1994) considers coarse-grained flows are much more common than fine-grained flows in the steep terrain of coastal B.C, but emphasizes that it is likely that a debris flow event displays more than one type of rheology during its movement down the travel path.

Laboratory studies by Takahashi (1991) have shown that the volumetric behaviour of debris flows is dependent on the velocity of the flow and the solids concentration within the flow. Entrainment of debris occurs in the transportation zone, where the slope angles of the travel path and flow velocity are generally high and the solids concentration within the flow is less than the equilibrium value. Deposition of debris from the flow occurs in zones along the travel path where the slope angle is flatter or the flow loses confinement, leading to a solids concentration within the flow which is greater than the equilibrium value. The relationships developed through laboratory testing do not account for woody debris as a third phase in the flow system, and consequently cannot be reliably used to predict the volumetric behaviour of full-scale debris flows from logged terrain.

The prediction of the travel distance (or runout distance from the onset of terminal deposition) for debris flows can be carried out using empirical/semi-empirical methods, or analytical methods. Empirical methods essentially estimate the volumes of entrainment and deposition along the debris flow path using the concept of a Volumetric Model. Semi-empirical methods, such as the runout equations of Takahashi and Yoshida (1979), utilize analytical concepts of momentum loss within the lower portion of the debris flow path but rely on empirical estimates of incoming flow discharge and a known, constant value for the friction angle along the base of the flowing debris. Analytical models have been developed which utilize implicit finite difference methodology to balance equations for momentum loss and continuity along all portions of the flow path, but often these models require a significant amount of input information such as topography, sediment gradation, and flow hydrographs that is difficult to compile with confidence. Moreover, the models use constitutive relationships which do not account for the large proportion of woody debris common in flows from logged terrain.

The current methods for predicting travel distance are also of limited use in a risk analysis as the methods return a single, deterministic value. A probabilistic method, accounting for the observed variability of full-scale debris flows, is necessary for risk assessment of debris flow impacts at locations along a potential debris flow runout path.



DEBRIS TORRENT /
CHANNELIZED DEBRIS FLOW

(confined flow over
portion of travel path)

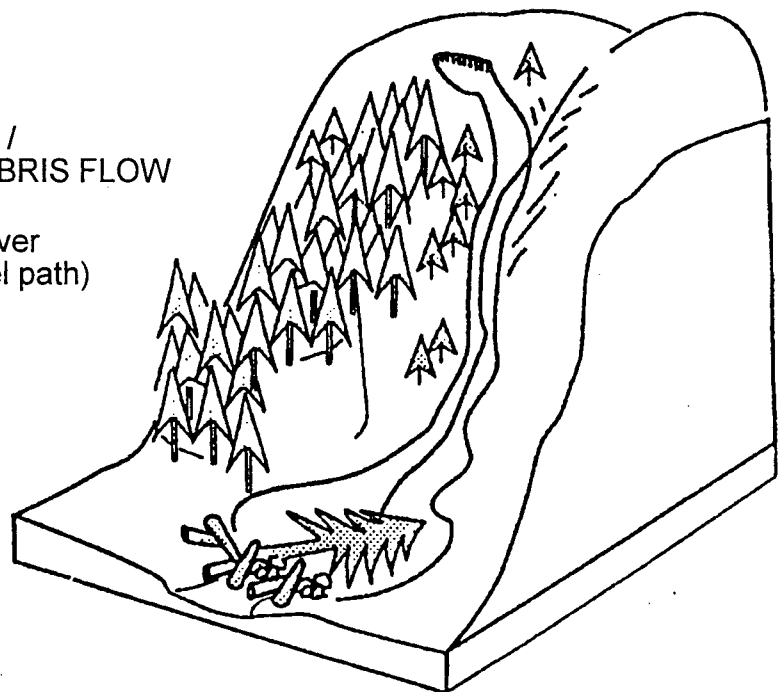


Figure 2.1: Schematic view of debris flow types (from Chatwin et al, 1994)

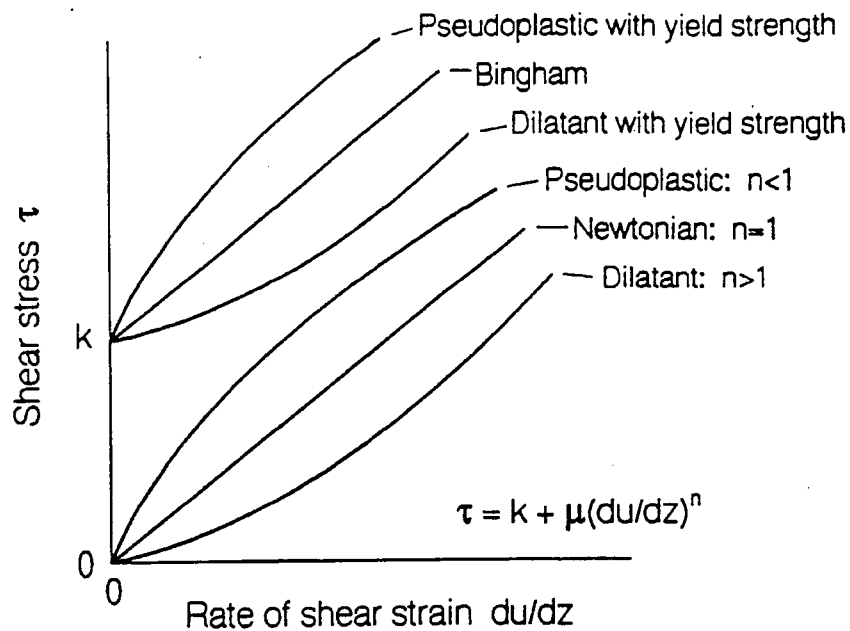


Figure 2.2(a): Flow curves for idealized liquid and plastic rheological models (after Jordan, 1994)

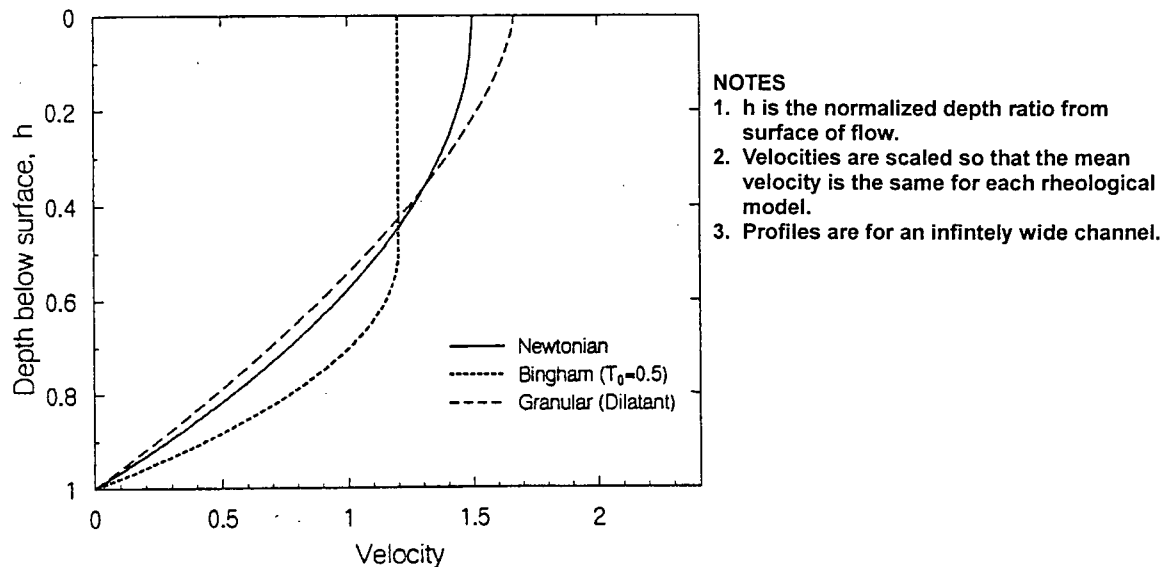


Figure 2.2(b): Dimensionless velocity profiles for a wide channel (after Jordan, 1994).

Chapter 3 DEBRIS FLOW SURVEYING

Research into debris flow behaviour has typically been previously carried out using forensic observations at debris flow sites, and laboratory studies designed to simulate debris flow. In most situations it is not possible to directly observe full-scale debris flow events, as a unique set of sediment storage and precipitation conditions are required to initiate a debris flow.

Forensic observations along the path of a debris flow event are important to develop an understanding of debris flow behaviour or response once a flow has initiated. In 1984 and 1985, the Land Use Planning and Advisory Team at MacMillan Bloedel carried out surveys of 449 debris flow events from logged terrain in the Queen Charlotte Islands to quantify the initiation (occurrence) and volumetric behaviour along the travel paths. These data form the Q.C.I. (Original) Data, which consists of surveyed forensic observations along the path of each debris flow event, studied previously by Rollerson (1992), and Fannin and Rollerson (1993).

This chapter describes the forensic observations recorded during the debris flow travel path surveys in the Queen Charlotte Islands and the methodology used. The advantages and limitations of using forensic observations to characterize debris flow volume behaviour along the travel path are also discussed.

3.1 Forensic Observations

Debris flows, while perhaps one of the most common of the mass-wasting geomorphic processes, are nevertheless difficult to predict both spatially and temporally. This is

particularly true in the case of debris flows relating to logging activities, as clearcut logging and forest road construction on hillslope areas can influence the slope stability and debris supply conditions along a potential debris flow travel path and increase the probability of debris flow occurrence in areas which may not be naturally prone to debris flows. Given these difficulties in predicting events, forensic observations are commonly used to examine debris flow behaviour.

For events such as those in the Queen Charlotte Islands related to logging activity, forensic observations can be used to establish the behaviour of the debris flow along the travel path. Such field observations may include trim lines along the sidewalls of a gully, deposition levees along the path, damaged trees outside of channel, "broomed" ends of logs, and organic material buried in granular sediment. Unsorted sediment deposits on a gully fan may also be indicative of debris flow occurrence. Sections 3.2 and 3.3 discuss the attributes recorded for each reach and the survey methodology used in the study.

The estimation of debris flow volume at the initiation point of the event can be carried out by measuring the thickness of the soil in the headscarp area and multiplying by the width and length of the first (initial) reach of the path. Another possible method for determining the initial volume is to examine the initial volumes of other failures with similar slope morphology and surficial geology, and combine these observations with site specific data.

For reaches in the transportation zone of the travel path, the depth of material entrained can be determined by looking for trim lines to establish the depth of material removed in gully channels. Minor scarps along the sides of the event can be used to determine the depth of material eroded for reaches with an unconfined morphology.

In the deposition zone, the length and average width of the deposit can be measured, and the depth estimated, to determine the volume. The volume of entrainment can be determined by multiplying the average width of and average estimated depth of entrainment in the reach by the reach length. If evidence of both processes is observed, then the average width for each process is recorded. For the debris flow events surveyed in the Queen Charlotte Islands, the measurements of average width, estimated depth, and reach length are recorded typically to the nearest 0.5 m. However, it is often the case that measurements are taken at a point determined to be the average (or representative) width and depth in a reach rather than averaging several measurements.

This survey procedure can lead to an error in long reaches, since a small error in the average width leads to a significant error in calculating the volume of entrainment and/or deposition. Also, since each event was surveyed by only one person, a systematic error may be introduced as an individual will often consistently over- or underestimate the average width or depth of a reach.

Different factors can lead to survey error in determining volumes of entrainment or deposition, leading to differences between the "observed" volume change (calculated from length, width, and depth measurements) within a reach and the actual volume change. For entrainment, error may result from the estimation of average depth of scour along reaches since there was no opportunity to take measurements immediately prior to the flow event. For deposition, volume error may be due to the incorrect estimation of the average depth of deposition for the debris flow event. This is most likely in the case of measurement of the deposition volumes on a debris flow fan, since the material deposited by previous events may inadvertently be included

in the average depth of deposited material for the debris flow event. Also, some material in the deposition may also be eroded by fluvial activity subsequent to debris flow deposition. Care must be exercised to avoid incorrect estimates of average deposition thickness. The clearing of debris flow deposits from logging roads prior to event surveying is also another source of error for estimation of deposition volumes. In general, the error in estimating deposition volume is likely greater than estimating entrainment volumes for reaches of equal length and average width since usually the deposition thickness is not known.

3.2 Reach Attributes of Event Path

The interpretation of survey measurements on recent debris flow event paths, as carried out in Fannin and Rollerson (1993), is based on forensic observations for each reach. A reach is a linear portion of the event path which has consistent slope morphology, slope angle, azimuth, width, and volumetric behaviour characteristics. Figure 3.1(a) shows the division of a debris flow path into reaches, and the attributes which describe a single reach of the path. These attributes consist of reach length L , reach orientation (slope angle TH and azimuth angle AZ), average flow width W_f , average entrainment width W_e and/or deposition width W_d as well as the average depth of entrainment and/or deposition within the reach. The change in path orientation both in profile (dTH) and azimuth (dAZ) can be determined by comparing the changes in slope angle and azimuth angle within the current reach to those of the reach immediately upslope, as shown in Figure 3.1(b).

Note that in some reaches, where entrainment and deposition were observed to have occurred within the same reach, the length of entrainment and deposition may differ. This would correspond to a reach which was predominantly entrainment, but some debris was deposited as a levee on the outer portions of the flow path. In these situations, the volume of entrainment is

calculated using the length of entrainment, and the volume of deposition is calculated using the length of deposition. The longer length is used as the length of the reach for purposes of determining the travel distance of the event.

Figure 3.2 shows examples of reaches from an event in the Queen Charlotte Islands for cases where debris from logging activities has accumulated in the channel and where the debris has been removed by a debris flow event.

The determination of average entrainment or average deposition depth within a reach is required to determine the debris flow volume change within reaches of the event path. Average entrainment depth can be estimated using the depth of the material present in the channel above the event path, or the depth of material in nearby gully channels where no event occurred. The trim lines along the sides of the path indicate the width and depth of the snout of the debris flow for gully reaches. On open slope, gully headwall, and other unconfined flow reaches the width of the flow can be measured by the lateral scar of the debris flow. The depth of entrainment for unconfined flow reaches is usually estimated by assuming a uniform ground surface prior to the event. Errors in determining entrainment depth within an event reach are often due to the assumption of a uniform ground surface. The average depth of deposition can be estimated based on the local relief of the debris flow deposit. For debris slides the deposition zone is often relatively thin and dispersed over a wide area, making estimation of the depth difficult in some cases to local variations in ground topography.

3.3 Survey Methodology

The systematic recording of reach attributes and debris flow volume change data was carried out using a methodology developed by the Land Use Planning and Advisory Team, Woodlands Services Division of MacMillan Bloedel. A slightly modified form of the field cards is available through the Ministry of Forests, Vancouver Forest Region (Appendix B). Although data for both the initiation point and the travel path were recorded, only the reach data along the travel path are considered in this study. Current research is using the initiation site data to develop a complementary model for probabilistic assessment of debris slide initiation (Fannin and Wilkinson, 1995).

Surveys of debris flow events were carried out by walking the travel path and recording the attributes of each reach. The length of each reach was measured using a hipchain, while widths of entrainment/deposition, as well as depth of entrainment/deposition, were either measured or estimated to the nearest 0.5 m. Slope angles and azimuth angles were measured for each reach. Slope morphology, observed bed materials, flow depth, as well as deposit texture and morphology were also noted.

Figure 3.3 presents an example data card of the event reaches for Event 1206, an event in the Queen Charlotte Islands. Note that this event was surveyed from the terminal deposition zone up to the initiation zone, due to ease of access in the field to the lower part of the event. The reach numbers are given in the left margin, and follow the flow path from the initiation point at Reach 1 to the terminal deposition point at the end of Reach 13. Lengths, widths, and depths of entrainment (or scour) are noted along the path, as are lengths, widths, and depths of deposition. The absence, or "non-occurrence" of entrainment in Reaches 12 and 13 are given

the value of zero entrainment volume. Similarly, in reaches 1 through 9, no deposition occurred and these values are taken as zero for later numerical analyses. Reaches 10 and 11, “dual mode” occurred as both entrainment and deposition were observed during the field survey. It is also important to note that the flow depth, as well as the gully floor width / depth data was not recorded for most gully events and thus these data are not used for subsequent analyses.

3.4 Remarks on Survey Methodology

The debris flow survey method described above has several advantages. These include a systematic and quantitative means of recording reach attributes and flow data, the relative ease of surveying for one person using inexpensive equipment, and a means of including important site observations in the survey.

Two limitations of the survey method are evident. The first is that it is most applicable to recording forensic data from debris flow events, and thus it is difficult to apply the methodology to survey potential travel paths. Secondly, errors can occur as a result of inaccurate estimates of entrainment or deposition depth within a reach, leading to errors where the total amount of debris flow material entrained may be significantly different than the total amount of material deposited.

Finally, it is important to note that during the survey the processes of entrainment and deposition are separated as the length, width, and depth of each process in each reach are recorded. The non-zero values for entrainment and deposition indicate the “non-occurrence” of the process in the reach, and non-zero values indicate the occurrence of the process as well as

the magnitude of the volume change in the reach. The non-zero data from selected events are used to develop regression equations for entrainment and deposition. The zero data are used to develop criteria for modelling the occurrence of entrainment and deposition processes, as discussed in Chapter 5.

debris flow path divided into reaches based on slope morphology, flow width, slope angle, azimuth angle, and flow behaviour along path

Notes:

1. Slope angle and azimuth angle refer to the orientation of the centerline of the reach

2. Reach width, entrainment width, and deposition width are average values over the length of the reach

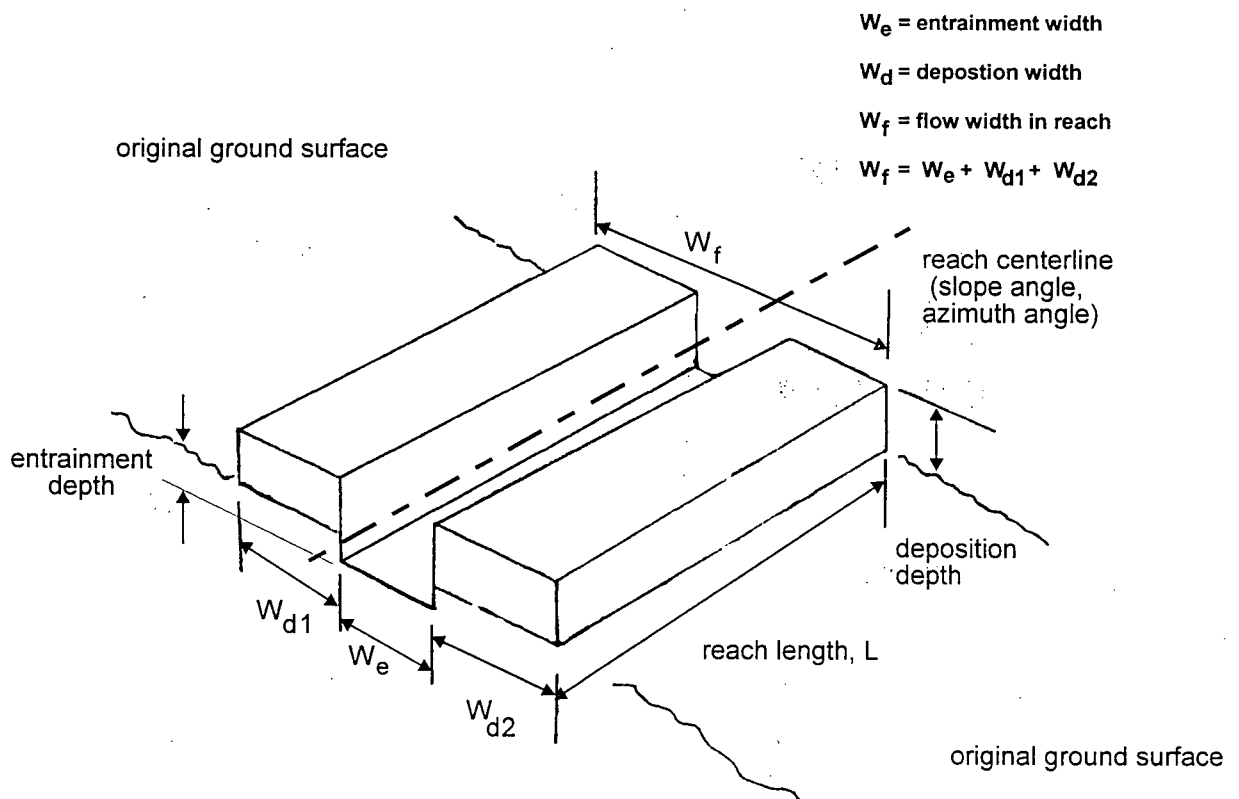
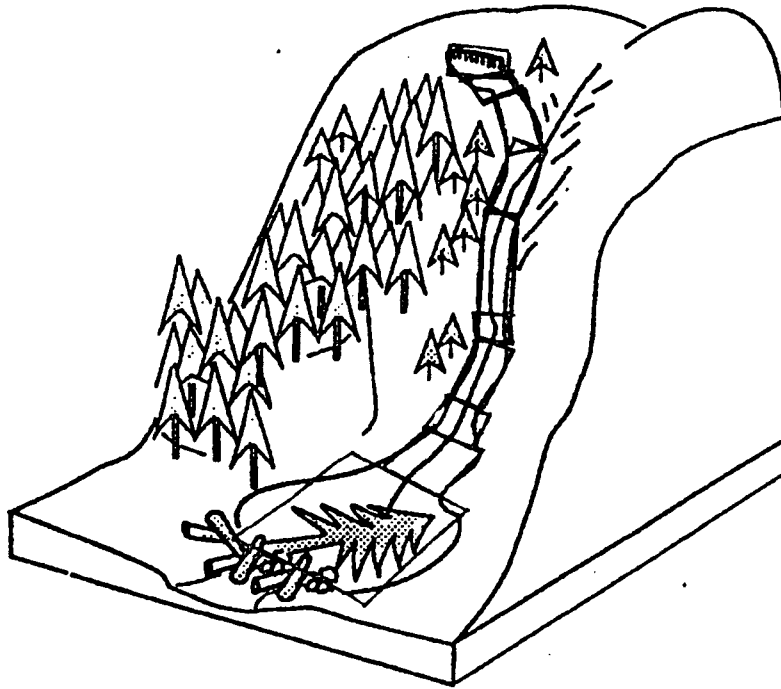


Figure 3.1(a): Attributes of a typical reach along debris flow event path

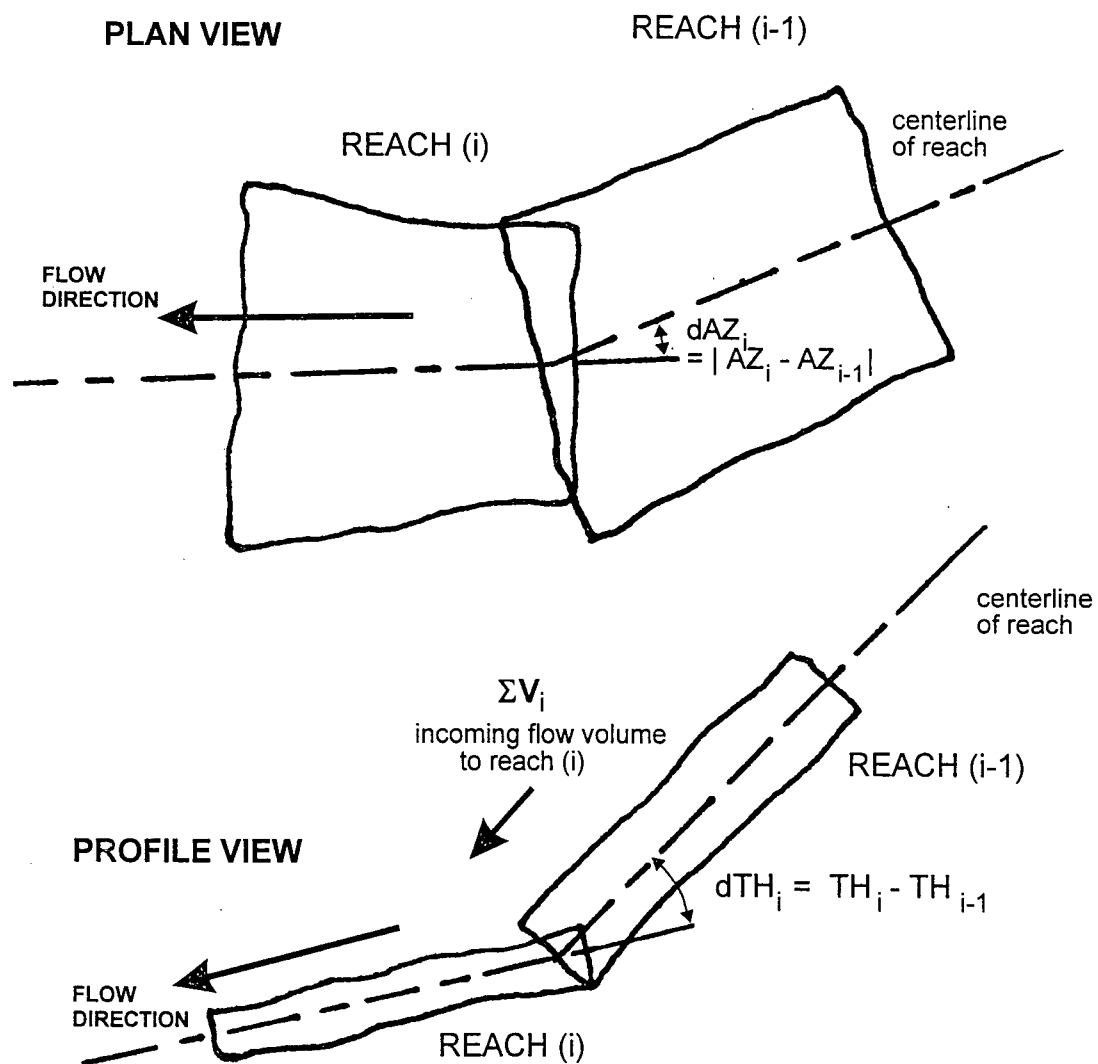
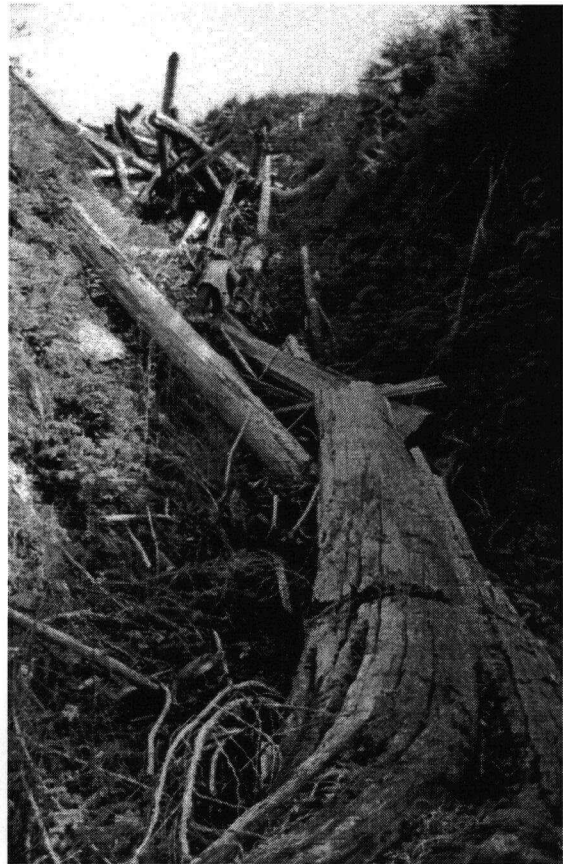


Figure 3.1(b): Attributes of reach relative to upslope reach

Example of reach along potential debris flow path. Note large proportion of woody debris in channel and logjam at top of photo.



Example of reach along travel path after debris flow event. Note trim lines visible below stumps to indicate maximum depth of material prior to entrainment.

Figure 3.2: Examples of reaches along debris flow travel paths

REACH
Number

2
1

Initiation point

Page 2 of 2

47

Chapter 4 DEBRIS FLOW DATA CHARACTERIZATION

A characterization of data for debris flow events from four study areas is carried out in this chapter. The events are characterized on the basis of event type, peak flow volume, and travel distance for each study area. Reach attributes of the events are characterized for different confinement flow conditions. This chapter also describes the basis for grouping debris flow events to form the Q.C.I. (Selected) Data. These events were extracted from the Q.C.I. (Original) Data to develop equations for debris flow modelling. Data analyses and the development of equations from the Q.C.I. (Selected) Data are described in Chapter 5.

4.1 Debris Flow Study Areas

Debris flow event data have been gathered from four different geographic areas in coastal British Columbia. The Q.C.I. (Original) data were gathered from the Queen Charlotte Islands in the mid-1980's by the Land Use Planning and Advisory Team at MacMillan Bloedel. Selection of these events is described in Rollerson (1992), with several areas logged 6 to 15 years prior to the field study selected for potential study in the Skidegate Plateau. These areas were then systematically numbered and randomly sampled. All landslide events greater than 0.05 ha were then surveyed in a given sample area. Supplementary events from the Queen Charlotte Islands, forming the Q.C.I. (Additional) Data set, were surveyed by the writer and Dr. R.J. Fannin in September, 1992. These events were surveyed to provide cases for testing of the model developed from the Q.C.I. (Original) Data. An additional 29 events were surveyed near the Mamquam River, the Eve River, and Nootka Island were obtained by the writer during field trips between May 1993 to December, 1993 as part of this research study.

The Q.C.I. (Additional) Data, Mamquam Data, Eve River Data, and Nootka Island Data are collectively termed the Supplementary Data. Figure 4.1 shows the locations of the four study areas in coastal British Columbia.

4.1.1 Skidegate Plateau (Queen Charlotte Islands)

Sutherland-Brown (1968) describes the Skidegate Plateau as a central area on the Queen Charlotte Islands archipelago which slopes gently eastward. Along the western edge of the Skidegate Plateau are the mountains of the Queen Charlotte Ranges, at an elevation of about 750 m above sea level, while the elevation along the eastern edge is typically less than 50 m. The Plateau landforms are generally dissected, rounded hills and ridges which separate moderately wide, low-gradient valleys. Bedrock in the area consists of volcanic (basalt) and metasedimentary (conglomerates, sandstone) formations. The Plateau was completely glaciated during the Pleistocene; consequently, glacial landforms dominate the hillslopes of the Plateau. Significant portions of the Queen Charlotte Islands have been logged since the mid-1950's.

The annual precipitation varies substantially across the Queen Charlotte Islands. The west side of the Islands, subjected to storms directly from the Pacific, has an annual precipitation of about 4500 mm. The annual precipitation decreases eastward across Skidegate Plateau, to the east coast which has an annual precipitation of about 1200 mm (Karanka 1986).

Figure 4.2 shows the Skidegate Plateau study area on the Queen Charlotte Islands and the sample locations where the 449 debris flow events were surveyed (after Rollerson, 1992). The locations for the six additional events surveyed in September, 1992 were in the central portion of Graham Island, near sample areas 10, 19, 20, and 26 (Figure 4.2). The young vegetation along the event paths (generally less than 5 years old) and the nature of the initiation points of

the additional events indicates that these events are more recent than the Q.C.I. (Original) Data which were surveyed in the mid-1980's. One exception is the debris avalanche above Riley Creek in Rennell Sound, which occurred about in the early 1980's. As this geographic area was not included in the original debris flow surveying of the mid-1980's, there is no potential duplication with the Q.C.I. (Original) Data.

4.1.2 Mamquam River (Squamish)

The Mamquam River is a tributary to the Squamish River, about 75 km north of Vancouver and south of Garibaldi Provincial Park. The valley in which the Mamquam River flows is V-shaped, with the northern portion of the valley formed by previous lava flows and the southern portion of the valley formed by granitic/dioritic intrusives common in the Coast Plutonic Complex (Jordan, 1994). Topography in the valley ranges from 600 m in the valley bottom to peaks as high as 1,676 m on the southern boundary of the watershed. The area was extensively glaciated during the Pleistocene period, and glacial landforms are found throughout the study area.

While there are no precipitation stations in the watershed with a substantial period of record, the annual precipitation for the Squamish area is 2247 mm. Jordan (1987) notes that rain sometimes falls at elevations of 2500 m during winter storms, while above elevations of about 1200 m, most of the annual precipitation falls as snow.

Figure 4.3 shows the Mamquam River watershed and the locations of the study areas where debris flow events were surveyed. Four debris torrents (channelized debris flows) and two debris slides were surveyed. These events were possibly triggered by the large storm events of November, 1990 or November, 1991.

4.1.3 Eve River (Tsitika Valley)

The Eve River watershed is located east of the Tsitika River, about 25 km west of Sayward, on the northern side of the Vancouver Island Mountain Range. This area was completely glaciated during the Pleistocene (Muller, 1977). Thus the topography in the Eve River valley is glacially-oversteepened, with the moderately narrow valley bottom at an elevation of 150 m rising to peaks of about 1700 m in the area. Bedrock types in the area are dominated by the Karmutsen Formation, with an upper member consisting of massive flows with interbedded pillow lava, breccia, and sedimentary layers with low-grade metamorphism (Muller, 1977).

Figure 4.4 shows the areas where four debris slides and two debris torrent events were surveyed in the Tlatlos Creek and Kunnum Creek tributaries, as well as the upper Eve River watershed. Of the six events surveyed, all had occurred a maximum of 5 years prior to the time of field surveying based on revegetation along the travel path and in the deposition areas.

4.1.4 Nootka Island (Kyuquot Sound)

Nootka Island is located in Kyuquot Sound, northwest of Clayquot Sound on Vancouver Island. The island was glaciated during the Pleistocene, and consequently the valleys in the study areas have glacially-oversteepened sideslopes. Topography in the study areas ranges from 50 m in valley bottoms to about 675 m at nearby peaks. Bedrock types in the area are dominated by the Westcoast Complex, consisting of gneisses, amphibolites, and diorites (Muller, 1977). From Figure 4.5, study sites in the Crawfish Lake watershed (Area 5000) would be impacted directly by large storms from the Pacific Ocean, whereas other study sites in Gunpowder Creek (Area 5200, 5300) and Area 5400 are in a slight rainshadow. Six debris slides were surveyed, in addition to 11 debris torrents. One multiple event was surveyed, with a single tributary, to provide a starting point for modelling of multiple flows in future

refinements of the model. Study areas 5100 and 5500 show the approximate locations of Events 5101, 5102, and 5501.

4.2 Formation of the Q.C.I. (Selected) Data Set

The Q.C.I. (Selected) Data Set is 131 debris flow events which have been extracted from the Q.C.I. (Original) Data Set on the basis of a single travel path, greater than two reaches, and the measured volumes along the path balancing to within a specified volumetric error. Figure 4.6 shows the criteria for extracting events from the Q.C.I. (Original) Data. The Q.C.I. (Selected) Data are used to develop regression equations to predict volumetric behaviour of debris flow events, discussed in Chapter 5.

Single events, as defined by Fannin and Rollerson (1993) have a unique travel path, whereas multiple events have one or more contributing channels and thus the travel path of each contributing channel is not unique. Multiple event data cannot be used for the development of regression equations due to the ambiguity of flow volumes associated with more than one initiation point and travel path. In total, there were 285 single events in the Q.C.I. (Original) Data (Fannin and Rollerson, 1993).

Events with three or more reaches were chosen since these events are much more likely to have fully developed debris flow behaviour. Many events with only two reaches are the result of very small debris slides or slumps from road cuts or gully sidewall areas. From the Q.C.I. (Original) Data, 79 events had two reaches or less, with 49 of these 79 events being tributaries for multiple events. The typical (average) number of reaches is 2.5 for the single unconfined events and 8.3 for single confined events in the Q.C.I. (Original) Data.

The normalized volumetric error for a debris flow event is a measure of the precision in the survey. This can be expressed as

$$VE(\%) = \frac{|V_e - V_d|}{V_e + V_d} \times 100 \quad [4.1]$$

where VE is the normalized volumetric error (expressed as a percentage), V_e is the total volume entrained over the travel path, and V_d is the total volume deposited. Events with VE greater than 40% were not selected since the accuracy of the volumetric data for the reaches in these events is suspect. Errors in surveying the debris flow volumes, discussed in Section 3.4, as well as changes in density along the flow path are factors which led to the arbitrary choice of 40% as the upper error limit for extraction of events into the Q.C.I. (Selected) Data. Appendix A contains a list of the events in the Q.C.I. (Selected) Data, as well as the reach data for the events.

It is important to note that the total volume of entrainment is not likely to equal the total volume of deposition, since a change in density will occur since the density of the deposited material is likely less than the *in situ* density of the material prior to the flow event. Hence, slightly larger volumes of deposition than entrainment are expected along the path due to dilation effects and some degree of volumetric error is to be expected as a result of forensic surveying of events.

4.3 Debris Flow Event Characterization

Debris flow events can be characterized by the type of event, peak flow volume, and the travel distance of the event. These characteristics are compared and contrasted for events from the Queen Charlotte Islands and the three other geographic study areas, Table 4.1.

Table 4.1: Characteristics for surveyed debris flow events.

Study Area / Data Set	n	Event Peak Flow (m ³)				Event Travel Distance (m)			
		mean	med	min	max	mean	med	min	max

Queen Charlotte Islands Events¹

Q.C.I. (Original) Data	449	922	467	38	11735	179	104	26	2100
Q.C.I. (Selected) Data	131	949	555	112	7810	171	115	26	1051

Supplementary Data²

Q.C.I. (Additional) Data	6	1748	1077	821	3346	411	401	217	627
Mamquam Data	6	1499	914	324	3303	443	302	141	1036
Eve River Data	6	1135	777	382	3099	298	312	128	431
Nootka Island Data	17	1784	710	67	7311	290	218	99	1029
Combined Supplementary	35	1594	914	67	7311	381	339	99	1036

Note: Event 5006 not included in Q.C.I. (Additional) Data

4.3.1 Types of Event

Since the most of the data employed in this study are the Q.C.I.(Original) Data used by Fannin and Rollerson (1993), a classification of the Supplementary Data by event type is carried out for comparison. Figure 4.7 shows the number of each event type for the study areas. Event types 1, 2, 3, and 4 are single event types, while event types 5, 6, and 7 are multiple event types. Comparing these data to event types in the Supplementary Data, there is a high proportion of types 1, 2, and 3 as single events were chosen preferentially during the field surveys. As discussed in Section 4.2, multiple events and Type 4 events (typically two reach events which terminate in gully channels) were not chosen for the Q.C.I. (Selected) Data as the material in the gully could be easily remobilized, and the focus of the model development is events which travel the full length of the gully system. Table 2.2 presents the classification criteria developed by Fannin and Rollerson (1993).

For the Supplementary Data from the Mamquam River, Eve River, and Nootka Island areas, Type 2 events were the easiest to locate in the field as often the travel path crossed logging

roads which provided vehicle access. Type 1 events were often difficult to find or access in areas with older tree regeneration. Type 3 events were relatively rare in the study areas, although in approximate proportion to the Type 3 events in the Q.C.I. (Original) Data. Most debris torrent events in the study areas for the Supplementary Data were Type 2 events, indicative of coarse-grained debris flow rheology and the local topography along the event path. Obtaining approximately equal numbers of confined and unconfined flow events was the goal when surveying events for the Supplementary Data. This fact is not expected to bias the conclusions of the study, since the Supplementary Data are used only for back-analyses to validate the debris flow model, rather than develop additional models for other geographic areas. Table 4.1 summarizes the event characteristics of the Supplementary Data.

4.3.2 Peak Flow Volume of Events

The peak flow volume of a debris flow event is indicative of the magnitude of the event and is calculated as the maximum cumulative flow volume of the event (see Figure 5.2 as an example). This may differ slightly from the magnitude of an event, which is the total volume of debris which is transported to the main deposition zone and is dependent on the size of the source area and the availability of debris for entrainment into the flow (Hung *et al*, 1984) as well as the extent of partial deposition along the travel path.

The peak flow volumes for the Q.C.I. (Original), Q.C.I. (Selected), and Supplementary Data are shown in Figure 4.8 for the different study areas. The peak flow volume of the Q.C.I. (Original) events varies from 38 m^3 to about $12,000 \text{ m}^3$, while the Q.C.I. (Selected) events range from 112 m^3 to about $8,000 \text{ m}^3$. Eliminating the multiple events (types 5,6,7) and the events with only two reaches has significantly reduced the number of small volume events. The number of larger events has decreased as some of these did not have a sufficiently small volumetric error. Note that the general distribution of the event volumes remains similar to the

Q.C.I. (Original), indicating the distribution of peak volumes is not likely to be biased by the elimination of events with two reaches or a volumetric error greater than 40%.

Comparison of the peak flow volumes from the Supplementary Data set with the Q.C.I. (Selected) Data indicates that the maximum peak flow volume for the Supplementary Data is less than the maximum value for the Q.C.I. (Selected) Data. The minimum is less than the value for the Q.C.I. (Selected) Data.

The difference between the mean and median values for all the peak flow data indicates these data are skewed. The histograms in Figure 4.8 show these data are positively skewed, indicative of natural processes which have a lower bound. These data also show the magnitude-frequency relationship common for landslide hazard, with a higher frequency of smaller events and a lesser frequency of large events. These peak flow volumes are also significantly less than the magnitudes of natural events as compiled by VanDine (1985), which range from about 7500 m³ to 61,000 m³. One exception to this is the large debris avalanche surveyed in Rennell Sound on the Queen Charlotte Islands as part of the Supplementary Data, which has a peak flow volume of about 20,000 m³.

4.3.3 Travel Distances of Events

The travel distance of a debris flow event is defined as the total slope distance from the initiation point to the termination point, as discussed in Section 1.2. Fannin and Rollerson (1993) have studied and characterized the travel distances and the terminal deposition zones for the Q.C.I. (Original) Data.

The travel distances for debris flow events in the Queen Charlotte Islands and other study areas are shown in Figure 4.9. The Q.C.I. (Original) events range from 26 m to 2,100 m, and the

elimination of events with two reaches to form the Q.C.I. (Selected) Data Set greatly decreased the number of shorter events. Only four events with relatively long travel distances were not selected from the Q.C.I. (Original) events, and were eliminated due to a large volumetric error. However, the general distribution of travel distances for the Q.C.I. (Selected) events with travel distances greater than 200 m is similar to the that of the Q.C.I. (Original) events, indicating the travel distances of the Selected events are representative of those of the Original events. Table 4.1 quantifies the distributions of these data which provide further evidence of the similarity between the Q.C.I. (Original) and Q.C.I.(Selected) Data Sets.

Comparison of the travel distances for the Supplementary events with the Q.C.I. (Selected) events indicate that the Supplementary events are longer than the range defined by the Q.C.I. (Selected) data. The minimum and maximum values of the Combined Supplementary Data indicate these data are within the bounds of the Q.C.I. (Selected) data. The mean and median values of the Combined Supplementary Data indicate these events are generally larger and longer than those in the Q.C.I. (Selected) Data, possibly due to the relatively large number of Type 2 and Type 3 events contained in the Supplementary Data.

4.4 Reach Characterization

Debris flow events were divided into reaches during the field survey, as discussed in Chapter 3. Figures 3.1(a) and 3.1(b) illustrate the attributes for an event reach. Several attributes are quantitative, such as those which characterize the geometry of the reach; others are qualitative, such as slope morphology which determines whether flow will be confined or unconfined flow in the reach. Both the geometry and morphology of a reach significantly influence the volume change behaviour of a debris flow passes through the reach.

Reach data are grouped by flow mode based on reach morphology, which determines flow confinement. Modes of flow recognized along a debris flow event are: unconfined flow on open slope, gully headwall, gully sidewall, and gully fan reaches; confined flow in gully channel reaches; and transitional flow, for the first reach of unconfined flow after a reach of confined flow. Reaches within each flow mode can be described by the geometry and changes in flow volume. Grouping of the reach data in this manner provides a means of developing relationships between the different flow modes (confined flow/unconfined flow), reach geometry, and volumetric behaviour.

Attributes of the Q.C.I. (Selected) Data reaches and the Supplementary Data reaches are characterized for flow modes of unconfined flow, confined flow, and transition flow (confined to unconfined), in Table 4.2. The range and distribution for each of the attributes is described and can be used as a basis for estimating values for the reach attributes in the field. Note that entrainment and deposition are considered separately, as discussed in Sections 3.3 and Chapter 5.

Table 4.2: Reach Characteristics for Q.C.I. (Selected) Data and Supplementary Data

Flow Mode	Statistic	L (m)	W_f (m)	W_e (m)	W_d (m)	TH (deg)	dTH (deg)	dAZ (deg)	$+dV$ (m ³)	$-dV$ (m ³)
<i>Q.C.I. (Selected) Reach Data</i>										
Unconfined Flow	mean	29.6	17.4	9.1	8.4	22.2	-4.6	0.3	156.7	-302.2
	median	23.0	14.0	6.0	5.0	22.0	-5.0	0.0	34.5	75.5
	st dev	21.7	12.9	12.6	11.0	11.5	12.6	14.6	315.8	737.2
Confined Flow	mean	34.6	10.3	7.4	3.0	22.1	-3.1	1.4	142.9	-141.5
	median	29.0	9.0	7.0	0.0	22.0	-3.0	0.0	89.0	0.0
	st dev	21.1	6.1	5.3	5.6	9.7	9.7	29.6	176.5	399.2
Transition	mean	33.4	12.3	2.4	9.9	14.7	-5.4	7.3	29.0	-554.0
	median	22.0	10.0	0.0	10.0	12.0	-5.0	0.0	0.0	-300.0
	st dev	39.7	6.7	5.5	6.9	12.8	11.7	22.1	81.6	821.0
<i>Supplementary Reach Data</i>										
Unconfined Flow	mean	32.1	17.3	8.1	9.1	20.6	-2.7	-0.4	380.0	-515.0
	median	24.0	10.0	3.0	1.0	12.5	-4.0	0.0	45.0	-12.0
	st dev	23.8	21.7	15.0	19.1	13.7	15.7	17.6	1340.0	2486.0
Confined Flow	mean	36.7	6.1	4.4	1.7	26.1	-2.1	3.2	177.6	-70.4
	median	31.5	4.0	4.0	0.0	26.0	-2.0	0.0	84.0	0.0
	st dev	22.3	6.5	4.7	4.8	9.2	12.9	25.4	261.5	265.3
Transition	mean	26.7	16.9	3.2	13.7	12.2	-10.6	-2.9	194.0	-463.0
	median	16.0	14.0	0.0	12.0	10.0	-8.0	0.0	0.0	-225.0
	st dev	23.2	9.9	7.2	8.1	9.9	12.6	13.1	483.0	508.0

4.4.1 Unconfined Flow Geometry and Morphology

Unconfined flow occurs on reaches with no lateral confinement to contain the flow event (such as open slope, gully headwall/sidewall, forestry road, and fan reaches). It is likely unsaturated, with the intergranular collisions within the flow determining the flow behaviour.

Figure 4.10a shows histograms of the reach attributes for unconfined flow reaches in the Q.C.I. (Selected) Data. It is apparent that, from these histograms, reach length L , flow width W_f , entrainment width W_e , and deposition width W_d have positively skewed distributions which appear lognormal. The slope angle of the reach, TH , appears to have a slightly skewed normal distribution. The slope morphology of most of these reaches is one of an open slope, with other unconfined morphologies (gully headwalls, gully sidewalls, gully fans, and forestry roads) represented in lesser numbers. The change in slope angle dTH and the change in

azimuth dAZ , both expressed relative to the previous reach, appear to have a normal distribution. More negative values for dTH indicates that most debris flow paths are concave upwards path in profile, with successive reaches having flatter slope angles. Both entrainment volume $+dV$ (volume entrained within the reach) and deposition volume $-dV$ (volume deposited within the reach) are highly skewed and appear to have lognormal distributions.

The characterization of the combined supplementary reach attributes is shown in Figure 4.10(b). Similar trends in the data are shown for these attributes as for the Q.C.I. (Selected) Data in Figure 4.10(a). The minima and maxima for the attributes in the Supplementary Data are comparable to the ranges in the Q.C.I. (Selected) Data, with the exception of the Riley Creek landslide in Rennell Sound (Event 3006).

4.4.2 Confined Flow Geometry and Morphology

Confined flow occurs in the gully reaches of debris torrents, and are identified by these slope morphologies in the data cards (Figure 3.1, for example). Flow through confined reaches is likely to contain a higher water content and fewer fine soils (due to previous fluvial erosion) than flow through unconfined reaches, and the flow behaviour is usually dominated by pore pressure effects.

Figure 4.11(a) shows the distributions for the reach attributes of confined flow reaches in the Q.C.I. (Selected) Data. The form of the distributions is generally similar to that for the unconfined flow reaches. Reach length L , W_f , W_e , and W_d all appear lognormally distributed. Slope angle TH , dTH , and dAZ all appear to be approximately normally distributed. The entrainment volume $+dV$ and deposition volume $-dV$ also appear to be lognormally distributed.

In comparison to the attributes of unconfined flow reaches, see Figure 4.10(a), the length of the confined flow reaches is roughly the equal but the W_f , W_e , and W_d are about half the values for unconfined flow reaches. The distribution of the reach slope angles appears to be similar. In terms of volumetric changes, the confined flow reaches typically have 50% lower entrainment volumes and much lower deposition volumes than unconfined reaches. The lower deposition volumes are the likely the result of the confinement of the gully reaches which increases the mobility of the flows by preventing lateral dissipation of the water within the flow event.

Figure 4.11(b) shows the distributions for confined flow reach attributes in the Supplementary Data Set. Comparison of the forms of these distributions with those of the Q.C.I. (Selected) Data show that the Supplementary Data have similar distributions. The minima and maxima of the Supplementary Data distributions are in reasonable agreement with the Q.C.I. (Selected) Data distributions.

4.4.3 Transitional Flow Geometry and Morphology

The unconfined reach immediately downslope of a confined flow reach is termed a transition reach. These reaches are typically the apex portions of gully fans, but may also include forestry roads which cross gully channels. Reaches with transition flow represent the change from the relatively mobile flow behaviour of confined channels to the less mobile behaviour associated with unconfined flow. Within transition flow reaches, the dominant effects on flow behaviour shift from pore pressures within the debris flow to granular interactions as water drains from the flow immediately following the loss of confinement.

Figure 4.12(a) shows the distributions of the reach attributes for the transition reaches in the Q.C.I. (Selected) data. Reach length L , W_f , W_e , and W_d appear to have a lognormal distributions. Reach slope angle TH appears to be distributed either normally or lognormally.

Change in slope angle dTH and change in azimuth angle dAZ appear to have normal distributions. The slope morphology for these data are mostly fan reaches.

The transition reaches for the Q.C.I. (Selected) Data have much lower values of reach slope angle than the unconfined reaches or the confined reaches. Also, the volumetric behaviour is very different: only minimal values of $+dV$ were observed, while $-dV$ values comparable to unconfined reaches were observed. It is concluded that the volumetric behaviour of the transition reaches is substantially different from other unconfined reaches, and sufficient to justify separating these into a distinct group for regression analyses and modelling purposes.

Figure 4.12(b) shows the transition reaches for the Supplementary Data. The form, as well as the minima and maxima, of these distributions are similar to the data in Figure 4.12(a) for the Q.C.I. (Selected) Data.

4.5 Summary

Debris flow events in the Q.C.I. (Original) Data contain reaches with modes of unconfined flow, confined flow, and transition flow (confined flow to unconfined flow). About one third of the events in the Q.C.I. (Original) Data were extracted, on the basis of single travel paths, minimum reaches, and normalized volumetric error, to form the Q.C.I. (Selected) Data. These data are used for developing regression equations for volumetric modelling.

The study areas where debris flows for the Supplementary Data were surveyed are described. These areas in coastal British Columbia have differences in bedrock geology, topography and climate when compared to the Queen Charlotte Islands. However, a comparison of the peak flow volumes and travel distances of events in the Supplementary Data to the Q.C.I. (Selected)

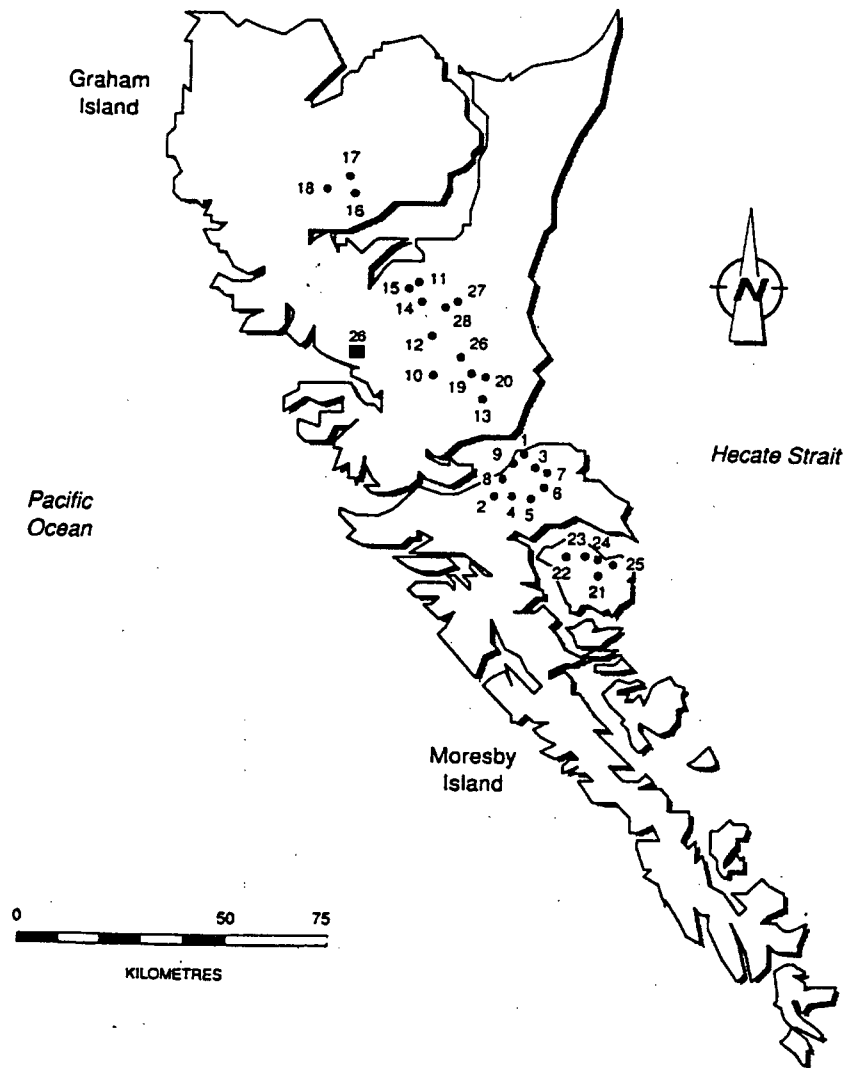
Data showed the two groups are essentially similar in scale. The similarities in events are expected, as previous studies of debris flows have noted similarities in types of debris flow behaviour in a variety of geographic locations with different climatic and geologic factors (Jordan, 1994; Hungr *et al*, 1984; VanDine, 1985).

A comparison of the reach attributes for the flow modes of unconfined flow and confined flow, as well as the transition reaches (confined flow to unconfined flow), shows that the volume change behaviour is typically different for each flow mode. Unconfined flow reaches have a large range of entrainment and deposition volumes, while confined flow reaches were observed to contribute moderate entrainment volumes and minimal deposition volumes were reported. Transition reaches have very low entrainment volumes and very high deposition volumes. Distributions for reach attributes in the Q.C.I. (Selected) Data appear either lognormally distributed or normally distributed, an interpretation which is investigated in Chapter 5. Pooling the reach attribute data for the Supplementary events illustrates similar trends and demonstrates that the Supplementary Data are within the ranges established by the Q.C.I. (Selected) Data to back-analyze debris flow volumetric behaviour.

The reach attributes characterized in this chapter are used in the development of equations for modelling volume change behaviour in Chapter 5. The back-analyses using equations to predict the volume change behaviour are discussed in Chapter 6.



Figure 4.1: Study areas for debris flow research



Notes:

Sample areas 1 through 25 represent sites for events in the Q.C.I. (Original) Data

Sample areas 21, 23, and 24 are not represented in the Q.C.I. (Selected) Data

Sample area 26 was added after compilation of the Q.C.I. (Original) Data and is included in the Q.C.I. (Additional) Data

Figure 4.2: Sample area locations on the Queen Charlotte Islands, B.C.
(after Rollerson, 1992)

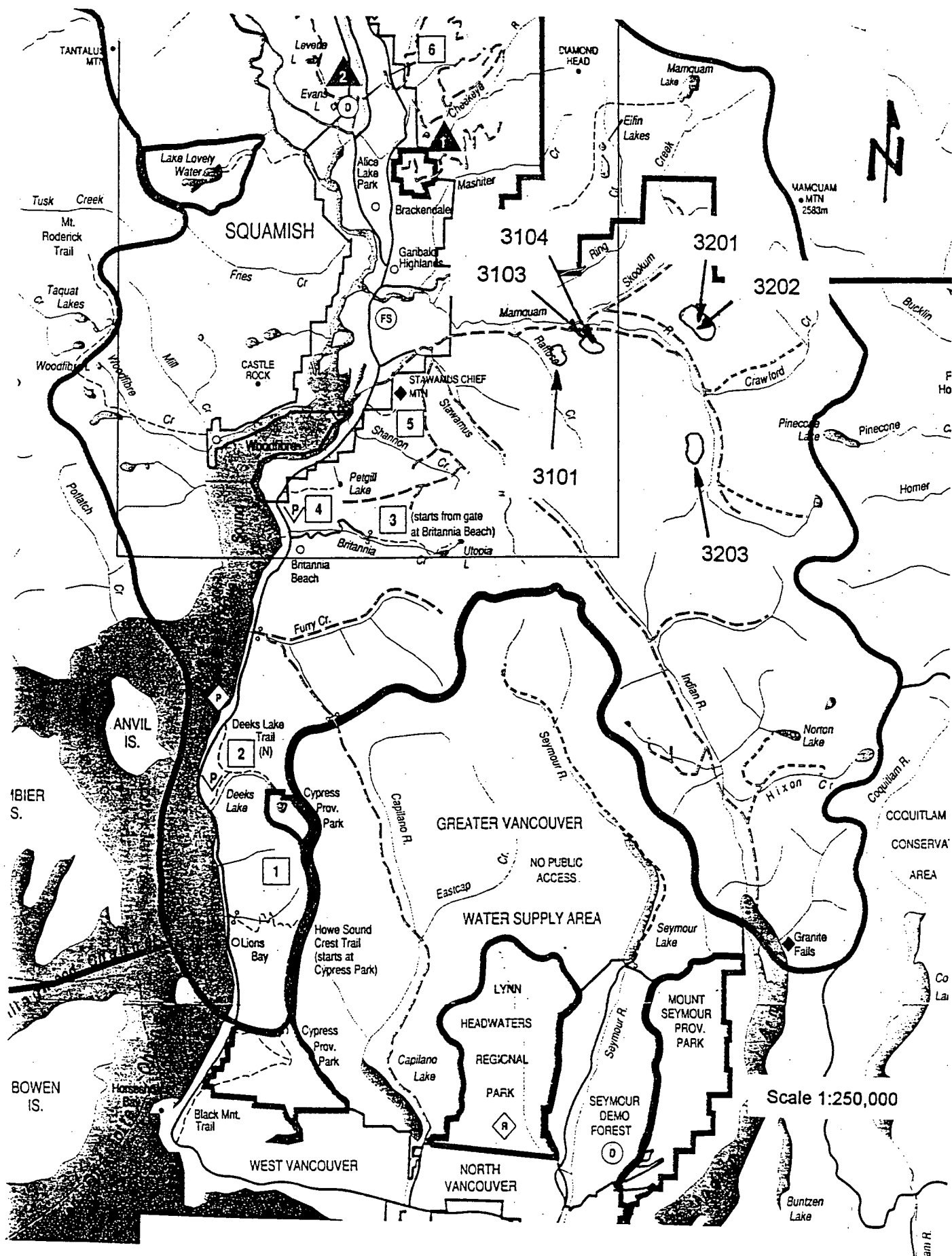


Figure 4.3: Sample area locations for Mamquam River study area, Squamish, B.C. 66

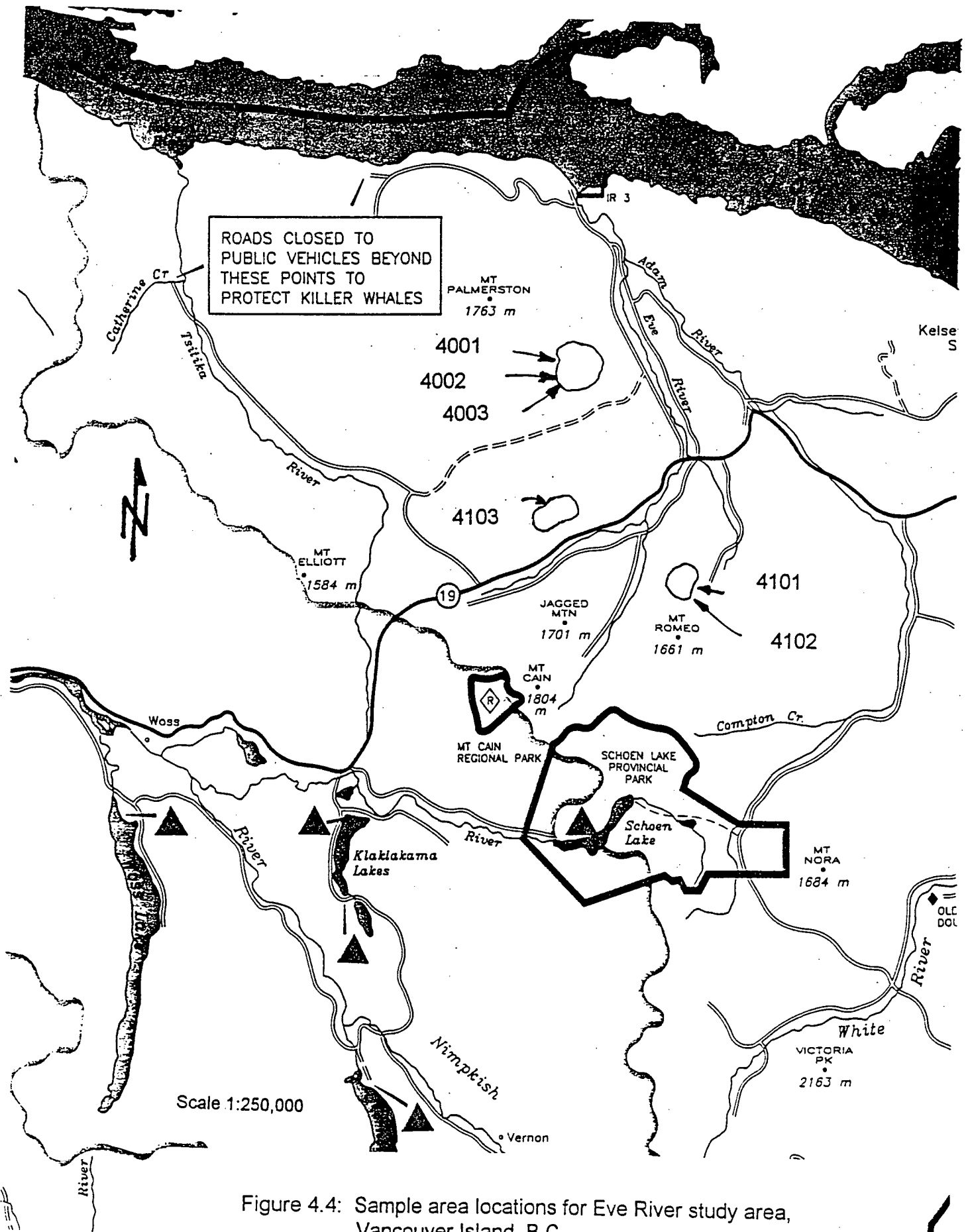
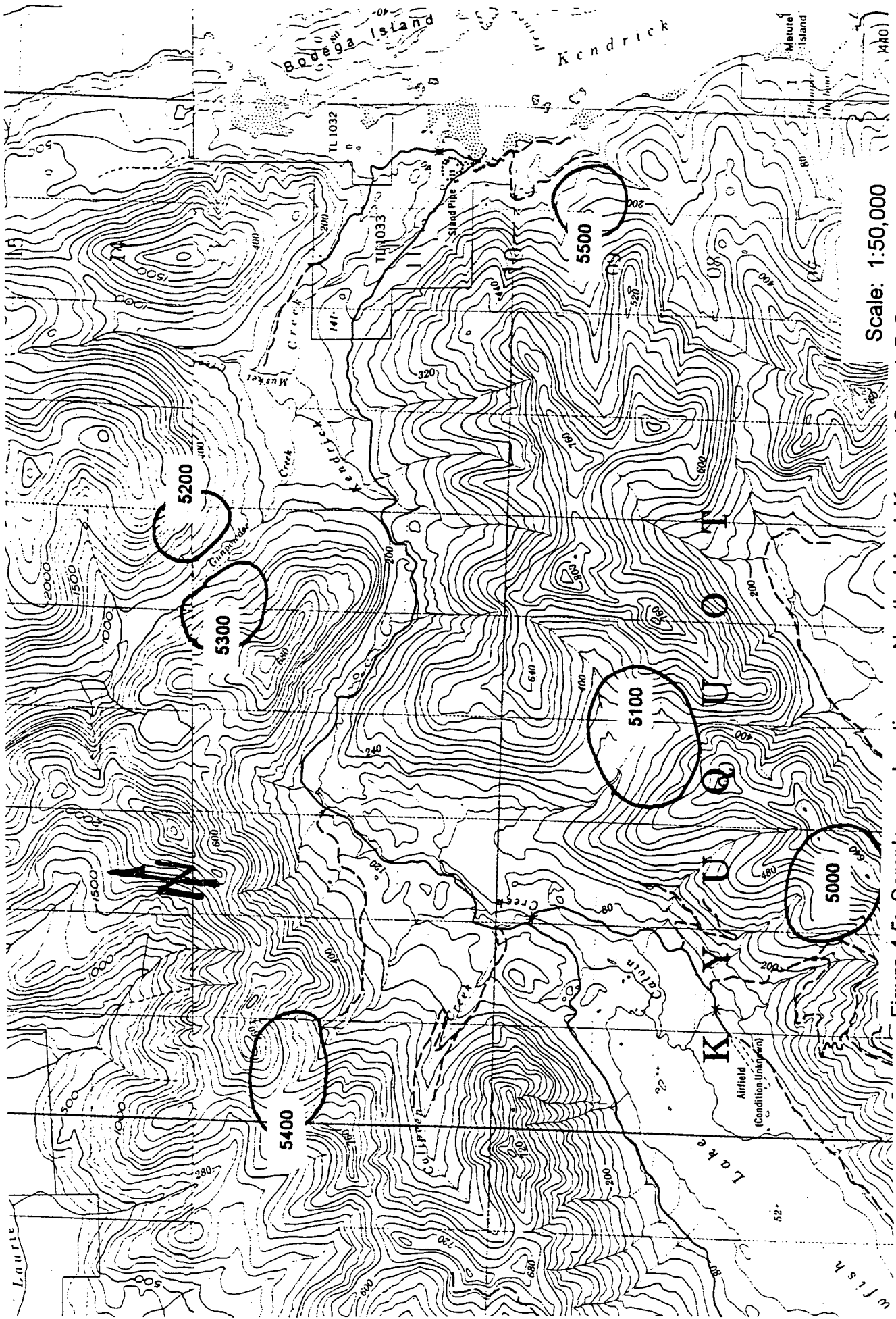


Figure 4.4: Sample area locations for Eve River study area, Vancouver Island, B.C.



Scale: 1:50,000

Figure 4.5: Sample area locations on Nootka Island, Kyuquot Sound, B.C.

Criteria for Selection of Events for Model Development and Back-Analyses

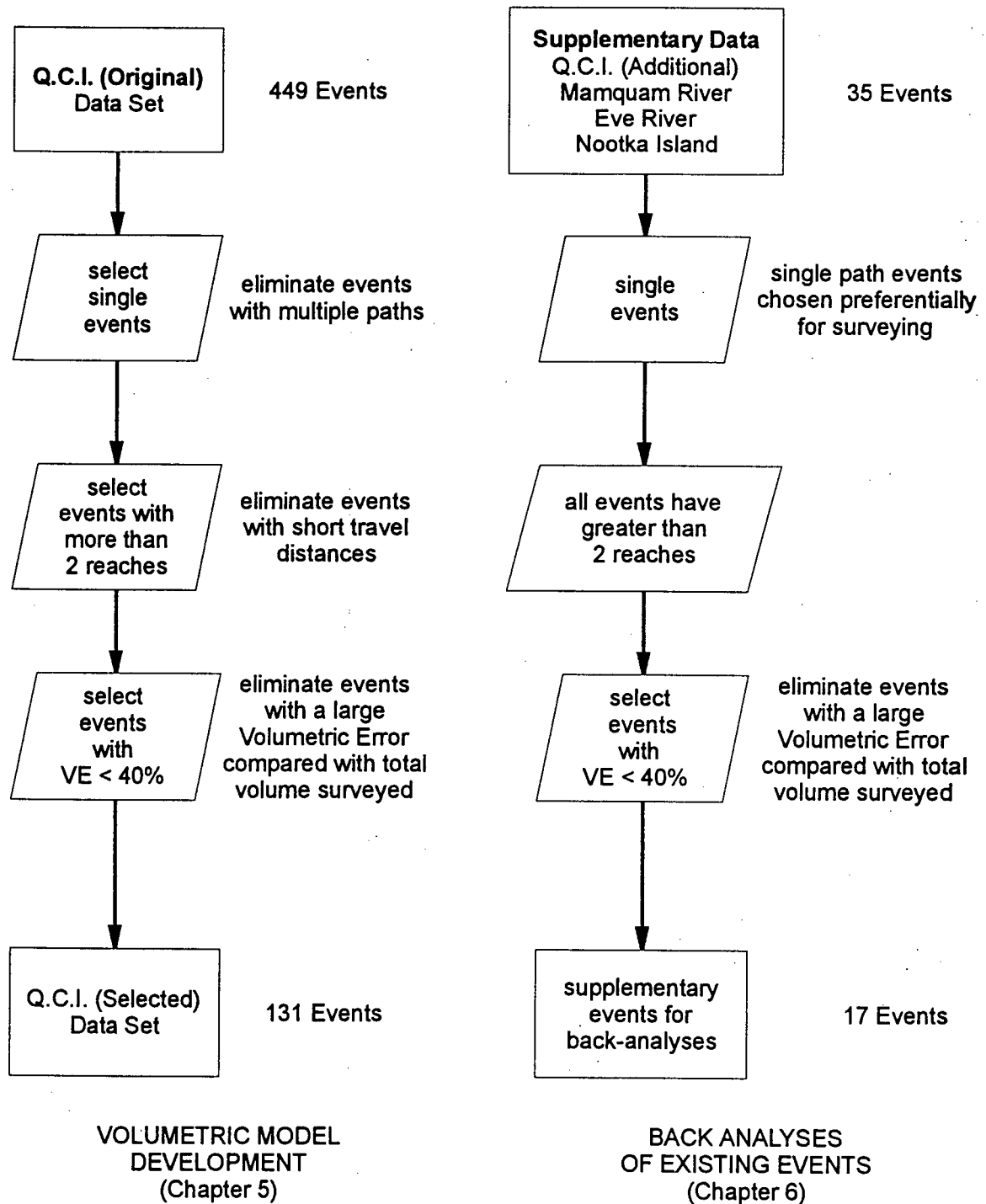
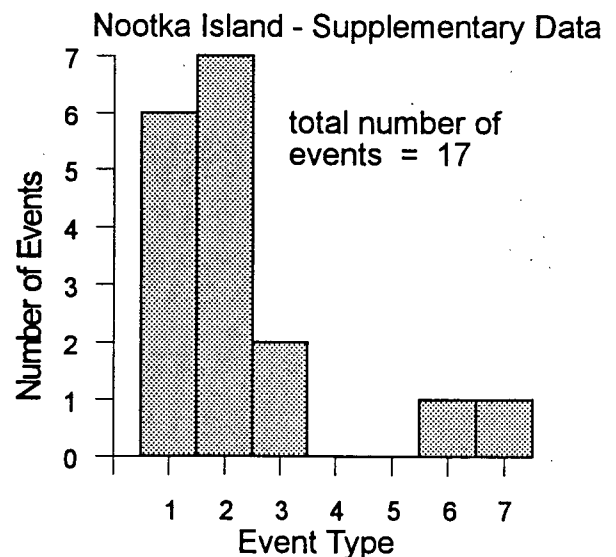
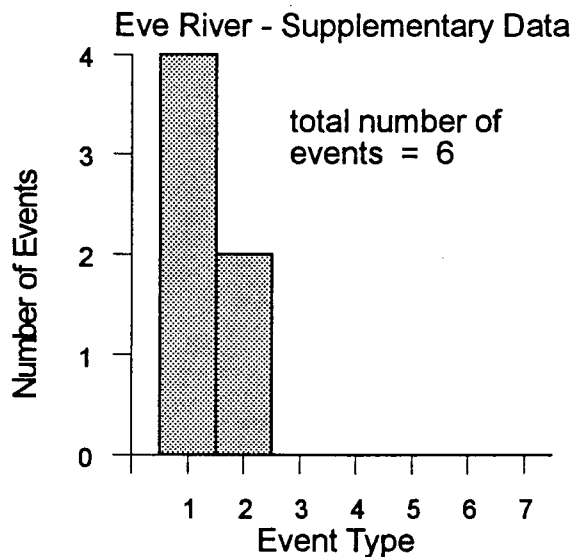
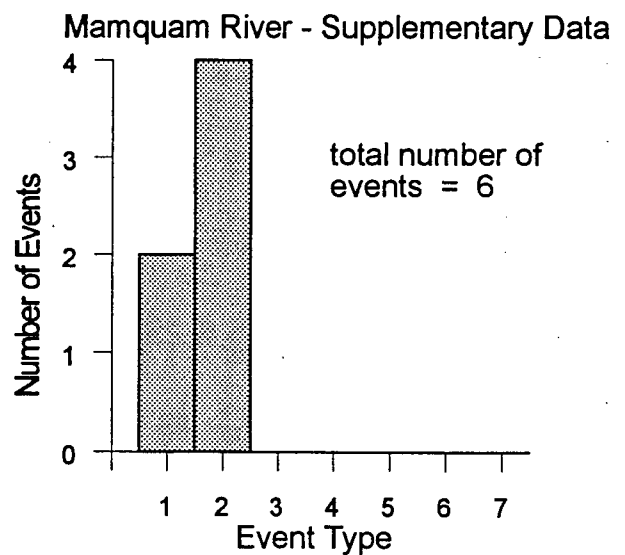
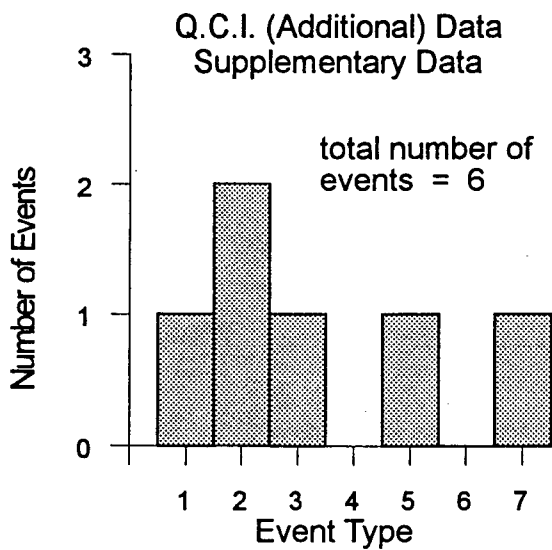
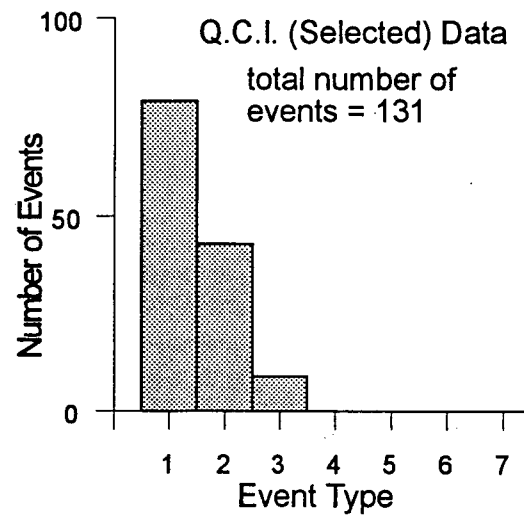
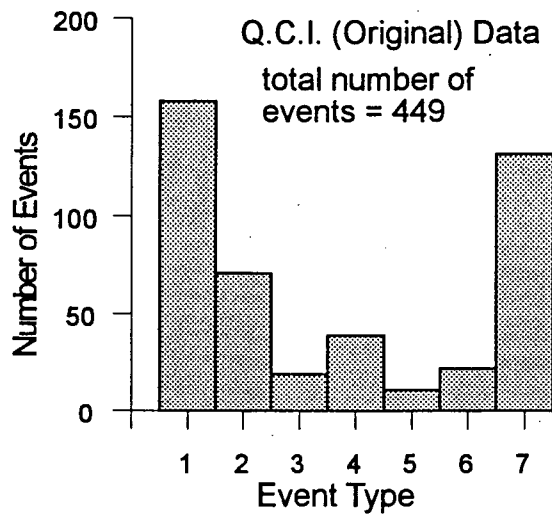


Figure 4.6: Flow chart showing criteria for extraction of events



NOTE: Event Types after Fannin and Rollerson (1993), presented as Table 2.2

Figure 4.7: Event types for surveyed debris flow events

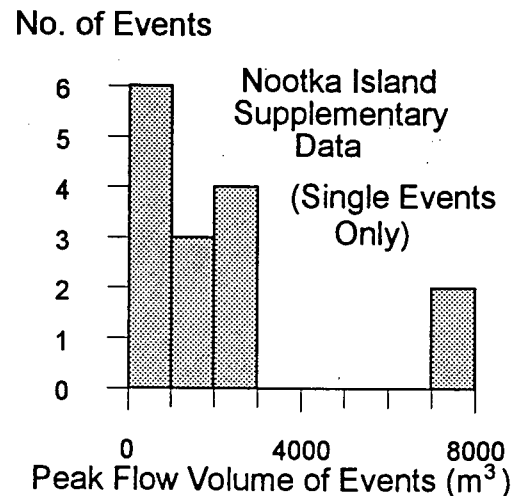
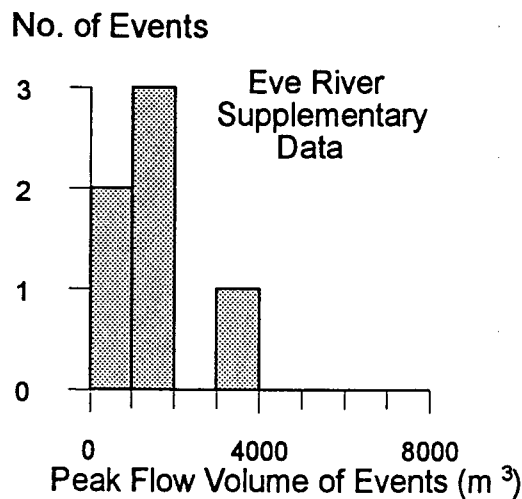
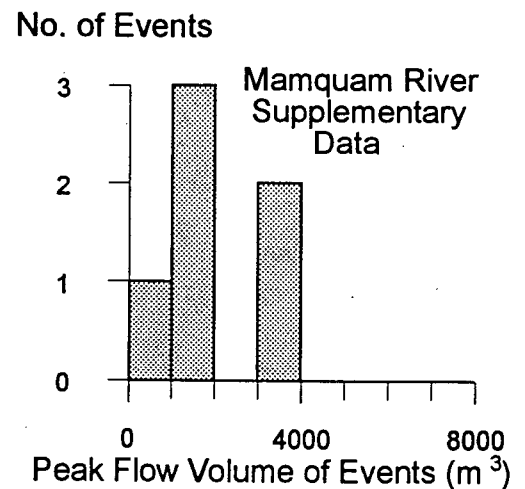
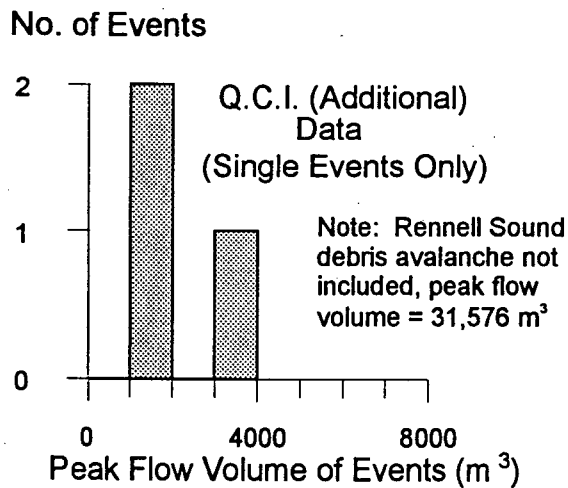
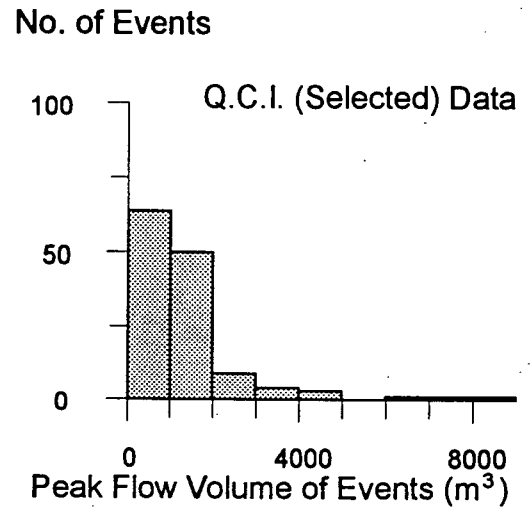
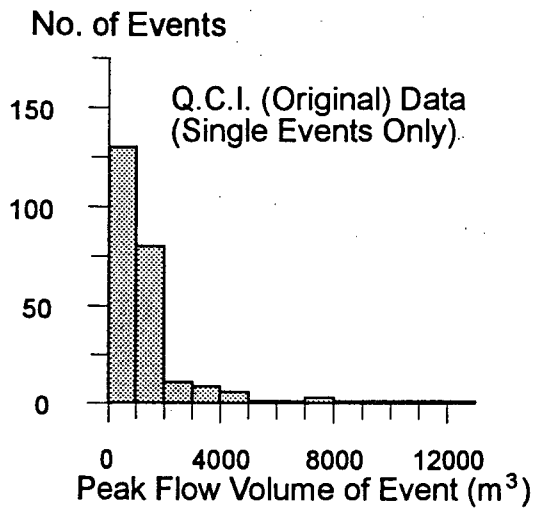


Figure 4.8: Peak flow volume of debris flow events

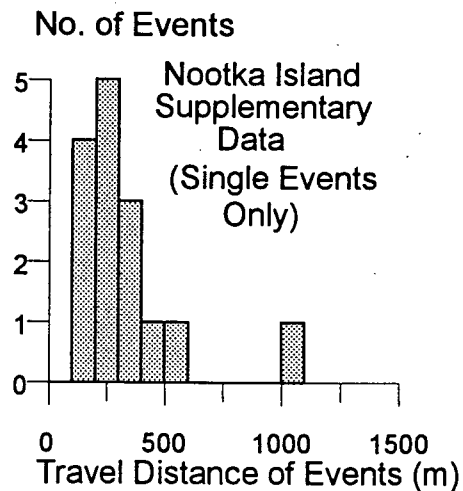
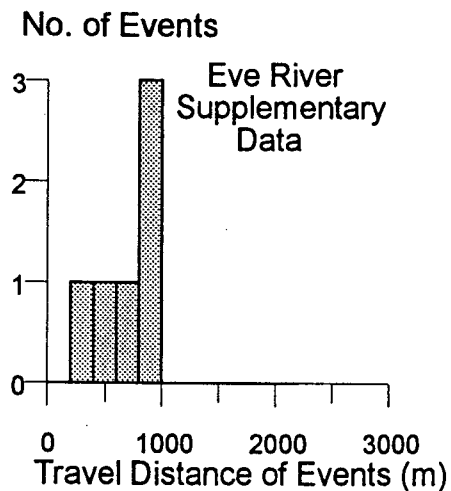
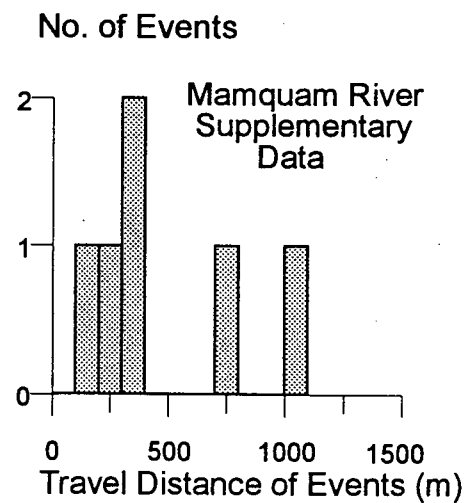
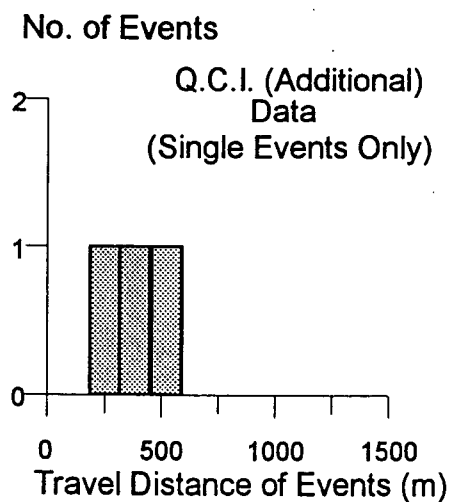
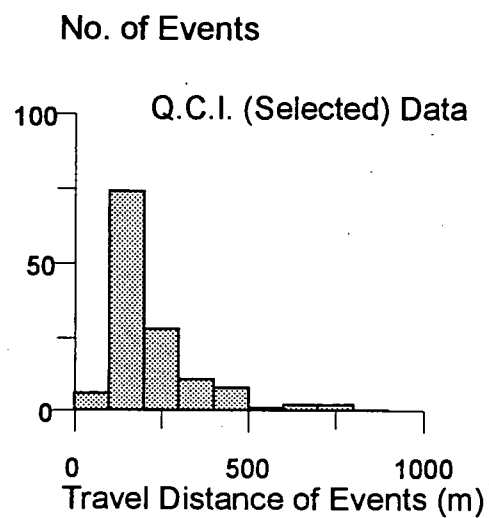
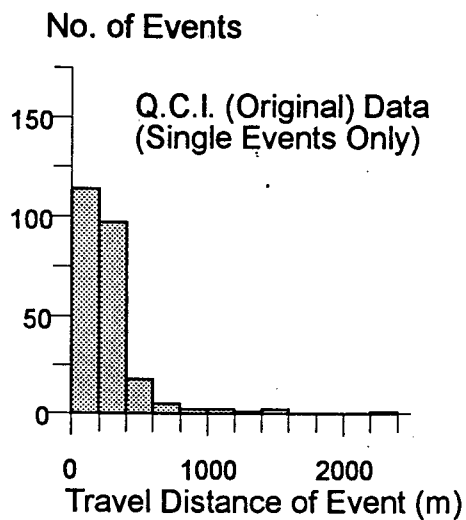


Figure 4.9: Travel distance of debris flow events

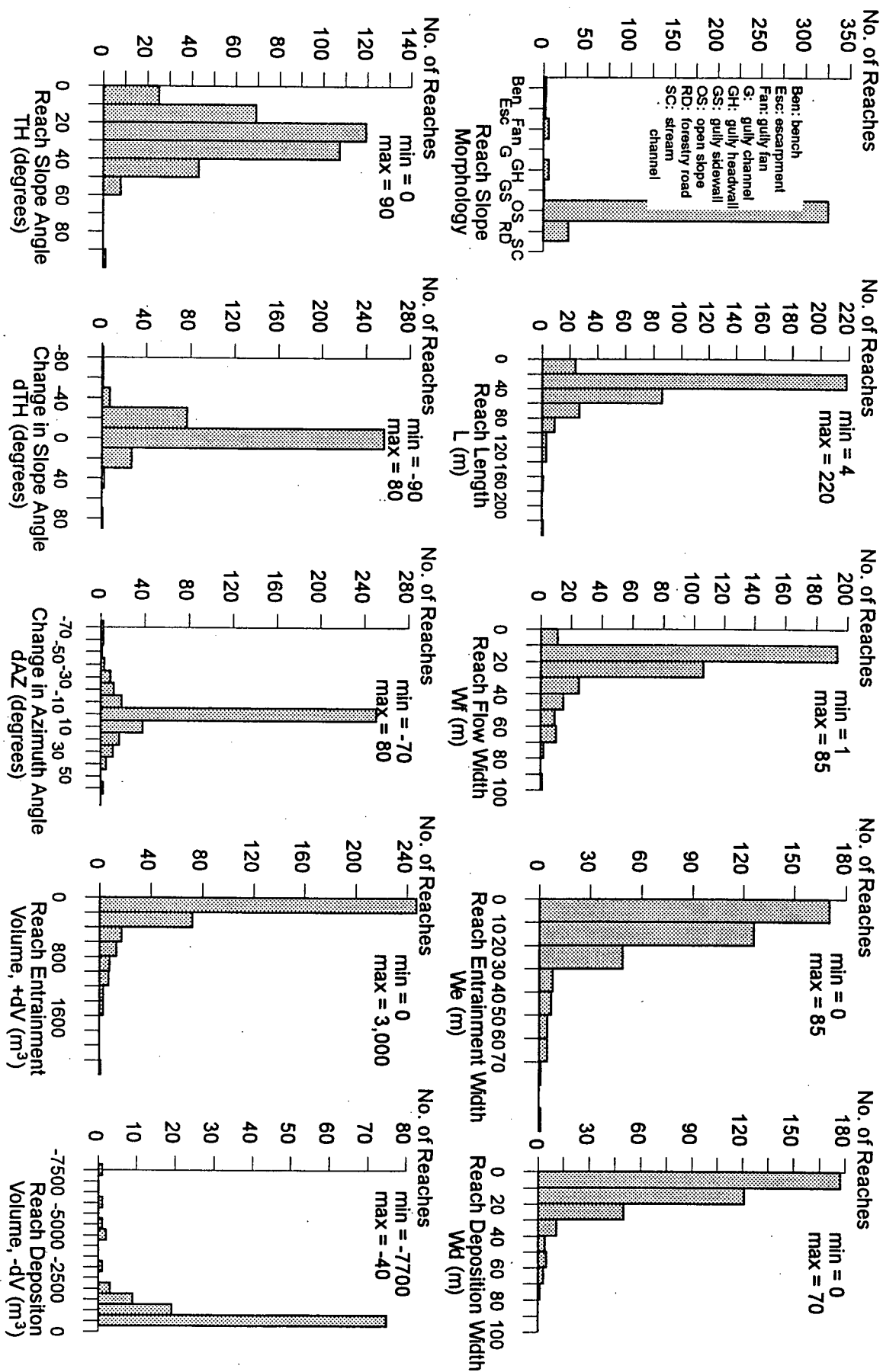


Figure 4.10(a): Reach Characteristics - Unconfined Flow Reaches, Q.C.I. (Selected) Data

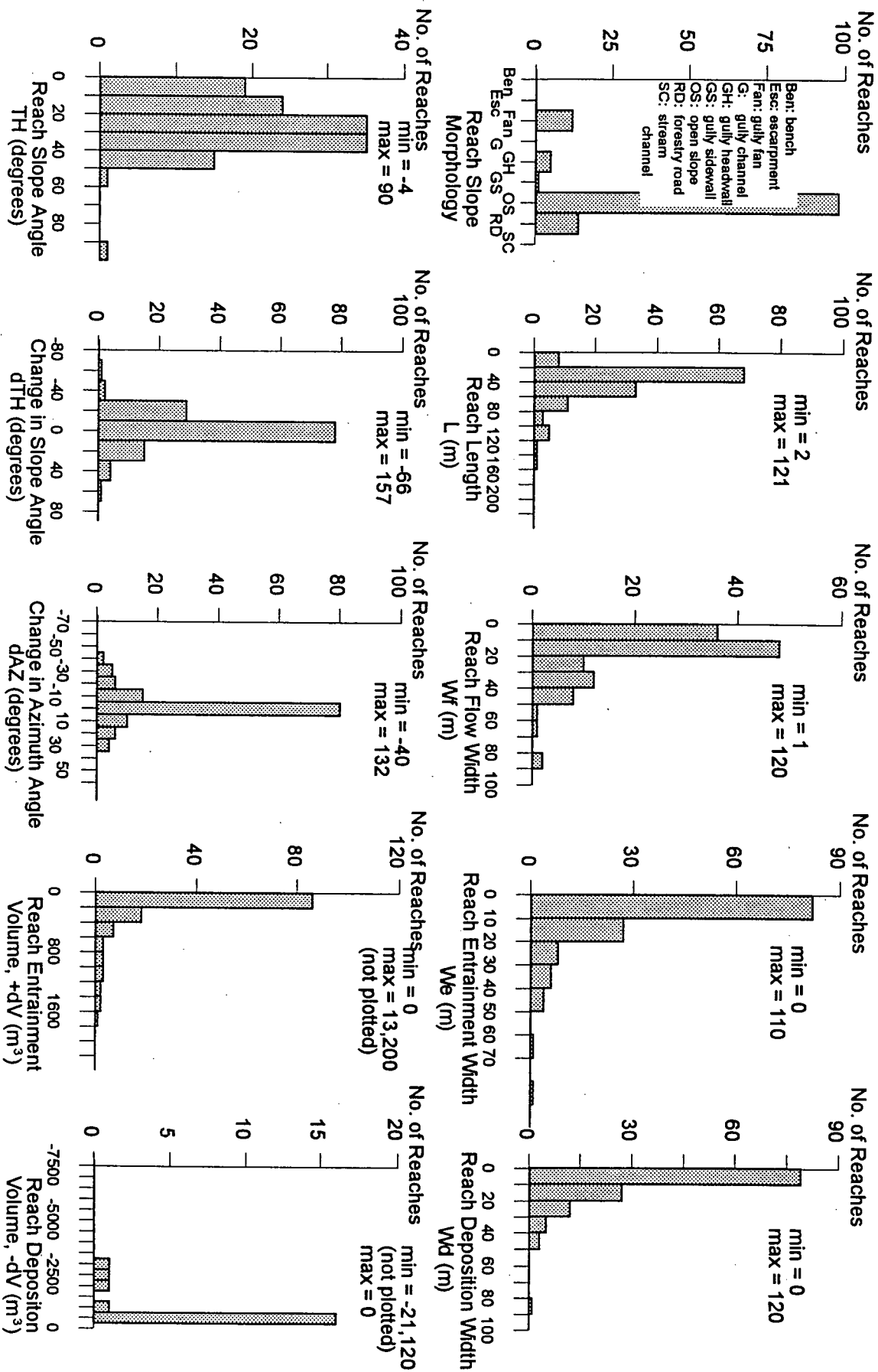


Figure 4.10(b): Reach Characteristics - Unconfined Flow Reaches, Supplementary Data

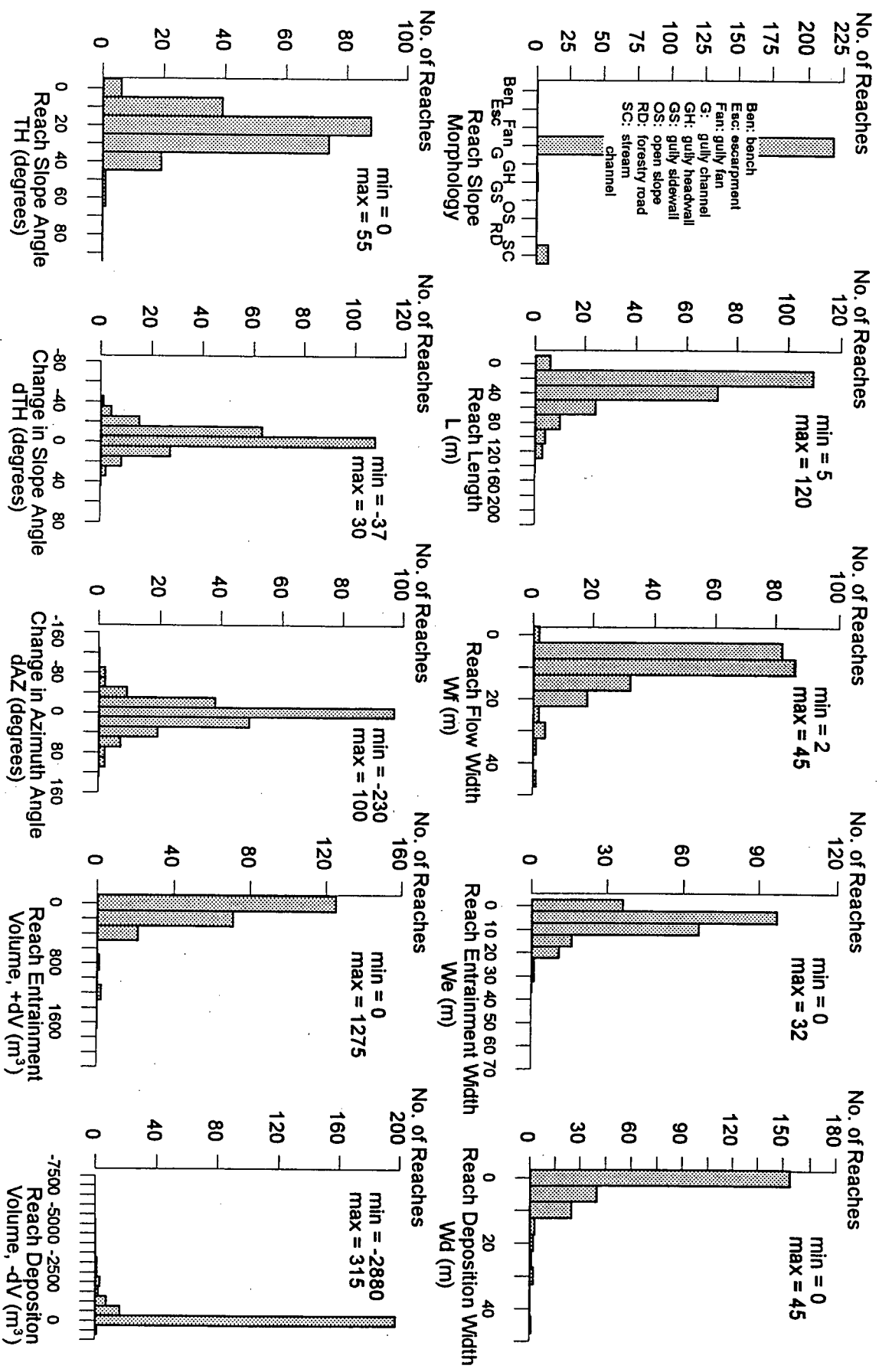


Figure 4.11(a): Reach Characteristics - Confined Flow Reaches, Q.C.I. (Selected) Data

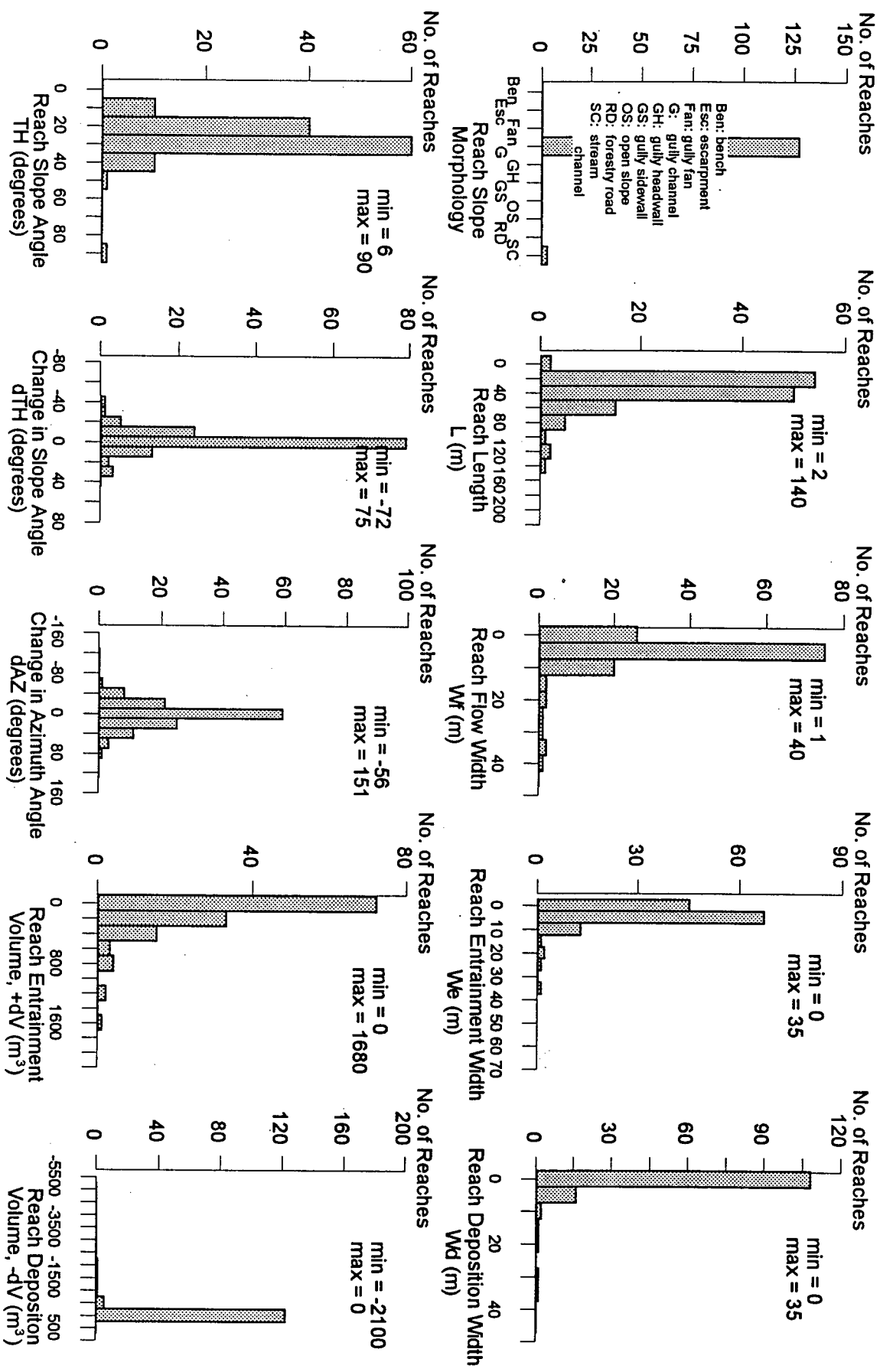


Figure 4.11(b): Reach Characteristics - Confined Flow Reaches, Supplementary Data

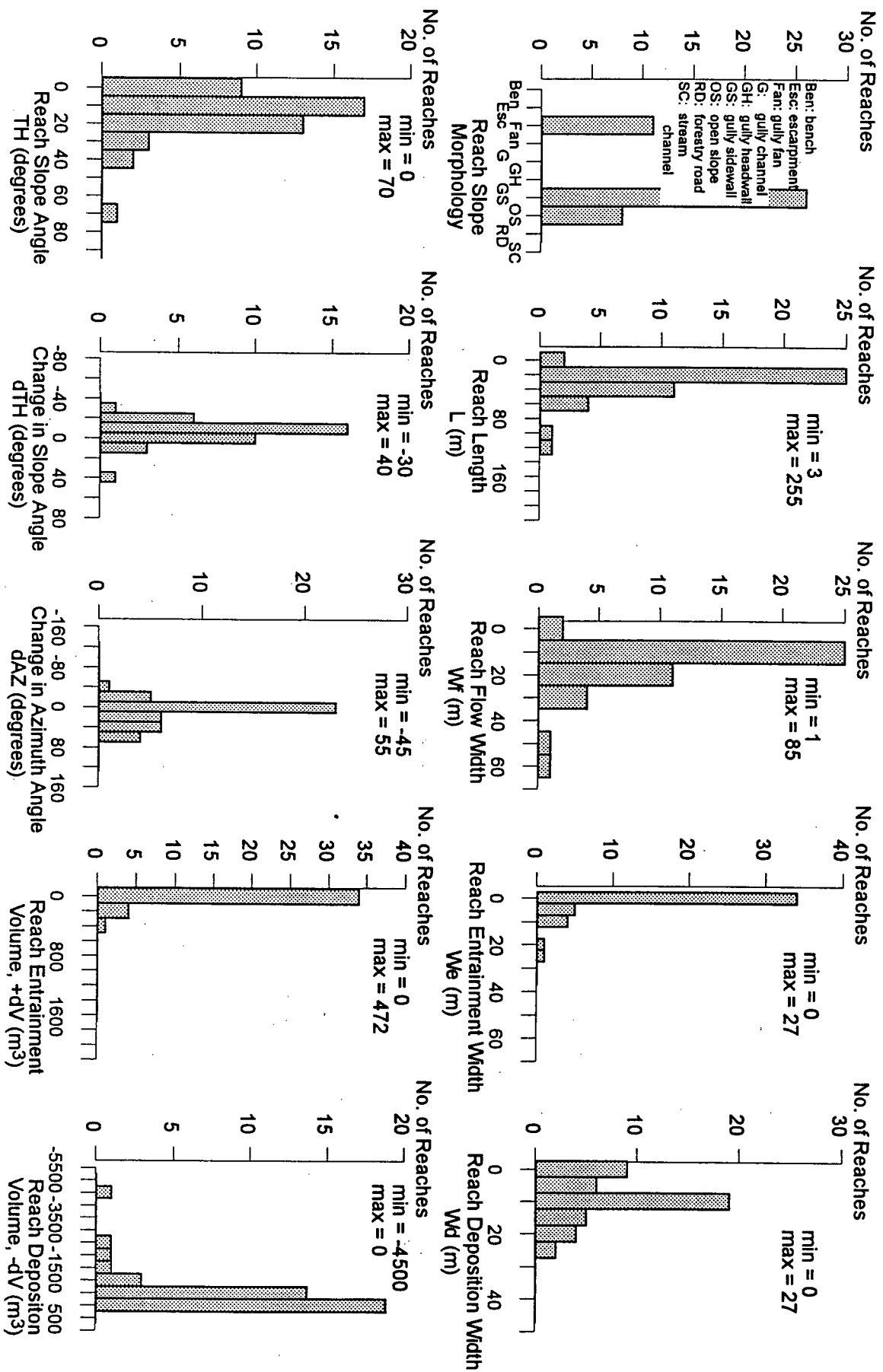


Figure 4.12(a): Reach Characteristics - Transition Reaches, Q.C.I. (Selected) Data

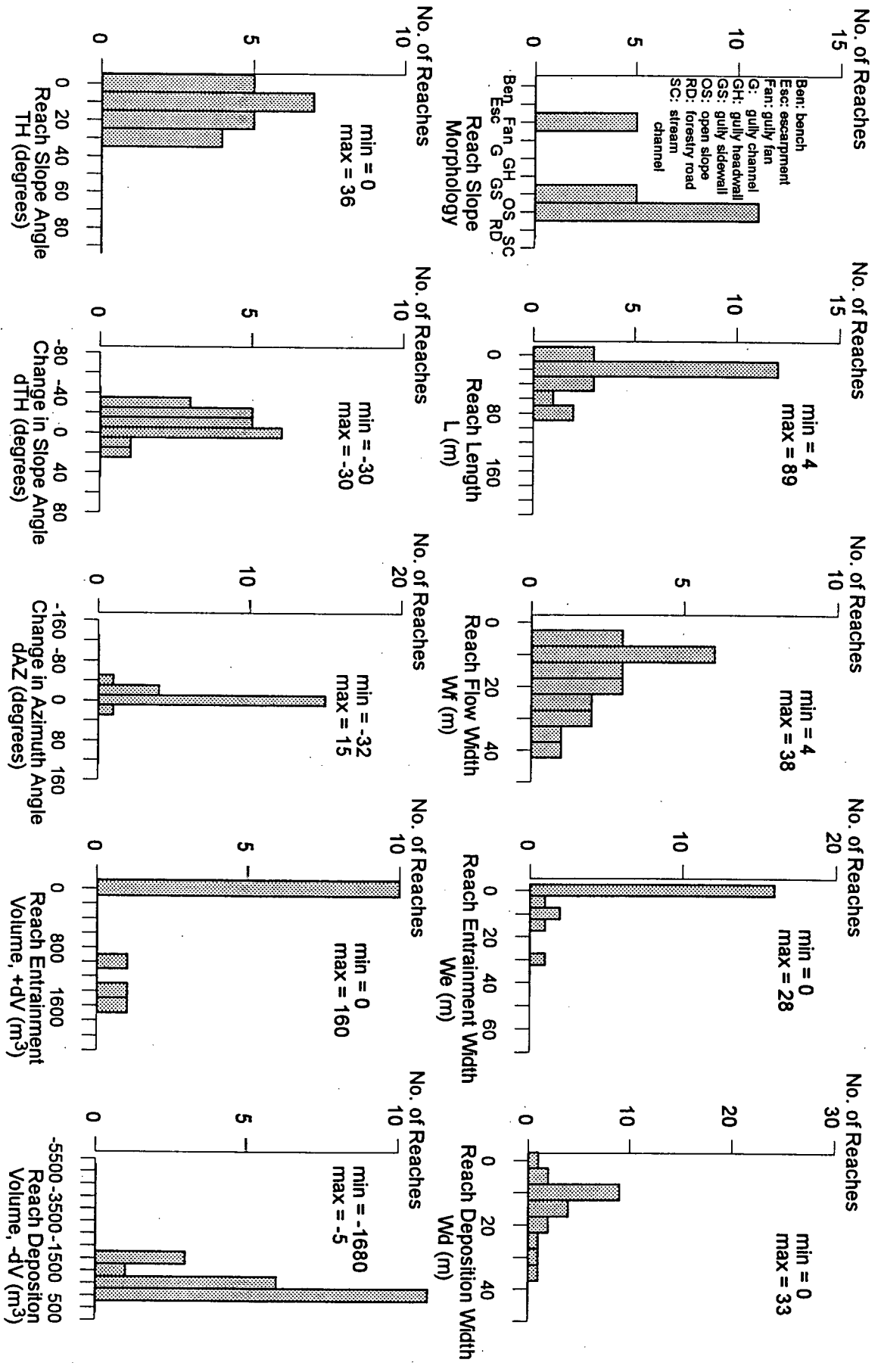


Figure 4.12(b): Reach Characteristics - Transition Flow Reaches, Supplementary Data

Chapter 5 DATA ANALYSIS AND MODEL DEVELOPMENT

The development of multiple regression equations for the back-analysis of debris flow volume behaviour and travel distance is discussed in this chapter. The objectives are to quantitatively relate the volume change along the path to the attributes of each reach, based on the Q.C.I. (Selected) Data. These data, characterized in Chapter 4, are divided into modes of unconfined flow, confined flow, and transition flow. Regression techniques are used to determine the change in debris flow volume for each of the flow modes. These regression equations are used in a Volumetric Model to determine the cumulative peak flow volume and the travel distance for a debris flow event. Back-analyses of debris flow events using the Volumetric Model are presented in Chapter 6.

5.1 Volumetric Model

A framework for the Volumetric Model, Figure 5.1, provides a methodology for determining flow volume along the path, on the basis of volumetric relationships. The framework is summarized as follows:

1. An open slope failure, a roadfill failure, or a gully headwall/sidewall/channel failure initiates a debris flow event with a known volume, V_{init} .
2. Based on attributes of the second reach, the volume of entrainment ($+dV_2$) or deposition ($-dV_2$) is determined and added to V_{init} . Figure 5.2 illustrates schematically how entrainment of material increases the cumulative volume of the debris flow and deposition decreases the flow volume. The resultant flow volume at the end of the second reach is ΣV_3 as the flow enters reach 3. Note that although some reaches showed both entrainment

and deposition in the observed data, this dual mode of volumetric behaviour could not be duplicated using a deterministic framework. Sections 3.3 and 5.3 contain discussions on this dual flow mode.

3. If the sum of calculated deposition volume $-dV$ and ΣV is negative, the flow is considered to deposit all of its volume and the event will terminate within the reach.
4. If the sum of the change in volume and incoming flow volume ΣV is positive, then the debris flow event continues to the next reach downslope.
5. The travel distance of the event is calculated as the sum of the reach lengths through which the flow has passed, as well as the reach in which the flow terminates. The full length of the final reach is conservative estimate of travel distance, since the flow will terminate within the reach.

Use of the Volumetric Model is contingent on the ability to calculate the entrainment volume $+dV$ and deposition volume $-dV$ for each reach, based on the attributes of the reach. Based on reach attributes and volume changes in the Q.C.I. (Selected) Data, empirical equations are developed to compute $+dV$ and $-dV$ for each reach.

5.2 Volume Corrections for Q.C.I. Selected Events

The total entrainment and deposition volumes for the Q.C.I. (Selected) Data should be equal for each event, neglecting minor changes in density which occur as the debris is entrained and subsequently deposited. However, random survey errors in estimating widths and depths of entrainment/deposition as well as systematic rounding errors during surveying can lead to differences in total entrainment and deposition volumes. The total volumes of entrainment (V_e)

and deposition (V_d) are often not equal and there exists some volumetric error (V_{err}) for a debris flow event, shown schematically in Figure 5.2. These can be expressed as

$$V_e = \sum_{i=1}^n (+dV_i) \quad [5.1]$$

$$V_d = \sum_{i=1}^n (-dV_i) \quad [5.2]$$

$$V_{err} = V_e - V_d \quad [5.3]$$

where $+dV_i$ and $-dV_i$ are the entrainment and deposition volumes along the travel path, divided into n reaches.

The correction of the entrainment and deposition volumes for each reach of an event must be carried out to ensure conservation of volume is satisfied for the debris flow event, before regression analyses are carried out. Two options for volume correction of the Q.C.I. (Selected) Data are: assigning an equal part of V_{err} to each reach of the event; or assigning a portion of V_{err} to each reach in proportion to the observed volume change in the reach. Assigning an equal part of V_{err} to each reach along the travel path would lead to volumes being added to reaches where only a minimal volume change was observed. However, reaches with large magnitudes of entrainment or deposition volumes are likely to be associated with proportionately larger errors than reaches with small volume changes. Therefore, the second option was chosen to best reflect the potential errors in the data. Assuming that V_e and V_d contribute equally to V_{err} , the following equations were derived for correction of the volumes (Figure 5.2):

$$+V_{corr} = -0.5 \cdot \left(\frac{+dV_i}{V_e} \right) \cdot V_{err} \quad [5.4]$$

$$-V_{corr} = +0.5 \cdot \left(\frac{-dV_i}{V_d} \right) \cdot V_{err} \quad [5.5]$$

where $+V_{corr}$ is the correction to the measured entrainment volume of reach i ; $+dV_i$ is the measured volume of entrainment in reach i ; and V_e is the total entrainment volume measured over the length of the debris flow. These definitions are analogous for variables in the deposition volume correction, $-V_{corr}$ (equation 5.5). The corrected entrainment volume for each reach is the sum of $-V_{corr}$ and $+dV_i$, while the corrected deposition volume is the sum of $-V_{corr}$ and $-dV_i$. After the volume corrections are applied, the volumetric error is zero.

These equations were applied to the Q.C.I. (Selected) Data to correct reach volumes prior to regression analyses. Note that in cases where there was a recorded volume of zero entrainment or deposition in a reach, these values remained as zero after the correction since $+V_{corr}$ or $-V_{corr}$ are equal to zero. This approach recognizes that during a field survey, it is often evident whether there has been entrainment or deposition in any given reach, but often the magnitude cannot be estimated accurately. Also, in the case of debris torrents with more reaches of entrainment than deposition, a larger proportion of the error is placed on the deposition volumes, which accounts for the likely greater errors associated with the measurement of deposition fan depth and width relative to the errors in the gully channel. Complete descriptions of debris flow survey methods and possible observations indicative of entrainment and deposition are contained in the first two sections of Chapter 3.

5.3 Response and Predictor Variables for Regression Analyses

Regression analysis techniques are well-suited to developing empirical relationships between predictor (independent) variables and response (dependent) variables. From the regression analysis techniques outlined in Wiesberg (1985), the first step in developing a regression

model is to select the response and predictor variables from the data. These choices must be made with a physical understanding of the phenomena in question.

At this point it is important to distinguish between the occurrence and magnitude of entrainment and deposition processes. Occurrence refers to whether a process, either entrainment or deposition, occurs within a given reach of the debris flow path. Magnitude refers to the volume amount of entrainment or deposition within the reach. As shown in Figure 3.3 and discussed in Section 3.3, a large number of zero values are present in the survey data which indicate the non-occurrence of a process within a given reach. These data are used for the single events in the larger Q.C.I. (Original) Data to partition the Q.C.I. (Selected) Data to determine the occurrence of entrainment / deposition processes based on slope morphology and slope angle, as discussed in Section 5.3.3. Regression analyses, discussed in the remainder of this section, are used to develop empirical relationships to determine the magnitude, or amount, of entrainment or deposition within a reach if it is assumed to occur.

The occurrence of both entrainment and deposition in a single unconfined reach, termed dual mode flow in Section 3.3, is not duplicated in the Volumetric Model. Early attempts to model the net change in cumulative flow volume along the path proved unsuccessful. This result is likely because the deterministic framework of the Volumetric Model dictates that if dual mode flow is to be considered, then dual mode flow must be present for each reach. Since dual mode flow is present in only about 35% of the unconfined flow reaches, then requiring dual mode flow causes an error in the other reaches. Thus, dual mode flow was not considered for the Volumetric Model and instead the data were partitioned to best reflect actual flow behaviour (Section 5.3.3). However, dual mode flow is subsequently incorporated using simulation techniques in the probabilistic model UBCDFLOW as discussed in Chapter 7.

5.3.1 Response Variables

Based on the discussion of the framework for the Volumetric Model in Section 5.1, it is apparent that the volume change through a reach of a debris flow travel path is the response of the flow to the attributes of the reach through which it passes. Indeed, flow volume change has been the response variable used by previous researchers (Takahashi *et al*, 1992; Cannon, 1993). Characterization of the Q.C.I. (Selected) Data in Chapter 4 has shown the volume change in a reach due to entrainment and deposition can best be determined separately and the results summed to determine the net volume change, rather than determining a single net volume. The calculation of a single net volume assumes that the same predictor variables have the same emphasis in governing both entrainment and deposition, but has nonetheless been used by Cannon (1993) and others.

Flow confinement, or slope morphology, of a reach for a debris flow event was shown in Chapter 4 to have a considerable influence on the volume of entrainment or deposition which occurred within a reach. Consequently, reaches with flow modes of unconfined flow, confined flow, and transition flow were separated for analysis. For each flow mode, the volumes of entrainment ($+dV$) and deposition ($-dV$) are chosen as the response variables for regression analyses. Full correlation tables are presented in Appendix C for the response variables and each of the possible predictor variables discussed below.

5.3.2 Choice of Predictor Variables

Possible predictor variables which can be utilized in regression analyses can be described as either measured variables or derived variables. Measured variables include reach attributes which describe reach geometry, such as length L , widths of entrainment W_e and deposition W_d , slope angle TH , as well as the changes in slope angle dTH and azimuth angle dAZ relative to

the upslope reach. Other variables include the incoming flow volume ΣV , and the bend angle function BAF which are indicative of the scale of the event and the potential for momentum transfer from the upslope reach. The relationships between possible predictor variables and response variables for the 615 reaches in the Q.C.I. (Selected) Data are discussed below.

Note that since the model can accommodate only one reach length L for the flow path, the W_e and W_d are assumed to be averages for the entire length of the reach. This is in slight contrast to some observed cases, where the lengths of entrainment and deposition differ along the same reach (see Section 3.2 for a discussion). For the purposes of regression analyses, the different lengths are used in calculating the volumes of entrainment or deposition in the reach. Thus, the different lengths are used in developing the regression equations for entrainment and deposition along the reach.

5.3.2.1 Unconfined Flow

Figure 5.3(a) shows the scatterplots of the possible predictor variables against reach entrainment volume, $+dV$, for 343 reaches with unconfined flow in the Q.C.I. (Selected) Data. All of the plots show unstable variances and poor correlation, although some trends are evident for L , W_f , and W_e . The scatterplot of W_d and $+dV$ shows virtually no correlation, which is expected since reaches with a W_d of zero usually have a W_e greater than zero (and vice versa). Also, there is also a significant number of reaches with an entrainment volume of zero, as these reaches showed no evidence of entrainment during the field survey. In these cases, minor amounts of entrainment may have occurred prior to deposition in the reach, but were not detected or not considered significant.

From the plot TH against $+dV$ in Figure 5.3(a), low values of $+dV$ were recorded for TH less than about 20° and greater than about 45° . For slopes less than 20° little entrainment is observed as the typical volume change behaviour is deposition. For angles greater than 45° , the material on the entrained on the slope was likely a very thin veneer of colluvial soils (weathered bedrock or weathered till), providing less material available for entrainment relative to intermediate slopes.

Figure 5.3(b) illustrates the response of deposition volume, $-dV$, with the possible predictor variables for unconfined flow reaches in the Q.C.I. (Selected) Data. As with many of the scatterplots in Figure 5.3(a), there are many data with a zero value for the response variable. Of particular note is the plot of TH against $-dV$, which has a large number of zero values for deposition, likely due to the large variation in moisture conditions of the flow on unconfined slope morphology since undersaturated flows will deposit on steeper slope angles than supersaturated flows. This variation in water content of the flow is very difficult to determine from forensic observations, and not appropriate in cases where the survey is carried out some years after the event occurred. In addition, for TH greater than 25° , most of the values of $-dV$ are near zero but some cases of deposition were observed. Many of these cases are associated with travel over a very flat reach, such as a forest road, and then onto a steep reach. The flatter reach will cause most of the momentum of the flow to be lost, and even though the flow continues downslope it will likely deposit the remainder of the flow volume on a relatively steep reach downslope of the road. In the scatterplots of $-dV$ against changes in slope angle and azimuth angle (Figure 5.6a), it is apparent that dTH is only a marginal predictor of $-dV$ while dAZ has little influence on $-dV$.

5.3.2.2 Confined Flow

Figures 5.4(a) and 5.4(b) show the scatterplots of the possible predictor variables against the response variables $+dV$ and $-dV$ for 221 confined flow (gully) reaches in the Q.C.I. (Selected) Data. From the correlation values for these plots, the predictor variables are marginally better correlated to the response variables than for unconfined flow, and the trends observed are similar to the data for unconfined flow reaches. A visual comparison yields similar results, when the zero values along the horizontal axis are ignored. The better correlation is likely a result of flow through confined reaches having less variation in water content, compared to unconfined flow reaches, and thus the confined flow events will likely behave in a rheologically similar manner.

The predictor variables L and W_e both show a comparable correlation with $+dV$ as for unconfined flow, but still a nonconstant variance is apparent. One possible explanation for the marked amount of variation for these data is the variation in the availability of debris material for entrainment along the reach length. For TH , entrainment of material occurs for reaches of virtually all slope angles with a high amount of variability.

Figure 5.4(b) shows scatterplots of deposition volume $-dV$ against possible predictor variables. With the exception of W_d , the other possible predictor variables show relatively little correlation with $-dV$. The scatterplot of $-dV$ against W_f shows that several reaches with nonzero values of W_f have a negative volume (nonzero $-dV$), possibly caused by the volume correction assigning a large negative value to a reach where there was a minimal entrainment volume. Reaches with slope angles greater than 15° show only minimal deposition of material.

5.3.2.3 Transition Flow

Scatterplots of the possible predictor variables against reach entrainment and deposition volume are shown in Figure 5.5 (a) and 5.5(b) for 39 reaches with confined to unconfined flow transitions. These reaches are located where gully channels emerge onto fans or where forest roads intersect gully channels. Since these cases are rare, there are fewer data compared to the confined flow and unconfined flow reaches.

Figure 5.5(a) shows entrainment volume $+dV$ plotted against the potential predictor variables. The variables L and W_e show reasonably good visual correlation with $+dV$, (ignoring the zero values of $+dV$). However, the data are sparse, with only about 12 out of 39 transition flow reaches showing evidence of entrainment. Many of these cases are likely marginally stable road fills which crossed gullies and were entrained as the debris torrent passed over the road surface, or very large debris flows which exit a gully channel with considerable momentum and are capable of entraining colluvial material stored at the apex of the debris fan. The outliers above 30° are likely due to the deposition of very small flows on roadfills where much of the flow volume has stopped on the road above.

Deposition of debris flow material is very common in transition reaches, with 37 out of 39 transition reaches exhibiting deposition. The potential predictor variables L , W_f and W_d show a reasonable correlation to the $-dV$ (Figure 5.5b). However, there are large variances in the response at higher ends of the predictor ranges, particularly for W_f and W_d against $-dV$. The plot of $-dV$ against TH indicates that all reaches below 18° show predominantly deposition behaviour. These nonconstant variances again suggest the need for transformation of the predictors.

5.3.2.4 Derived Variables

Derived variables considered as potential predictors include change in slope angle dTH , change in azimuth angle dAZ , incoming flow volume ΣV , and the bend angle function BAF . Figure 3.1(b) shows how dTH , dAZ , and ΣV are determined. The BAF is expressed as

$$BAF = \cos(dTH) \cdot \cos(dAZ) \cdot \ln(\Sigma V) \quad [5.6]$$

where dTH and dAZ denote the change in slope angle and change in azimuth angle, respectively. Note that the use of the cosine of the change in slope angle is used by Takahashi and Yoshida (1979) to quantify momentum losses for debris flow events as the flow emerges from a gully channel and encounters an abrupt change in bed slope angle; inclusion of dAZ incorporates additional changes in path azimuth which can also cause momentum losses.

These derived variables are considered potential predictors since changes in path orientation can affect the amount of momentum lost by the flow between reaches, and incoming flow volume can determine the amount of momentum transferred between reaches, as smaller flows are not able to transfer momentum effectively (Hung *et al*, 1984). The bend angle function combines dTH , dAZ , ΣV as a measure of momentum losses due to changes in path orientation, relative to incoming flow volume. Note that the BAF differs from the junction angle as evaluated by Benda and Cundy (1990). Their evaluation was carried out to determine if changes in the potential path would cause an event to terminate; however, the BAF is related to the momentum flux between reaches, with smaller BAF values indicating a significant change in path direction and/or a small incoming flow volume, both of which favour deposition in a transition reach or an unconfined reach.

For unconfined reaches, Figure 5.6(a), dTH appears to have only a minimal effect on the entrainment of material. It is likely that the availability of material is more important than

changes in slope angle. Although large negative values for dTH may be expected to cause deposition, often the upslope reach is very steep so that even a 20° decrease in TH will still result in a reach with a sufficiently steep slope to entrain rather than deposit material. The change in azimuth dAZ does not appear to have any influence on the entrainment volume, which is to be expected since unconfined flow follows the gradient of the micro-topography on the open slope and directional changes to the flow path likely do not cause a large loss in flow momentum. The plots of ΣV and BAF against $-dV$ shows a reasonable correlation, but other plots show only weak correlations. Figure 5.6(b) shows the derived predictor variables plotted against $-dV$ for unconfined reaches. As for the entrainment data, little correlation is evident between $-dV$ and either dTH or dAZ . There appears to be a reasonable correlation between $-dV$ and ΣV . In transition reaches, Figure 5.6(c), weak correlations are evident between dTH , dAZ and volume change. While there is a reasonable correlation between ΣV and $-dV$, correlations between ΣV , BAF , and $+dV$ volume are weak.

For confined reaches, Figure 5.6(c) has similar non-constant variance trends as observed in the unconfined reaches. However, the correlation coefficients are lower with the exception of the plot of cumulative flow volume against entrainment volume. This is likely due to the fact that larger debris flows usually occur in gully reaches which significant amounts of material available for entrainment. Figure 5.6(d) shows the deposition volumes observed in confined flow reaches in the Q.C.I. Selected Data. Although limited amounts of deposition were observed, many of these were only of minimal amounts when compared to the entrainment volumes. (See Section 5.3.3, below).

Figures 5.5(e) and 5.5(f) show entrainment and deposition volumes plotted against the derived variables. In Figure 5.5(e), the sparse character of the data are evident and no trends are

discernible. In Figure 5.5(f), some trends are evident in the data, particularly for BAF , dTH , and ΣV vs $-dV$. However, the relationship between dTH and $-dV$ is non-linear and transformation is necessary if dTH is to be used in the development of a regression equation for transition flow. Also, the BAF variable is derived from dTH and ΣV , and the scatterplot of BAF vs $-dV$ shows trends which are present in the plots of dTH and ΣV vs $-dV$.

5.3.3 Partitioning of Q.C.I. (Selected) Data Based on Slope Angle

Analysis of the relationship between reach slope angle, TH , and volume change behaviour ($+dV$, $-dV$) in the Section 5.3.2 has shown a large amount of variability. This variability is likely due to differences in water content of the debris flow for deposition processes and availability of material for entrainment processes. To establish a more definite relationship between TH and volume change behaviour, all reaches from the single path events in the Q.C.I. (Original) Data were used to determine the typical flow behaviour on various slope angles. The typical volume change behaviour is described as the dominant process of either entrainment or deposition for a reach with a given TH .

Debris flow events with a single travel paths from the Q.C.I. (Original) Data were chosen for analysis of volume change behaviour. These events are of types 1,2,3, and 7 as classified by Fannin and Rollerson (1993). Since these events, most of which are not in the Q.C.I. (Selected) Data, have a normalized volumetric error (VE) of greater than 40%, the magnitude of the volume change for each reach cannot be used with confidence in regression analyses. However, whether entrainment or deposition was evident for a particular reach should be related to the slope angle of the reach.

Examination of the occurrence of entrainment only, entrainment and deposition, as well as deposition only reaches within these data for various TH provides a basis for determining the typical volume behaviour occurrence. A filter was applied to reduce the number of reaches exhibiting both entrainment and deposition, since there is a significant proportion of these present. The filter grouped reaches which showed only a minor amount of entrainment or deposition together with reaches which demonstrated the dominant volume behaviour. The threshold for the filter was arbitrarily set at 20%, to ensure all the reaches which are grouped as both entrainment and deposition have significant amounts of both entrainment and deposition. For example, a reach with 18 m³ of deposition and 100 m³ of entrainment would be termed as an "entrainment only" reach after filtering. Figure 5.7 shows the occurrence of entrainment, entrainment and deposition, and deposition reaches for the complete range of TH values present in the Q.C.I. (Original) Data.

For unconfined flow there is some variability in the range of 11° to 35°, there is a bound below 19° where over 80% of the reaches are deposition only or deposition and only small proportions of the reaches showing entrainment only. The data for TH equal to 0° and 1° are likely the result of travel over forestry roads in the upper portion of the travel path, with unstable roadfill entrained or incorporated into the flow. Entrainment only is dominant in reaches with slopes of about 30° or more, with approximately 80% of the reaches showing signs of entrainment only. Slopes above 38° show predominantly entrainment only behaviour.

Data for confined flow show that a similar lower bound exists for entrainment behaviour. At slope angles of about 10° about 60% of the reaches show at least some entrainment behaviour. At slope angles below 6°, deposition is dominant. For reaches with transition flow, deposition is dominant for slope angles up to about 18°; and other reaches showed both entrainment and

deposition up to 22° . There are limited data above 22° to characterize flow behaviour.

Deposition in transition reaches is expected at this location in the flow path, since these reaches are where the flow often encounters both a flatter slope angle and a loss of confinement.

To summarize, examination of the larger number of the events in the Q.C.I. (Original) Data provides more information on the typical volume change response related to slope angle. For unconfined flow, slope angles of 18° or less show a significant trend towards deposition. Slope angles above 18° and below 24° show some cases of dual mode behaviour (both entrainment and deposition). Reaches in this slope range may have either entrainment, or deposition, or both as volume change responses in these intermediate angles. Entrainment is dominant on unconfined reaches with slopes of 24° or above, although cases of deposition are present in the data. For confined flow, entrainment is the dominant process down to slope angles of 6° or less; however, most of the reaches below 10° are stream channels and are not included in this study. Transition flow has deposition as the dominant flow response up to slope angles of 18° , with some entrainment observed for reaches on slopes up to 22° . These bounds indicate the slope angles for typical flow behaviour and are used to partition the reach data in the Q.C.I. (Selected) Data. Reach data within these bounds were used for data transformations and regression analyses. Table 5.1 shows the partitioning of the Q.C.I. (Selected) Data for regression analyses based on the volume behaviour occurrence for a larger data set, the Q.C.I. (Original) Data.

Although there is some overlap in slope range, and hence the potential for dual mode behaviour, for unconfined flow, it should be noted that after regression analyses the application of the regression equation for deposition is restricted to 18° . This range is expanded to 24° for purposes of probabilistic modelling in Chapter 7.

Table 5.1: Partitioning of Q.C.I. (Selected) Data based on slope angle and flow mode

Flow Mode	Volume Behaviour (Dominant)	Applicable Slope Angle Range	
		Minimum	Maximum
Unconfined Flow	deposition	0°	24°
	entrainment	19°	55°
Confined Flow	entrainment	10°	55°
Transition Flow	deposition	0°	22°

5.3.4. Transformations of Variables

Based on the scatterplots of the response and predictor variables discussed in Section 5.3.2, transformations of both the response variables and predictor variables are required for all flow modes. Transformation of the response variable is typically carried out to ensure normality (normal distribution) of the response variable after regression, a key assumption in linear regression analyses. For the predictor variables, normality is less important, but the predicted response (sum of predictor variables multiplied by coefficients) should be normal with a stable variance (Weisberg, 1985). A number of transformations for variables are possible, and the most common are listed in Weisberg (1985). Only successful transformations which were used in the regression analyses of this study are reported.

In general, natural logarithmic transformations proved to be the most beneficial to increase the normality of the response variables and stabilize the variances of the predictor variables.

Logarithmic transformations are commonly used for analysis of geographic and geologic phenomena, since often the values of variables cannot go below zero or some other physically-based lower bound. Log transformations were also beneficial in that any zero values of $+dV$ or $-dV$ resulted in computation errors and thus were eliminated from the data for the regression analyses. These zero values are due to the non-occurrence of either entrainment or deposition

in a reach, and thus bias many scatterplots of the untransformed data (Section 5.3.2). Note that the elimination of the zero data values will not bias the regression equations, since these values indicate the absence of a given processes, and are used to determine the occurrence of entrainment or deposition within a reach (see Section 5.3, above).

5.3.4.1 Unconfined Flow

Entrainment response for unconfined flow is shown in Figures 5.8(a) and 5.8(b). Based on Figure 5.7 and 5.3(a), the lower bound of the entrainment for unconfined flow taken as 19° . Data for slope angles 19° and greater were examined and broken into two groups, since at slope angles above 30° there are lesser amounts of material entrained on steeper slopes as shown by the negative correlation on slopes greater than 30° , evident in Figures 5.8(a) and 5.8(b).

For data with a reach slope between 19° and 29° inclusive, Figure 5.8(a) plots the transformed entrainment volume $\ln(+dV)$ and the predictor variables. In comparison to Figure 5.3(a), a greater correlation results for the transformed data, particularly for $\ln(L)$. Moreover, the logarithmic transformations have stabilized the variances in the scatterplots. The correlation with reach slope TH has also improved, based on a visual assessment. However, based on these scatterplots the predictor variables dTH and dAZ appear to correlate poorly with $\ln(+dV)$ or $\ln(-dV)$ as shown in Figure 5.11(a).

Figure 5.8(b) shows scatterplots for $\ln(+dV)$ and the transformed response variables for unconfined flow data with TH 30° or greater. These scatterplots show a marked increase in the stability of variance in comparison to Figure 5.3(a), with $\ln(L)$, $\ln(W_p)$, and $\ln(W_e)$ reasonably well correlated with the response $\ln(+dV)$. The non-constant variance has almost been

eliminated for TH and $\ln(+dV)$ as compared to Figure 5.3(a); however, a significant amount of scatter remains in the data.

For deposition of unconfined flow, Figure 5.8(c) contains scatterplots of the transformed response $\ln(-dV)$ plotted against transformed predictor variables with TH less than or equal to 24° , based on Figure 5.7. The similarity of the plots for $\ln(W_p)$ and $\ln(W_d)$ against $\ln(-dV)$ indicate that most of these reaches exhibit deposition. The transformation used on the variables $-dV$, L , W_e , and W_d improves the correlation significantly with the response $-dV$ as compared to Figure 5.3(b). A visual comparison of Figures 5.3(b) and 5.8(c) shows the correlation between TH and $\ln(-dV)$ improves both due to the $-dV$ transformation and the exclusion of data on slope angles greater than 25° .

5.3.4.2 Confined Flow

Figure 5.9 shows the transformed variables for entrainment by confined flow on reaches with slopes of 10° or greater. Deposition reaches are not included in further analyses since these cases were observed to be only about 17% of the cases, based on confined flow reaches in the Q.C.I. (Original) Data. Log transformations were applied as for the unconfined flow data. The large number of data points in the Q.C.I. (Selected) Data serves to reinforce the correlations between the predictor variables and $\ln(+dV)$. The lack of correlation between TH and $\ln(+dV)$ may indicate that the amount of material available for entrainment is more important than the slope angle of the confined reaches.

5.3.4.3 Transition Flow

The transformed variables for transition reaches for confined flow to unconfined flow are plotted in Figure 5.10. As is the case with confined and unconfined flow, log transformations

lead to increased normality of $\ln(-dV)$ and increased correlation in W_f and W_d . The transformation has also stabilized the variances of the predictors, especially L . Reach slope angle TH appears to be better correlated with the response variable $\ln(-dV)$ than for the other flow modes.

5.3.4.4 Derived Variables

Scatterplots showing the transformed volume change and the transformed derived variables are presented in Figures 5.11 through 5.13 for the Q.C.I. (Selected) Data. Logarithmic transformations were used for the ΣV data, and the absolute value transformation has been used on dAZ since changes in azimuth for either direction (left or right) should have an equal influence on the flow.

For entrainment, Figures 5.11(a) and (b) show that the transformations lead to a more constant variance in the predictor variables ΣV and BAF , as well as an increased correlation for reaches with TH between 30° and 55° . For deposition on slopes of 24° or less, Figure 5.11(c), the variance in both ΣV and BAF is markedly decreased, and correlations increased, as a result of the transformations.

Confined flow data in Figure 5.12 show only a weak correlation between $\ln(\Sigma V)$ and $\ln(+dV)$, but a moderate correlation between $\ln(-dV)$ and $\ln(\Sigma V)$. No significant correlations are evident between dTH , dAZ , and both $\ln(+dV)$ and $\ln(-dV)$. For transition flow, Figure 5.13 shows good correlations for $\ln(\Sigma V)$ and BAF with $\ln(-dV)$, but weak correlations between dTH and dAZ . These results suggest that $\ln(\Sigma V)$ and BAF may be suitable predictors for $\ln(+dV)$ and $\ln(-dV)$.

5.4 Regression Analyses

The entrainment and deposition behaviour of a debris flow within a given reach can be separated into occurrence and magnitude. The preceding section has been used to determine the occurrence of entrainment or deposition within a reach of an event, based on the slope morphology and the slope angle of the reach. Regression analyses are used to develop empirical relationships which can calculate the amount of entrainment or deposition within a reach.

Regression analyses were carried out on the partitioned and transformed Q.C.I. (Selected) Data, as discussed previously, to develop regression equations. These regression equations are used in the back-analysis of debris flow events carried out in Chapter 6.

Multiple regression was carried out on predictors chosen as a result of best subset regression analyses, using the computer program MINITAB (Version 8, 1991). This technique develops numerous regression equations for a given group of data and reports the results in terms of the coefficient of determination R^2 , the standard deviation in the response variable, and Mallows' $C-p$. Mallows' $C-p$ is a criteria for selection of a subset of predictors based on the mean square error of the fitted values of the subset model (Weisberg, 1985). The use of $C-p$ as a selection criterion allows for comparison of several subset models. Weisberg (1985) recommends that subset models with a $C-p$ value approximately equal to the number of predictors, and models which minimize the standard deviation in the response, will be good models. The examination of subsets of predictors as a alternative to stepwise regression techniques is suggested by Weisberg (1985) in situations where there is an intuitive relationship between one or more of the predictor variables and the response. Further, Weisberg (1985) cautions that stepwise

regression techniques can produce regression equations using subsets of predictors which have no physical basis and produce equations with biased, and possibly artificially large, values of R^2 .

Table 5.2 presents a summary of the regression equations and the results of diagnostics tests. Section 5.4.1 through 5.4.3 contain a discussion of the diagnostic tests used in the regression analyses for each flow mode. The regression parameters and diagnostic tests in Table 5.2 include the number of data points n used in the regression, the number of outliers n_{out} deleted from the partitioned data group (on the basis of a t -test), the standard deviation of the regression equation s , the coefficient of determination R^2 , as well as the p -value and the F -test results for analysis of variance. The scatterplots for normal scoring of the residuals (errors) of the regression are also described to demonstrate the normality of the residuals.

5.4.1 Unconfined Flow

For unconfined flow, deposition was found to dominate on reaches with slope angles of 24° or less. One regression equation was developed from these data:

$$\ln(-dV) = -0.514 - 0.988 \ln(W_d) - 0.101 BAF - 0.731 \ln(L) + 0.0155 TH \quad [5.7]$$

where $-dV$ is the modelled deposition volume in the reach, W_d is the width of deposition in the reach, BAF is the bend angle function, L is the length of the reach, and TH is the slope angle.

The coefficient R^2 is 0.882 indicating a good, reasonably precise relationship as determined by the predictors. The p -value of the regression indicates that the regression is significant at the 0.01 level, and the value of 216 for the F -test indicates that most of the variance in the

Table 5.2: Summary of Regression Equations

FLOW MODE	FLOW BEHAVIOUR (Note 1)	REGRESSION EQUATION	n	n _{out}	s	R ²	p-value	F-Test	Q-Q Plot
UF	Deposition 0° ≤ TH ≤ 24° (Note 2)	$\ln(-dV) = -0.514 - 0.988\ln(W_d) - 0.101BAF - 0.731\ln(L) + 0.0155TH$	121	6	0.3755	0.882	0.001	216.41	linear
	Entrainment 19° ≤ TH ≤ 29°	$\ln(+dV) = 1.13\ln(W_d) + 0.787\ln(L) - 0.0636\ln(\sum V_i)$	91	3	0.6244	0.758 Note 3	0.001	(90.74) Note 4	linear, some steps
	Entrainment 30° ≤ TH ≤ 55°	$\ln(+dV) = 0.728 + 1.31\ln(W_d) + 0.742\ln(L) - 0.0464TH$	73	9	0.6026	0.793	0.001	87.92	linear, minor steps
CF	Entrainment 10° ≤ TH ≤ 55°	$\ln(+dV) = 0.344 + 0.851\ln(W_d) + 0.898\ln(L) - 0.0162TH$	170	21	0.4377	0.763	0.001	185.57	linear
TR	Deposition 0° ≤ TH ≤ 22° Note 5	$\ln(-dV) = -1.54\ln(W_d) - 0.90\ln(L) + 0.123BAF$	36	3	0.3203	0.946 Note 3	0.001	(192.82) Note 4	linear, some steps

Notes:

- Slope ranges indicate the slope range for the data used in the regression analyses.
- Equation applied on slopes of 18° or less to prevent dual flow mode in deterministic model (entrainment and deposition in same reach)
- Coefficient of Determination calculated after Kozak and Kozak (1995).
- F-test value given for the full model regression (intercept included), and intercept proved to be insignificant in both cases.
- Equation applied on slope angles of 20° in cross-validation testing.

regression equation is small compared to the variance in the data. The linear Q-Q plot (Normal Score Test) indicates that the variance in the regression errors is normally distributed over the predictor interval under consideration.

For entrainment, two regression equations were developed due to the apparent nonlinear relationship between TH and $+dV$ for slope angles 19° or greater, from Figures 5.11(a) and (b). The first, for reach slope angles of 19° to 29° , is

$$\ln(+dV) = 1.13 \ln(W_e) + 0.787 \ln(L) - 0.0636 \ln(\Sigma V) \quad [5.8]$$

where $+dV$ is the modelled entrainment volume in the reach, W_e is the width of entrainment in the reach, L is the length of the reach, and ΣV is the incoming flow volume to the reach. From the diagnostic tests of this equation, the low t -test value of the constant during regression analyses led to the elimination of the constant for the regression. Although MINITAB does not calculate the R^2 for the regression equation, a value was calculated using the procedure described in Kozak and Kozak (1995). Using this method, the R^2 value is calculated to be 75.8%. The low t -ratio calculated as part of the full model (intercept included) provides justification for elimination of the regression constant and use of the no-intercept model. The overall linear trend in the Q-Q plot indicates that the residuals from the regression are essentially normally distributed. Only three outliers were deleted during the regression procedure, indicating the relatively tight grouping of data in this set.

A second equation was developed for entrainment on unconfined slopes of greater than 29° . This equation is

$$\ln(+dV) = 0.728 + 1.31 \ln(W_e) + 0.742 \ln(L) - 0.0464 TH \quad [5.9]$$

where the predictor variables are as described for equation 5.8, and TH is the slope angle of the

reach. During regression analyses, the diagnostic tests indicated that this regression equation is statistically significant, and the R^2 value is 0.79. The Q-Q plot is essentially linear, attesting to the overall normality of the residuals from the regression, and hence the normality of the $\ln(+dV)$.

5.4.2 Confined Flow

A total of 172 data points were used to develop the regression equation for confined flow in gully channels. From the best regression test, three variables were found to produce a regression equation with an acceptable R^2 and $C-p$. The final form of the regression equation is

$$\ln(+dV) = 0.344 + 0.851\ln(W_e) + 0.898\ln(L) - 0.0162TH \quad [5.10]$$

The R^2 value for this equation is 76.3%, after 21 outliers were deleted from the data on the basis of the t -ratio from the regression analyses. The p -values and the F -test results, as well as the Q-Q plot, show this regression is statistically significant with an acceptable variance.

Note that although TH did not have a particularly strong correlation to $\ln(+dV)$ in Figure 5.9, it does appear to be a useful predictor in the regression equation, based on the best subset regression analyses and the t -ratio. This phenomenon is likely due to an added variable effect whereby the usefulness of TH as a predictor is a result of its interaction with the other predictors used during regression.

5.4.3 Transition Flow

For transition reaches, data on slopes of 22° or less were used in the regression analysis. One equation was developed using predictor variables of W_d , L , and BAF :

$$\ln(-dV) = -1.54\ln(W_d) - 0.90\ln(L) + 0.123BAF \quad [5.11]$$

The constant for the equation was eliminated during analysis on the basis of a *t*-test. Consequently, there is no R^2 value calculated by MINITAB, but the R^2 value calculated using the method of Kozak and Kozak (1995) is 94.6%. The high *t*-ratio in the diagnostic testing of the full model regression equation (including the intercept) provides evidence that the constant is not significant in the final regression equation (Appendix C).

5.5 Cross Validation of Regression Analyses

The Q.C.I. (Selected) Data were separated into two subsets for cross-validation of the regression equations discussed in Section 5.4. Validation of the regression analyses for predicting volumes of debris flow entrainment and deposition within a reach is important to ensure the Volumetric Model can accurately predict volume changes, and thus the cumulative flow volume and travel distance, along the event path.

Events from the Q.C.I. (Selected) Data were separated into a construction set, the Q.C.I. (S-C) Data, and a validation set, the Q.C.I. (S-V) Data. Table C2 (Appendix C) contains a list of the events in the construction and validation sets. The events, after being separated into sets of unconfined flow events and confined flow events, were ordered from most accurate to least accurate in terms of normalized volumetric error. Reach data from every second event was chosen to create the Q.C.I. (S-C) Data. These data were used to create the subset regression equations and are tested using events in the Q.C.I. (S-V) Data. Weisberg (1985) contains a discussion of cross-validation methods for applied regression analyses.

The regression equations developed from the Q.C.I. (S-C) Data are presented in Table 5.3. Generally, the quality of the subset regression equations was poorer than the regressions

carried out in Section 5.4. This deterioration can likely be attributed to the use of fewer data points, which did not reinforce trends observed in earlier regressions. This slight shift in the emphasis of some predictors caused the values of the coefficients to change in magnitude, but not in sign during regression. The diagnostic tests on the subset regression equations indicate that all the regressions are satisfactory, although the R^2 value for the confined flow equation indicates some lack of precision for this equation. Regression analyses for the subset equations are contained in Appendix C.

5.5.1 Unconfined Flow

For deposition, Figure 5.14 shows the cross-validation of the regression equation for deposition of unconfined flow. The plots show the regression results before and after the log transformation. The correlation of the predicted values to the corrected values in the Q.C.I.(S-V) Data is 0.845. For these results, a regression equation was developed (not shown) to determine if the relationship between the actual and predicted results is significantly different from the 1:1 correlation line in Figure 5.15. Note that this is equivalent to evaluating the significance of the regression coefficients in comparison to the theoretical values of the intercept equal to zero and the slope equal to unity. On the basis of a t -test for the 0.001 confidence level, the intercept was found to be not significantly different than zero and the slope was found to be not significantly different from unity.

Figure 5.15 shows the results of using the equations 5.13 and 5.14 in the Subset Model to predict entrainment for unconfined flow. The correlation between the log of the predicted values and actual values is 0.743. Significance testing of the regression coefficients of this relationship revealed that the intercept is not significantly different than zero and the slope is not significantly different than unity.

Table 5.3: Summary of Subset Regression Equations (used in Cross-validation Testing)

FLOW MODE	FLOW BEHAVIOUR (Note 1)	REGRESSION EQUATION	n	n_{out}	s	R^2	P-value	F-Test	Q-Q Plot
UF	Deposition $0^\circ \leq TH \leq 24^\circ$ (Note 2)	$\ln(-dV) = -0.424 - 1.18\ln(W_d) - 0.0713BAF - 0.681\ln(L) + 0.0141TH$	59	3	0.4991	0.828	0.001	65.13	linear
	Entrainment $19^\circ \leq TH \leq 29^\circ$	$\ln(+dV) = 1.24\ln(W_d) + 0.788\ln(L) - 0.103\ln(\sum V_i)$	42	2	0.5871	0.783 Note 3	0.001	(46.06) Note 4	linear, some steps
	Entrainment $30^\circ \leq TH \leq 55^\circ$	$\ln(+dV) = -0.10 + 1.19\ln(W_d) + 0.732\ln(L) - 0.0062TH$	38	3	0.8181	0.705	0.001	26.28	linear
CF	Entrainment $10^\circ \leq TH \leq 55^\circ$	$\ln(+dV) = 0.613 + 0.976\ln(W_d) + 0.640\ln(L) - 0.00152TH$	85	4	0.5657	0.562	0.001	35.07	linear, some steps
TR	Deposition $0^\circ \leq TH \leq 22^\circ$ Note 5	$\ln(-dV) = -1.47\ln(W_d) - 1.02\ln(L) + 0.162BAF$	19	1	0.3175	0.961 Note 3	0.001	(126.11) Note 4	linear, some steps

Notes:

1. Slope ranges indicate the slope range for the data used in the regression analyses.
2. Equation applied on slopes of 18° or less to prevent dual flow mode in deterministic model (entrainment and deposition in same reach)
3. Coefficient of Determination calculated after Kozak and Kozak (1995).
4. F-test value given for the full model regression (intercept included), and intercept proved to be insignificant in both cases.
5. Equation applied on slope angles of 20° in cross-validation testing.

5.5.2 Confined Flow

The plot of predicted entrainment volumes against the actual (corrected) volumes for the cross-validation of the confined flow regression equations is shown in Figure 5.16. The correlation for these results is 0.779, which is greater than for the case of unconfined flow. This higher correlation is due to the tighter grouping of the data. It should also be noted that the corrected data is present over a more limited range, which reflects the restricted widths of these reaches. Significance testing of the regression coefficients revealed that the intercept is not significantly different than zero and the slope is not significantly different than unity for the relationship between the observed and corrected results.

5.5.3 Transition Flow

Figure 5.17 shows the results of the cross-validation of the regression equation for transition flow. The predicted volumes of deposition are well correlated for the results, with r equal to 0.811. More test cases would add confidence to this relationship. Significance testing on the regression equation of this relationship determined that there is no significant difference between the intercept value and zero, and the slope of the regression and unity.

5.6 Summary

Debris flow events can be modelled using the volume change behaviour along the travel path of the event. A Volumetric Model is presented to predict the cumulative flow volume of the event and calculate the travel distance. Regression equations are developed to calculate the change in debris flow volume for each reach along the debris flow path as a critical component within the Volumetric Model.

Regression analyses are carried out using the Q.C.I. (Selected) Data, a group of debris flow events within the Q.C.I. (Original) Data, described in Chapter 4. The change in volume for each reach of these events is corrected to ensure that the total entrainment and total deposition volumes balance over all the reaches of an event. The change in entrainment or deposition volume over the length of a reach are used as the response variables in separate regression analyses for each flow mode. Measured predictor variables include the reach length, width of entrainment, width of deposition, and slope angle. The derived variables of incoming flow volume and bend angle function are also used as predictor variables and quantify the size of the debris flow entering the reach and the amount of momentum lost due to changes in the direction of flow, respectively.

Cross-validation of the regression equations was carried out by developing subset regression equations using about half of the events in the Q.C.I. (Selected) Data. The subset regression equations are developed in a form identical to the regression equations created from the Q.C.I. (Selected) Data using the same predictor variables for each flow mode. Diagnostic tests for the regression analyses indicate that the subset regression equations are statistically significant, yet less precise, than the equations developed using the Q.C.I. (Selected) Data. The subset regression equations were successfully validated by predicting entrainment and deposition volumes for the other half of the Q.C.I. (Selected) Data not included in the regressions. Significance testing of the regression relationships (best fit lines) between the corrected values and predicted values showed that the intercepts of the equations are not significantly different than zero and the slopes are not significantly different than unity at the 0.001 level.

The regression equations developed using the Q.C.I. (Selected) Data set are used to back-analyze debris flow volume behaviour and predict the travel distance using the Volumetric Model. The results of the back-analyses are presented and discussed in Chapter 6.

Framework for Volumetric Model

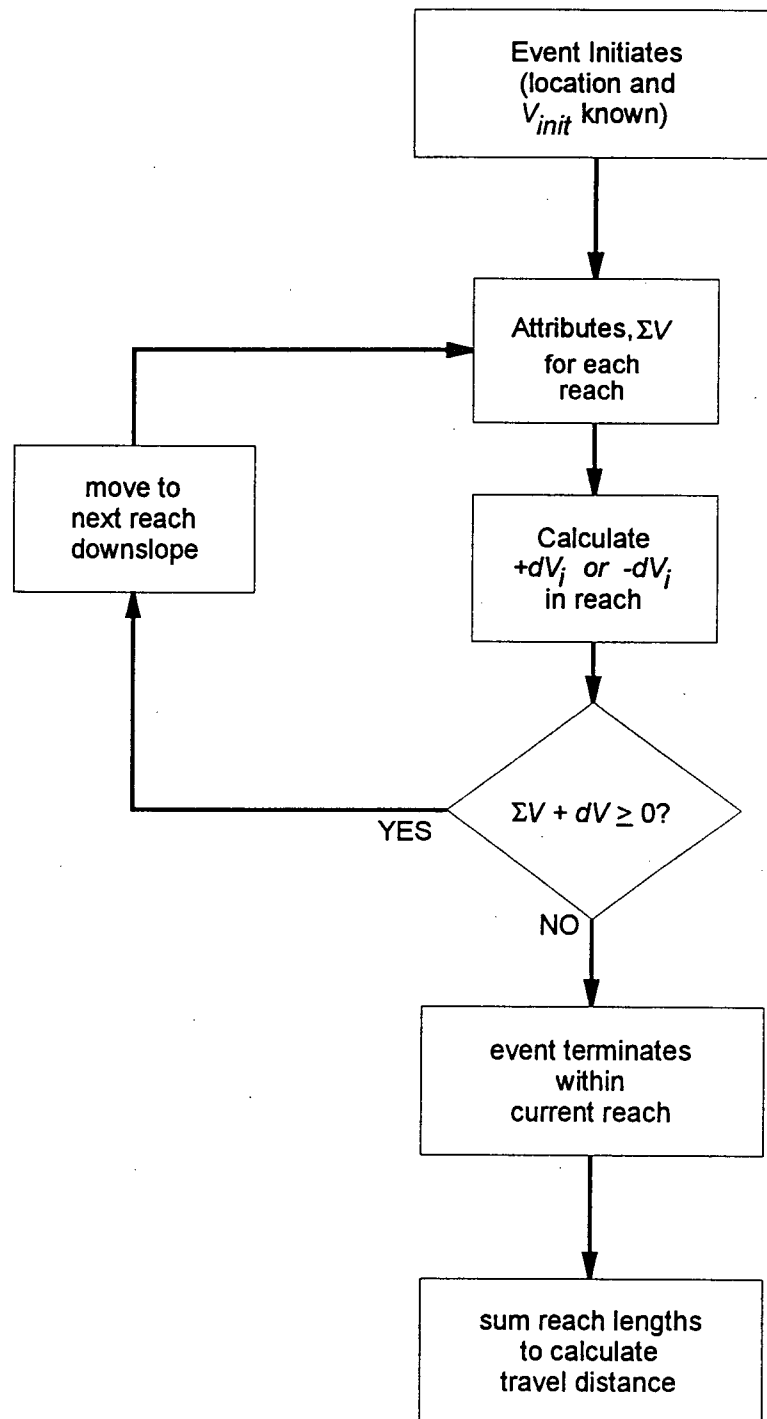
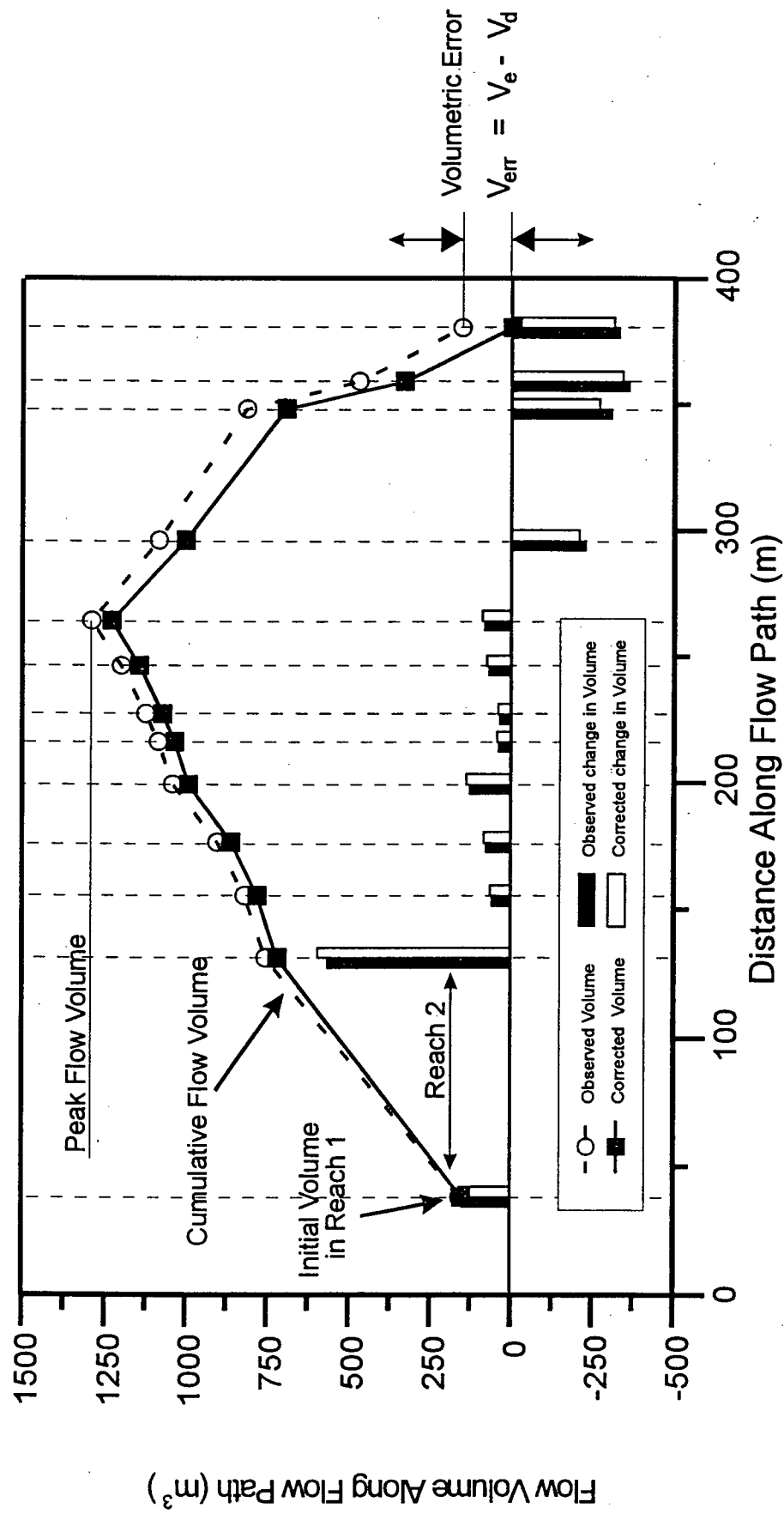


Figure 5.1: Flow Chart of Volumetric Modelling Framework



NOTE: $V_e = \Sigma(+dV_i)$ = total volume entrained along path

$V_d = \Sigma(-dV_i)$ = total volume deposited along path

$V_{err} = V_e - V_d$ = volumetric error

$$VE(\%) = \frac{V_{err}}{V_e + V_d} \times 100$$

Figure 5.2: Schematic plot of cumulative flow volume and volumetric error for Event 1206, Q.C.I. (Selected) Data

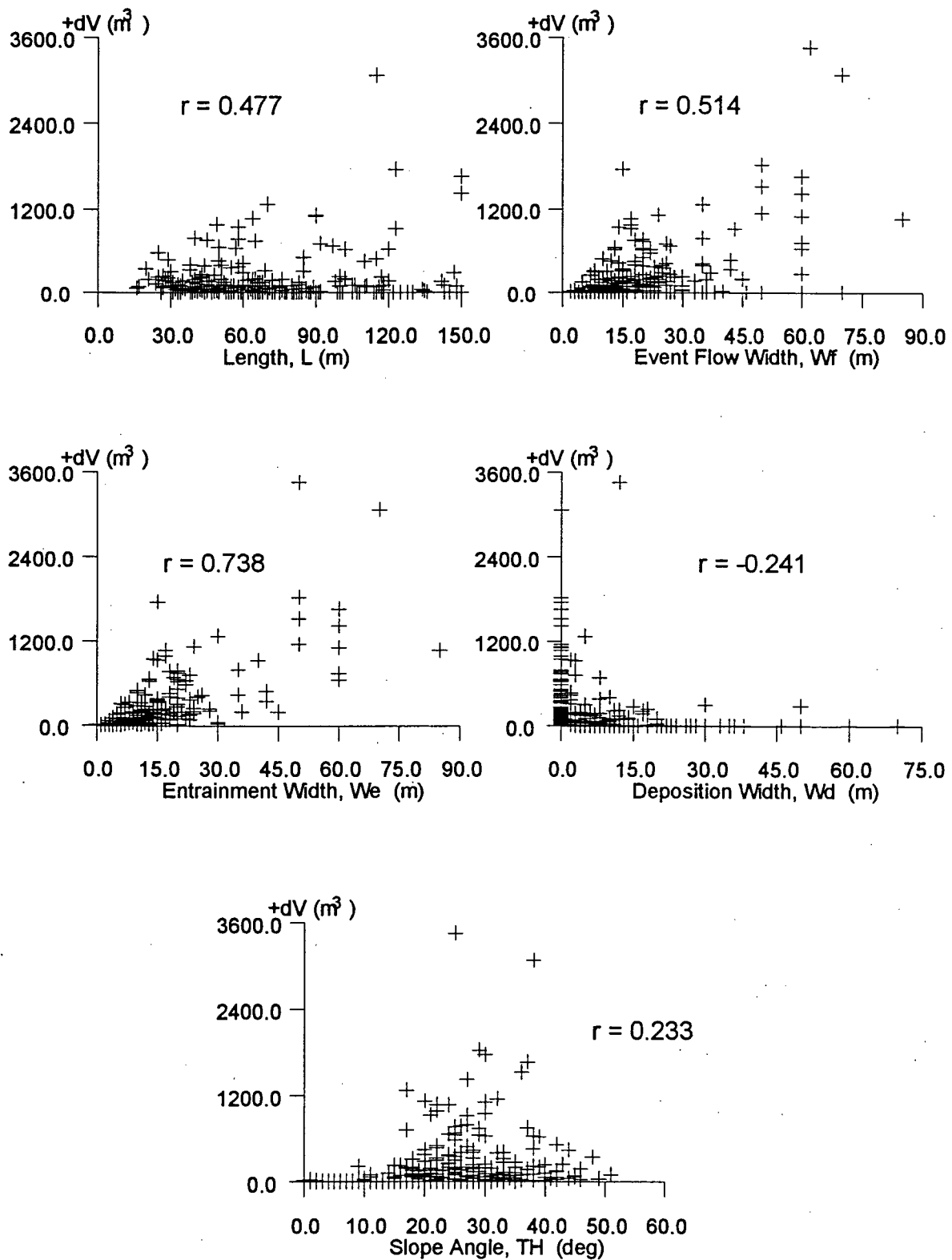


Figure 5.3(a): Scatterplots of reach entrainment volume $+dV$ vs measured predictor variables
Unconfined Flow Reaches; Q.C.I. (Selected) Data

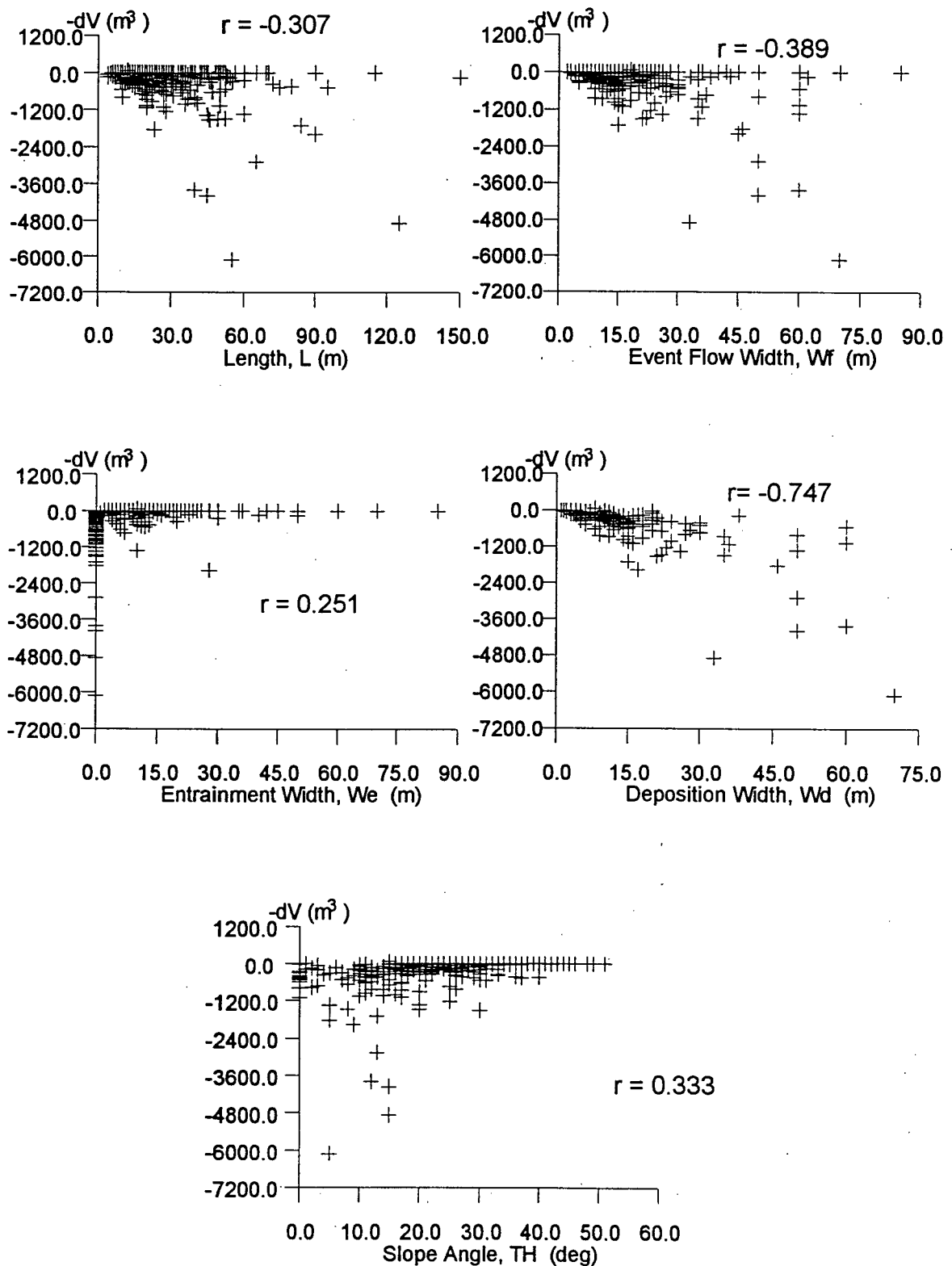


Figure 5.3(b): Scatterplots of reach deposition volume $-dV$ vs measured predictor variables
Unconfined Flow Reaches; Q.C.I. (Selected) Data

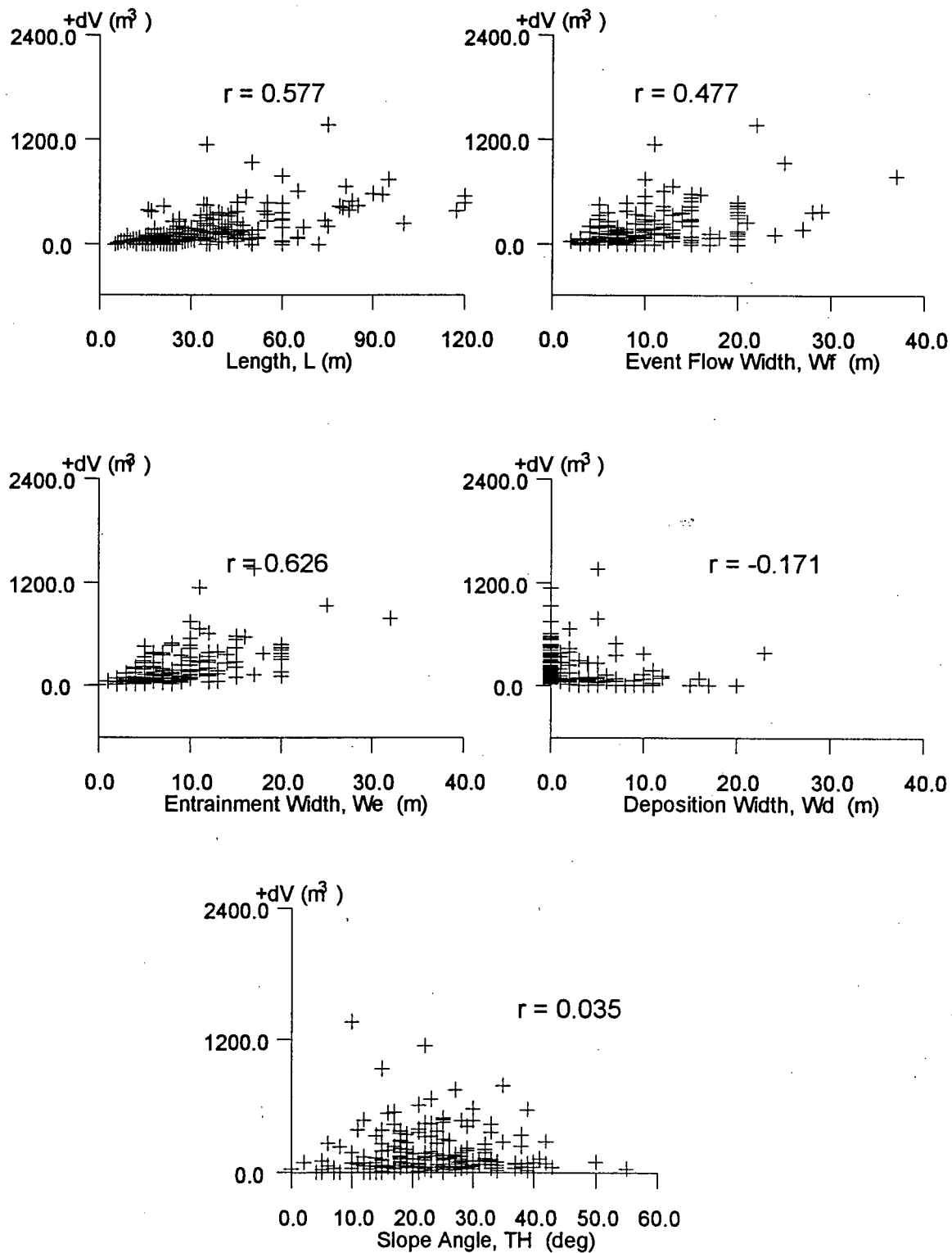


Figure 5.4(a): Scatterplots of reach entrainment volume $+dV$ vs measured predictor variables
Confined Flow Reaches, Q.C.I. (Selected) Data

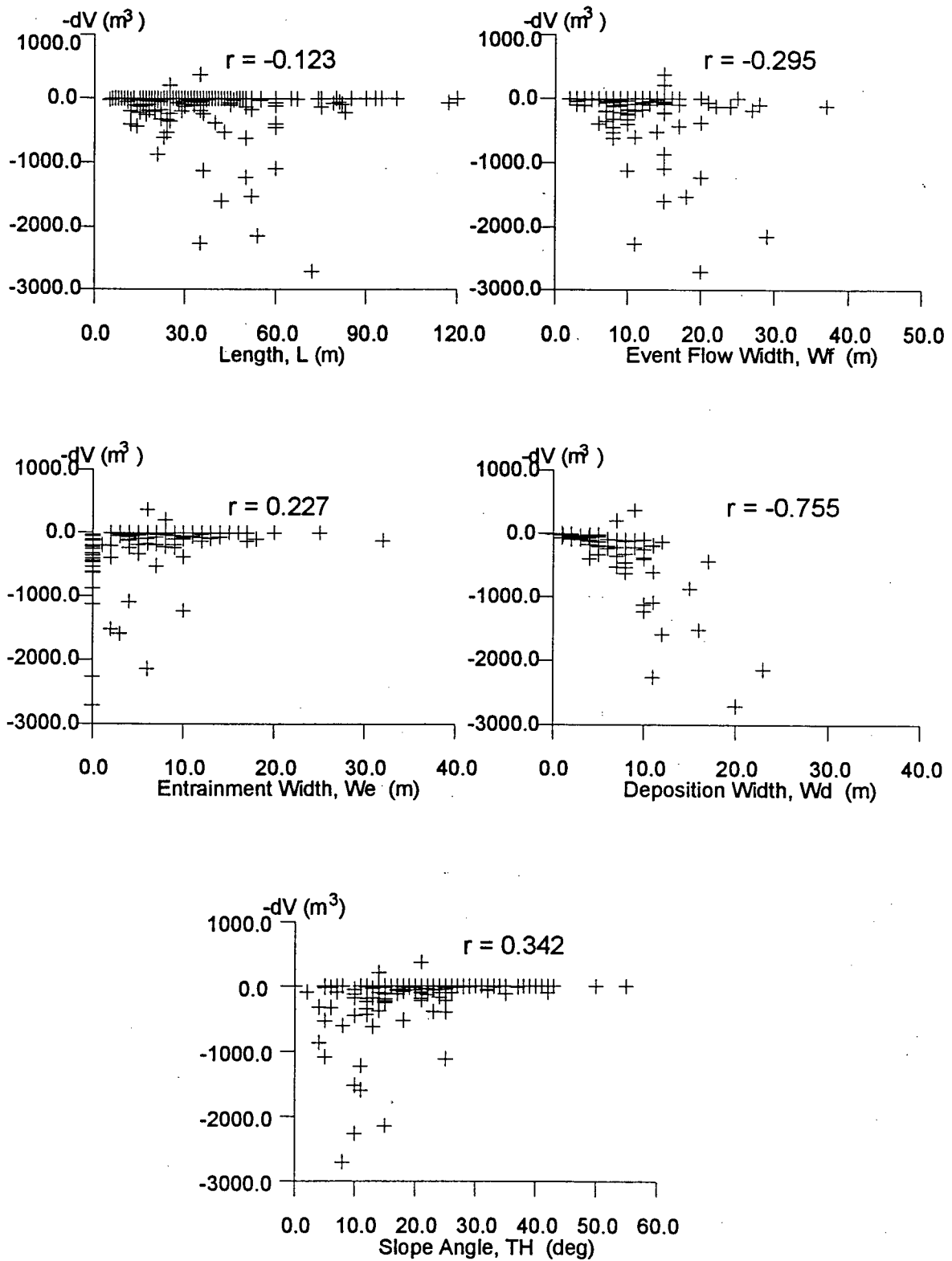


Figure 5.4(b): Scatterplots of reach deposition volume $-dV$ vs measured predictor variables
Confined Flow Reaches, Q.C.I. (Selected) Data

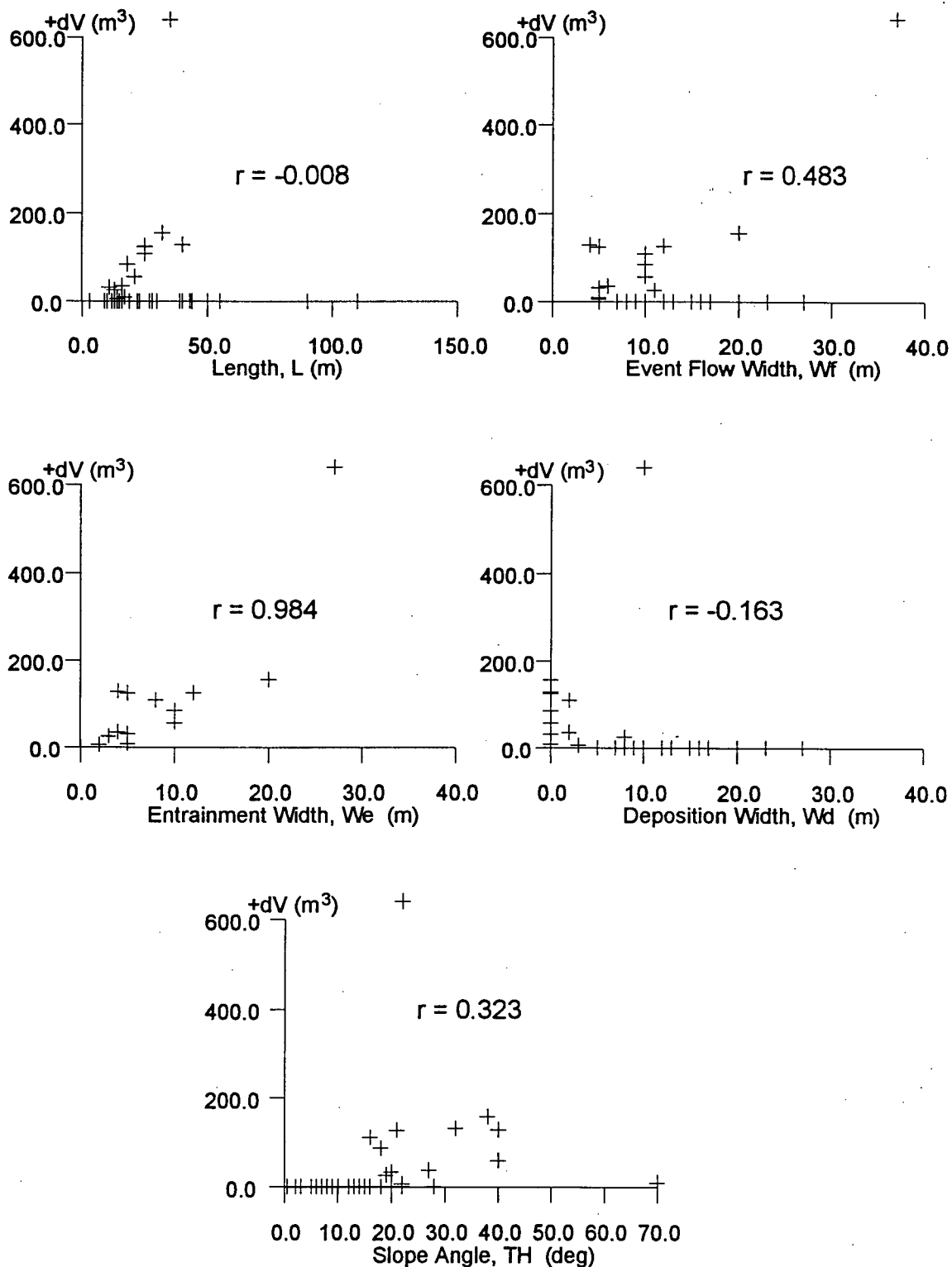


Figure 5.5(a): Scatterplots of reach entrainment volume $+dV$ vs measured predictor variables
Transition Reaches, Q.C.I. (Selected) Data

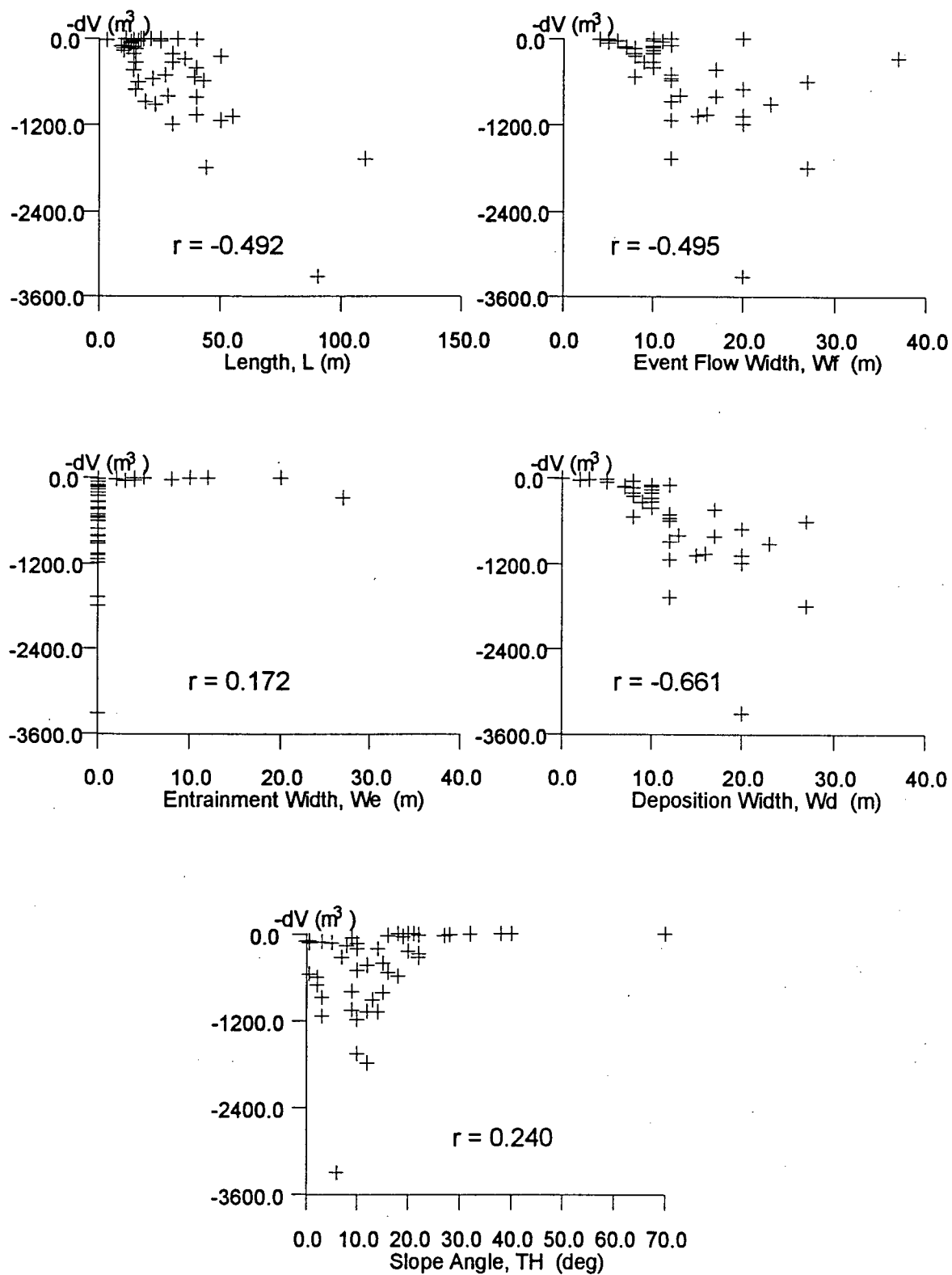


Figure 5.5(b): Scatterplots of reach deposition volume $-dV$ vs measured predictor variables
Transition Reaches; Q.C.I. (Selected) Data

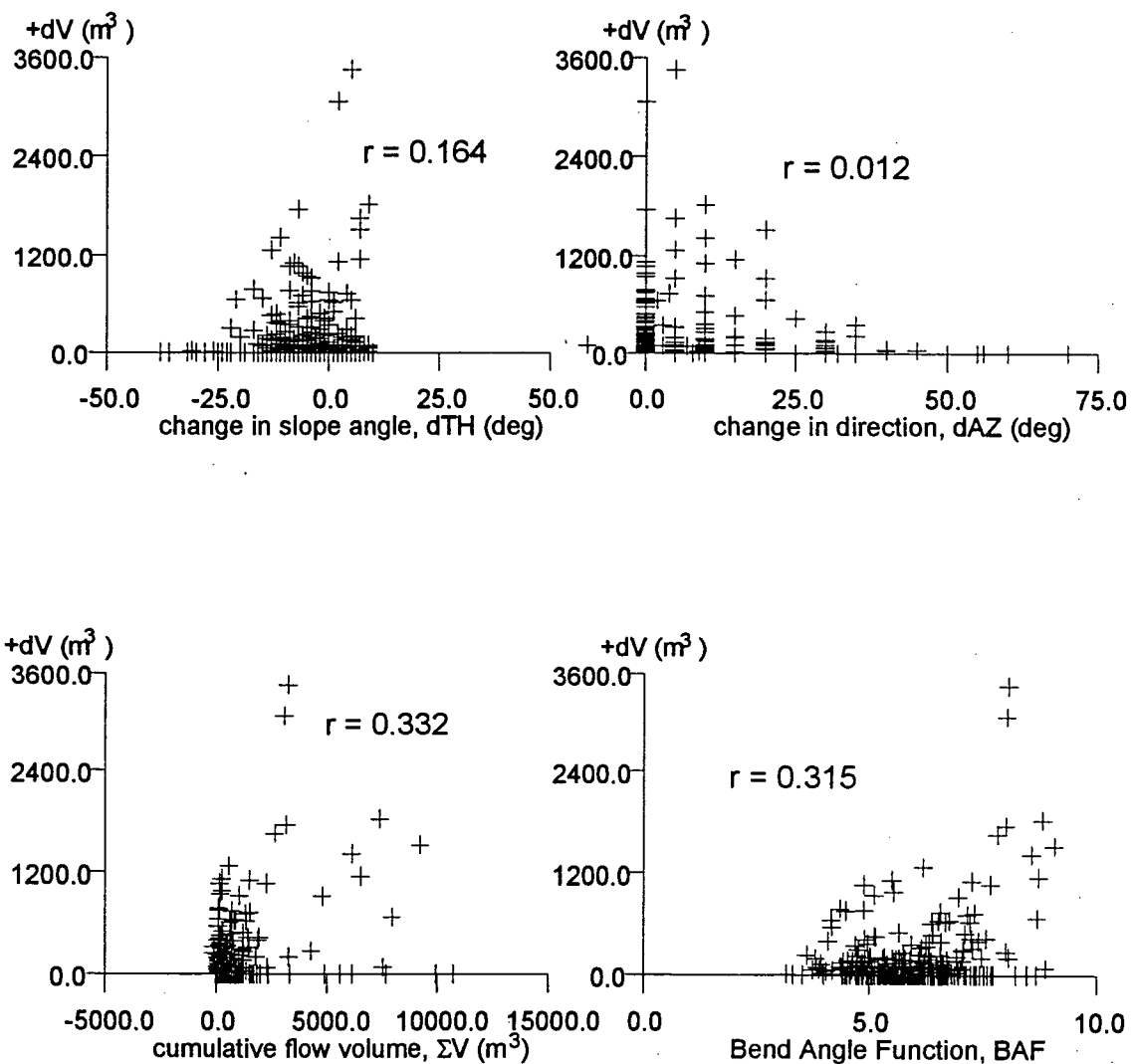


Figure 5.6(a): Scatterplots of reach entrainment volume $+dV$ vs derived predictor variables
Unconfined Reaches, Q.C.I. (Selected) Data

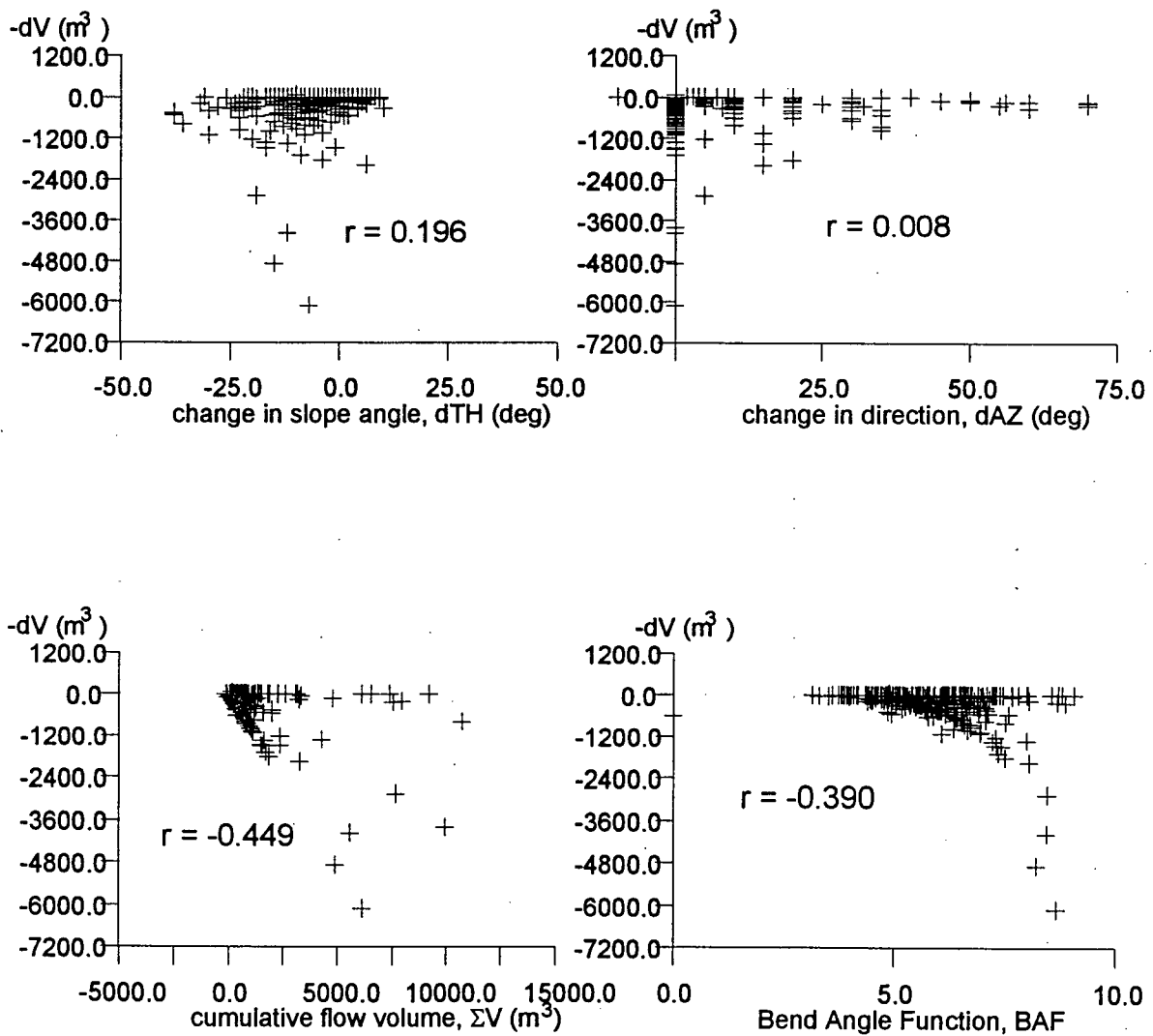


Figure 5.6(b): Scatterplots of reach deposition volume $-dV$ vs derived predictor variables
Unconfined Reaches, Q.C.I. (Selected) Data

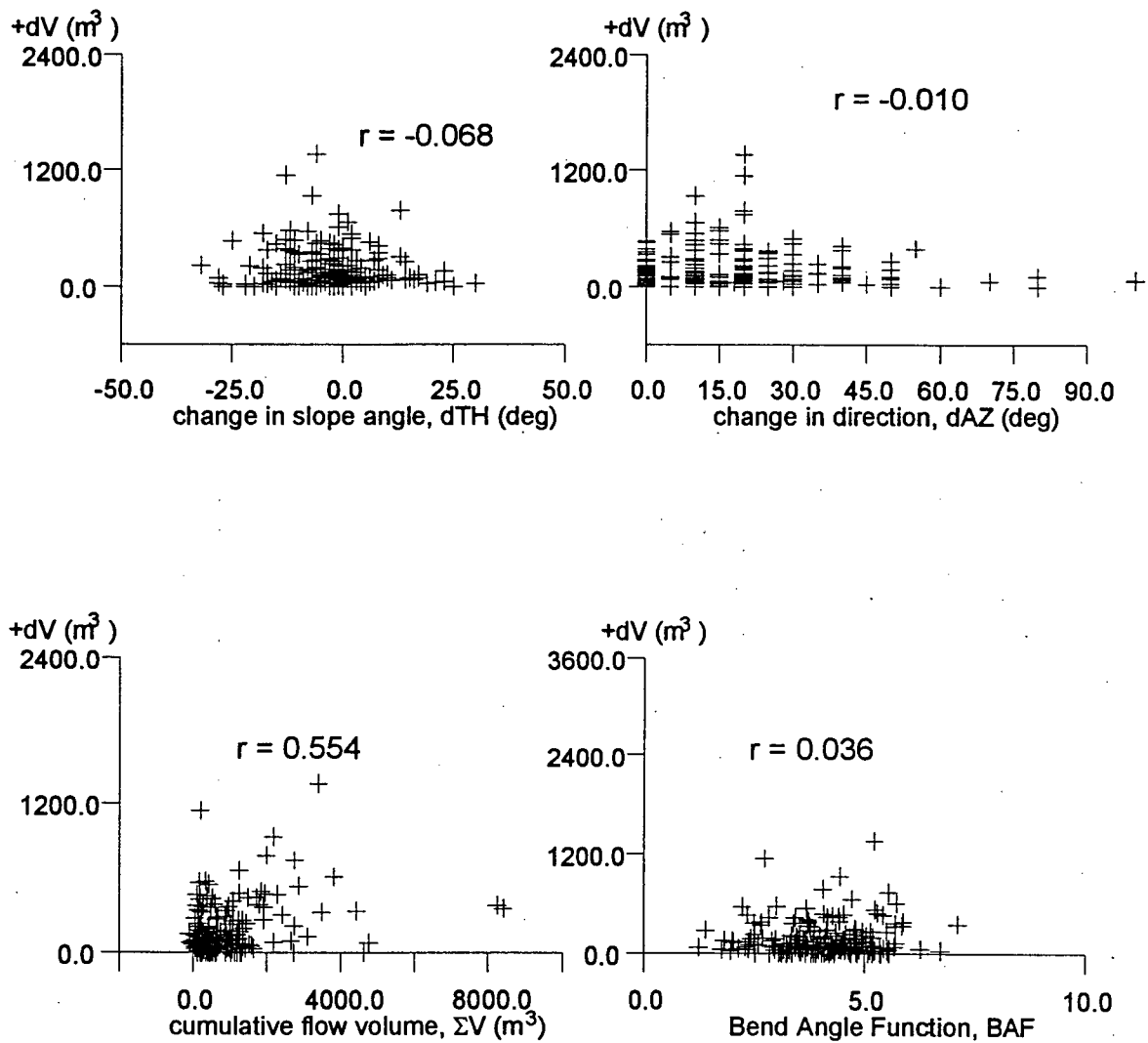


Figure 5.6(c): Scatterplots of reach entrainment volume +dV vs derived predictor variables
Confined Reaches, Q.C.I. (Selected) Data

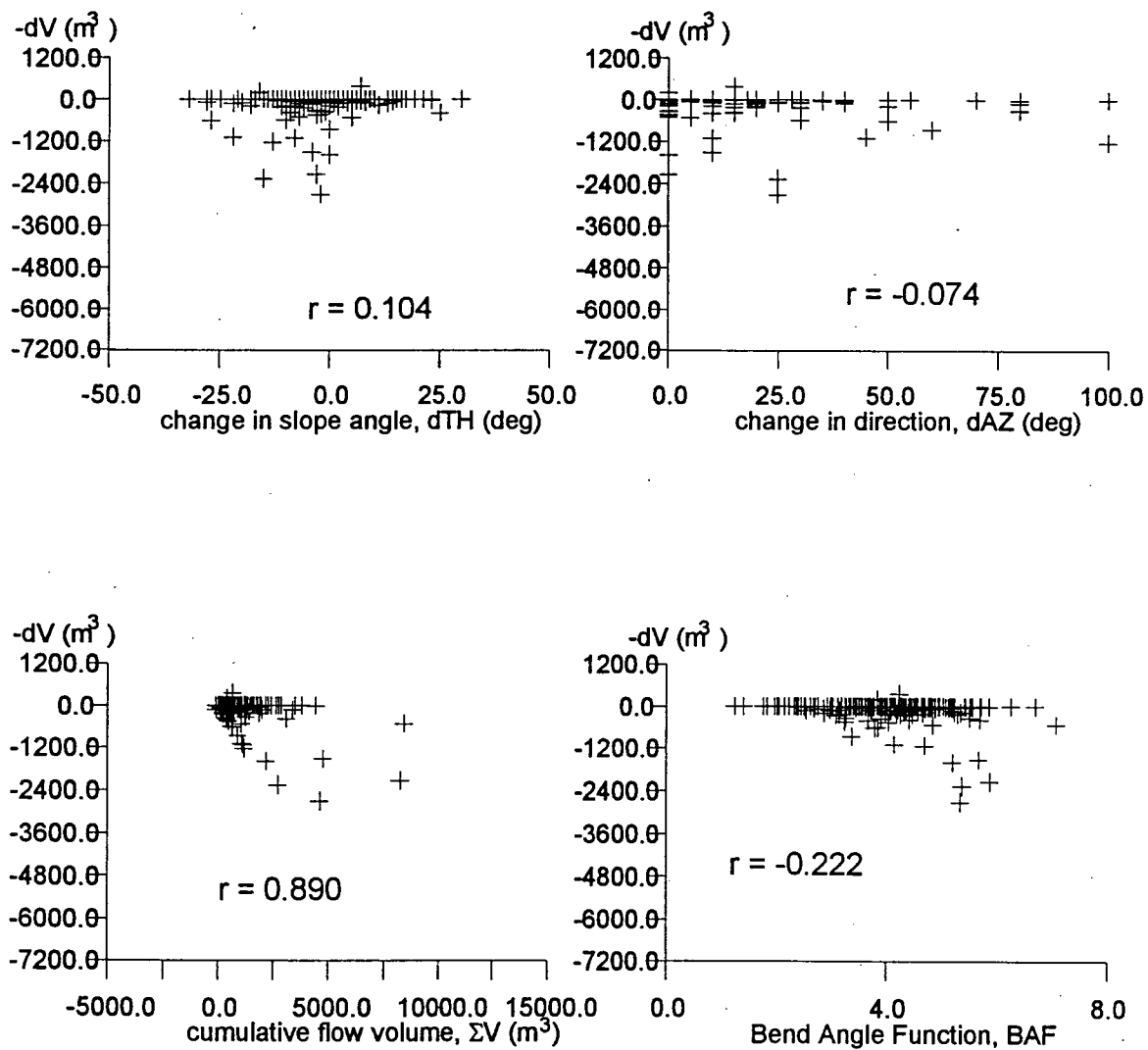


Figure 5.6(d): Scatterplots of reach deposition volume $-dV$
vs derived predictor variables
Confined Reaches, Q.C.I. (Selected) Data

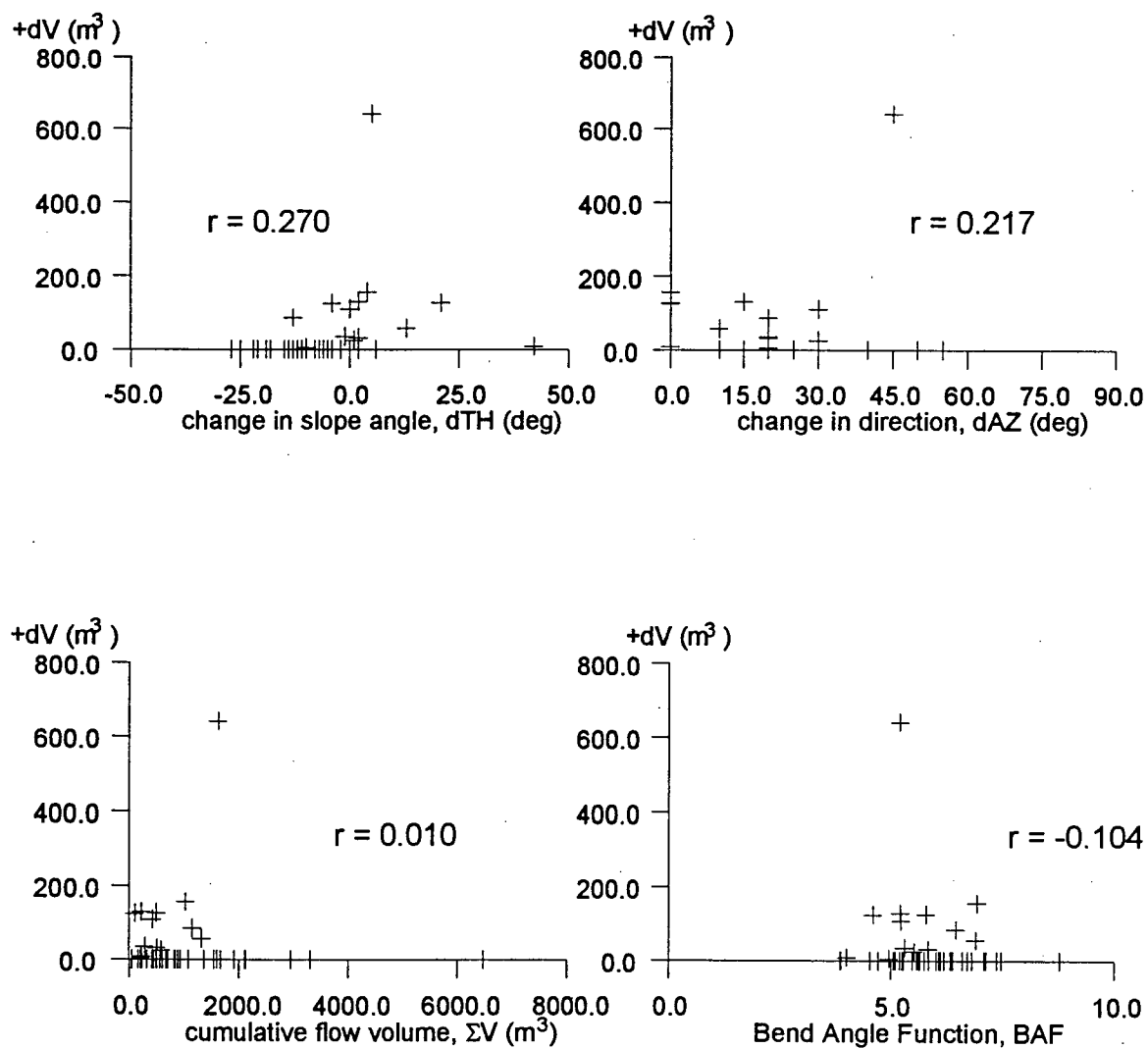


Figure 5.6(e): Scatterplots of reach entrainment volume $+dV$ vs derived predictor variables
Transition Reaches, Q.C.I. (Selected) Data

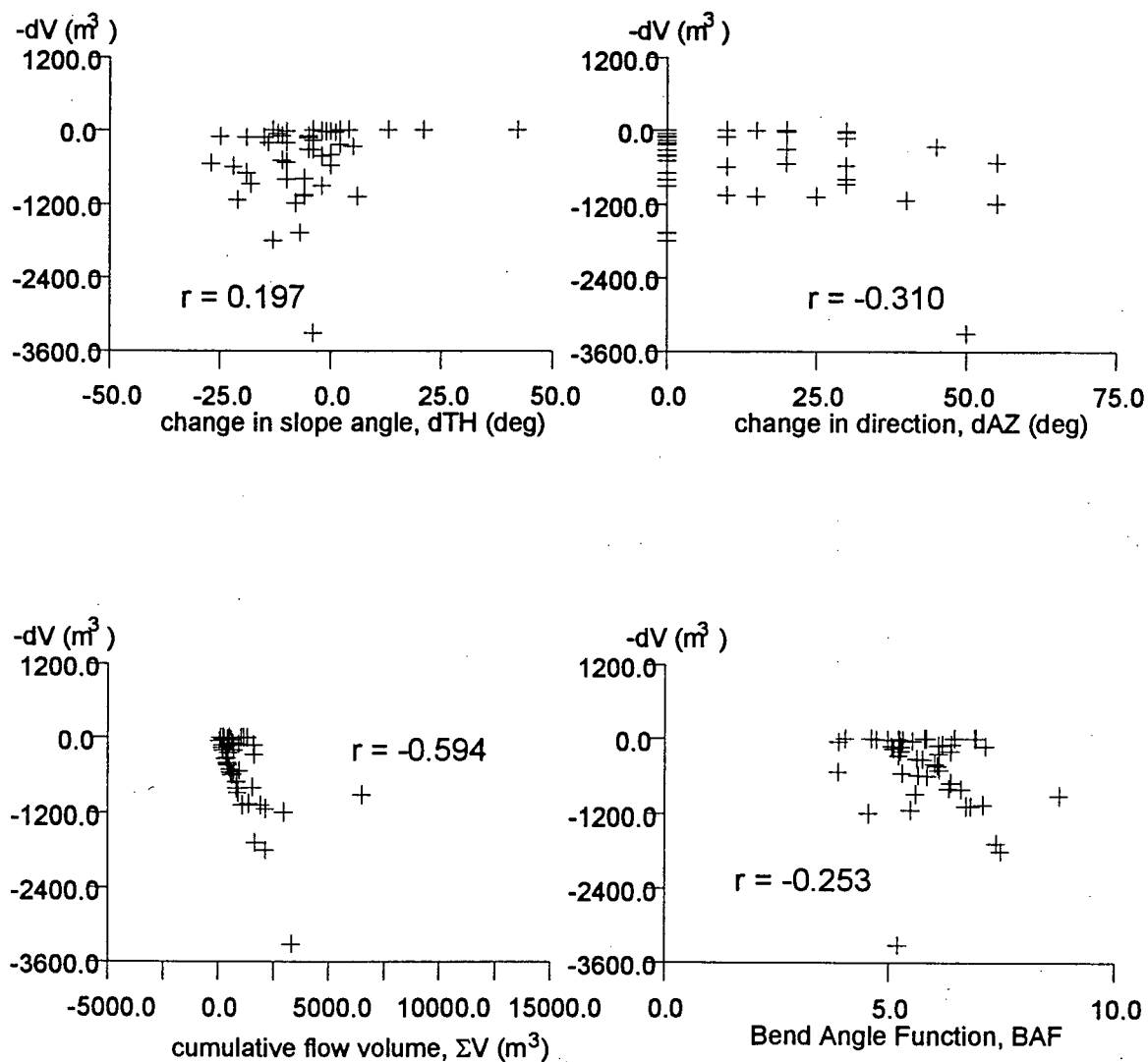
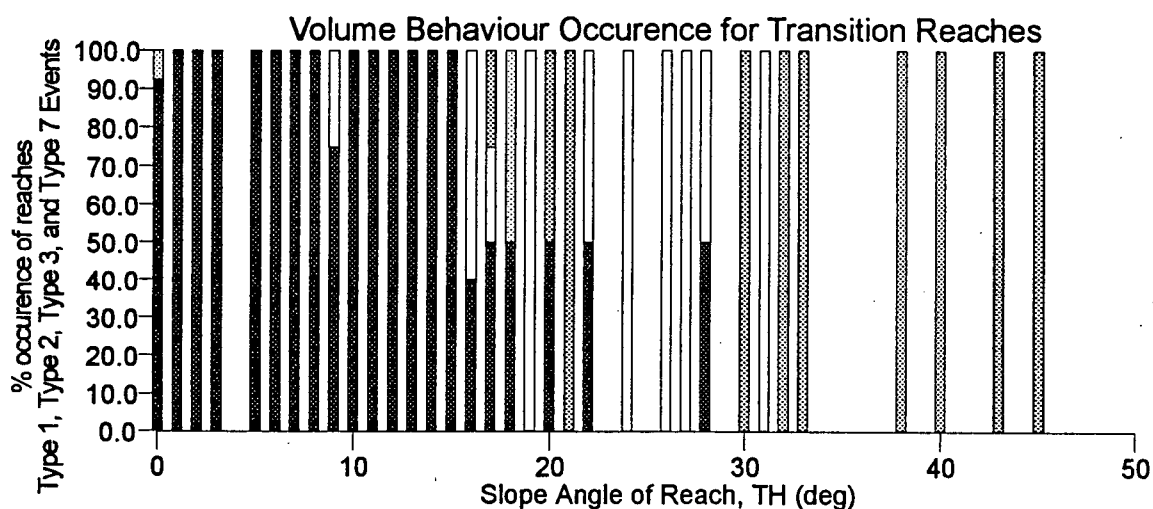
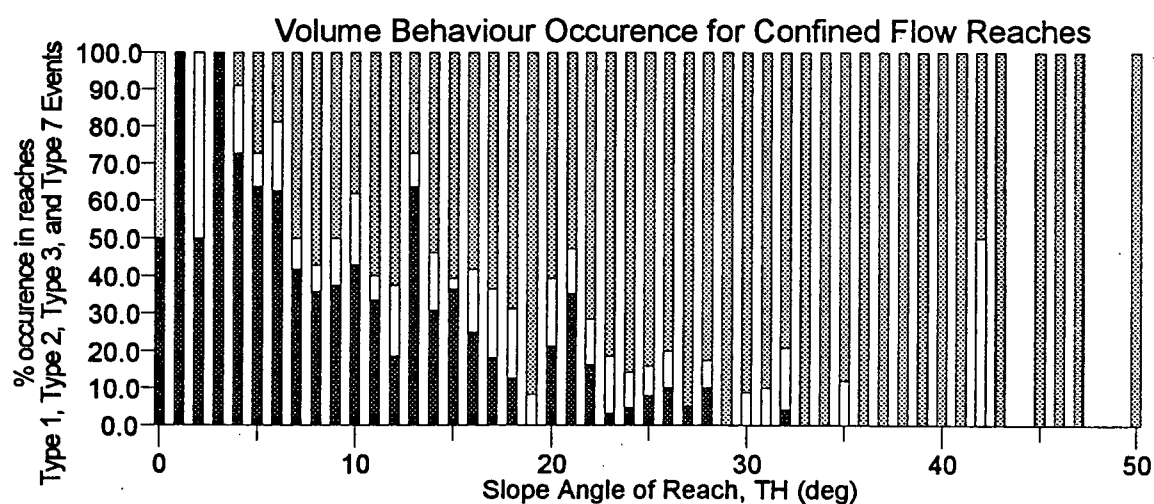
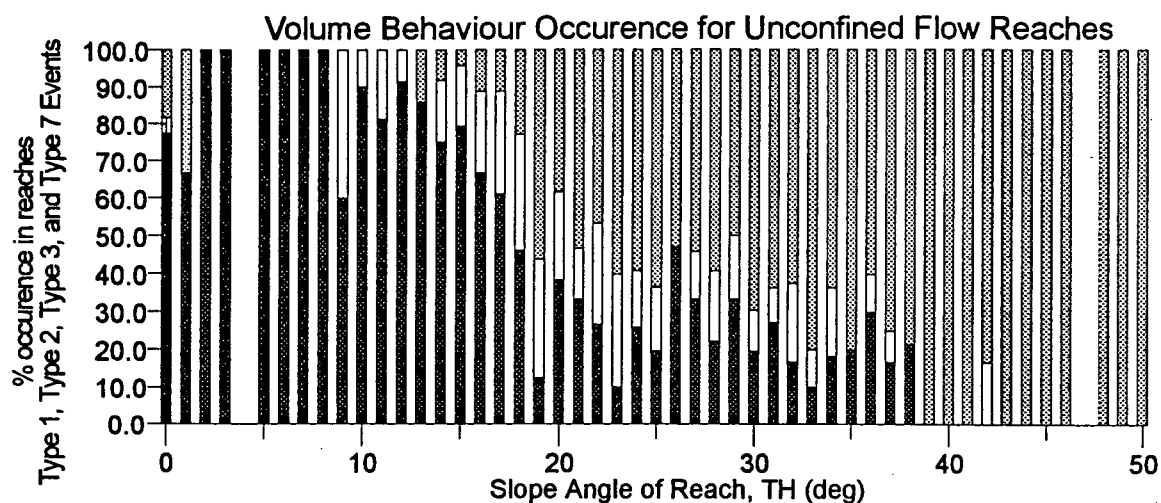


Figure 5.6(f): Scatterplots of reach deposition volume $-dV$ vs derived predictor variables
Transition Reaches, Q.C.I. (Selected) Data



Legend for all Barcharts

- Deposition Observed
- Deposition and Entrainment Observed (Dual Flow Mode)
- Entrainment Observed

Filter applied to group reaches with both deposition and entrainment into deposition/entrainment only if lesser volume change < 20% of total volume change

Figure 5.7: Filtered Volume Change Behaviour for Q.C.I. (Original) Data

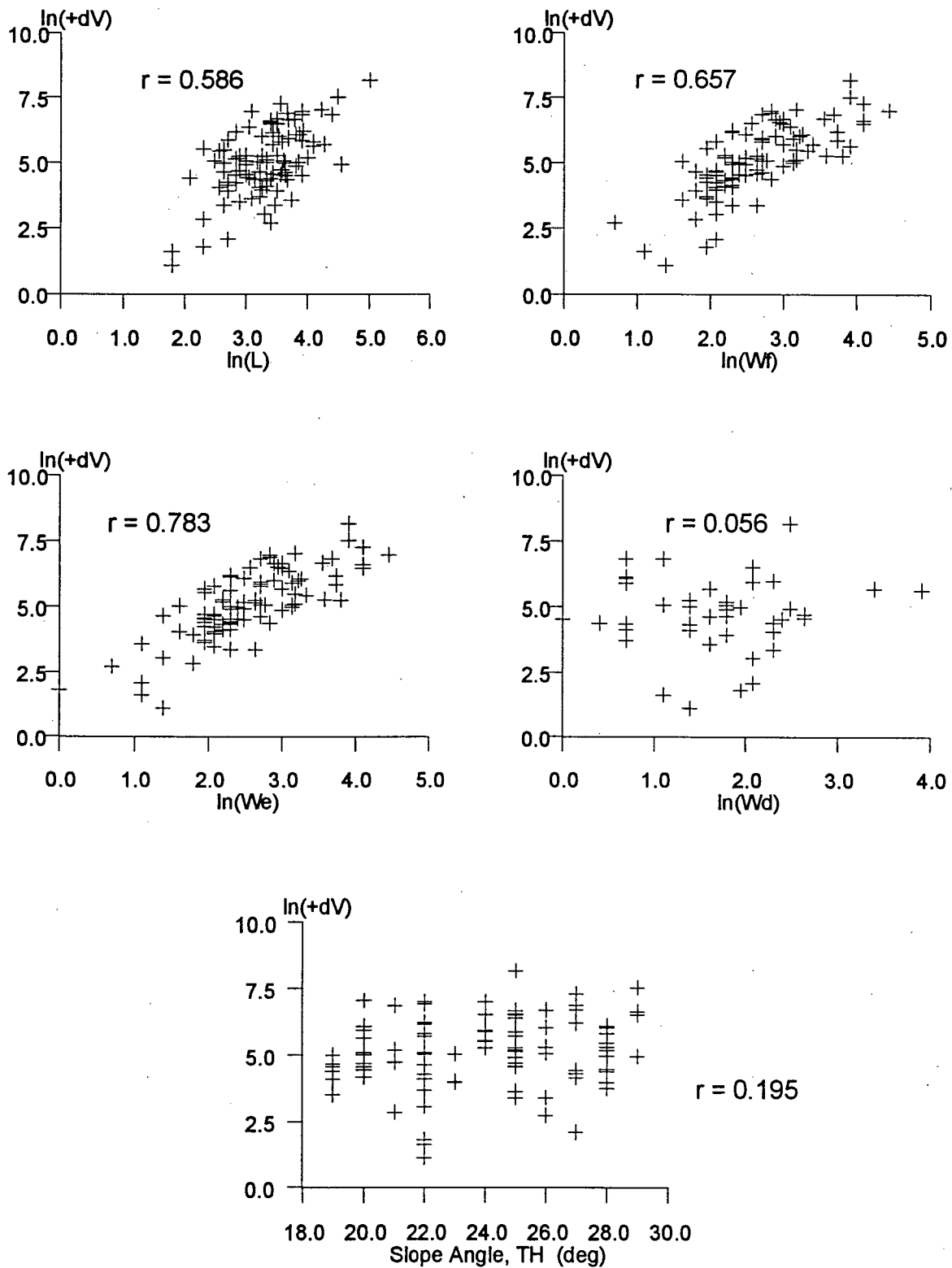


Figure 5.8(a): Scatterplots of transformed entrainment volume $+dV$ vs transformed predictor variables
Unconfined Flow reaches, $19 \leq TH \leq 29$, Q.C.I. (Selected) Data

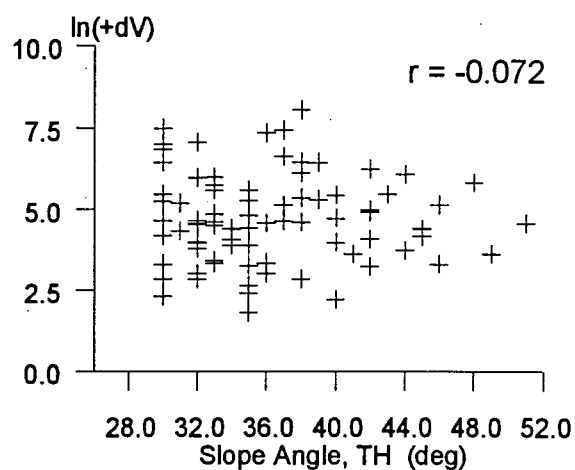
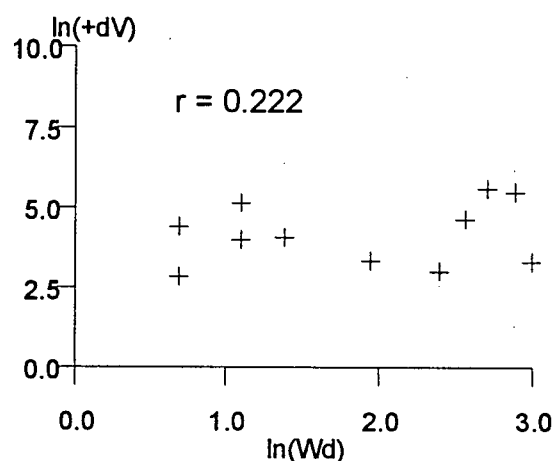
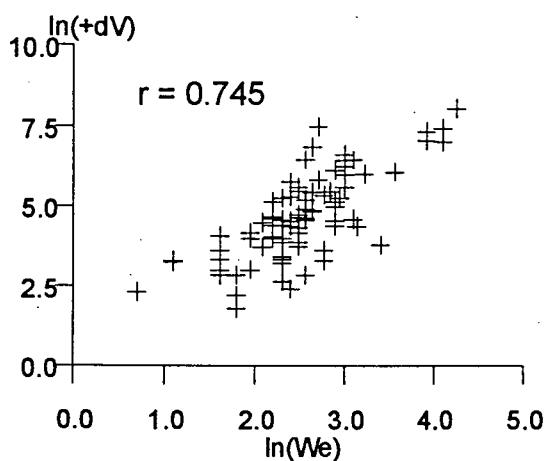
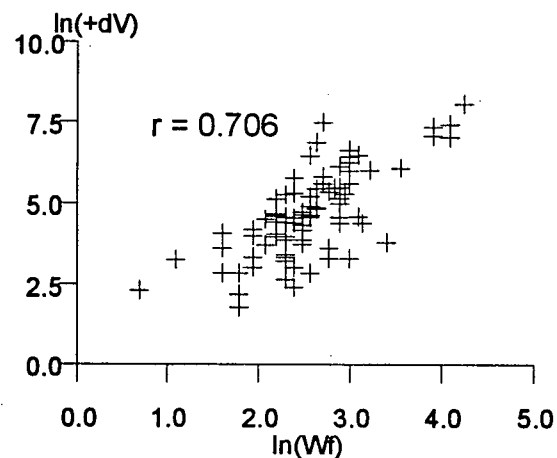
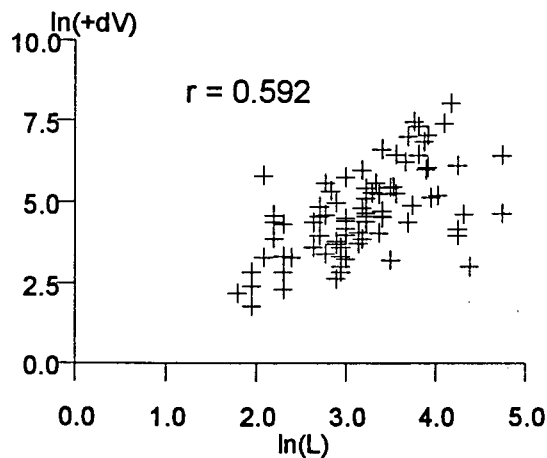


Figure 5.8(b): Scatterplots of transformed entrainment volume +dV vs transformed predictor variables
Unconfined Flow reaches, $30 \leq TH \leq 55$, Q.C.I. (Selected) Data

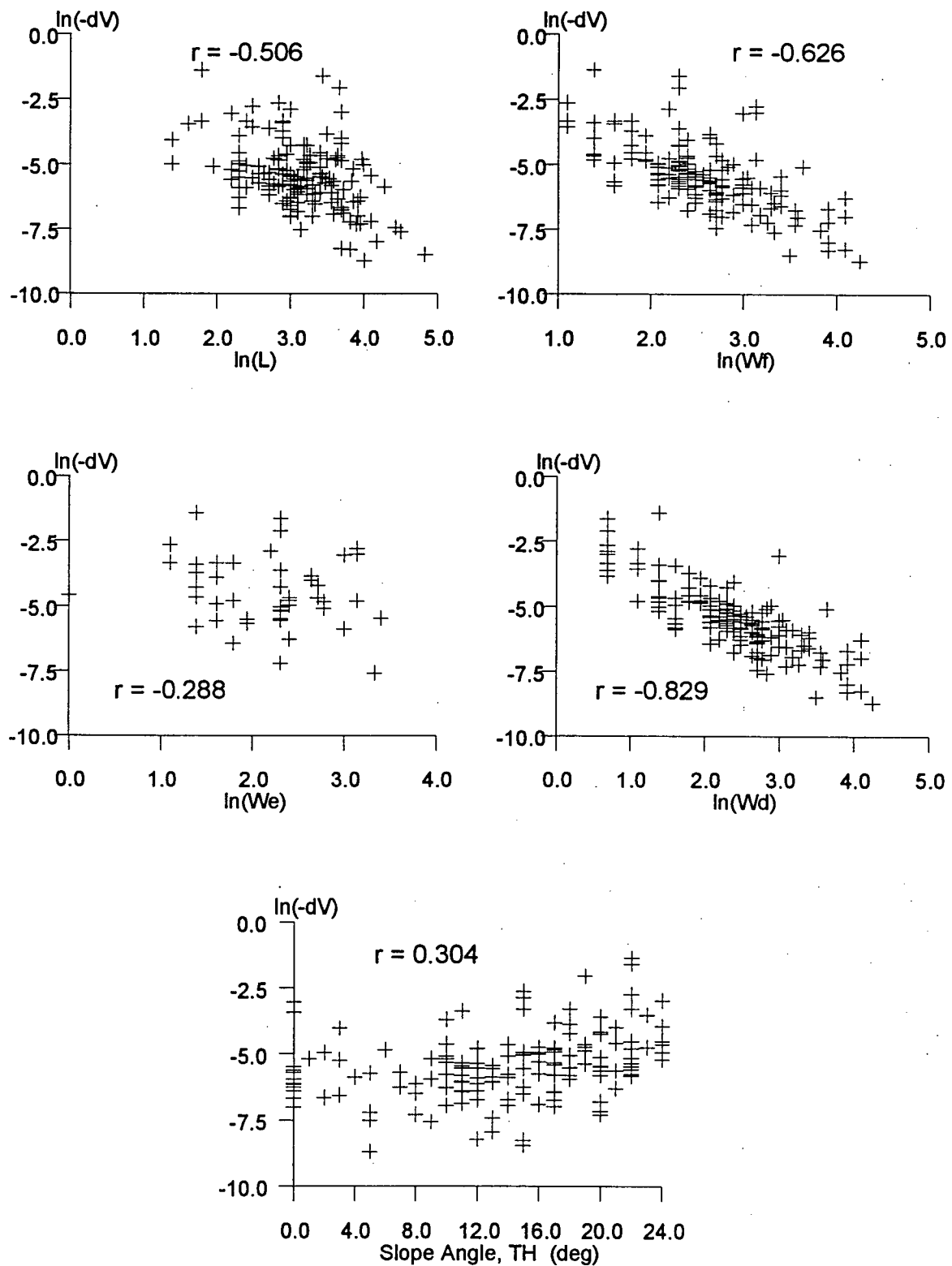


Figure 5.8(c): Scatterplots of transformed deposition volume $-dV$ vs transformed predictor variables
Unconfined Flow reaches, $0 \leq TH \leq 24$, Q.C.I. (Selected) Data

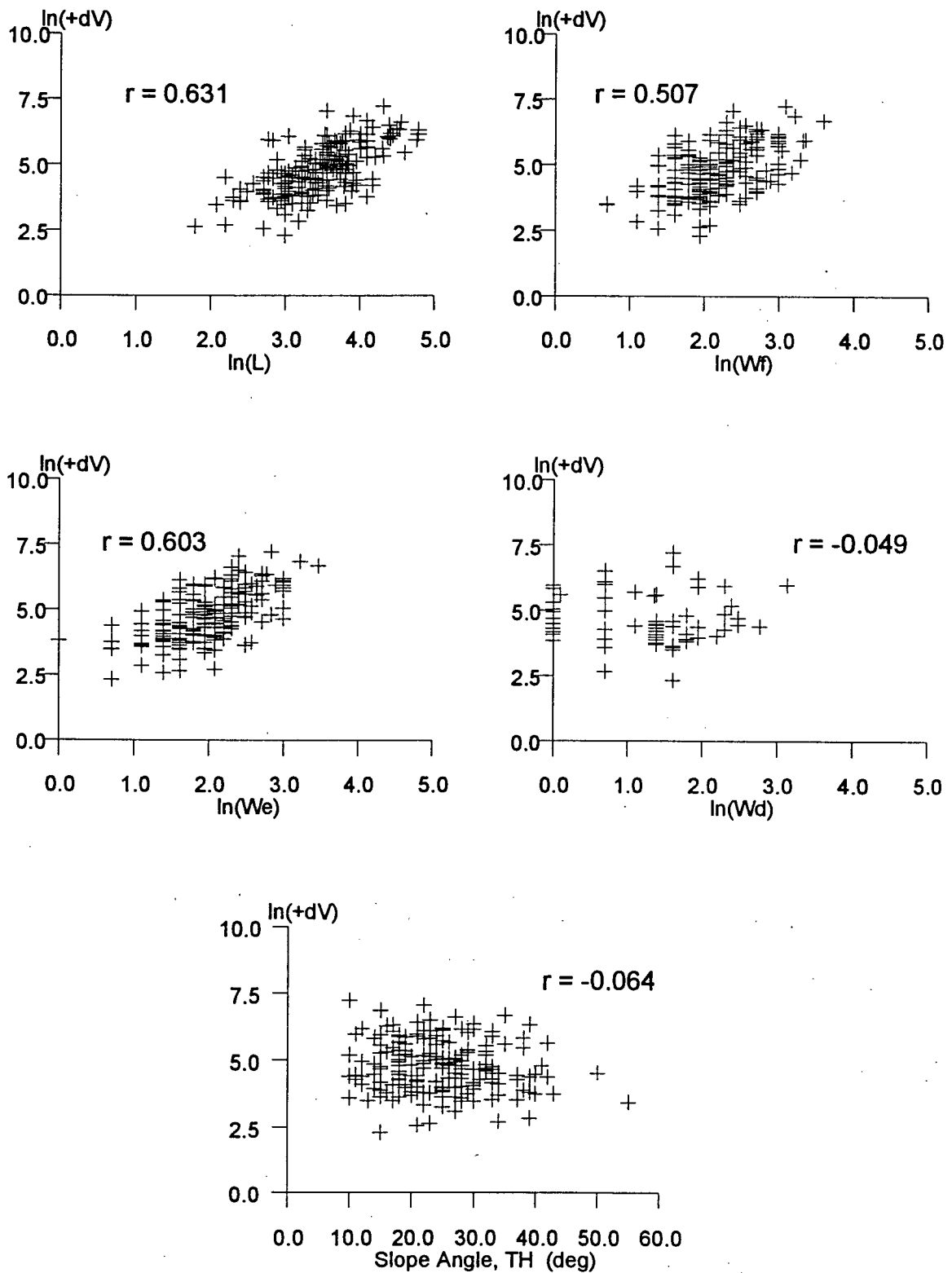


Figure 5.9: Scatterplots of transformed entrainment volume $+dV$ vs transformed predictor variables
Confined Flow reaches, $10 \leq TH \leq 55$, Q.C.I. (Selected) Data

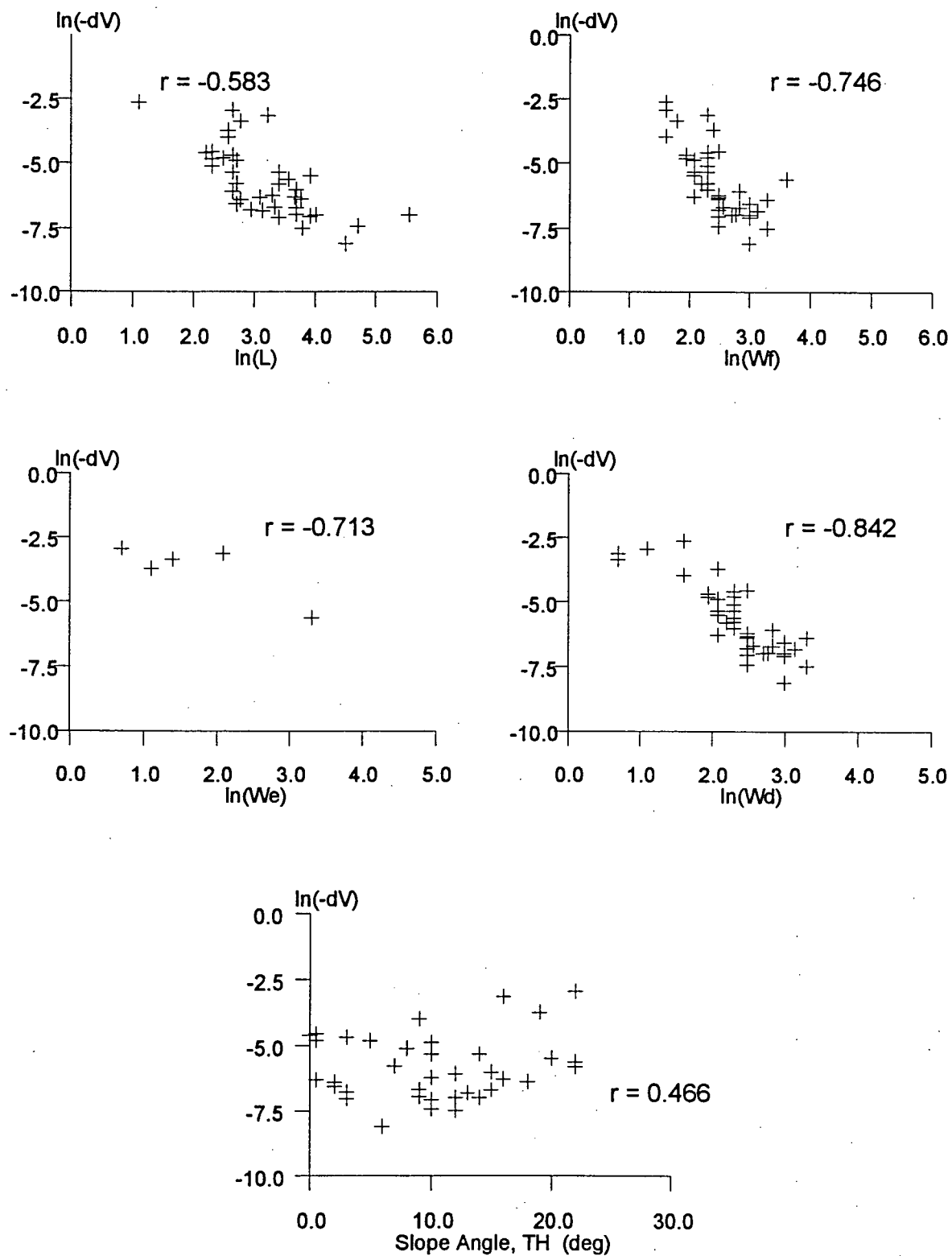


Figure 5.10: Scatterplots of transformed deposition volume $-dV$ vs transformed predictor variables
Transition Flow reaches, $0 \leq TH \leq 22$, Q.C.I. (Selected) Data

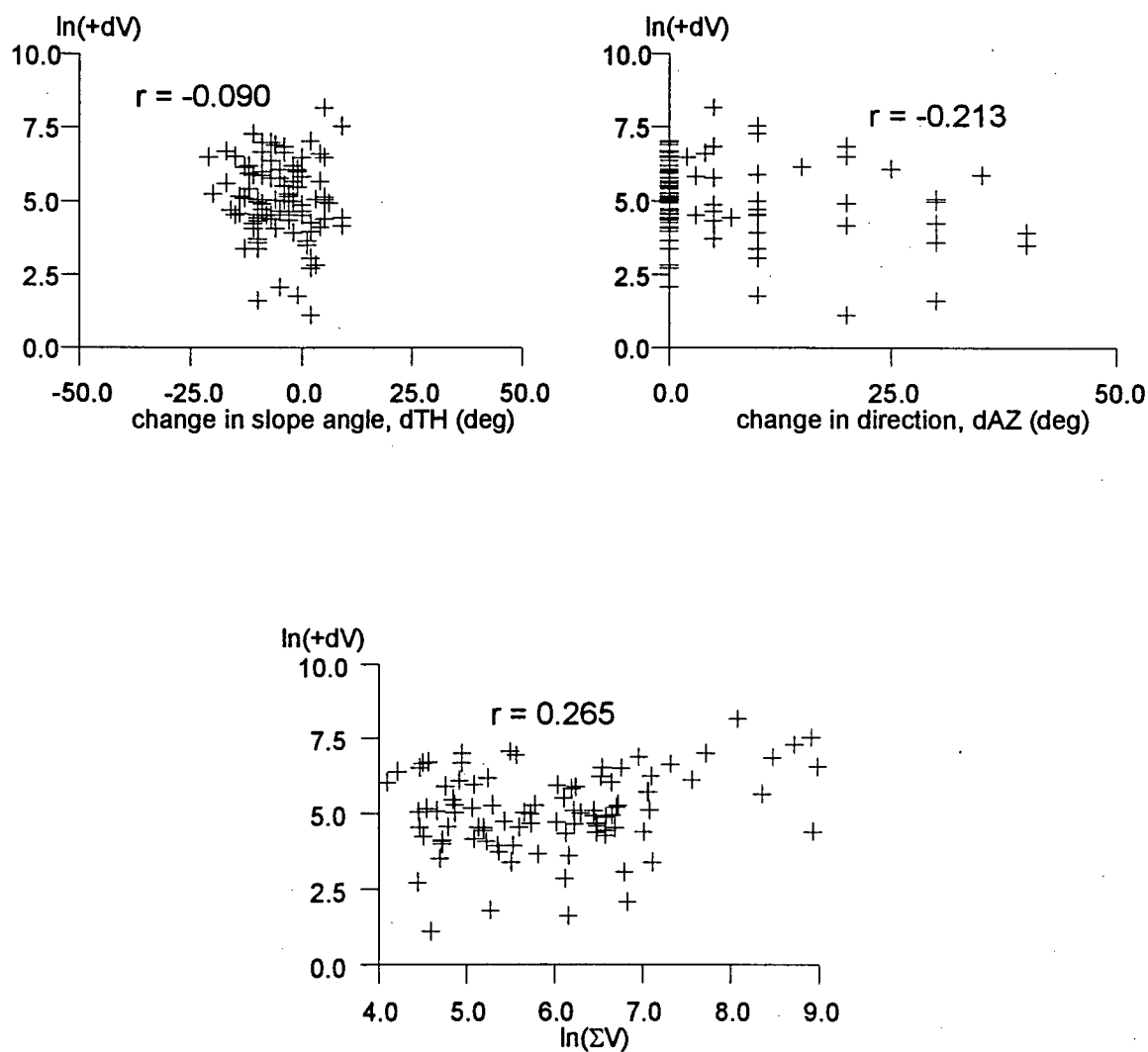


Figure 5.11(a): Scatterplots of transformed entrainment volume +dV vs transformed derived variables
Unconfined Flow reaches, $19 \leq TH \leq 29$, Q.C.I. (Selected) Data

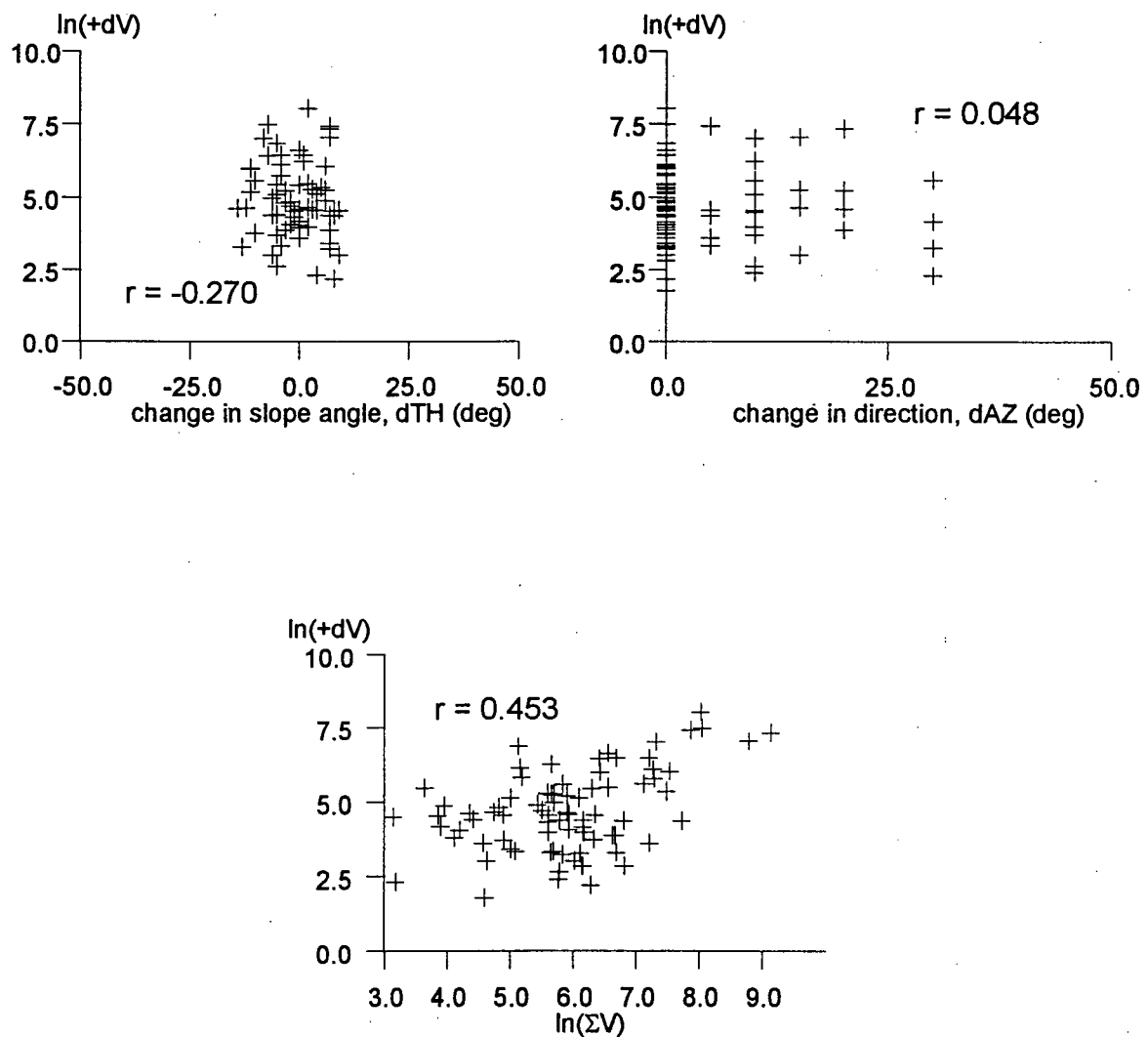


Figure 5.11(b): Scatterplots of transformed entrainment volume $+dV$ vs transformed derived variables
Unconfined Flow reaches, $30 \leq TH \leq 55$, Q.C.I. (Selected) Data

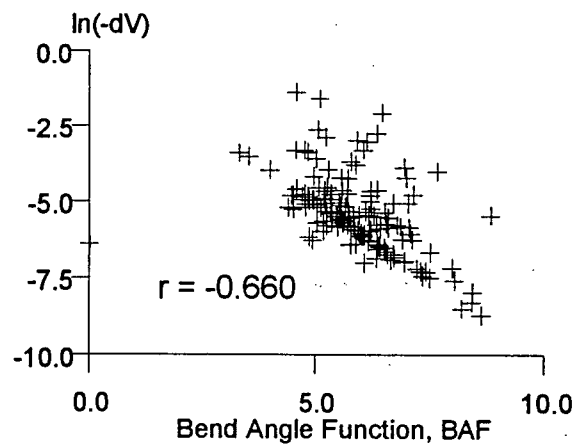
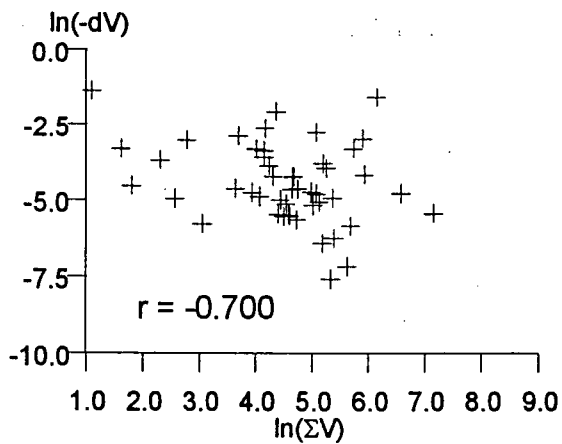
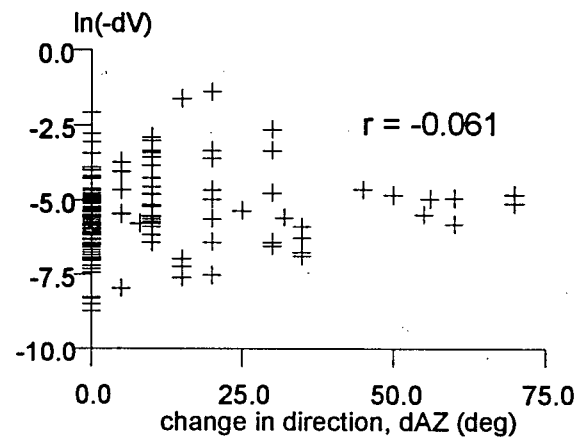
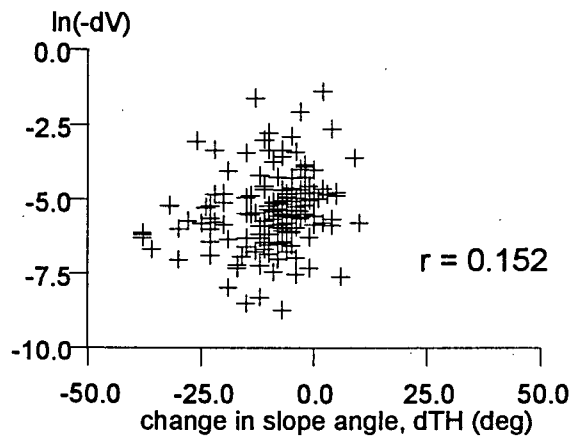


Figure 5.11(c): Scatterplots of transformed deposition volume $-dV$ vs transformed derived variables
Unconfined Flow reaches, $0 \leq TH \leq 24$, Q.C.I. (Selected) Data

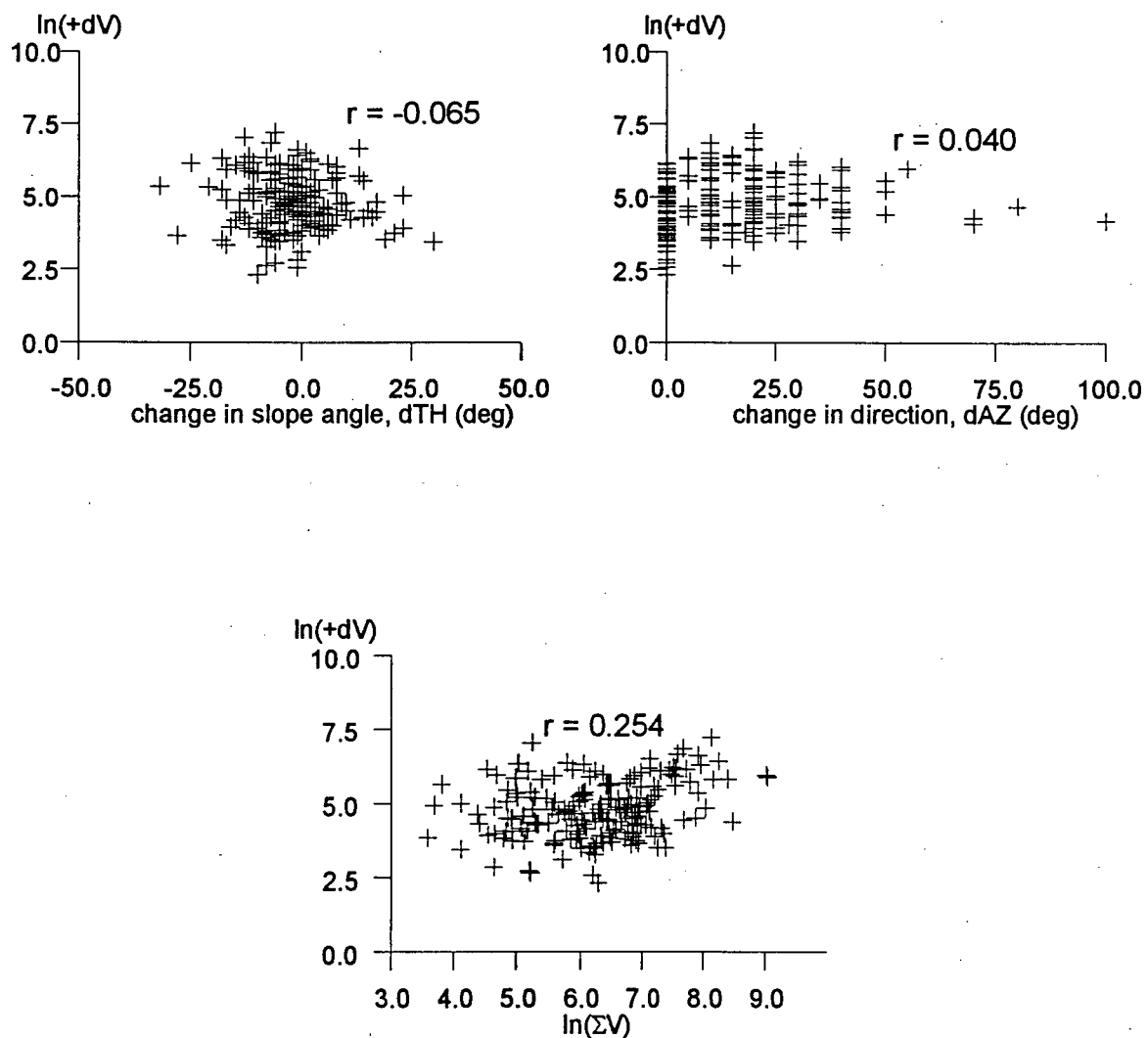


Figure 5.12: Scatterplots of transformed entrainment volume $+dV$ vs transformed derived variables
Confined Flow reaches, $10 \leq TH \leq 55$, Q.C.I. (Selected) Data

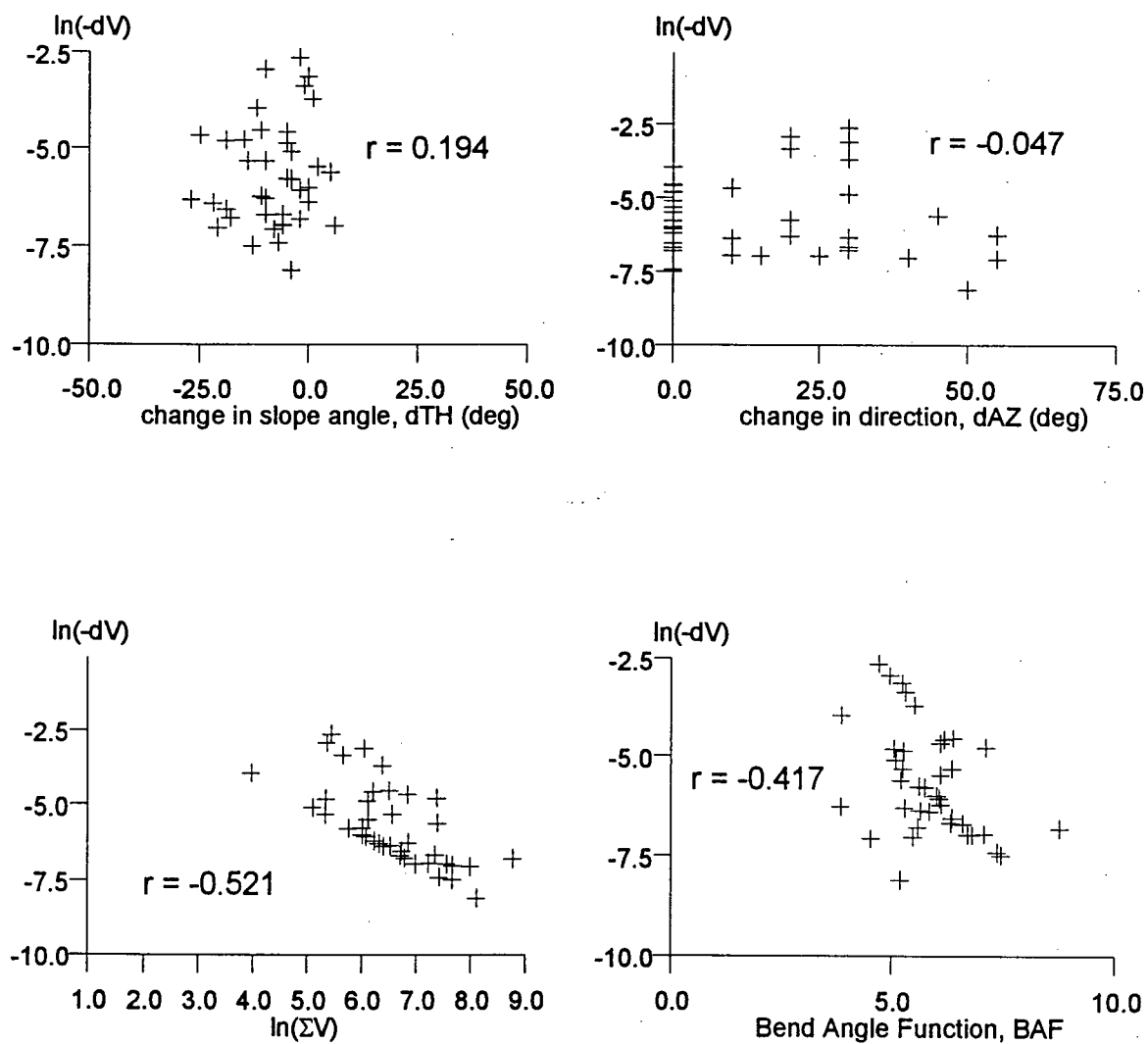


Figure 5.13: Scatterplots of transformed deposition volume $-dV$ vs transformed derived variables
Transition Flow reaches, $0 \leq TH \leq 22$, Q.C.I. (Selected) Data

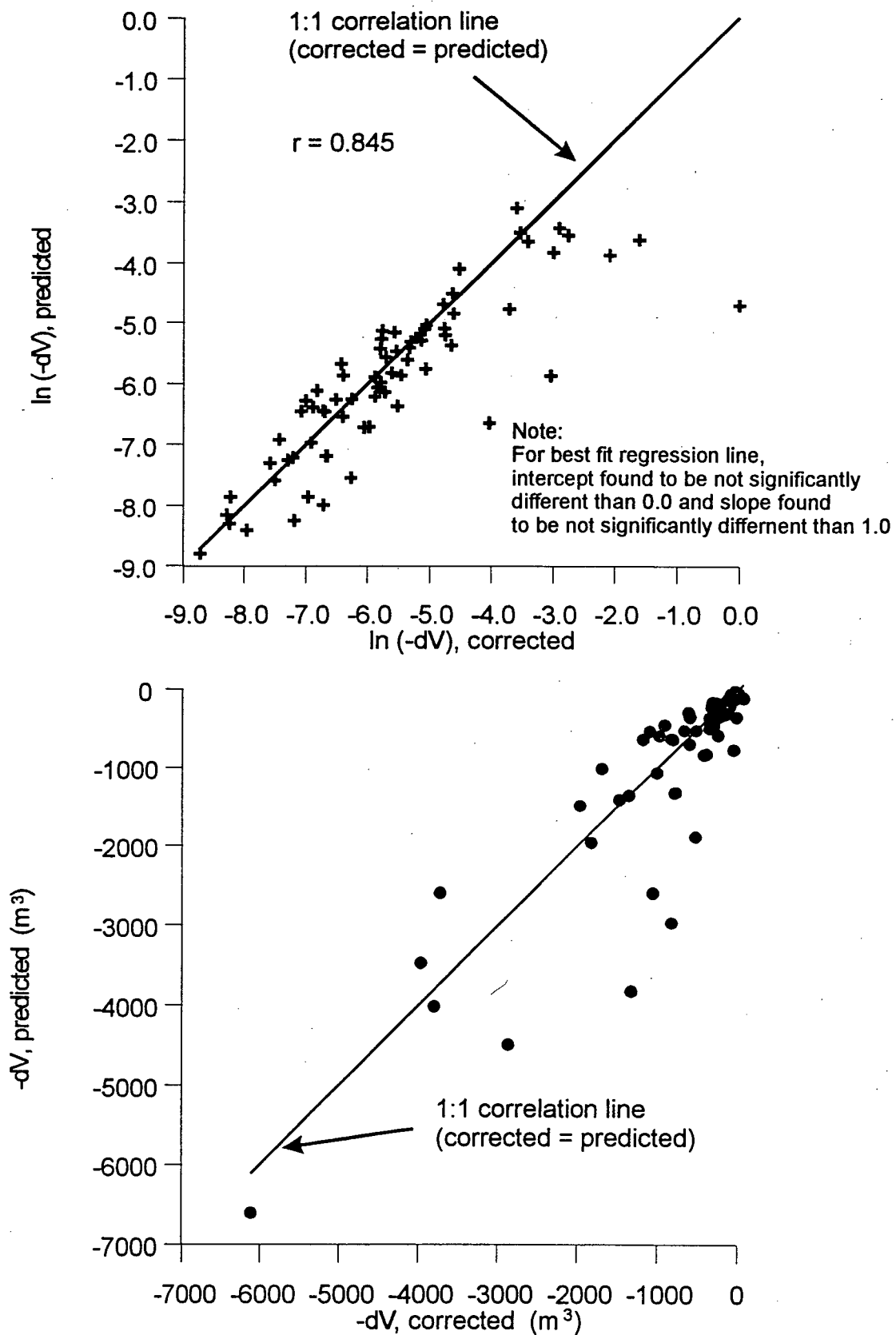


Figure 5.14: Test of subset regression equations, deposition
Unconfined Flow Reaches, $0 \leq TH \leq 24$, Q.C.I. (Selected) Data

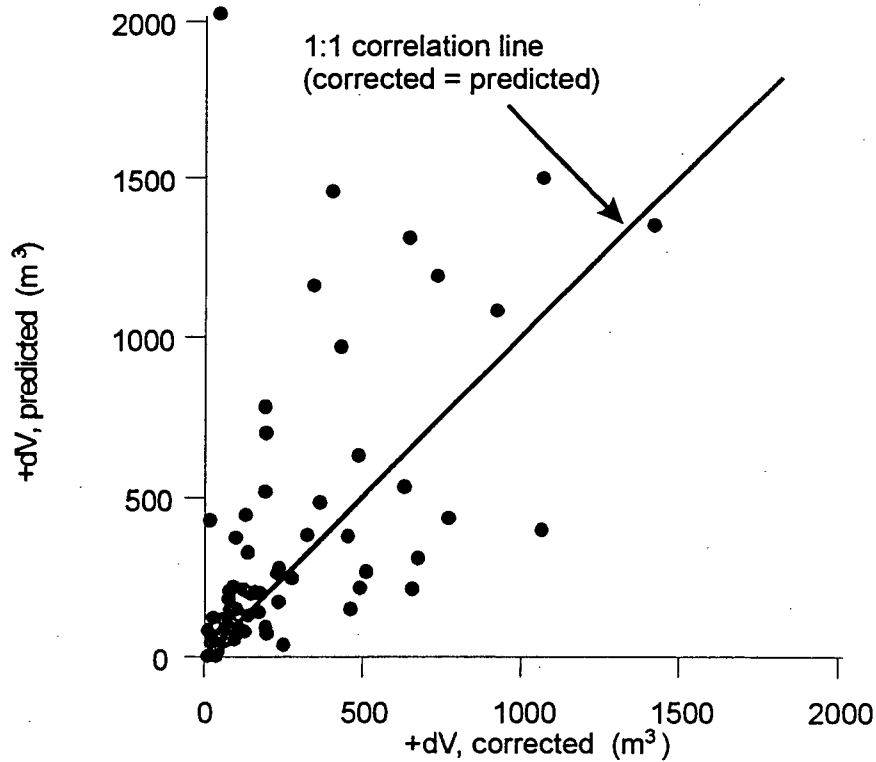
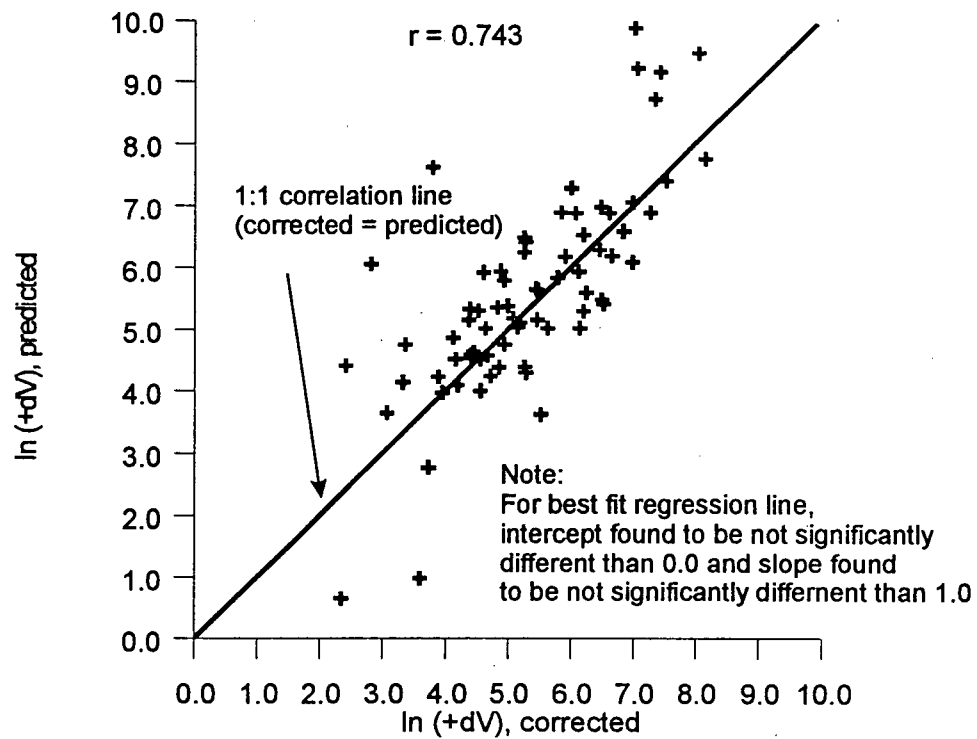


Figure 5.15: Test of subset regression equations, entrainment
Unconfined Flow Reaches, $19 \leq TH \leq 55$, Q.C.I. (Selected) Data

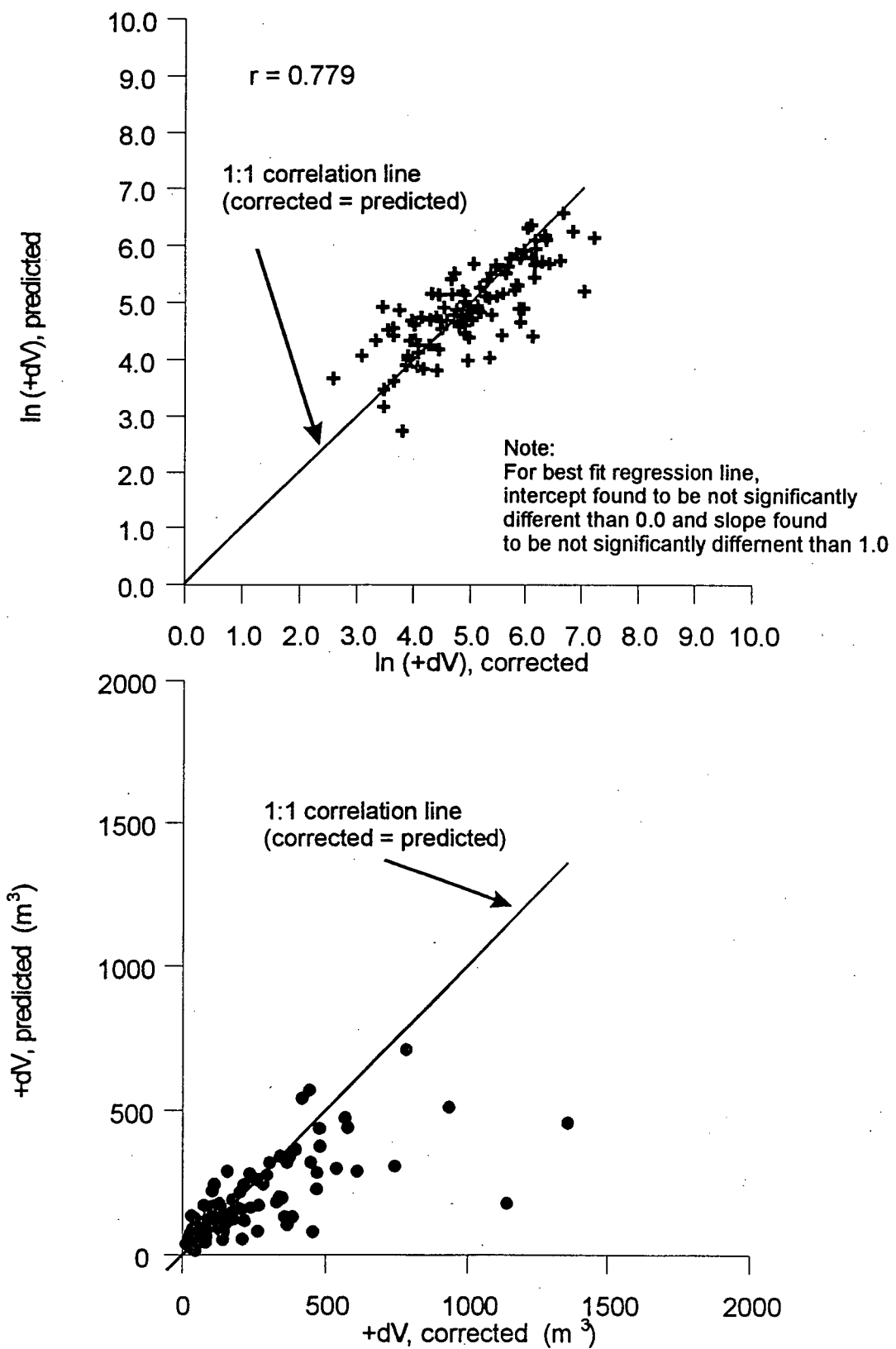


Figure 5.16: Test of subset regression equations, entrainment
Confined Flow Reaches, $10 \leq TH \leq 55$, Q.C.I. (Selected) Data

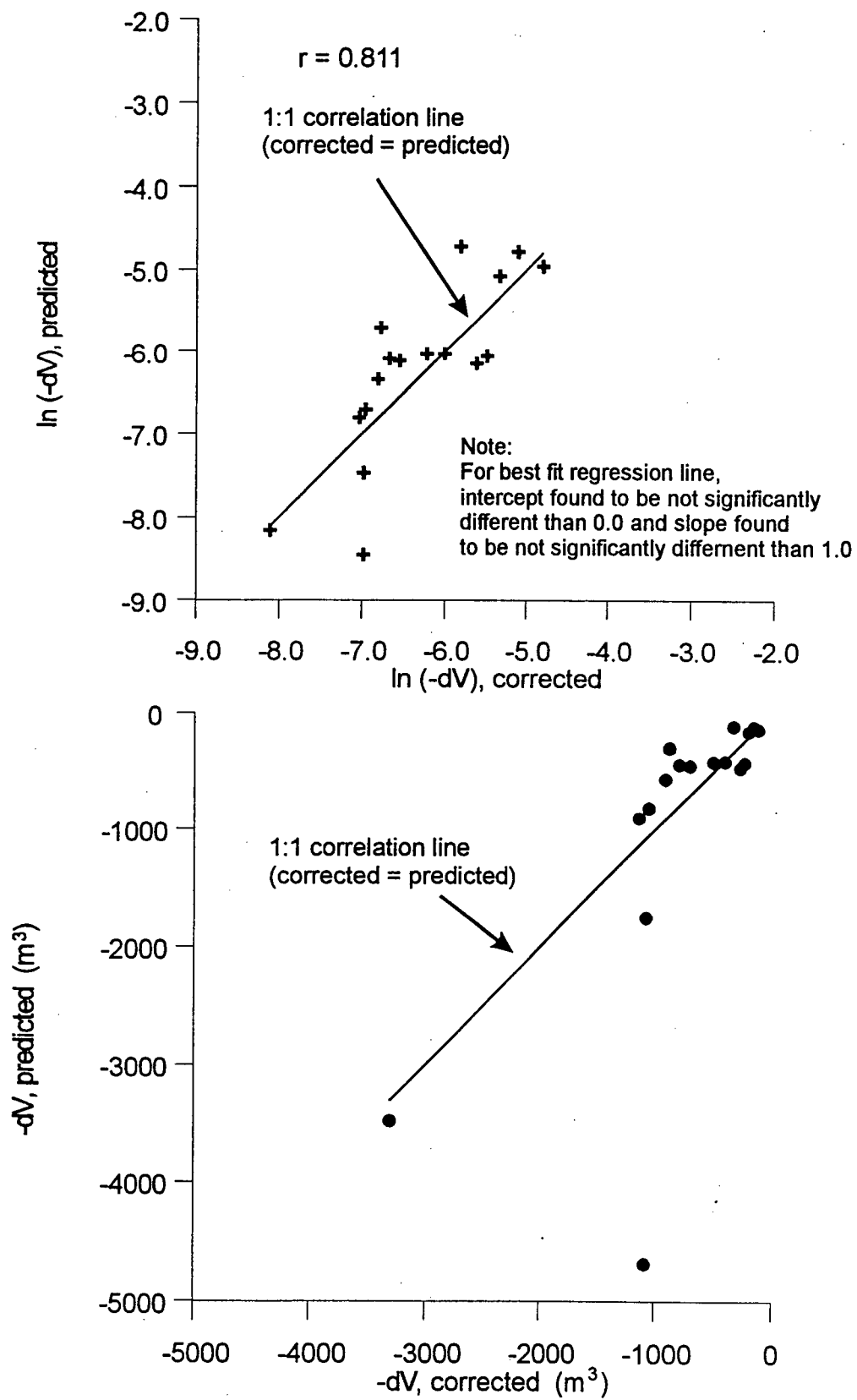


Figure 5.17: Test of subset regression equations, deposition
Transition Flow Reaches, $0 \leq TH \leq 20$, Q.C.I. (Selected) Data

Chapter 6 BACK-ANALYSES OF DEBRIS FLOW EVENTS

A back-analysis of 37 actual debris flow events was carried out to determine whether the Volumetric Model is able to predict the cumulative flow volume and travel distance for each event. The regression equations developed in Chapter 5 from the Q.C.I. (Selected) Data are used in the Volumetric Model. These regression equations, listed in Table 5.2, are used to calculate the entrainment or deposition volume for each reach of an event path, given the slope morphology and slope angle of the reach, as well as the length, width of entrainment/deposition, incoming flow volume, and bend angle function.

Selected Type 7 events from the Q.C.I. (Original) Data and Type 1, 2, and 3 events from the Supplementary Data were used for back-analyses. The selection criteria for these events was similar to that used for the Q.C.I. (Selected) Data: namely, the events must be three reaches or greater and the volumetric error (VE) must be less than or equal to 40% (Section 5.2). Note that Q.C.I. (Original) Type 7 events were not used to develop the regression equations in Table 5.2, since the total entrainment and total deposition volumes cannot be balanced for these truncated events. Events from the Supplementary Data were deliberately excluded from the regression analyses to provide independent data for testing. Consequently, both data sets are independent of the model development.

Table 6.1 summarizes the regression equations for different flow behaviour based on flow confinement and slope angle for each reach. The slope angles for the data used in the regression analyses are also given in square brackets to show the TH range for which the regression equations are valid. Note that for simplicity, the regression equation for transition

flow is applied to slopes of 20° or less, since there are few examples of deposition only behaviour above this slope angle. The slope angle ranges of the given flow confinement (slope morphology) conditions to determine the occurrence of entrainment or deposition, which stipulates which regression equation is used. Field observations (as recorded on the field data cards) for the reach length, width of entrainment or deposition, and slope angle are used as inputs into the regression equations for each reach. These data represent the observed volumes for the test cases, and no survey corrections were applied before they were input into the Volumetric Model. Initial volumes for the first reaches of the back-analyses were taken as equal to the initial volumes from field data.

Table 6.1: Summary of Regression Equations used in Deterministic Model

FLOW MODE	FLOW MODE*	REGRESSION EQUATION	Equation Number	Applicable Slope Range
UF	Deposition [0° ≤ TH ≤ 24°]	$\ln(-dV) = -0.514 - 0.988\ln(W_d) - 0.101BAF - 0.731\ln(L) + 0.0155TH$	[5.7]	(0° ≤ TH ≤ 18°)
	Entrainment [19° ≤ TH ≤ 29°]	$\ln(+dV) = 1.13\ln(W_e) + 0.787\ln(L) - 0.0636\ln(\Sigma V_i)$	[5.8]	(19° ≤ TH ≤ 29°)
	Entrainment [30° ≤ TH ≤ 55°]	$\ln(+dV) = 0.728 + 1.31\ln(W_e) + 0.742\ln(L) - 0.0464TH$	[5.9]	(30° ≤ TH ≤ 55°)
CF	Entrainment [10° ≤ TH ≤ 55°]	$\ln(+dV) = 0.344 + 0.851\ln(W_e) + 0.898\ln(L) - 0.0162TH$	[5.10]	(10° ≤ TH ≤ 55°)
TR	Deposition [0° ≤ TH ≤ 22°]	$\ln(-dV) = -1.54\ln(W_d) - 0.90\ln(L) + 0.123BAF$	[5.11]	(0° ≤ TH ≤ 20°)

*Slope angle range indicates range from data used in regression analyses

The back-analysis results from four events in the Type 7 Q.C.I. (Original) Data and four events in the Supplementary Data are discussed. Graphical results of the all events are presented in Appendix D. Discussion of the first two events for each set involves the success of the Volumetric Model in calculating the cumulative flow volume and change in flow volume when compared to the observed volumes. Discussion of the second two events addresses the lack of

agreement between observed volumes and the volumes calculated during the back-analysis using the Volumetric Model in specific types of reaches. These cases are the result of assumptions related to the slope ranges for use of the regression equations, restricting deposition on steep reaches and entrainment on relatively gentle slope angles.

Note that although Equation 5.7 to predict deposition in unconfined reaches is developed from data up to 24° , the application of the equation is restricted to slope angles of 18° or less. This is done to prevent dual mode flow, which was present in only a fraction of the reaches in the Q.C.I. (Selected) Data. Early attempts in using the Volumetric Model to back-analyze debris flow events with dual mode flow were unsuccessful, with the model predicting much lower cumulative flow volumes than the observed values. This result was due to the cancellation of entrainment and deposition volumes for every reach with TH in the range of 19° to 24° , when in fact much more often the reaches exhibited single mode flow behaviour. Thus, dual mode behaviour was eliminated from the Volumetric Model to facilitate modelling of typical, single mode flow behaviour.

6.1 Model Validation Using the Q.C.I. (Original) Data

The Volumetric Model was used to back-analyze 20 Type 7 events from the Q.C.I. (Original) Data. These events have a truncated deposition zone, and form the tributary branches to the main channel of a multiple debris flow event (Fannin and Rollerson, 1993), as described in Section 2.1.

Only Type 7 events with three reaches or more were used; events with fewer reaches are less likely to exhibit fully developed debris flow behaviour. The main channels of multiple events

(Types 5 and 6, see Table 2.2) were not chosen for back-analyses since the entrainment of debris volumes from the Type 7 tributary events cannot accurately be modelled by the regression equations due to the ambiguity of determining entrainment volumes in the reaches and on the fan of the main channel.

The regression equations used in the Volumetric Model were tested using the reach data from the Type 7 events and the Supplementary events. Figure 6.1 illustrates scatterplots of the results, showing observed against predicted volumes of entrainment and deposition, on a reach basis for all flow modes. There is reasonably good agreement in the results, with a correlation coefficient of 0.827 for unconfined flow and 0.772 for confined flow for entrainment. For deposition, correlation coefficients of 0.936 for unconfined flow and 0.907 for transition flow were calculated. Regression relationships were developed to test the significance of the results, comparing the best fit regression line to the correlation line shown in Figure 6.1. The regression relationships were found to be significantly different than the 1:1 correlation lines shown in Figure 6.1. However, the results show good visual agreement between the observed and modelled volumes, for both entrainment and deposition, when the regression equations are used to predict changes in volume for the Type 7 events and the Supplementary events.

The change in debris flow volume along the path of the Type 7 events is calculated for the events listed in Table 6.2. Appendix D contains the tabulated results and plots of the back-analyzed cumulative flow volume along the profile of each event, along with the observed flow volume based on the field survey data. A statistical analysis of the results of the back-analyses is carried out using the paired *t*-test to determine whether the differences between the modelled results and observed volumes are statistically significant. This is done by testing if the mean of the differences between the observed and calculated values is significantly different from zero,

given as hypothesis H_0 in Table 6.2, as discussed by Kennedy and Neville (1976). These tests were carried out on both the volume change for each reach and the cumulative flow volume. Testing with a 80% confidence level, 11 of the 20 Type 7 back-analyses proved to be statistically accurate with respect to the cumulative flow volume, with no significant difference in the observed and calculated values. On a reach-by-reach basis, paired t -tests proved that 18 of the 20 events have differences which are not statistically significant with respect to the change in volume along the path of the event. These results indicate that even if an error occurs in calculating the volume change in one reach of the event, these errors are likely small compared to the cumulative flow volume.

6.1.1 Event 2294

Figure 6.2(a) shows the observed and calculated cumulative flow volume, as well as changes in flow volume, along the path for Event 2294, Q.C.I. (Original) Data. This event is a tributary of a larger, multiple path debris torrent. The event initiated on an unconfined gully headwall with a V_{init} of 450 m³ and flowed through a gully channel (with one short, unconfined reach), and then joined the main channel of the multiple event some 365 m from the initiation point. The volume at the end of the first reach, a distance of 45 m along the flow path, is input into the model as equal to the observed volume from the actual event. The line connecting the crosses in Figure 6.2(a) indicates the "observed" total debris flow volume based on the measured field data; the light bars at the end of each reach illustrate the magnitude of the change in flow volume through the reach. The back-analysis results are shown by the line connecting the squares, indicating the modelled cumulative debris flow volume along the event path. The dark bars show the modelled change in flow volume in each reach of the debris flow path, calculated using the regression equations.

Table 6.2: Paired t-tests on Type 7 Events, Q.C.I. (Original) Data Σ

Event	n	$H_o: [(\Sigma V_{im} - \Sigma V_{io}) = 0]$		$H_o: [(dV_{im} - dV_{io}) = 0]$		Sig?
		t_{n-1}	t_m	t_m	t_m	
426	4	2.353	0.88	No	0.94	No
477	3	2.920	2.74	No	0.32	No
1011	4	2.353	-2.67	Yes	0.44	No
1410	4	2.353	1.09	No	0.73	No
1417	7	1.943	0.70	No	-0.58	No
1804	7	1.943	2.35	Yes	1.56	No
1913	3	2.290	-1.01	No	1.00	No
2255	3	2.290	3.65	Yes	1.01	No
2259	7	1.943	1.43	No	1.15	No
2274	10	1.883	-0.82	No	0.36	No
2287	4	2.353	-2.25	No	-0.94	No
2288	2	6.314	5.64	No	2.51	No
2290	5	2.132	2.14	Yes	0.31	No
2292	9	1.860	1.41	No	-0.64	No
2294	8	1.895	-7.74	Yes	1.78	No
2295	5	2.132	-15.30	Yes	-1.68	No
2296	7	1.943	5.14	Yes	1.95	No
22101	9	1.860	-3.54	Yes	-0.92	No
22111	21	1.725	-0.98	No	0.63	No
22112	4	2.353	-2.36	Yes	-0.22	No

Notes:

1. **Sig?** indicates whether the H_o (null hypothesis) is significant at $\alpha = 0.20$.
2. Two-tail test used to determine significance.
3. ΣV_i is the cumulative flow volume at the end of the reaches of the event path
4. dV_i is the change in flow volume within the reaches of an event
5. subscripts o and m indicate observed and modelled values, respectively

These results show that the back-analysis using the Volumetric Model accurately calculates the change in flow volume along the path of Event 2294. Although the calculated volumes are slightly less than the observed volumes, the model accurately characterizes the increase in cumulative flow volume along the path. From Table 6.2, The t -test value for the difference of

the total flow volumes is -7.74, indicating the difference between the modelled flow volume and the observed flow volume over the event path is significant at the 80% confidence level. For the changes in reach volumes, the *t*-test value is -1.78 indicating that the difference between the calculated and observed volumes is also not significant on a reach basis.

6.1.2 Event 22101

Figure 6.2(b) shows the back-analysis for Event 22101 from the Q.C.I. (Original) Data, another Type 7 event. This event was unconfined for the first six reaches (to a distance of 210 m along the flow path), and deposited material as it crossed a logging road (reach 4). At 210 m distance the flow moved into a gully and became confined. As for the plot showing the back-analysis of Event 2294, the line connecting the squares and dark bars show the calculated results from the Volumetric Model, and the line connecting the crosses and the light bars show the observed flow data. The initial volume of 1000 m³ is input as equal to the observed value.

Close agreement is evident between the values calculated in the back-analysis and the observed values. The *t*-test value for the volume difference at the end of the event path is -3.54, indicating that the differences between the calculated and observed values are insignificant at the 80% confidence level. The differences between the change in volume for each reach proved to be insignificant, with a *t*-test value of 0.038. This indicates that although differences between the cumulative flow volumes were significant, the differences in the change in volume between each reach was not significant. This may be a result of differences canceling out for reaches along the flow path.

6.1.3 Event 2290

Event 2290, a Type 7 Event in the Q.C.I. (Original) Data, was unconfined over its entire length of 310 m (Figure 6.3a). The initiation volume of the event was reported as 360 m³ and the event entrained an additional 310 m³ over its length. The observed volumes, calculated from field measurements of average entrainment width and depth for the length of each reach, imply that the event should have terminated after reach 2. However, this was not the case as the event flowed down to the main channel of a larger, multiple event.

Back-analysis using the Volumetric Model shows that due to the assumed behaviour of entrainment only on a reach slope angle of 29° does not account for the observed volume change in Event 2290. Thus, in reach 2, the slope angle of 29° leads to a model prediction of entrainment despite the observed deposition. Paired *t*-test results in Table 6.2 show that the differences between the changes in flow volumes are not significant. This result is due to the reasonable agreement between the calculated and observed changes in flow volumes along the event path. In this case the model predicts, with reasonable accuracy, the volume at the end of the event path but not the cumulative flow volume between the initiation point and the end of the path.

6.1.4 Event 2296

The back-analysis of Event 2296 is presented in Figure 6.3(b). Field survey data indicate this event was unconfined over its entire length. At a distance of about 300 m along the flow path from the initiation point, the event entered a gully channel, contributing a total of 951 m³ of material to the main channel of a multiple event.

The back-analysis of the cumulative flow volume is in approximate agreement with the observed flow volume for reaches 2 and 3; however, in reaches 4 and 5 the model calculates entrainment even though deposition only was recorded for these reaches in the field survey. As the 27° slope angle for reaches 4 and 5 is greater than 18° , the model assumes entrainment of material through these reaches. Volumes of entrainment calculated for the remainder of the reaches along the event path are approximately equal to the observed volumes.

6.2 Model Validation Using Supplementary Events

A back-analysis of 17 selected events in the Supplementary Data was also carried out using the Volumetric Model. Events were selected for back-analysis from the Supplementary Data if the volumetric error for the event is less than 40%. Volume corrections were applied to the events prior to back-analysis to balance total entrainment and total deposition volumes, as described in Section 5.2, to provide a consistent framework for evaluation of the model.

As before, inputs to the model included the initial volume as observed in the field and data for each reach of the event path. On a reach basis, the input data used are the reach morphology (to determine flow confinement), the reach slope angle, as well as the necessary predictors for the regression equations: measured reach length, measured width of entrainment or deposition, and measured slope and azimuth angles.

Paired *t*-tests were carried out to compare the results for the cumulative flow volume along the path as well as the change in volume for each reach. The results of the tests are presented in Tables 6.3, comparing the modelled results with the observed volumes. For the back-analyses of these 17 supplementary events, 16 of the events proved to show no significant difference

between the observed cumulative flow volume and the calculated cumulative flow volume (for an 85% confidence level). However, 15 of the events proved to have a significant difference in the change in volume between the observed data and the calculated results of the back-analysis. As was the case for the back-analyses of the Type 7 events, this difference can be attributed to the differences in the reach change in volume being large relative to the observed volume change but not large relative to the cumulative flow volume of the event.

Table 6.3: Paired t-tests using Supplementary Events

Event	<i>n</i>	$H_o: [(\Sigma V_{im} - \Sigma V_{ic}) = 0]$			$H_o: [(dV_{im} - dV_{ic}) = 0]$	
		t_{n-1}	t_m	Sig?	t_m	Sig?
3001	9	1.860	-3.72	Yes	-0.06	No
3005	13	1.782	-4.51	Yes	0.17	No
3006	10	1.833	-3.77	Yes	-0.13	No
3104	3	2.290	-3.73	Yes	-0.44	No
3201	10	1.833	1.70	No	0.99	No
3202	7	1.943	-0.59	No	0.27	No
3203	8	1.895	-2.00	Yes	0.44	No
4001	16	1.753	-1.21	No	0.38	No
4002	4	2.353	-0.08	No	-0.49	No
4102	6	2.015	-4.94	Yes	-3.24	Yes
5001	8	1.895	-5.62	Yes	-1.13	No
5002	10	1.833	-4.78	Yes	-0.66	No
5003	9	1.860	-8.44	Yes	-1.35	No
5101	5	2.132	3.17	Yes	2.87	No
5301	7	1.943	-2.65	Yes	-0.78	No
5402	18	1.740	-9.50	Yes	0.54	No
5501	4	2.353	-4.62	Yes	-0.32	No

Notes:

1. **Sig?** indicates whether the H_o (null hypothesis) is significant at $\alpha = 0.20$.
2. Two-tail test used to determine significance.
3. ΣV_i is the cumulative flow volume at the end of the reaches of the event path
4. dV_i is the change in flow volume within the reaches of an event
5. subscripts o and m indicate observed and modelled values, respectively

Using the same format as Section 6.1, the back-analyses of four events are discussed.

Tabulated values and graphical results of back-analyses for the remaining events are contained in Appendix D.

6.2.1 Event 4001

Event 4001 initiated on an open slope and flowed into a gully channel at a slope distance of 49 m along the event path. The flow continued down the gully and onto a fan at the base of the gully, some 375 m from the initiation point, and would be classified as a Type 2 event according to Fannin and Rollerson (1993). The event was surveyed in the Eve River Watershed, southeast of the Tsitika Valley on Northern Vancouver Island.

Figure 6.4(a) shows the observed, corrected, and calculated volumes for Event 4001. The calculated total flow volume for the back-analysis is in good agreement with the corrected total flow volume, particularly along the first portion of the event where the flow is entraining material both through unconfined reaches and confined gully reaches. The model estimate of travel distance is also in reasonable agreement with the observed data, as termination of the modelled flow would be expected in the reach immediately following the end of the surveyed geometry.

In reach 14, a predicted zero change in flow volume is the result of the model assumption that only entrainment is possible at slope angles greater than 19° . Since only deposition was observed in this reach, an input of zero width recorded for entrainment and the constraint that no deposition is possible above 18° resulted in a zero value for change in flow volume through reach 14. Although this discrepancy could have been much larger if the reach was longer, the

magnitude of the difference relative to the total flow volume is small such that only a minor error is introduced.

Note that if dual mode behaviour was permitted in the Volumetric Model, the error in Reach 14 would have been less than that with the single mode of flow behaviour which is modelled. However, the majority of reaches, which exhibit single mode behaviour, would have larger errors with the dual mode behaviour leading to underestimates of deposition and entrainment for reaches in the slope range of 19° to 24° .

A comparison of the difference between the observed flow volume with the calculated flow volume at the end of the event path yields a paired *t*-test value of -1.21, indicating the difference between these two sets of volumes is insignificant at the 80% confidence level. On a reach basis, the difference between the corrected and calculated change in volume is also not significant, indicating that the errors for each reach are small relative to the magnitude of the volume change in the reach. Small errors in the calculation of change in volume are evident, but these do not greatly affect the ability of the Volumetric Model to calculate the cumulative peak flow volume or the travel distance of the event.

6.2.2 Event 3202

Results from the back-analysis of Event 3202 in the Mamquam Watershed near Squamish are presented in Figure 6.4(b). This debris slide (Type 1) event initiated on an open slope and remained unconfined over its entire path. The calculated total flow volume at the end of the surveyed path was 104 m^3 , at a distance of 266 m from the initiation point of the flow.

The assumed applicable slope ranges for application of the regression equations, Table 6.1, resulted in differences between the observed and calculated changes in flow volume. In reaches 3 and 4 of the event, the modelled flow behaviour is opposite to that of the observed behaviour: for reach 3 TH is 21° , and the Volumetric Model assumes the flow would entrain material; for reach 4, the Model assumes the flow would deposit on a slope of 17° , but the observed response was one of entrainment. However, these differences proved to be relatively minor compared to the initial volume of the flow and the prediction of both cumulative peak flow volume and travel distance appear to be in good agreement with the observed flow data.

An examination of the results of the corrected total flow volume and the calculated total flow volume reveal that the two are in excellent agreement. The paired t -test value comparing the observed and modelled cumulative flow volumes is -0.59 , providing evidence that the differences are not significant at the 80% confidence level. The differences between the change in volume for the observed data and the modelled results are also statistically not significant.

6.2.3 Event 5501

Event 5501 is a Type 1 (debris slide) event on Nootka Island that remained unconfined over its entire length of 99 m. For this event, the volume correction applied to the observed data decreased the volumes of deposition over the event path length to balance total entrainment and deposition volumes (Figure 6.5a). The dark line showing the back-analyzed cumulative flow volume compared with the plot of the corrected total volume illustrates another instance where the flow behaviour is different to that assumed in the Volumetric Model in reaches 3 and 5. In these cases, the observed flow response was deposition on slopes steeper than 18° , while the

model calculated an entrainment volume equal to zero since the surveyed W_e measurements were zero for these reaches.

6.2.4 Event 3006

Event 3006 represents a very large debris avalanche on the west side of the Queen Charlotte Islands in Rennell Sound, above Riley Creek. The volumes in this event are much larger than any of the other events in either the Q.C.I. (Original) Data or the Supplementary Data. The path length for the event is 461 m, with the flow being unconfined over the entire length. The cumulative flow volume plot is presented in Figure 6.5(b).

The results of back-analysis of the event show that the calculated volumes are consistently much less than the observed volumes in the field. Inspection of the flow volume along the profile of the event shows the volumetric model does not calculate the peak volume of the event accurately.

One possible reason for the error in the results calculated by the model is due to the difference in volume scale Event 3006 and all the others in the data. Based on observations by Takahashi (1980) and Hungr *et al* (1984) smaller debris flow events often terminate earlier than large events, since the larger events are able to transfer momentum between reaches more efficiently. This example illustrates that a limitation for application of the Volumetric Model is that only smaller debris slide events on unconfined slopes, such as many of those which occur after clearcut logging, can be modelled successfully using the regression equations developed in this study.

6.3 Summary

From the results of a deterministic back-analysis of 37 debris flow events using the Volumetric Model, the calculated debris flow volume changes for 36 events proved to have insignificant differences when compared to actual total flow volumes. For the truncated Type 7 events, the observed flow volumes were used as the basis for comparison of the modelled results, whereas the corrected volumes of the Supplementary Data were used for comparison of results. Errors in the calculated cumulative flow volumes for each reach proved to be statistically significant in most cases. However, favourable results were obtained from a visual comparison of the results and significance testing on the changes in flow volumes along the reaches of the events. These results indicate that although some differences may exist between the calculated and actual volumes, they do not appear to greatly influence the prediction of a zero flow volume (and hence event termination) along the debris flow path.

Discrepancies in the assumption of flow behaviour affect the calculated total flow volume for back-analyses. These discrepancies occurred in reaches where the model assumed entrainment behaviour due to a steep slope angle, but in fact deposition was observed. Conversely, in some reaches deposition was expected due to flat slope angles, but only entrainment was reported. These situations are considered atypical flow behaviour. For debris flow events, deposition on steep slope angles (greater than 19°) is likely attributed to flow with a low water content or loss of confinement. Entrainment of material on slopes flatter than 19° may occur when the debris flow volume is significantly larger than the flows modelled by the regression equations, or the flows have an unusually high water content.

Since a deterministic model is constrained to modelling typical behaviour, Chapter 7 discusses how probability is incorporated to simulate the variation in flow behaviour in unconfined reaches with intermediate slope angles. Also, Monte-Carlo type sampling is used to generate repeated simulations for probabilistic modelling, which in turn can be used to determine the probability of travel distance excellence for locations along the event path, an important parameter for risk assessment of debris flow hazards.

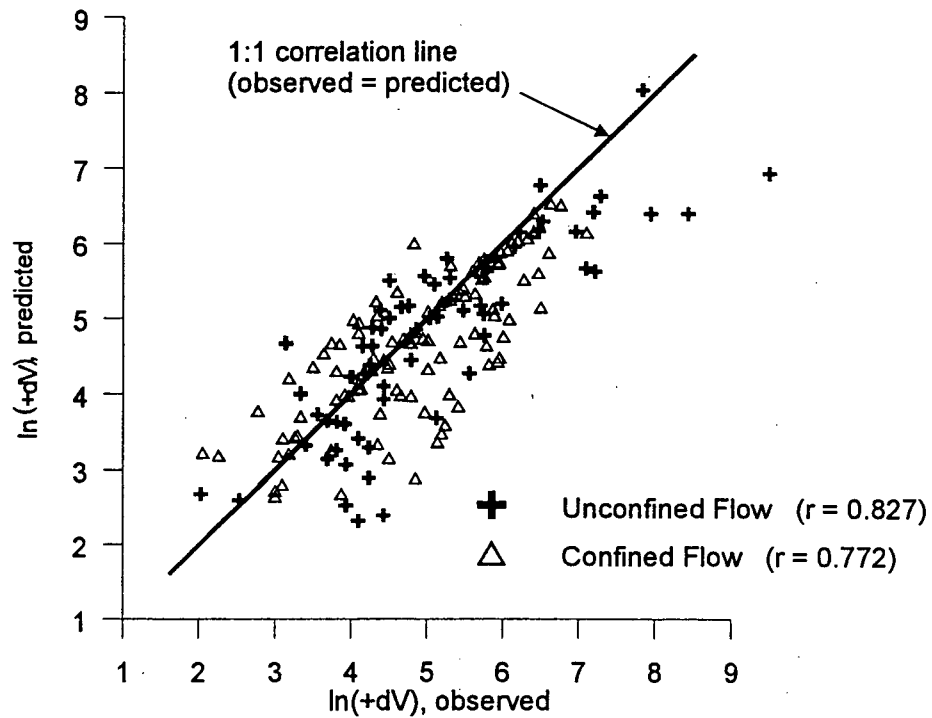


Figure 6.1(a): Test of entrainment regression equations using Type 7 Q.C.I. (Original) Data and Supplementary Data

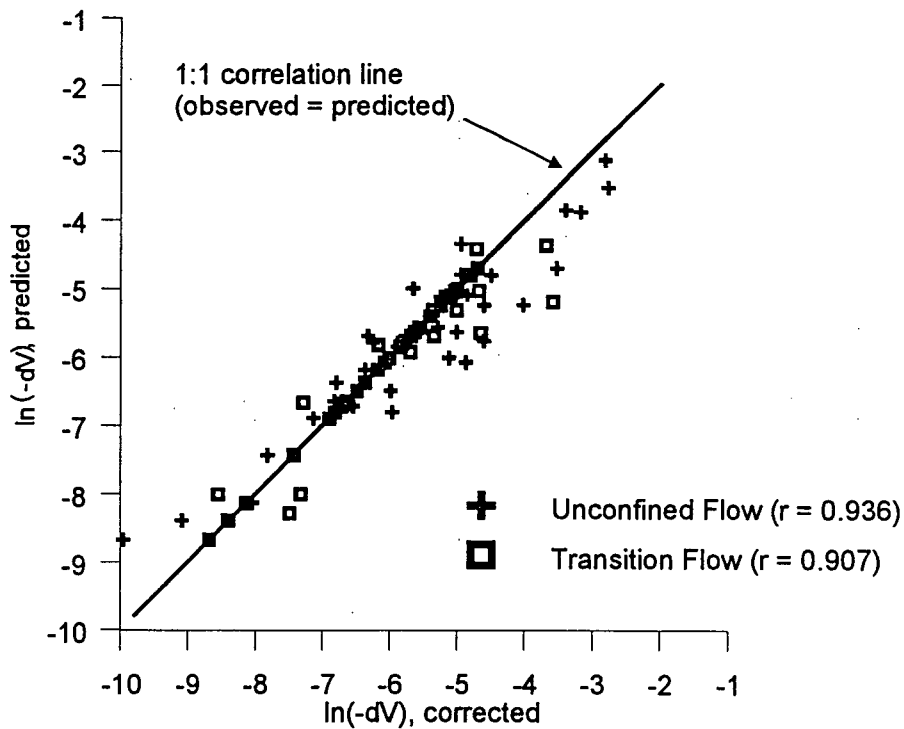


Figure 6.1(b): Test of deposition regression equations using Type 7 Q.C.I. (Original) Data and Supplementary Data

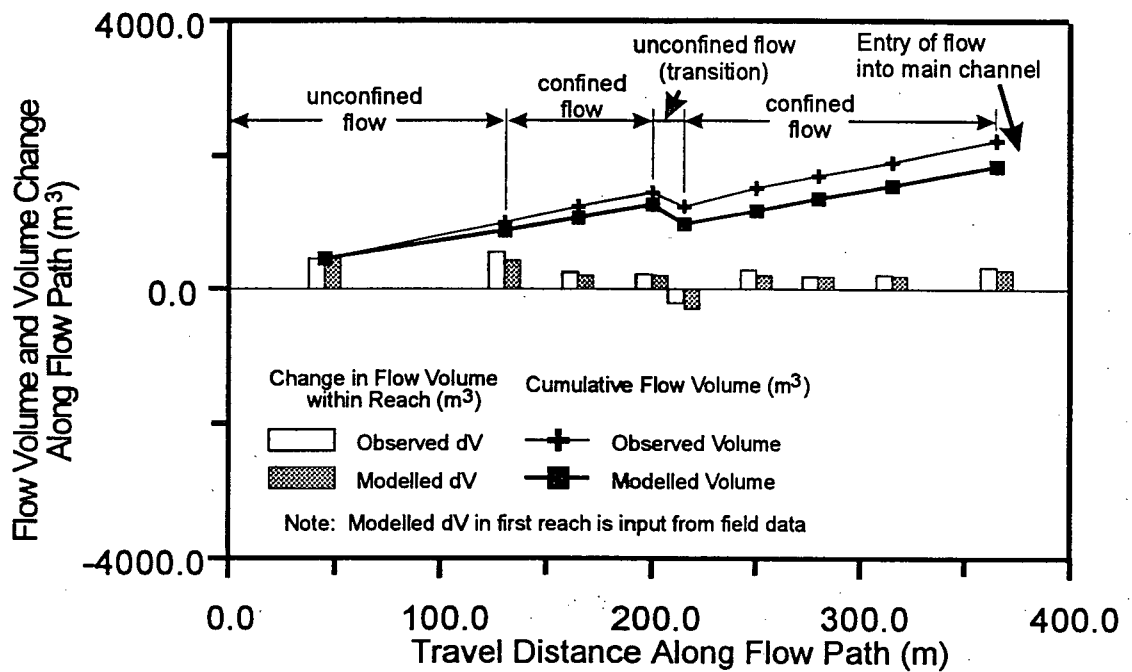


Figure 6.2(a): Back-Analysis of Event 2294, Q.C.I. (Original) Data

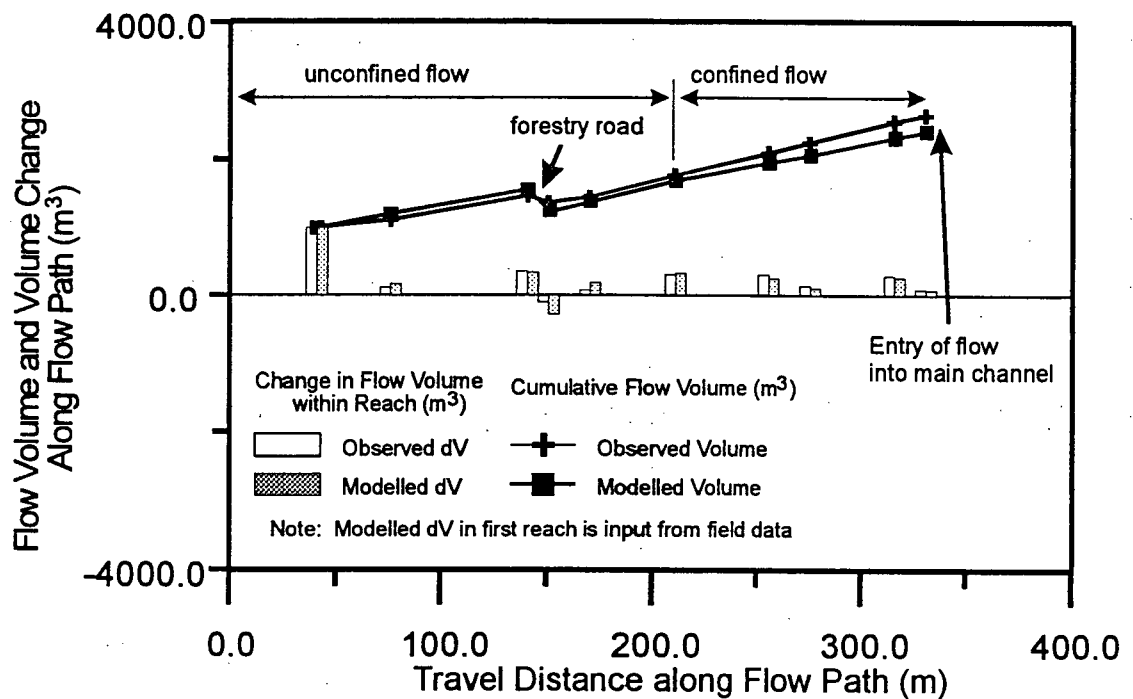


Figure 6.2(b): Back-Analysis of Event 22101, Q.C.I. (Original) Data

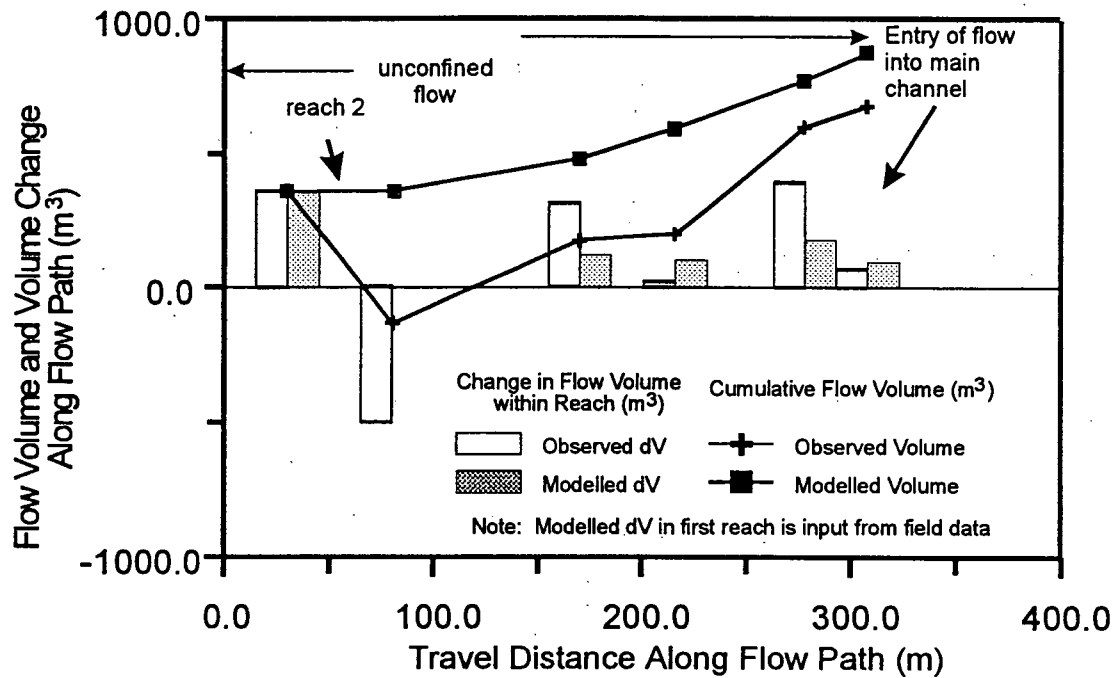


Figure 6.3(a): Back-Analysis of Event 2290, Q.C.I. (Original) Data

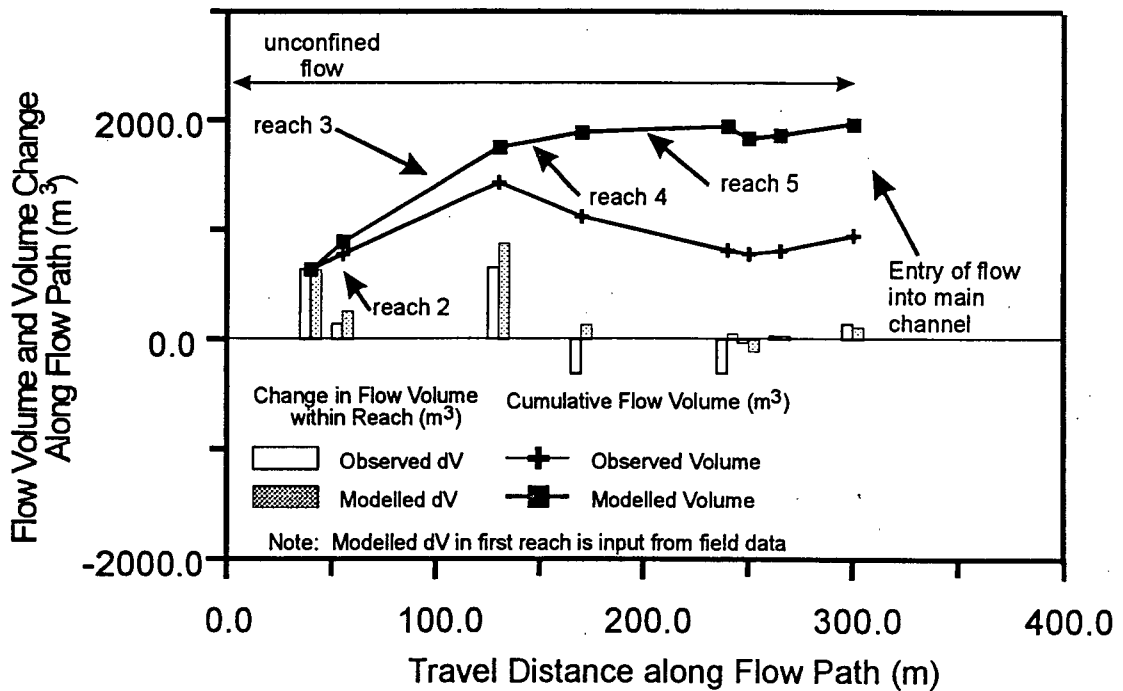


Figure 6.3(b): Back-Analysis of Event 2296, Q.C.I. (Original) Data

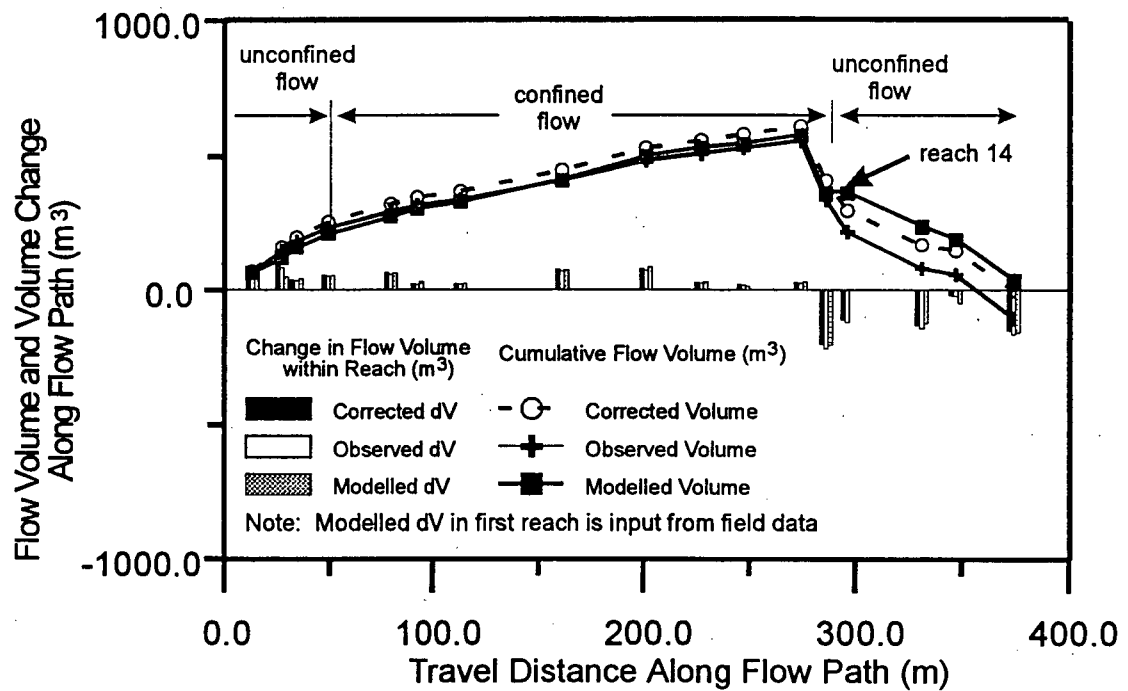


Figure 6.4(a): Back-analysis of Event 4001, Eve River Data

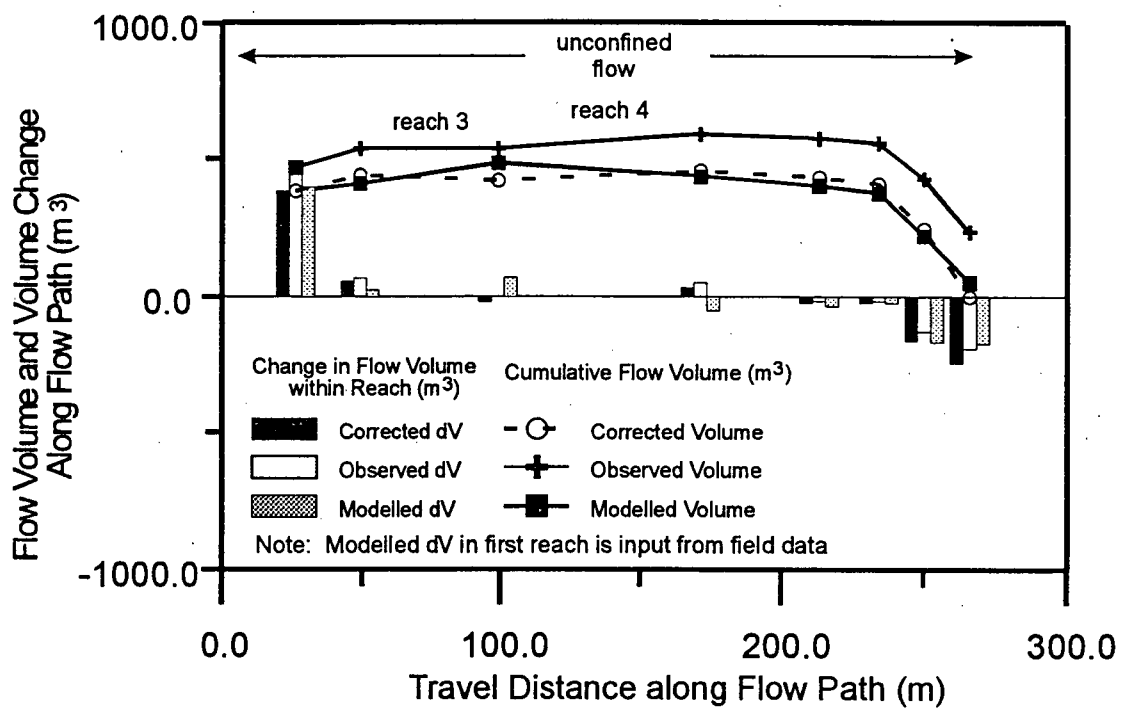


Figure 6.4(b): Back-analysis of Event 3202, Mamquam River Data

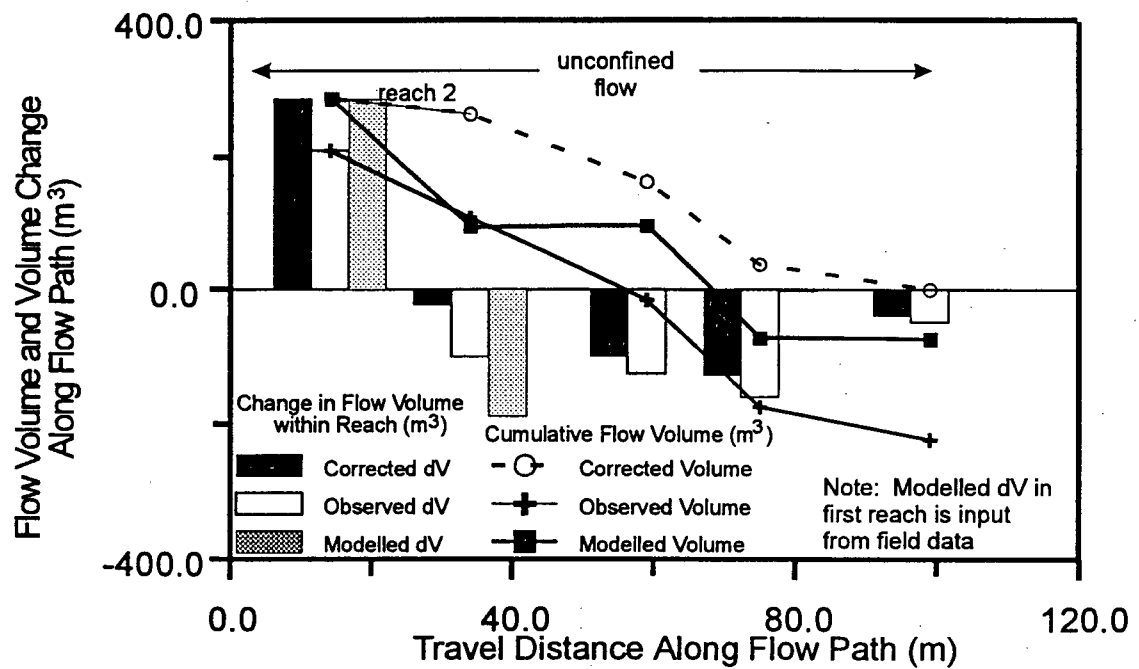


Figure 6.5(a): Back-analysis of Event 5501, Nootka Island Data

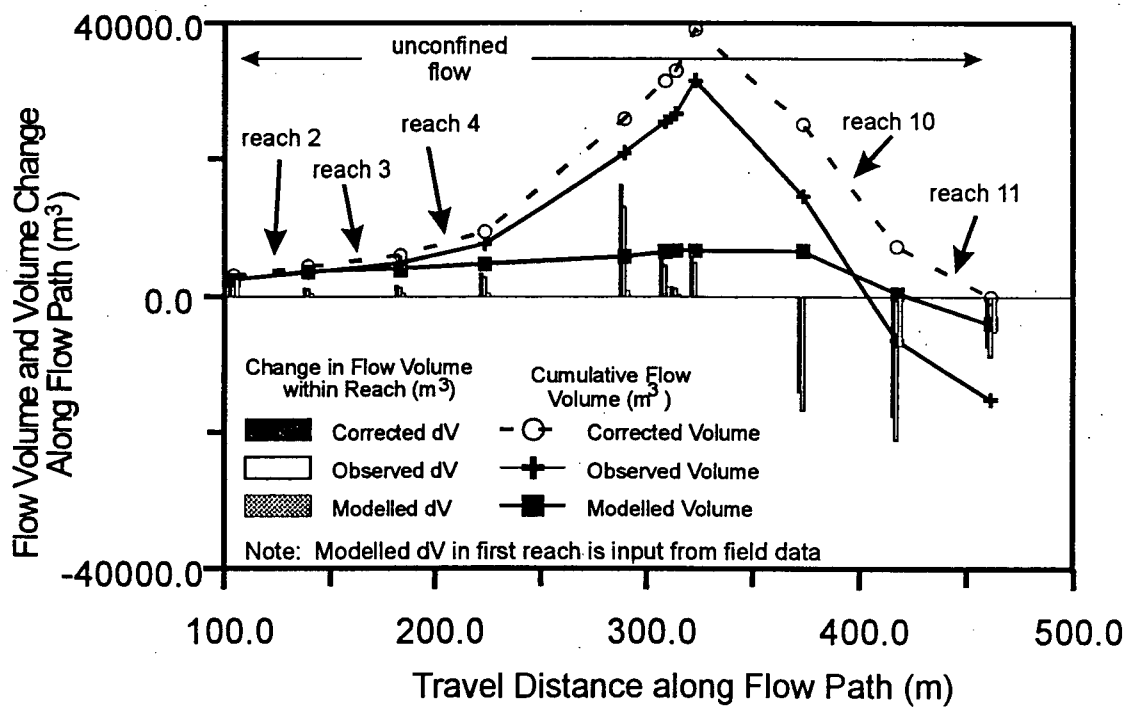


Figure 6.5(b): Back-analysis of Event 3006, Q.C.I. (Additional) Data

Chapter 7 PROBABILISTIC MODELLING USING *UBCDFLOW*

7.1 General

The creation of *UBCDFLOW* from the Volumetric Model used in Chapter 6 for the back-analyses of debris flow events is discussed. Six examples are presented showing the application of *UBCDFLOW* to calculate the probability of a debris flow travelling to a point of interest along the path, based on the cumulative flow volumes and travel distances of simulated flows.

From the back-analyses of events in Chapter 6 using the Volumetric Model, it was concluded that a deterministic framework could not adequately characterize the variability observed in cumulative flow volumes of actual debris flow events. Discrepancies between the observed and modelled behaviour are attributed to the assumed flow mode on ranges of slope angles for unconfined flow, which is a result of application of the regression equations over specific slope ranges. Similar discrepancies were observed related to the assumption of deposition in confined flow reaches, and entrainment in transition reaches. For the regression equations, the single set of input parameters for the Volumetric Model can also present a problem in terms of prediction: the widths of entrainment and deposition are not known precisely for each reach prior to an event, but often can be estimated as a probable range of values. Also, based on field observations, both entrainment and deposition may occur in the same reach, and it is difficult to determine this combined flow behaviour using a deterministic model as this behaviour does not occur in every reach and there is no means of applying specific regression equations in some reaches and not others, and dual mode flow cannot be modelled (see Section 6.0). The

case of prediction is also subject to uncertainty in the initial volume from the first reach, which cannot be characterized by a deterministic model where only a single value is used.

UBCDFLOW incorporates probability density functions (p.d.f.'s) to account for the uncertainty in the initial volume, V_{init} , of potential flows as well as the flow widths, W_f , for each reach. The calculation of entrainment width, W_e , and deposition width, W_d , are discussed in Section 7.2 for different flow modes. Each simulation of the Volumetric Model uses different values sampled from the p.d.f.'s to calculate a single cumulative flow volume along the travel path. The travel distance for this simulated flow can be calculated as the sum of the reach lengths until the cumulative flow volume decreases to zero. Repeated simulations are carried out to determine the cumulative flow behaviour along the debris flow event path, and the probability of exceedance, $P(Ex)$, at the end of each reach along the travel path based on the flow volumes of the simulations. The probability of exceedance is required for a quantitative risk assessment of the potential debris flow hazard at a given location, as discussed in Chapter 1.

The remainder of Section 7.1 describes the assumptions and criteria which must be satisfied for the valid application of *UBCDFLOW* along a potential debris flow travel path. Section 7.2 discusses the incorporation of probability into the Volumetric Model by introducing p.d.f.'s to account for the uncertainty governing the input data (predictor variables) for the regression equations of the Volumetric Model. Comments regarding the field application of the model are also made. Six example scenarios, at two debris flow sites, are presented in Section 7.3 to demonstrate the application of *UBCDFLOW*.

7.1.1 Assumptions for the Application of *UBCDFLOW*

The application of *UBCDFLOW* to the risk assessment for debris flow hazards can be carried out for potential debris flow event paths which meet criteria based on the applicability of the regression equations developed from the Q.C.I. (Selected) Data, Table 7.1. Situations where the regression equations are considered valid are described below.

Table 7.1: Summary of Regression Equations used in *UBCDFLOW*

Flow Mode	Flow Behaviour	REGRESSION EQUATION		Deterministic Applicable Slope Range	<i>UBCDFLOW</i> Applicable Slope Range
UF	Deposition $0^\circ \leq TH \leq 24^\circ$	$\ln(-dV) = -0.514 - 0.988 \ln(W_d) - 0.101 BAF - 0.731 \ln(L) + 0.0155 TH$	[5.7]	$0^\circ \leq TH \leq 18^\circ$	$0^\circ \leq TH \leq 24^\circ$
	Entrainment $19^\circ \leq TH \leq 29^\circ$	$\ln(+dV) = 1.13 \ln(W_e) + 0.787 \ln(L) - 0.0636 \ln(\Sigma V_i)$	[5.8]	$19^\circ \leq TH \leq 29^\circ$	$19^\circ \leq TH \leq 29^\circ$
	Entrainment $30^\circ \leq TH \leq 55^\circ$	$\ln(+dV) = 0.728 + 1.31 \ln(W_e) + 0.742 \ln(L) - 0.0464 TH$	[5.9]	$30^\circ \leq TH \leq 55^\circ$	$30^\circ \leq TH \leq 55^\circ$
CF	Entrainment $10^\circ \leq TH \leq 55^\circ$	$\ln(+dV) = 0.344 + 0.851 \ln(W_e) + 0.898 \ln(L) - 0.0162 TH$	[5.10]	$10^\circ \leq TH \leq 55^\circ$	$10^\circ \leq TH \leq 55^\circ$
TR	Deposition $0^\circ \leq TH \leq 22^\circ$	$\ln(-dV) = -1.54 \ln(W_d) - 0.90 \ln(L) + 0.123 BAF$	[5.11]	$0^\circ \leq TH \leq 20^\circ$	$0^\circ \leq TH \leq 20^\circ$

1) Topography and Land Use. The site for the debris flow risk assessment is in areas of coastal B.C. with generally similar surficial geology, topography, and precipitation as the Queen Charlotte Islands. These conditions include relatively thin, coarse grained soil veneers/mantles over compact glacial till or bedrock and relatively steep slopes. The contact between the soil strata and the competent strata usually forms the failure plane for the initiation of debris flow events. Periods of intense precipitation must also occur sufficiently often to create moist soil conditions. As the data used in the model were obtained from terrain where clearcutting has been carried out, the model is not applicable to determine the travel distances from natural (unlogged) terrain.

- 2) **Input Parameters.** The potential debris flow path must be surveyed in the field, typically from the assumed initiation point down to the point(s) of interest along the debris flow path. The ends of the survey reaches must coincide with the points of interest along the debris flow path. Table 7.2 contains a list of the six parameters which must be included in a field survey of a potential debris flow initiation point and event path, as well as the recommended measurement ranges for these parameters. Note that ΣV , the incoming flow volume for each reach after the initial reach, is calculated within the model and the result is used as an input into the regression equations.
- 3) These ranges are based on the Q.C.I. (Selected) Data used in the development of the regression equations. Section 7.2 discusses the development of p.d.f.'s for the initial volume and flow width.

Table 7.2: Input parameters for UBCDFLOW

Parameter	Description	Measurement
V_{init} (m ³)	Initial volume from assumed initiation point	see Section 7.2.1
For each reach of potential debris flow path		
SM	Slope morphology (to determine flow mode)	landform type
L (m)	reach length	field measurement
TH (deg)	average slope angle over reach length	0° to 55°
AZ (deg)	average azimuth angle over reach length	0° to 360°
W_f (m)	estimated width of event though reach	field measurement

- 4) The peak flow volume of the potential debris flow event should not exceed an upper limit, taken arbitrarily as 4000 m³. This bound is recommended since it is approximately equal to the upper bounds for debris flow events in the Q.C.I. (Selected) data which were used in the development of the regression equations and the largest event which was successfully back-analyzed in Chapter 6.

7.2 Probabilistic Modelling

Figure 7.1(a) presents a flow chart which demonstrates the simulation procedure using the Volumetric Model. For a known initiation location and travel path, an initial volume is selected from a user-defined p.d.f.. The flow is routed downslope into the second reach. Based on a user-defined p.d.f. for W_f , a flow width is selected and from the slope morphology and slope angle of the reach, is designated as entirely deposition (W_d), entirely entrainment (W_e), or proportioned into W_e and W_d (see Section 7.2.3). The entrainment volume $+dV$ and/or deposition volume $-dV$ is calculated using the regression equations. If the sum of the incoming flow volume ΣV and the net change in volume dV (equal to the sum of $+dV$ and $-dV$) is greater than zero, the flow is routed into the next reach; if the sum is less than zero, negative volumes are calculated for all remaining reaches.

The probability density functions within *UBCDFLOW* are sampled using the Latin Hypercube Technique (Pallisade, 1994). This technique is an alternative to traditional Monte Carlo sampling whereby the cumulative probability distribution for a p.d.f.. is stratified into five intervals, and then samples without replacement are obtained from each interval. The advantage of Latin Hypercube over Monte Carlo sampling is that Monte Carlo sampling can lead to "clustering" of sample locations in the middle of the cumulative probability distribution, particularly for limited simulations of some types of distributions. The Latin Hypercube technique is also preferable for modelling low probability outcomes, since it ensures that outlying portions of the p.d.f. are adequately sampled for each scenario.

Repeated simulations within a scenario form the basis for calculating the $P(Ex)$ at the end of each reach as outlined in Figure 7.1(b). After the specified number of simulations (2000 for

these analyses) have been completed, the number of simulations which terminate within each reach are identified. Subsequently, the number of events passing the end of each reach can be determined and are used to calculate $P(Ex)$, discussed in Section 7.2.4.

7.2.1 Prediction of Initial Volume, V_{init}

Measurements and other information from the field survey of a potential debris flow site can provide information for the prediction of the initial volume of the failure. Locations identified as being potentially unstable can be examined and the downslope length and width of the unstable soil mass, as well as the estimated depth to the failure plane, can be measured or estimated. Even if these dimensions are not known precisely, they can typically be bounded by estimates of the minimum, maximum, and most likely values for each dimension. These data can then be used as a triangular p.d.f. distribution for the initial volume at the potential failure site, although other types of p.d.f.'s can be used in *UBCDFLOW*. Figure 7.2(a) shows the p.d.f. of an initial debris flow volume based on estimated averages for length, width, and depth to failure plane of an unstable soil mass. The initial volume is then assumed to be equal to the flow volume exiting reach 1 of the debris flow path.

Existing failures in an area and statistical analyses of failures for various slope geometries may also provide information which can be used to estimate the initial volumes of failures. Nearby areas with similar surficial geology and topography which have experienced failures can also be used as a basis for determining a p.d.f. for V_{init} . Histograms of initiation volumes on four common slope morphologies in the Q.C.I. (Original) Data are presented in Figure 7.2(b). Together they account for 96% of all the initiation points in the Q.C.I. (Original) Data Set, with the remainder of the events having initiated on stream escarpments or road cutslopes. For these data, open slope reaches have the largest initial volumes, while gully channel and gully

sidewall morphologies have the smallest. In addition, Figure 7.2(c) illustrates how V_{init} from roadfill failures can be determined by multiplying an average cross-sectional area of the road prism by the estimated length of road which would be incorporated, with both the cross-section area and/or the length input as a p.d.f.

7.2.2 Prediction Reach Flow Width, W_f

The predicted flow width, W_f , must be determined at the time of a field survey for each reach of a potential debris flow path. Based on slope morphology, the reaches can be divided into unconfined flow, confined flow, and transition flow.

The width of confined reaches can be estimated based on measurements of the average width of the gully channel during the field survey. A schematic distribution for a confined flow reach is presented in Figure 7.3. Minimum and maximum values for the triangular distribution should reflect the variability in reach width along the gully reach. Note that other distributions, such as normal or lognormal, can be used to characterize the variability of flow width along the reach if sufficient data are available to calculate the standard deviation in the mean.

Determining the potential event width of unconfined reaches can be carried out by carefully considering the effect of micro-topography in the reach. For example, slight open slope depressions and local high points on the hillslope can define the likely maximum values for W_f . Minimum values should also reflect the relative size of the initiation volume. Also, the W_f for unconfined reaches should be chosen in conjunction with the estimated widths for reaches immediately upslope and downslope of the reach under consideration: unless a change in the microtopography dictates otherwise, W_f can be estimated as having the same p.d.f. as the reach immediately upslope. Note that the p.d.f. for unconfined flow has a larger spread between

minimum and maximum values than the p.d.f. for confined flow, which is indicative of the larger possible variability expected in W_f for unconfined flow.

The W_f for transition reaches is the average width of that reach where the flow emerges from a gully channel. Existing failures in the area or the relative divergence of debris fans at the base of the gully, as well as the depth of incision of a channel on the fan, may provide guidance in characterizing the p.d.f. for the transition reach.

7.2.3 Prediction of Deposition Width, W_d

The widths of deposition and/or entrainment are used in the regression equations to calculate change in volume within each reach of an event. The calculation of W_d and/or W_e for each reach is different for each flow mode, and based on observed flow behaviour for reaches in the Q.C.I. (Original) Data. The calculation of both W_d and W_e for a single unconfined reach is the means by which UBCDFLOW models dual mode flow. Since the occurrence of dual mode flow within UBCDFLOW is based on actual data, as described below, its presence reflects its actual occurrence in the Q.C.I. (Selected) Data. Further discussion on volume change behaviour and its use in partitioning the Q.C.I. (Selected) Data prior to regression analyses is presented in Section 5.3.3.

7.2.3.1 Unconfined Flow

The behaviour of unconfined flow on intermediate slope angles was observed to include single mode behaviour (entrainment only, deposition only) and dual mode behaviour (both entrainment and deposition) for the events in the Q.C.I. (Original) Data (Section 5.3.3, Figure 5.7). The deterministic Volumetric Model was constrained to entrainment on slopes 19° or greater, and deposition on slopes of 18° or less (Table 7.1) to prevent modelling of dual mode

flow. As discussed in Section 5.3.3, attempts to include dual mode behaviour in the Volumetric Model were not successful in modelling typical flow behaviour. A probabilistic sampling technique, discussed below, is developed to model dual mode behaviour in unconfined reaches of intermediate slope angle in *UBCDFLOW*.

The probabilistic sampling technique is based on Figure 7.4, which shows the volume behaviour occurrence for unconfined flow reaches in the Q.C.I. (Original) Data. Note that this plot does not apply a filter (to group entrainment and deposition reaches which displayed less than 20% entrainment or deposition), and consequently differs from Figure 5.7. The boundary between single mode (entrainment only) behaviour and dual mode behaviour is approximated by Line E, which represents a visual fit to the boundary. Similarly, the lower boundary between the deposition only reaches and the dual mode reaches is approximated as a bilinear boundary, Line D. Reaches above Line E, noted as Region E, have only entrainment, hence W_d is equal to zero for these reaches. The opposite is true for Region D: W_e is equal to zero since only deposition was observed. The volume behaviour occurrence for each value of TH is normalized by the total number of reaches, and presented as a stacked bar graph (Figure 7.4).

Note that Figure 7.4 illustrates that dual mode flow occurs often for unconfined reaches of 15° to 30° . However, the regression equation for deposition which can be applied up to 24° , given the slope range over which the data was developed. Similarly, the regression equation for entrainment can be applied down to slopes of 19° . Thus, the sampling technique models non-entrainment on slopes above 24° in effect neglecting deposition on these steeper reaches. Non-deposition on slopes less than 19° was also assumed, neglecting entrainment on these flatter slopes. An overall range of 16° to 27° was chosen for the probabilistic sampling technique in

UBCDFLOW, based on the lower bound for TH vs $+dV$ and the upper bound for TH vs $-dV$ in Figures 5.3(a) and 5.3(b).

The region between Lines D and E represents the occurrence of reaches which exhibit dual mode behaviour, for which the W_d / W_f is between zero and unity. Assuming the region between W_d / W_f of zero and W_d / W_f of unity can be approximated as linear, W_d / W_f as a function of occurrence can be plotted for specific slope angles. Figures 7.5(a) and 7.5(b) present plots for the range of slope angles of 16° to 27° , where dual mode behaviour is modelled in *UBCDFLOW*. For these plots, a random variable $X(TH)$ with a uniform p.d.f. is sampled for each slope angle TH , and its value used to select the volume change behaviour from the given relationship for TH . The resulting value of W_d / W_f can be used to predict W_d since W_f is known, sampled from a user-defined p.d.f. For example, let $X(21)$ be a random variable, sampled from 0 and 100 inclusive, for a 21° reach. For values of $X(21)$, W_d can be determined based on W_f :

$$W_d \begin{cases} \text{if } X(21) < 29, & W_d = W_f \\ \text{else if } X(21) > 74, & W_d = 0 \\ \text{else } & W_d = W_f(-0.0217X(21) + 1.609) \end{cases} \quad [7.1]$$

Since both deposition and entrainment can be calculated for a slope angle of 21° (Table 7.1), the width of entrainment W_e can be calculated as

$$W_e = W_f - W_d \quad [7.2]$$

and these values of W_d and W_e are used in the regression equations to calculate $+dV$ and $-dV$ in each reach.

Volume changes on reaches with slope angles of 25° to 27° , and 16° to 18° , are determined in a similar fashion. For a slope of 17° , W_d can be calculated:

$$W_d \begin{cases} \text{if } X(17) < 52, & W_d = W_f \\ \text{else if } X(17) > 88, & W_d = 0 \\ \text{else } & W_d = W_f(-0.0278X(17) + 2.444) \end{cases} \quad [7.3]$$

However, since the equation for entrainment is not applicable to slopes less than 19° , W_e is zero regardless of the value calculated for W_d at this slope angle. In practical terms, this would correspond to a flow which travels through a 17° reach with no net change in volume. For slopes greater than 24° , the regression equation for deposition is not applicable. Thus, for a reach with a slope angle of 26° , the W_e can be calculated as the complement to deposition:

$$W_e \begin{cases} \text{if } X(26) < 23, & W_e = 0 \\ \text{else if } X(26) > 57, & W_e = W_f \\ \text{else } & W_e = W_f[1 - (-0.0294X(26) + 1.677)] \end{cases} \quad [7.4]$$

An outcome of W_e equal to zero would simulate no net volume change as the flow travelled through the reach.

It should also be noted that another approach to modelling dual mode behaviour is to extend the ranges of the regression equations. This would allow for modelling of entrainment on flatter slopes (less than 19°) and deposition on steeper slopes (greater than 24°). A preliminary set of regression equations was developed for the range of 16° to 27° , with the result of a marked decrease in the precision and significance of these equations due to the small amount of data in these ranges. The survey of additional data in these ranges in a future study may further define the trends which are present, and lead to satisfactory regression analyses.

In the absence of these data, however, deposition on slopes greater than 24° and entrainment on slopes less than 19° are neglected for the purposes of probabilistic modelling in *UBCDFLOW*, as described immediately above.

7.2.3.2 Confined Flow

From Figure 5.7, most of the confined flow reaches showed evidence of entrainment, with only 17% having any deposition. To reflect this, it was assumed in *UBCDFLOW* that no deposition occurs in confined reaches and that W_e is equal to the sampled value of W_f . This conservative assumption of only single mode flow in gully channels will lead to larger volumes transported down to the mouth of the gully channel.

In a practical sense, if a debris flow event does deposit material in a confined channel, it will be moved to the fan of the gully either by alluvial processes or remobilization of as a debris flow. Alluvial processes will scour any material which has been deposited, carrying this material down to the fan below. In cases where the gully channel has a direct hydraulic connection to a stream, this material will still impact the stream processes. Debris material stored in the channel may also be remobilized by high water levels in the gully, in effect continuing the flow down to the fan. Due to the forensic nature of the observations, it is not possible to determine if events which were deposited on gully fans were the result of a single, non-interrupted flow or the remobilization of stored debris.

7.2.3.3 Transition Flow

The loss of confinement in transition reaches dominates the volume change behaviour of these reaches. From Figure 5.7, most of the reaches showed deposition, while only a few showed entrainment. In the deterministic model, transition reaches were assumed to only deposit material and no entrainment was permitted. This is reflected in *UBCDFLOW*, with W_d equal to W_f for all transition reaches.

7.2.4 Prediction of Debris Flow Travel Distance

Calculation of the potential debris flow travel distance, based on simulation of the cumulative flow volume, is carried out for *UBCDFLOW* using the measured deterministic input values of TH , L , AZ , as well as values sampled from user-defined p.d.f.'s of V_{init} , W_f . These values are measurements obtained during a field survey of the potential travel path. Based on the flow mode and TH for each reach, the W_d is equal to W_f , zero, or proportioned with W_e according to variable observed flow behaviour as discussed in the previous section. The incoming flow volume for each reach, ΣV , is also used as a predictor in one regression equation used by *UBCDFLOW*, but is calculated internally within the model.

The repeated simulation of debris flow events for a scenario can be used to determine the debris flow travel distance and probability of exceedance $P(Ex)$ at a point of interest along the path. Figure 7.6(a) shows a schematic plan view of a potential debris flow travel path. The path begins on a gully headwall, shown in the left of the figure and moves right to the gully fan. Along the path, changes in confinement occur as the flow modes change from unconfined flow, to confined flow, to a transition reach, and back to unconfined flow on the gully fan. Point X represents a point of interest on the gully fan, which coincides with the end of reach 9.

Repeated simulations of the cumulative debris flow volume along the path can be carried out using the Volumetric Model. A histogram of the number of flows which terminate within each reach of the path can be determined, and an example is presented in Figure 7.6(b). Simulated flows which did not terminate within the surveyed geometry of Figure 7.5 can be assumed to terminate at further points down the debris flow path. These are shown conceptually by the white bars plotted in Figure 7.6(b). The sum of the flow terminations represented by both the solid bars and the dotted bars in the histogram equals the total number of flows simulated in the

analysis. The shaded bars in the histogram represent simulated flows which terminate upslope of point X.

The histogram may then be converted from a discrete distribution to a continuous distribution, shown as a solid line for reaches in the surveyed geometry, and a dotted line for reaches beyond the surveyed geometry. Normalizing the area under this curve as unity creates a probability density function for the flow terminations for the reaches of the travel path. The p.d.f. can be divided into two areas: the area to the left of reach 9 (the point of interest), noted as Area C in Figure 7.6(b); and the area under the dotted line, noted as Area B. For a large number of simulations, the probability of the simulated flows exceeding point X along the travel path is equal to the number of flows which travel farther than point X divided by the total number of flows, and represented as Area B.

As the distribution of event terminations is not known beyond the surveyed geometry of the potential debris flow path, the Area B cannot be computed explicitly. However, since the area of the p.d.f. is equal to unity, Area B, and hence the probability of exceedance at X, can be calculated as

$$P(Ex) = B = 1 - C \quad [7.5]$$

Applying this procedure for the end of each surveyed reach of a potential debris flow path, $P(Ex)$ at the end of each reach can be determined. Plotting these values and joining them by a line, Figure 7.6(c), shows the $P(Ex)$ along the travel path. For the initial portion of the event, and along the gully channel, the probability of impact is certain at 1.0. In the later reaches of the event on the gully fan, the impact is less certain with $P(Ex)$ less than 1.0. The dashed portion of the plot in Figure 7.6(c) indicates the possible distribution of $P(Ex)$ beyond the

surveyed geometry, represented by the dotted bars in Figure 7.6(a). The $P(Ex)$ decreases to zero as all the simulated flows terminate before or within reach 15.

7.3 Example Scenarios

Using *UBCDFLOW* the $P(Ex)$ is determined for three debris torrent scenarios and three debris slide scenarios. The example gully geometry for the torrent scenarios is based on Event 4001, from the Eve River Watershed on Vancouver Island. The debris torrent scenarios are used to determine the relative influence of initiation point on $P(Ex)$. The debris slide examples are based on the unconfined flow geometry of Event 3202 from the Mamquam Watershed near Squamish, B.C. and are used to investigate the relative importance of V_{init} in the calculation of $P(Ex)$ for unconfined events. Table 7.3 summarizes the test parameters for the *UBCDFLOW* examples discussed in this Chapter. Both Event 4001 and Event 3202 were back-analyzed using the deterministic Volumetric Model in Chapter 6 and are presented in Figures 6.4(a) and 6.4(b), respectively.

Table 7.3: Summary of Test Parameters for *UBCDFLOW* Examples

Geometry	Scenario	V_{init}	Initiation Location
Gully System	A1	constant (as observed)	gully headwall (as observed)
	A2	variable	gully headwall (as observed)
	A3	variable	gully sidewall
Open Slope	B1	constant (as observed)	open slope (as observed)
	B2	variable (low volume)	open slope (as observed)
	B3	variable (high volume)	open slope (as observed)

Note: (as observed) indicates the values/parameter values are used/based on those recorded during the field survey.

7.3.1 Scenario A1: Gully Headwall Failure

The input data for modelling Event 4001 using *UBCDFLOW* are presented in Figure 7.7(a). The triangular distributions for W_f are based on likely variations for each of the reaches. The distribution of the initial volume for the gully headwall failure is taken as a constant value of 100 m^3 , similar to the 71 m^3 volume surveyed at the initiation site. Other data entered as single values into *UBCDFLOW* are unchanged from the measured values obtained during the field survey.

Repeated simulations of the volume change behaviour along Event 4001 are also presented in Figure 7.7. For this example, the initial volume was constant at 100 m^3 but variability was assumed along the remainder of the event path, both in the gully channel and the fan area at the base of the gully. Reaches 2 and 3 are unconfined with a large estimated variation in flow width, and then a gully confines flows for reaches 4 to 12 with much less possible variation. Reach 13 is a transition reach where the flow moves from confined flow to unconfined flow, and reaches 14 through 17 are the unconfined fan portion of the flow path, again with more possible variation than the gully channel reaches. Reach slope angles, TH , range from 35° in the gully headwall area to about 12° on the fan. Based on the applicable slope ranges for determining volumetric behaviour, all reaches are entrainment only until the transition reach (13), which is deposition only. Reach 14, with a slope angle of 23° , is assumed to have entrainment and/or deposition (see Section 7.2.3).

The lower portion of Figure 7.7(a) shows the variation in cumulative flow volume along the travel path. The bounds are plotted for one standard deviation in the results, as well as the 95% confidence intervals. Along the bottom of the plot the number of events which terminate

within each reach is shown for the 2000 simulations. Of the 2000 simulations carried out, 622 did not terminate within the surveyed geometry.

Histograms of the cumulative flow volumes in three of the last six reaches of the travel path are plotted in Figure 7.7(b). The histogram of volumes at the end of reach 13, the upper plot in the figure, characterize the cumulative flow volumes at the mouth of the gully channel as between 400 and 1000 m³. For each successive reach down the fan, more of the cumulative flow volumes are negative corresponding to the termination of increasing numbers of simulated events. At the end of reach 17, all but 622 volumes are negative, signifying that 1,378 of the 2000 simulations have terminated prior to the end of this reach. The cumulative flow volumes from histograms such as these can be used to determine the flow volume, or severity of impact, at a point of interest along the debris flow path.

7.3.2 Scenario A2: Variable Gully Headwall Failure

Scenario A2 is carried out on the same path geometry as Scenario A1. However, for Scenario 2, the V_{init} is input as a p.d.f. The triangular p.d.f. was chosen with a lower bound of 50 m³, the mode as 100 m³, and the upper bound as 250 m³. Figure 7.8(a) contains the input data for Scenario A2.

Simulations for cumulative flow volumes are shown in the lower portion of Figure 7.8(a). The variation in initial volumes leaving reach 1 is shown by the various starting points of the flows on the left side of the plot, at the beginning of reach 2 on the gully headwall. As for the previous scenario, the flows are unconfined in reach 3, confined in reaches 4 through 12, and emerge on the fan at reach 13. The lower portion of Figure 7.8(a) shows the variations in cumulative flow volume, with bounds of one standard deviation in of the results as well as the

95% confidence intervals. In comparison with the flow volume plot in Figure 7.7(a), more simulations travelled farther down the path for Scenario A2; indeed, 1075 of the 2000 simulations did not stop within the surveyed geometry, an increase from 622 for Scenario A1.

Figure 7.8(b) presents histograms characterizing the volumes of the simulated flows at the end of reaches 13, 15, and 17. For reaches 13 and 15, no values are below zero as no flows terminate within these reaches in Scenario A2. In reach 17 some flow volumes are negative (indicating that flows have terminated) and range from 600 to -400 m³.

7.3.3 Scenario A3: Gully Sidewall Failure

Scenario A3 was carried out to model a gully sidewall failure using a modified version of the same potential debris flow path given in the first example. The first gully channel reach (reach 2) corresponds with Reach 9 of the first example. An unconfined flow reach is inserted as reach 1 to represent the gully sidewall initiation point, with a triangular distribution based on the initiation volumes of the reported gully sidewall failures from the Q.C.I. (Original) Data, Figure 7.2(b).

The variations in initial volume are shown on the on the cumulative flow plots, as the flow moves off the gully sidewall and into the gully channel. The flows then move down the gully channel and into the unconfined transition and fan reaches. All of the simulated flows in this scenario terminated within the surveyed geometry; in fact, only 331 of the 2000 simulations continued beyond reach 15 at a path length of 148 m downslope from the initiation point on the gully sidewall. These flows terminate earlier than the flows in Scenarios A1 and A2 since less material is entrained along the gully path.

The histogram plots for volumes at the ends of the reaches quantitatively describe the size of the flows in the simulations, Figure 7.9(b). The values for reach 13 are between about -300 and 450 m³, a decrease from the 500 to 1100 m³ range in Scenario A2. Similarly, the volumes of the simulated flows at the end of reach 17 are virtually all negative, since only one simulation continues beyond this point along the path compared to 1075 simulations for Scenario A2.

7.3.4 Calculation of Probability of Exceedance for Scenarios A1 to A3

A comparison of the probability of exceedance along the event path for each of the above examples is presented in Figure 7.10 for Scenarios A1, A2, and A3. Scenario A2 (the gully headwall failure with a variable initial volume) has the highest range of $P(Ex)$ along the path with Example A1 (constant initial volume) only slightly lower. The gully sidewall failure (Example A3) has the lowest range of $P(Ex)$ along the event path. This comparison illustrates that for events in gully channels, the initiation location is more important than the initiation volume: as the initiation point is moved further upslope in the gully system, there is more available material for the flow to entrain as it moves down the gully channel. When the flow emerges onto the fan, a larger flow event will travel farther by virtue of its size than a smaller flow, leading to higher values of $P(Ex)$. Variation of the initial volume is less important than the initiation location, since the $P(Ex)$ values for Scenario A1 (constant volume) were very similar to those for Scenario A2 (variable initial volume).

7.3.5 Scenario B1: Open Slope Failure

As for the first three scenarios, the input data for scenarios B1 through B3 are based on the likely variations of event width and initial volume. Essentially, the triangular distribution for W_f along the travel path is chosen as the same distribution for each reach with minimum,

maximum, and mode values chosen based on the surveyed measurements of W_f for the actual event.

The input data for Scenario B1 are presented in the top portion of Figure 7.11(a). A constant initial volume of 400 m^3 was chosen for this scenario, similar to the observed initial volume of 468 m^3 for this event. As the entire length of the event is unconfined, variations are expected in entrainment and/or deposition along reaches with TH between 16° and 27° , inclusive.

Section 7.2.3 discusses the methodology used to calculate the W_d and/or W_e for each reach, based on W_f and TH , and the occurrence of dual mode behaviour in the Q.C.I. (Original) Data. Thus, entrainment and/or deposition are permitted on reach 3, with no deposition on reach 2 and no entrainment on reaches 4 through 8.

The lower portion of Figure 7.11(a) plots the variation in cumulative flow volumes calculated by *UBCDFLOW*. Compared to Scenarios A1 through A3, the flows terminate in a more disperse pattern along the travel path which is characteristic of unconfined flow. For this scenario, 130 of the 2000 simulations did not terminate within the surveyed geometry.

The flow volumes at the ends of three of the last six reaches are presented in Figure 7.11(b). These results show the volumes the end of reach 4, where the shortest flows terminate, are less than 700 m^3 . The flow volumes at the end of the surveyed geometry, reach 8, are calculated as less than 300 m^3 .

7.3.6 Scenario B2: Small Open Slope Failure

The *UBCDFLOW* results, along with the input data and simulated flows, are presented in Figure 7.12(a). The initial volume of the flow was input as a triangular distribution, with a

minimum of 75 m³, a mode of 150 m³, and a maximum of 400 m³. This distribution was chosen to provide values less than the observed V_{init} at the site.

The lower portion of Figure 7.12(a) shows that more of the simulated flows terminate within the surveyed geometry, due to the smaller initial volumes. For this scenario, only 61 simulated events did not terminate within the surveyed geometry. Figure 7.12(b) characterizes the flow volumes at the ends of three of the last six reaches, with the maximum flow volumes ranging from about 600 m³ in reach 4 to about 300 m³ at the end of the reach 8. The initial volumes of the simulated flow events appear to play a strong role in determining the cumulative flow volume, in comparison to the confined flow scenarios.

7.3.7 Scenario B3: Large Open Slope Failure

Taking the same path geometry and initiation location as the Scenario B2, the effect of increasing the initial volume is considered. The p.d.f. of V_{init} , as well as the other input data and the plots of the simulated flows, are presented in figure 7.13(a).

As with the previous scenario, the size of the initial volumes for the simulated events are important. With the larger initial volumes, much fewer of the flows terminate within the surveyed geometry. Of the 2000 simulated flows, 343 did not terminate before the end of Reach 8.

Figure 7.13(b) illustrates the histograms of the debris flow volumes for three of the last six reaches of the flow path. Comparison of these distributions with the results of the Scenario B2 shows that these flows are larger, on average.

7.3.8 Calculation of Probability of Impact for Scenarios B1 to B3

For open slope Scenarios B1 to B3, the results differ from the gully scenarios. Figure 7.14 shows the plots of the probability of impact along the path for Event 3202, Examples B1 through B3. In this plot there is a larger variation in the $P(Ex)$ values as compared to Figure 7.10 for the gully scenarios. In these analyses, the large open slope failure (Scenario B3) has the highest $P(Ex)$ at the end of the path with a value of about 0.17. The small open slope failure, Scenario B2, has the lowest $P(Ex)$ along the event path, with $P(Ex)$ about 0.03 at the end of the surveyed geometry. The differences in $P(Ex)$ between Scenarios B2 and B3 are due to the range of initial volumes used in these analyses relative to the event path length: flows from small initial volumes are much more likely to terminate within a given reach than those with large initial volumes. It is also likely that another factor contributing to this result is that larger flow volumes will entrain proportionately more material than flows with smaller volumes. These results show that for unconfined events, the size of the initiation volume is an important factor in determining the travel distance of the simulated flows, and hence $P(Ex)$ along the path.

7.4 Summary

The incorporation of probability into the Volumetric Model to create *UBCDFLOW* provides a method for modelling the variability of the initial volume for a flow event, estimating the width of a debris flow event, and accounting for the variability of flow responses on intermediate slope angles for unconfined flow. Probability distributions are determined based on site survey information for initial volume and flow width. Observations of flow behaviour from the Q.C.I. (Original) Data are used as the basis of an expert system to determine the unconfined flow

response on intermediate slope angles of 16° to 27° , inclusive. Other input values necessary for the regression equations in the Volumetric Model are obtained during a site survey of the potential debris flow path. These values are used as single (deterministic) values by *UBCDFLOW* in the calculation of volume change for each reach of a potential flow path.

The deterministic values and a single set of sampled values from the appropriate probability distributions are used to simulate the cumulative flow volume of a single debris flow event along the travel path. The cumulative flow volume is used to calculate the travel distance of the simulated flow. Repeated sampling and simulations are used to model a range of possible flow behaviour.

Identifying the number of simulated flows which terminate in each reach, and determining the number of flows passing through each reach, leads to a calculation of the $P(Ex)$ for the end of each reach. $P(Ex)$, the probability of exceedance, is equal to the proportion of simulated flows passing the endpoint of the reach. Plotting $P(Ex)$ for the ends of the reaches in a potential debris flow path can be used approximate the $P(Ex)$ for points of concern along the potential path. Simulated flow volumes at the end of each reach can be used to characterize the likely severity of a debris flow event. The calculated $P(Ex)$ must be multiplied by the probability of initiation of a debris flow to determine the risk at a specific point of concern along the path.

UBCDFLOW was used to determine the $P(Ex)$ for three different scenarios on gully channel and open slope morphologies. For debris torrents, the initiation location is more influential than for open slope events, as gully events will entrain a large amount of material during movement along the gully channel relative to the initial volume. Smaller $P(Ex)$ values were calculated where the simulated flows initiated closer to the end of the mouth of the gully.

Open slope events are able to deposit material on intermediate slope angle reaches, and thus the size of the initiation volume is more important for open slope events. Smaller initiation volumes resulted in smaller $P(Ex)$ values along the travel path relative to larger initiation volumes. For gully events, the size of the initial volume is likely much smaller than the total amount of material entrained during movement down the gully, and thus the size of the initiation volume is less important for gully events.

Probabilistic Modelling for a Single Simulation

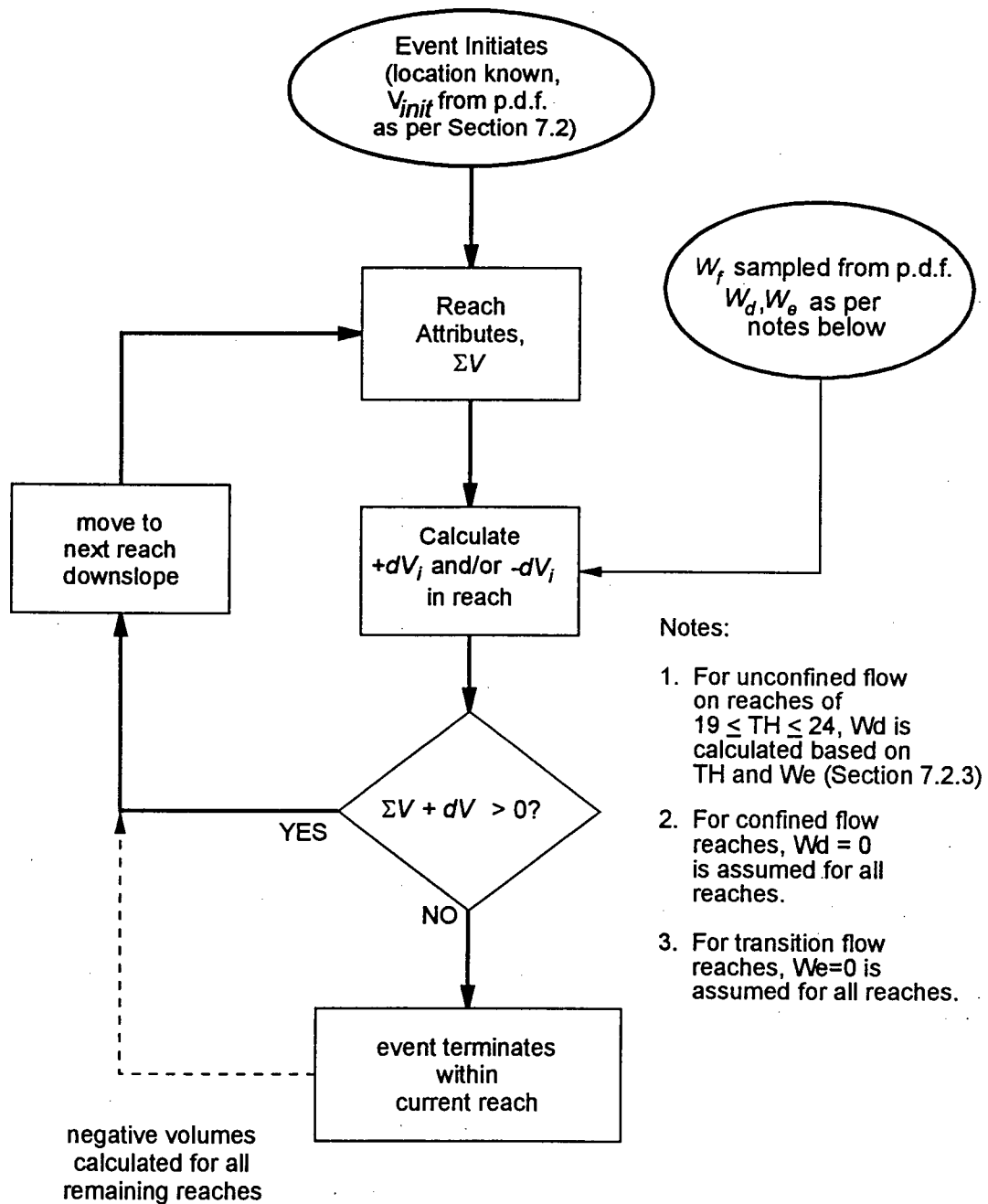


Figure 7.1(a): Flow chart showing probabilistic modelling for a single simulation

Probabilistic Modelling for single Scenario (many Simulations)

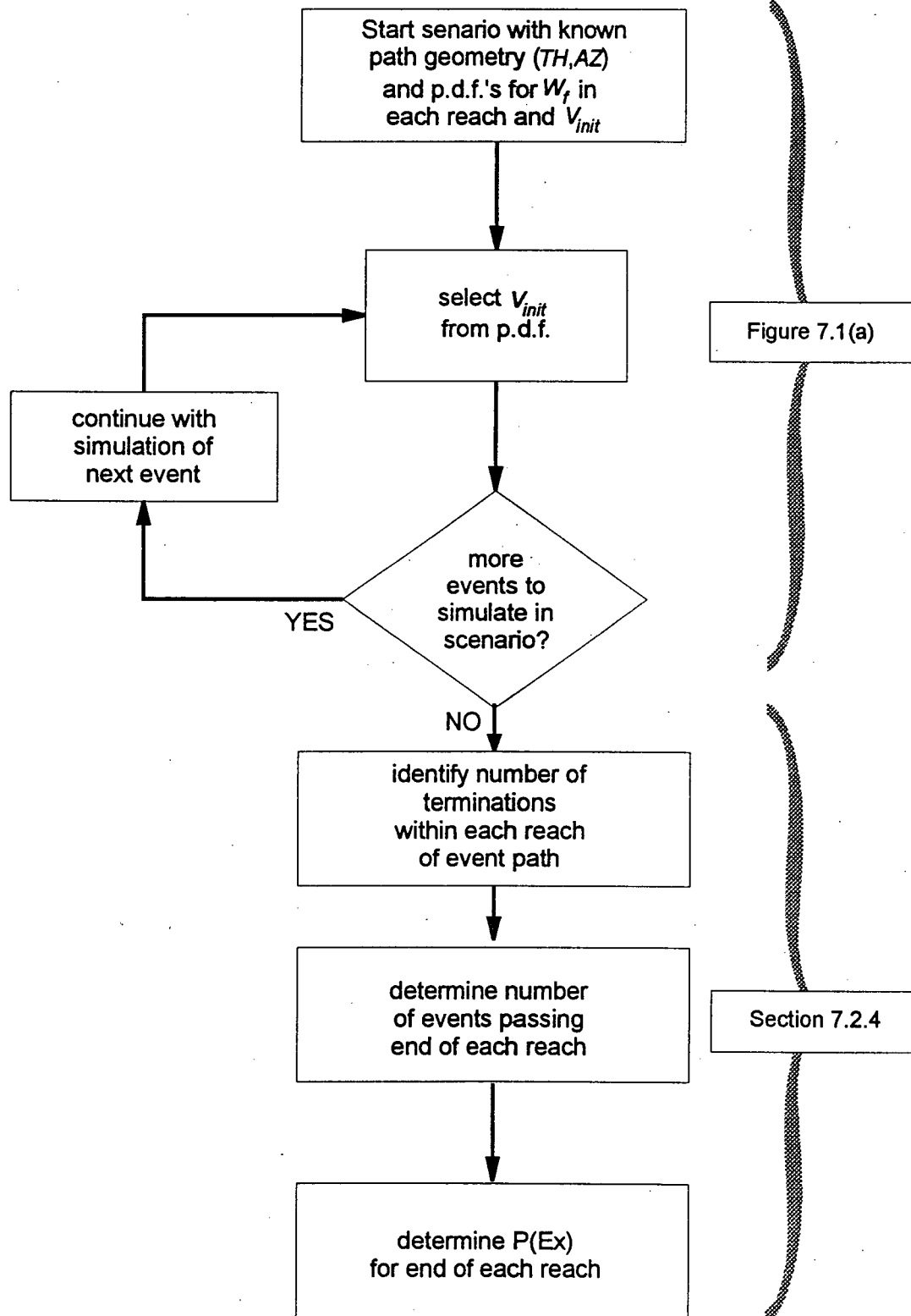
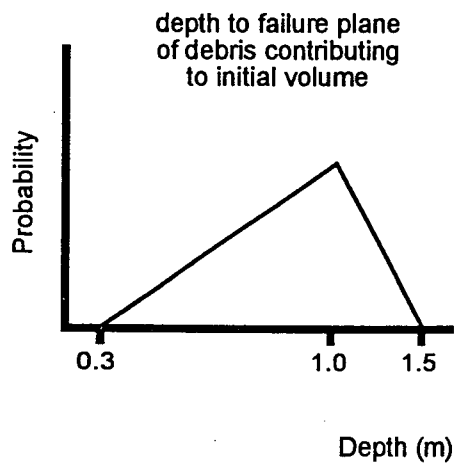
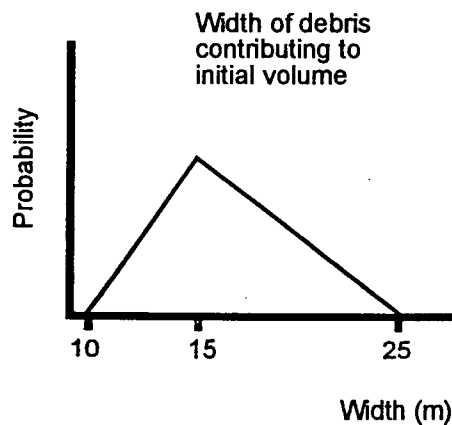
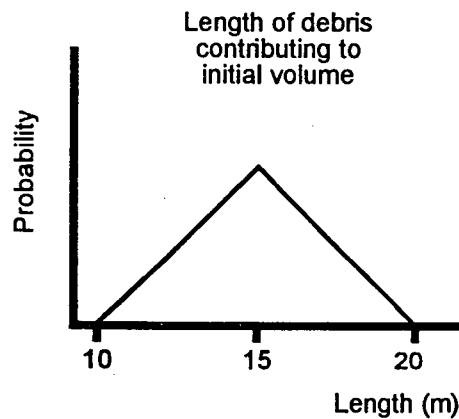
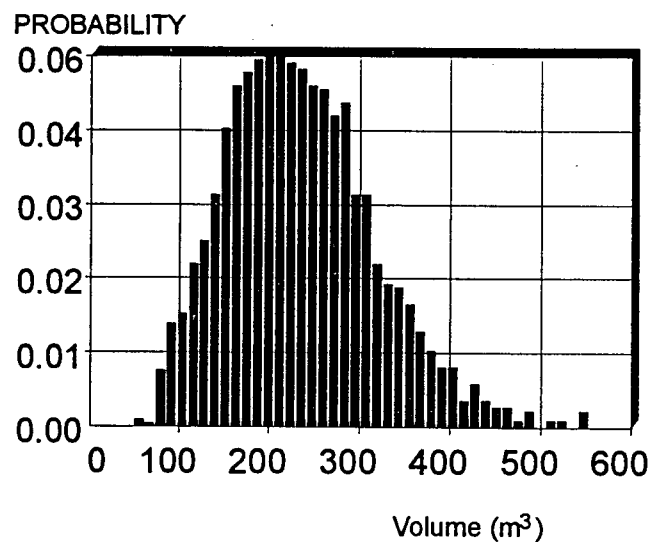


Figure 7.1(b): Flow chart showing probabilistic modelling for scenarios

Field Observations at Initiation Location



Initial Volume
 $V = L \times W \times D$



Notes:

1. Length is measured parallel to the direction of potential flow. Width is measured transverse to the potential flow. Depth is measured perpendicular to the flow.
2. Triangular distributions represent the minimum, most likely, and maximum values for each parameter. Other types of p.d.f. distributions can be chosen.

Figure 7.2(a): Determination of initial volume for a potential open slope failure

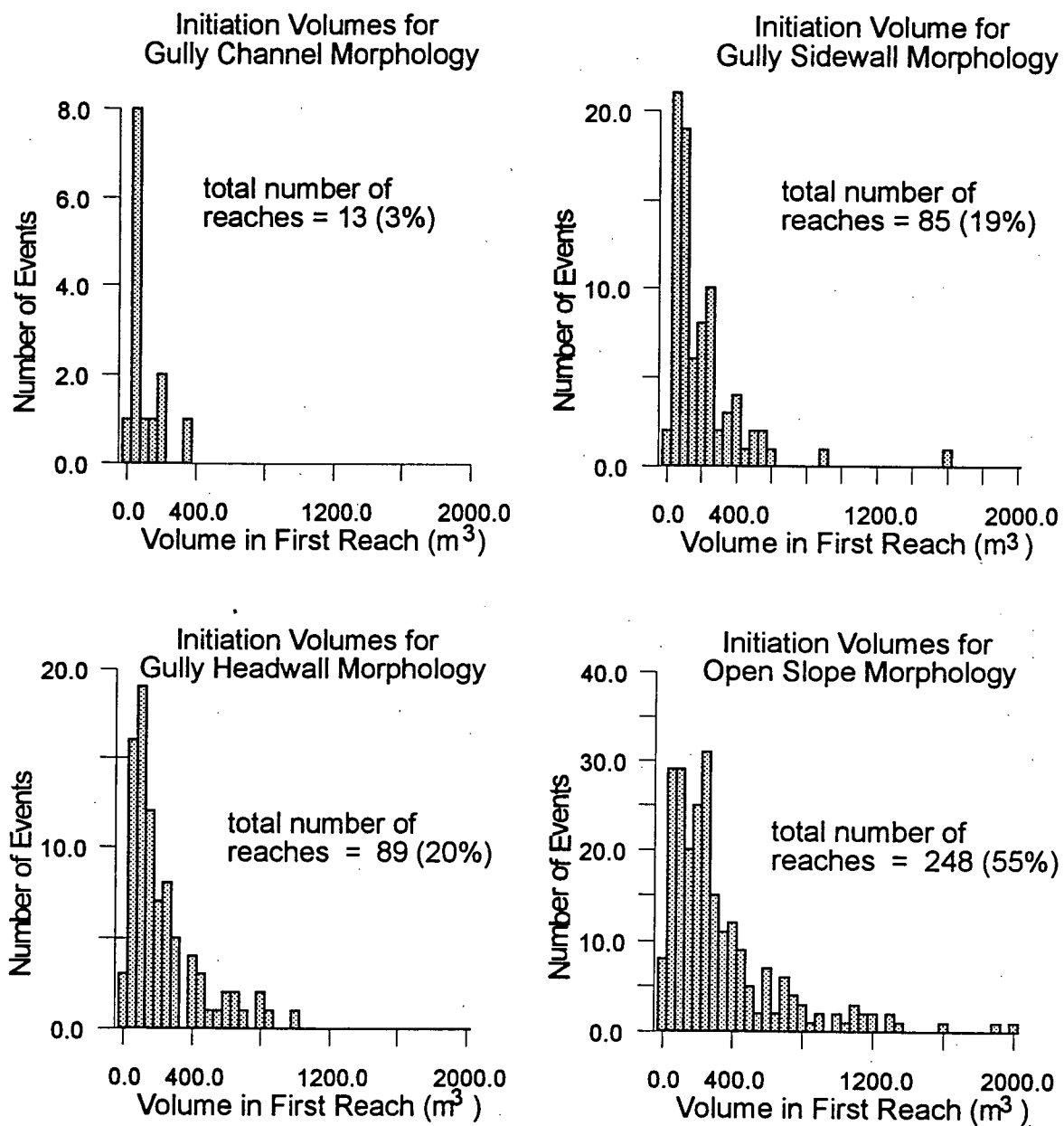
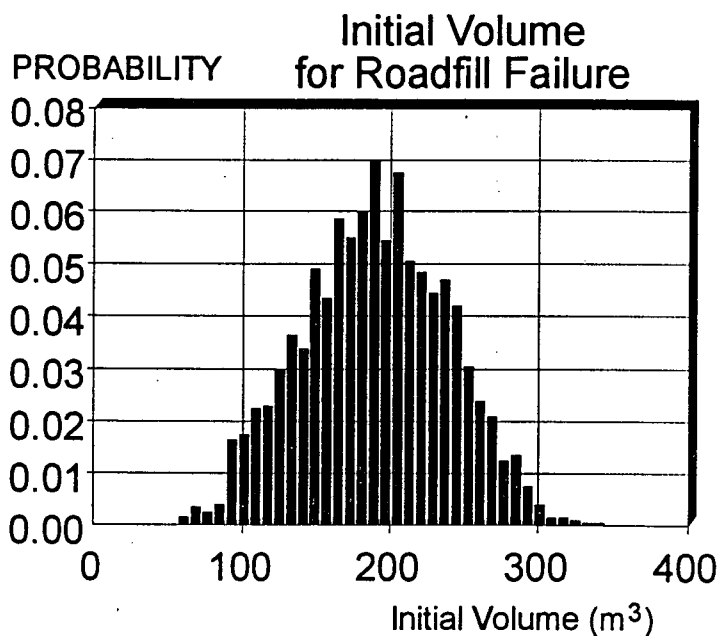
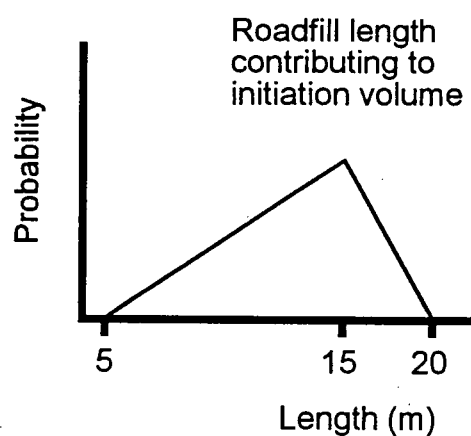
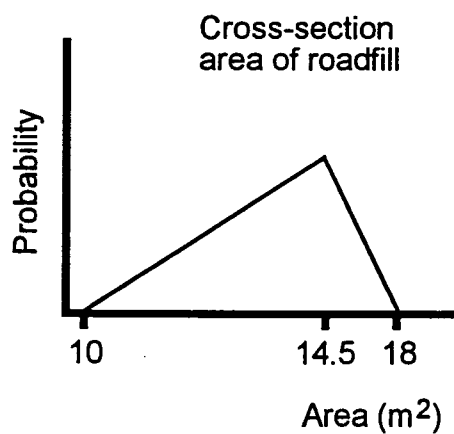
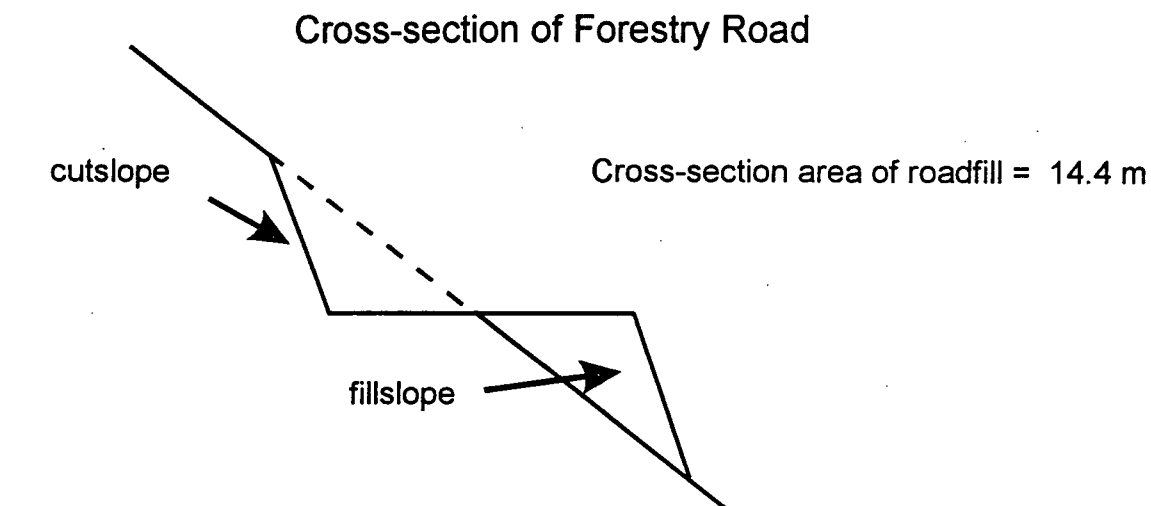


Figure 7.2(b): Initial volumes for various slope morphologies from Q.C.I. (Original) Data

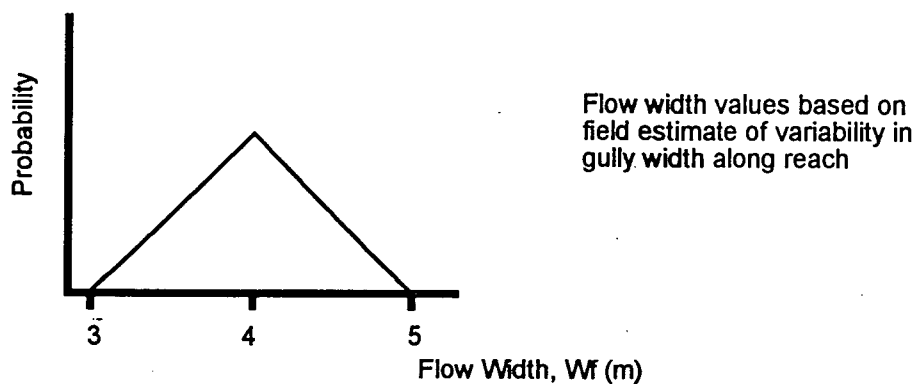


Notes

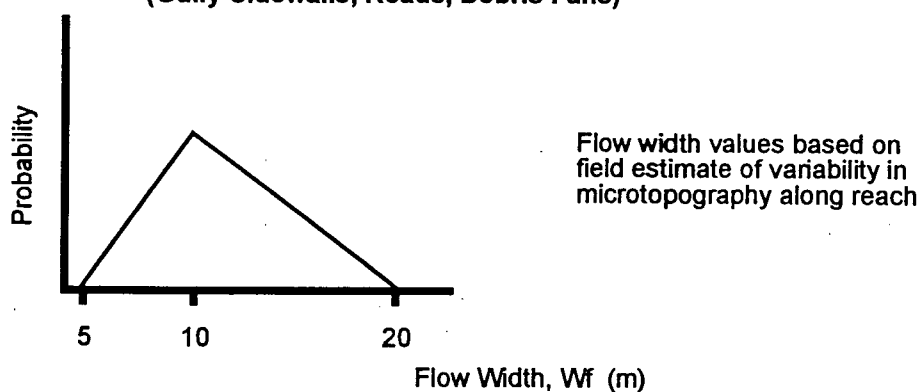
Area of roadfill should include any native soil under the roadfill which may also contribute to the initial volume

Figure 7.2(c): Determination of initial volume for a potential roadfill failure

CONFINED FLOW (Gully Channels)



UNCONFINED FLOW (Open Slopes, Gully Headwalls, Gully Sidewalls, Roads, Debris Fans)



TRANSITION FLOW (Gully Channels to Debris Fans)

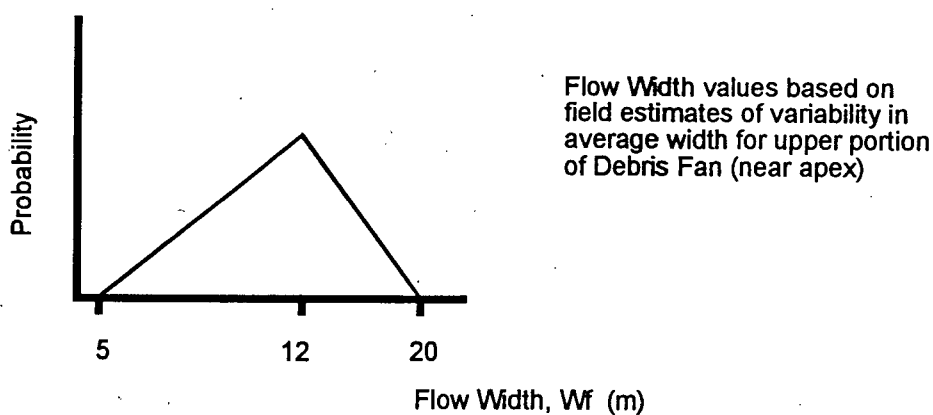
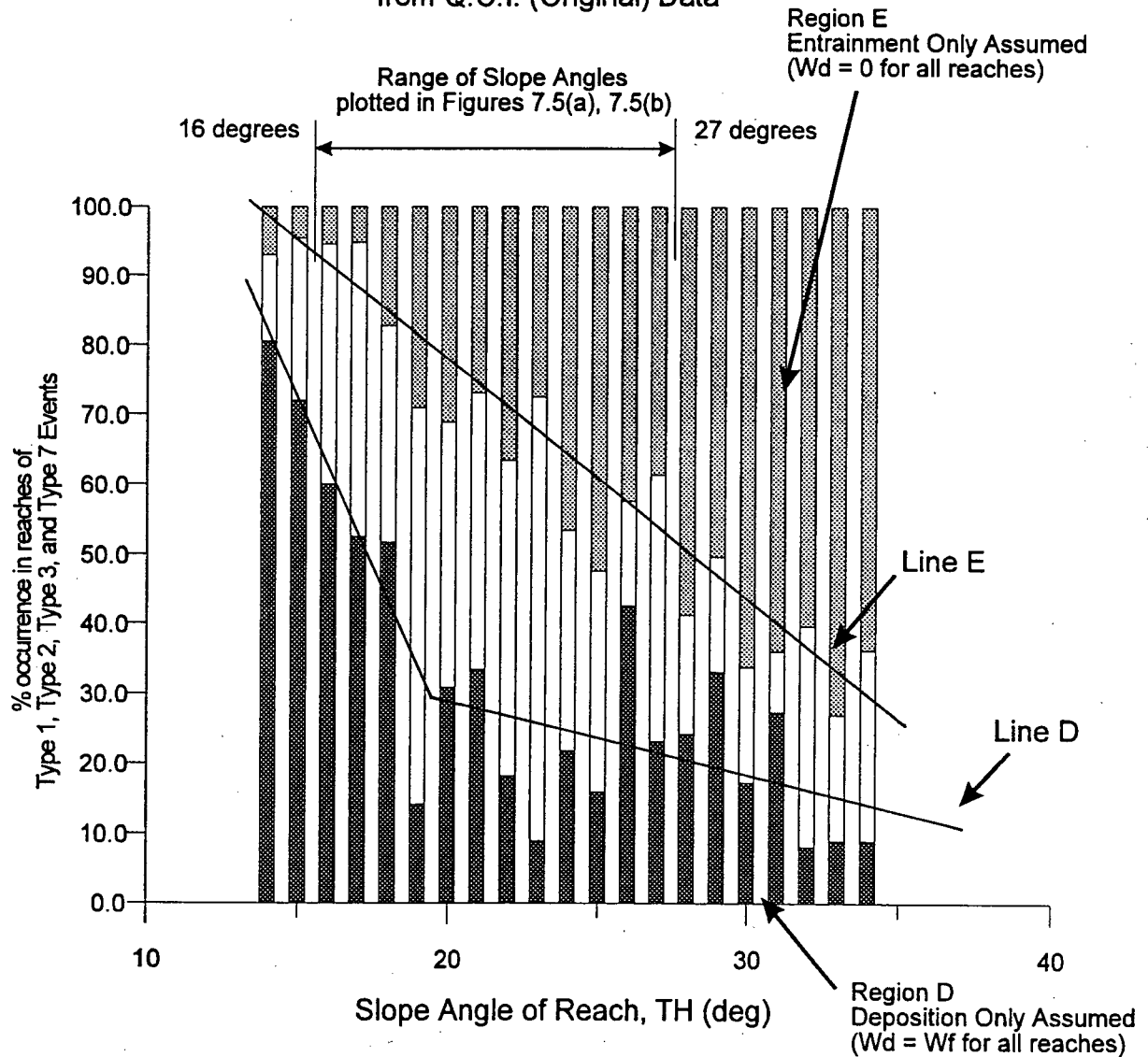


Figure 7.3: Schematic triangular p.d.f. distributions for Flow Width W_f based on Flow Mode

Volume Behaviour Occurrence for Unconfined Flow Reaches from Q.C.I. (Original) Data



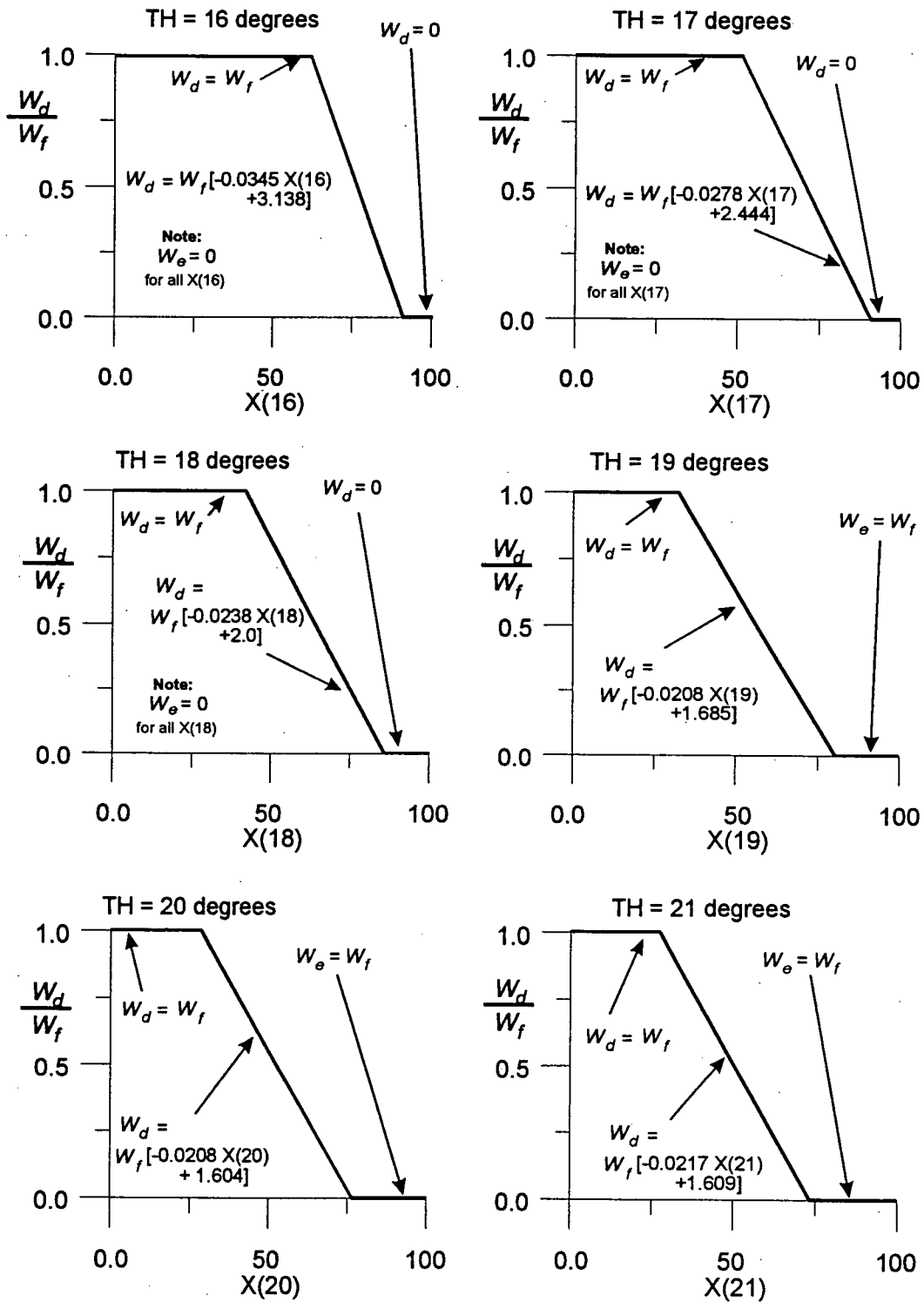
Legend

- Deposition Observed
- Deposition and Entrainment Observed (Dual Mode Behaviour)
- Entrainment Observed

NOTES

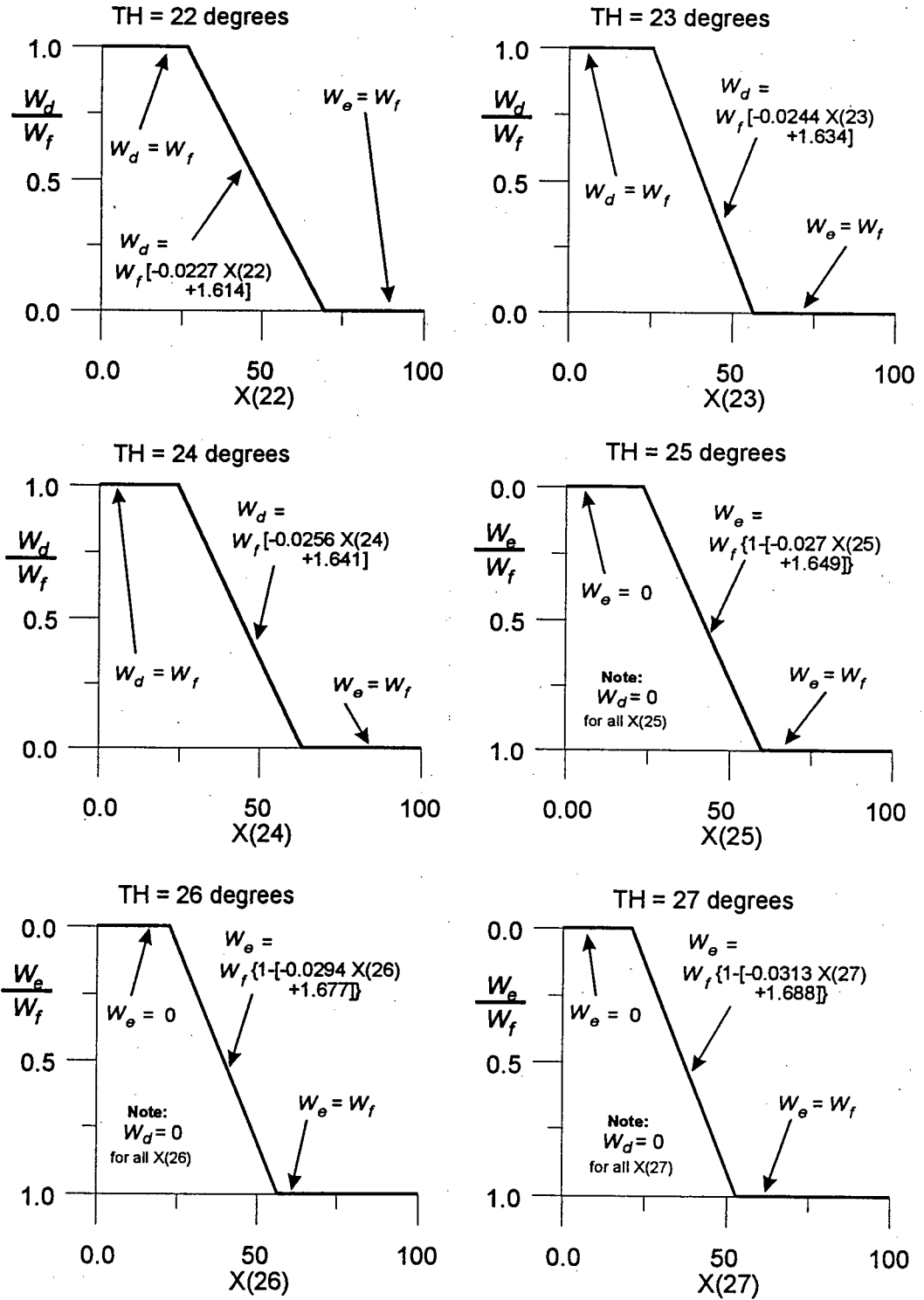
1. No filter applied; all reaches which were observed to have both entrainment and deposition are grouped together (see text).
2. Lines plotted using a visual fit to ends of histogram bars.
3. See Table 7.1 for slope angle range used for probabilistic modelling in *UBCDFLOW*

Figure 7.4: Unfiltered volume change behaviour for Q.C.I. (Original) Data, $14 \leq TH \leq 34$



Note: $X(TH)$ sampled from a uniform p.d.f.

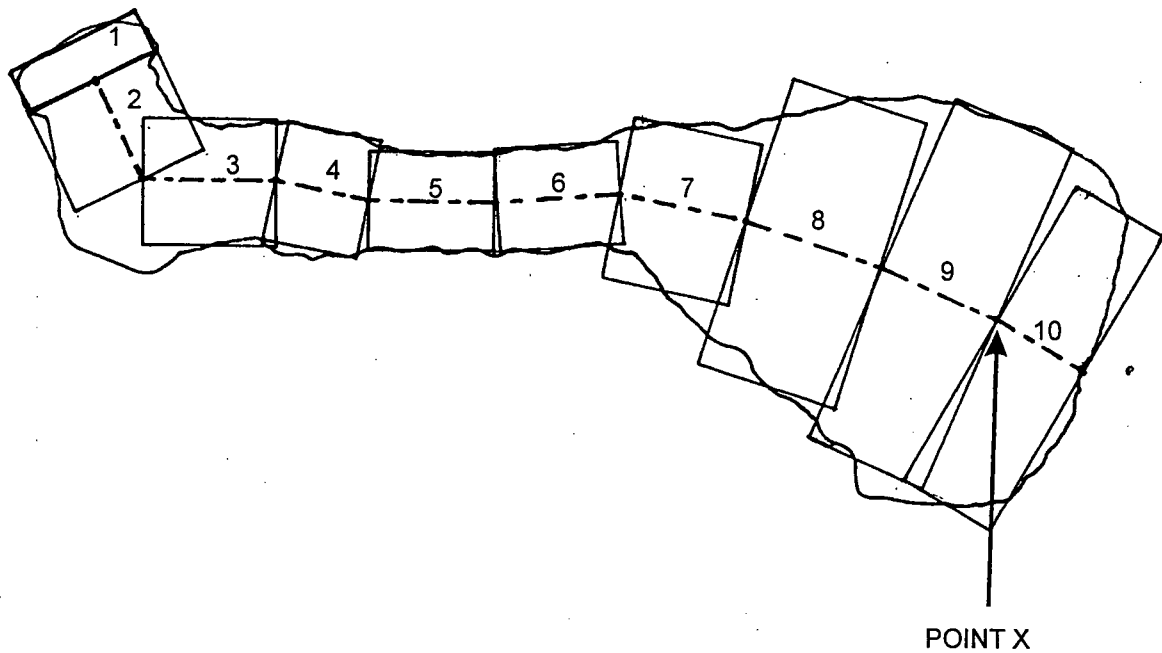
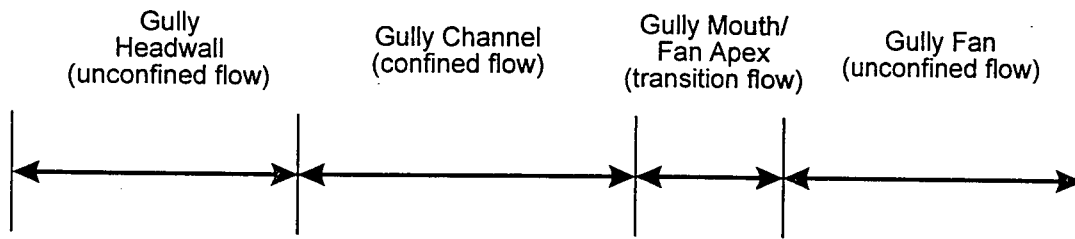
Figure 7.5(a): W_d/W_f functions for reach slope angles of 16 to 21 degrees, inclusive



Note: X(TH) sampled from a uniform p.d.f.

Figure 7.5(b): $W_d, W_e / W_f$ functions for reach slope angles of 22 to 27 degrees, inclusive

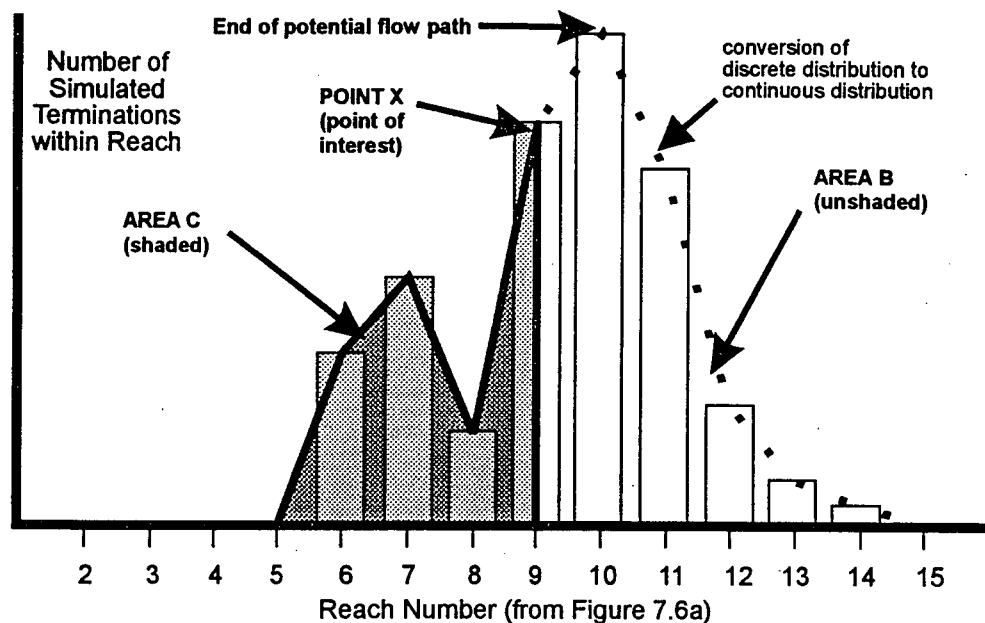
SLOPE MORPHOLOGY OF GULLY SYSTEM



NOTES

1. Boxes along potential debris flow path indicate reach width
2. Point X represents a point of interest along the potential path

Figure 7.6(a): Schematic plan view of potential debris flow path



NOTES

1. Number of terminations is based on the number of simulated flow events which terminate within a given reach along the potential flow path
2. For a probability density function, (AREA C) + (AREA B) = 1

Figure 7.6(b): Histogram of simulated flow terminations along flow path

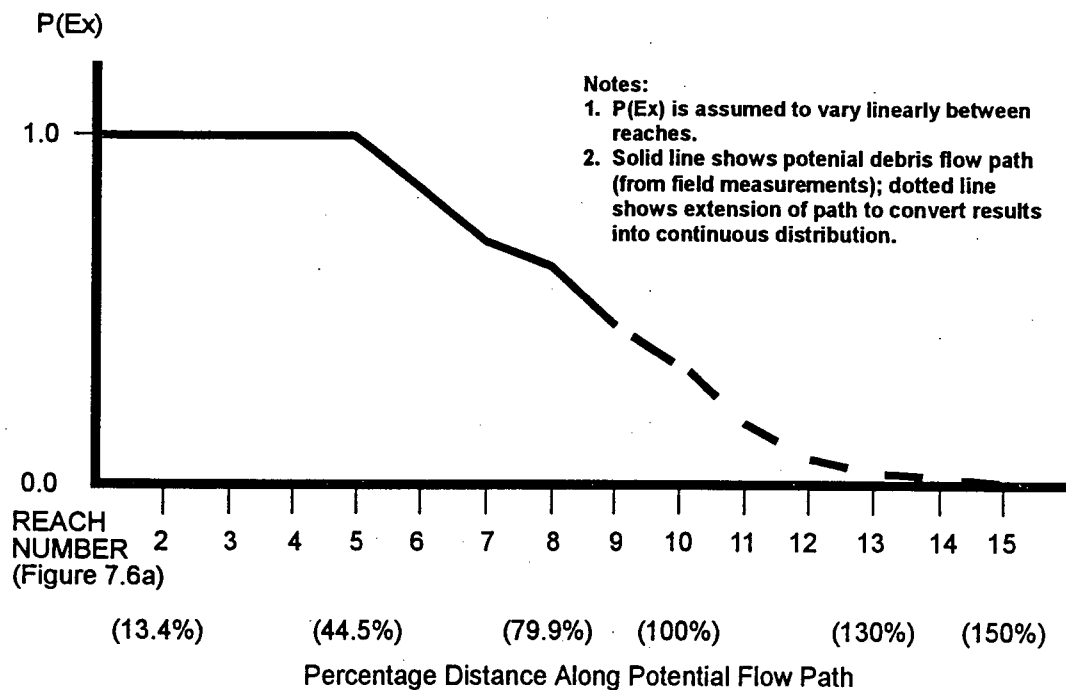


Figure 7.6(c): Probability of Exceedance, $P(Ex)$, along debris flow path for simulated debris flow events

INPUT DATA FOR SCENARIO A1: EVENT 4001, Constant Initial Volume
Initiation Volume: constant 100 m³

Reach	SM	Path Length	Reach Length	W_f	W_e	W_d	TH	dTH	dAZ
1	U	13	13	n/a	n/a	n/a	35	n/a	n/a
2	U	27	14	(5,10,30)	W_f	0	43	8	0
3	U	34	7	(5,10,30)	W_f	0	31	-12	-31
4	C	49	15	(5,7,10)	W_f	0	28	-3	2
5	C	79	30	(3,4,7)	W_f	0	27	-1	5
6	C	92	13	(3,4,6)	W_f	0	25	-2	-2
7	C	113	21	(3,4,6)	W_f	0	30	5	-5
8	C	161	48	(2,3,5)	W_f	0	27	-3	14
9	C	201	40	(4,5,7)	W_f	0	22	-5	8
10	C	227	26	(2,3,5)	W_f	0	26	4	-10
11	C	247	20	(2,3,6)	W_f	0	24	-2	17
12	C	274	27	(2,3,6)	W_f	0	27	3	10
13	U	286	12	(5,10,25)	0	W_f	8	-19	3
14	U	296	10	(4,8,12)	W_f $W_d(23)$	$W_d(23)$	23	15	-10
15	U	331	35	(4,8,12)	0	W_f	15	-8	19
16	U	347	16	(4,8,12)	0	$W_d(18)$	18	3	5
17	U	374	27	(4,8,12)	0	W_f	12	-6	-8

Scenario A1: UBCDFLOW Results

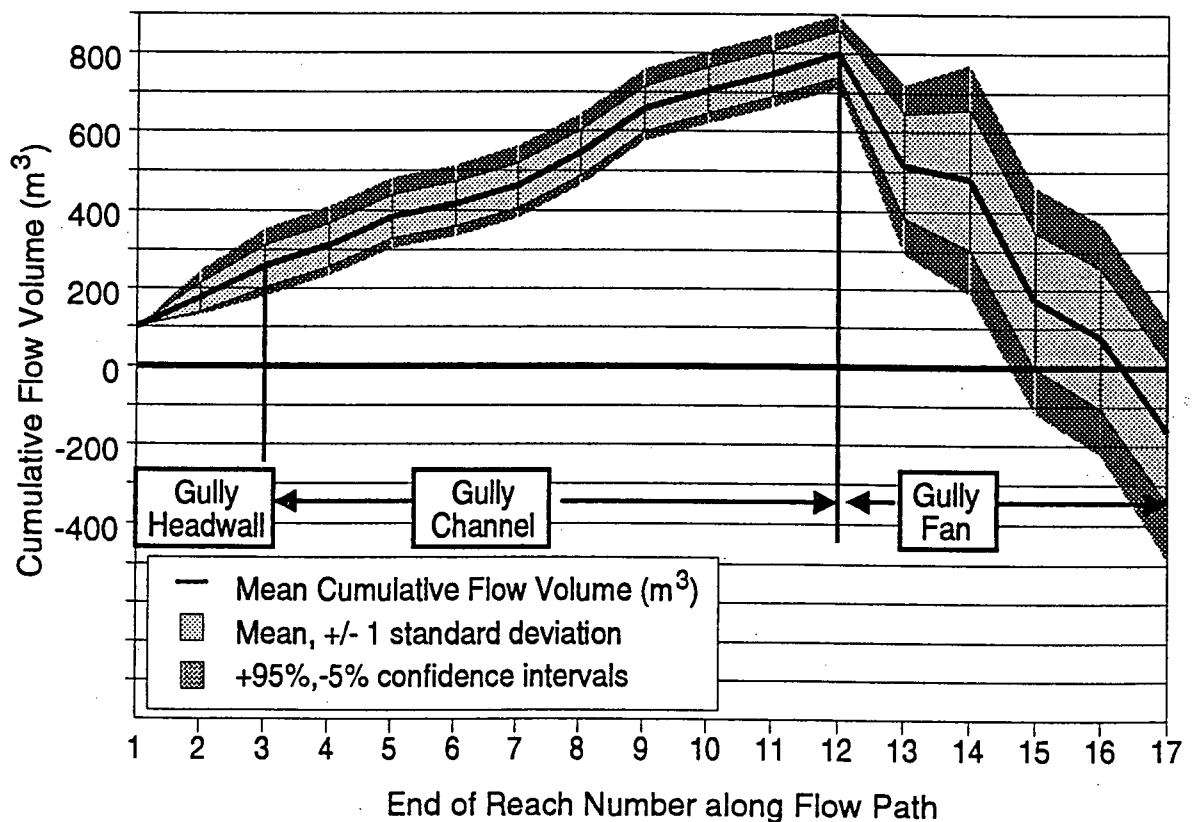


Figure 7.7(a): Input data and results for Scenario A1

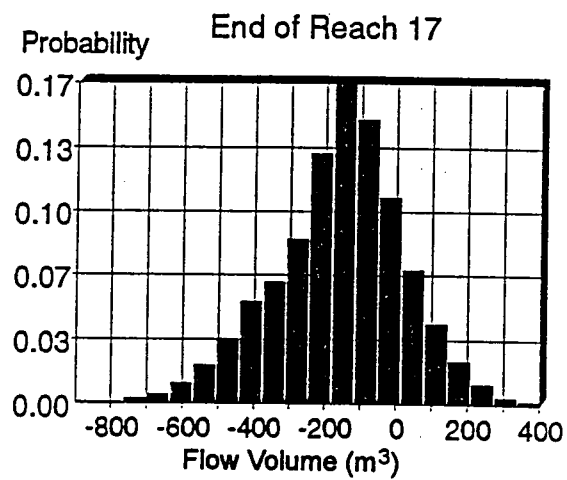
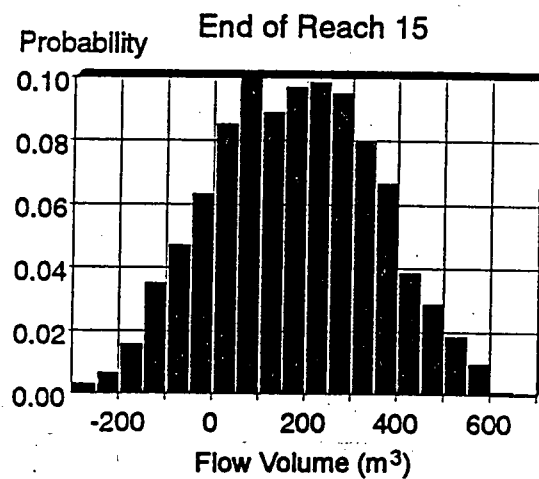
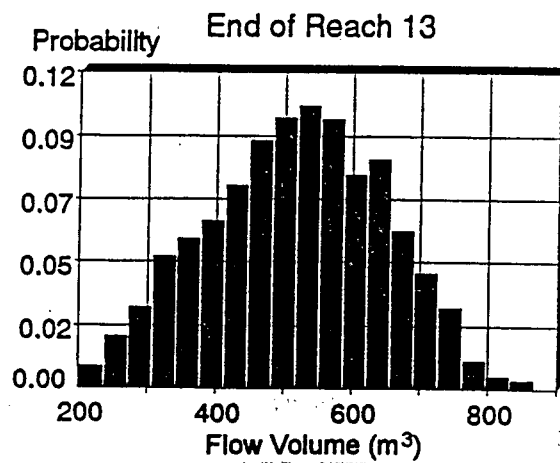


Figure 7.7(b): Flow volumes at ends of selected reaches, Scenario A1

INPUT DATA FOR EXAMPLE A2 , EVENT 4001 Variable Initial Volume
Initiation Volume: triangular distribution of (50,100,250 m³)

Reach	SM	Path Length	Reach Length	W_f	W_e	W_d	TH	dTH	dAZ
1	U	13	13	n/a	n/a	n/a	35	n/a	n/a
2	U	27	14	(5,10,30)	W_f	0	43	8	0
3	U	34	7	(5,10,30)	W_f	0	31	-12	-31
4	C	49	15	(5,7,10)	W_f	0	28	-3	2
5	C	79	30	(3,4,7)	W_f	0	27	-1	5
6	C	92	13	(3,4,6)	W_f	0	25	-2	-2
7	C	113	21	(3,4,6)	W_f	0	30	5	-5
8	C	161	48	(2,3,5)	W_f	0	27	-3	14
9	C	201	40	(4,5,7)	W_f	0	22	-5	8
10	C	227	26	(2,3,5)	W_f	0	26	4	-10
11	C	247	20	(2,3,6)	W_f	0	24	-2	17
12	C	274	27	(2,3,6)	W_f	0	27	3	10
13	U	286	12	(5,10,25)	0	W_f	8	-19	3
14	U	296	10	(4,8,12)	W_f	$W_{d(23)}$	23	15	-10
15	U	331	35	(4,8,12)	0	W_f	15	-8	19
16	U	347	16	(4,8,12)	0	$W_{d(18)}$	18	3	5
17	U	374	27	(4,8,12)	0	W_f	12	-6	-8

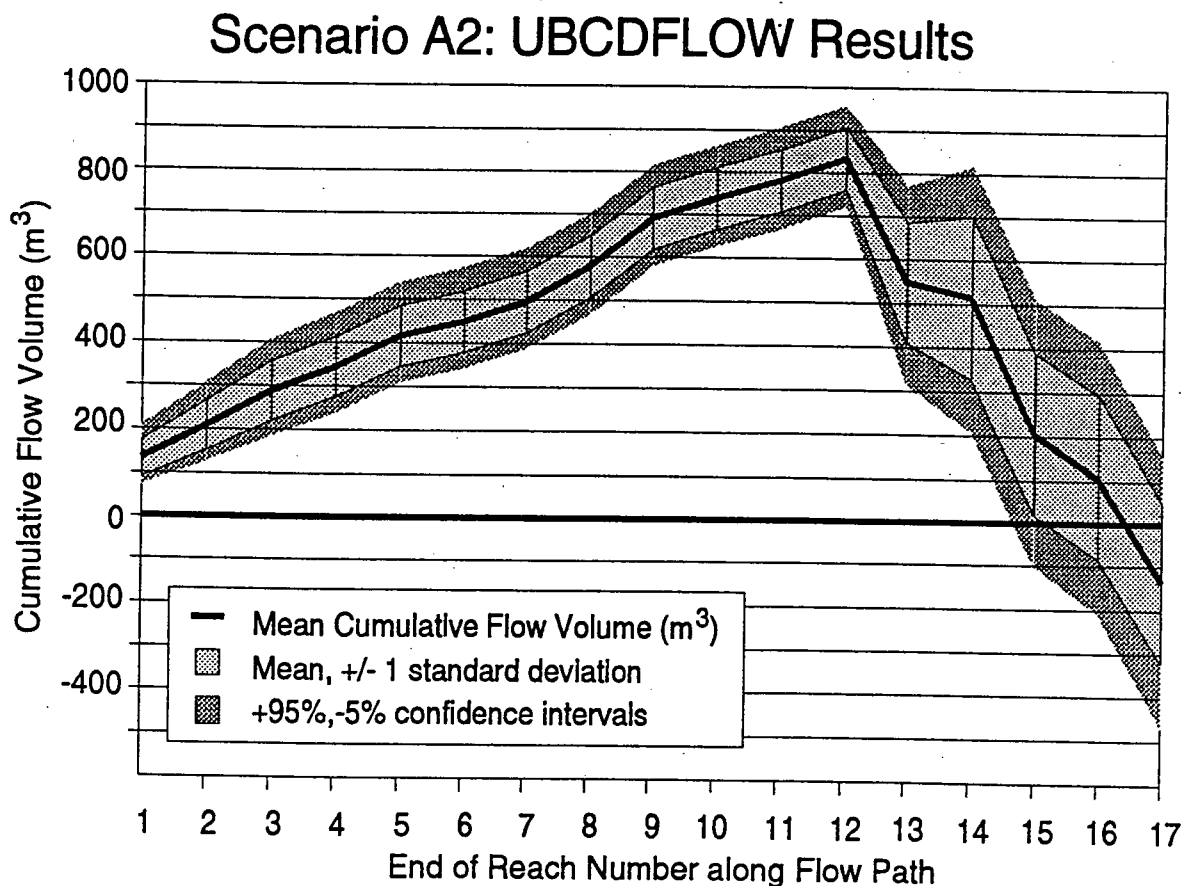


Figure 7.8(a): Input data and results for Scenario A2

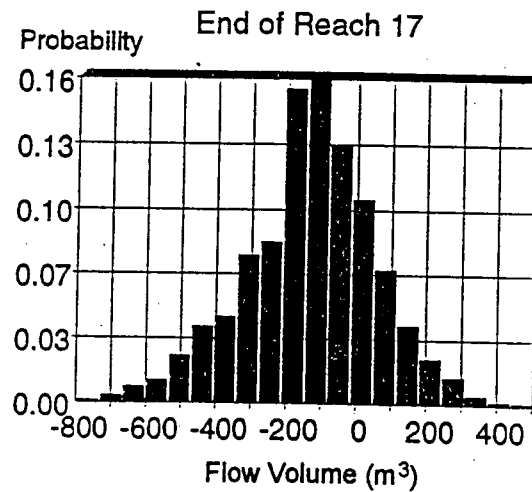
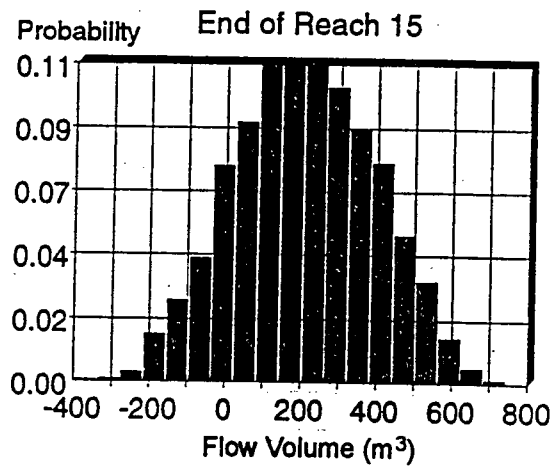
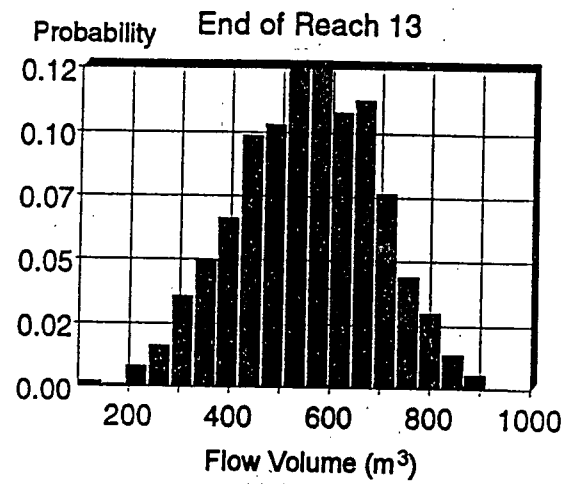


Figure 7.8(b): Flow volumes at the ends of selected reaches, Scenario A2

INPUT DATA FOR SCENARIO A3, EVENT 4001, Variable Initial Volume
Initiation Volume: triangular distribution of (50,100,250 m³)

Reach	SM	Path Length	Reach Length	W_f	W_e	W_d	TH	dTH	dAZ
1	U	13	13	n/a	n/a	n/a	35	n/a	n/a
9	C	53	40	(4,5,7)	W_f	0	22	-13	7
10	C	79	26	(2,3,5)	W_f	0	26	4	-10
11	C	99	20	(2,3,6)	W_f	0	24	-2	17
12	C	126	27	(2,3,6)	W_f	0	27	3	10
13	U	138	12	(5,10,25)	0	W_f	8	-19	3
14	U	148	10	(4,8,12)	W_f	$W_d(23)$	23	15	-10
15	U	183	35	(4,8,12)	0	W_f	15	-8	19
16	U	199	16	(4,8,12)	0	$W_d(18)$	18	3	5
17	U	226	27	(4,8,12)	0	W_f	12	-6	-8

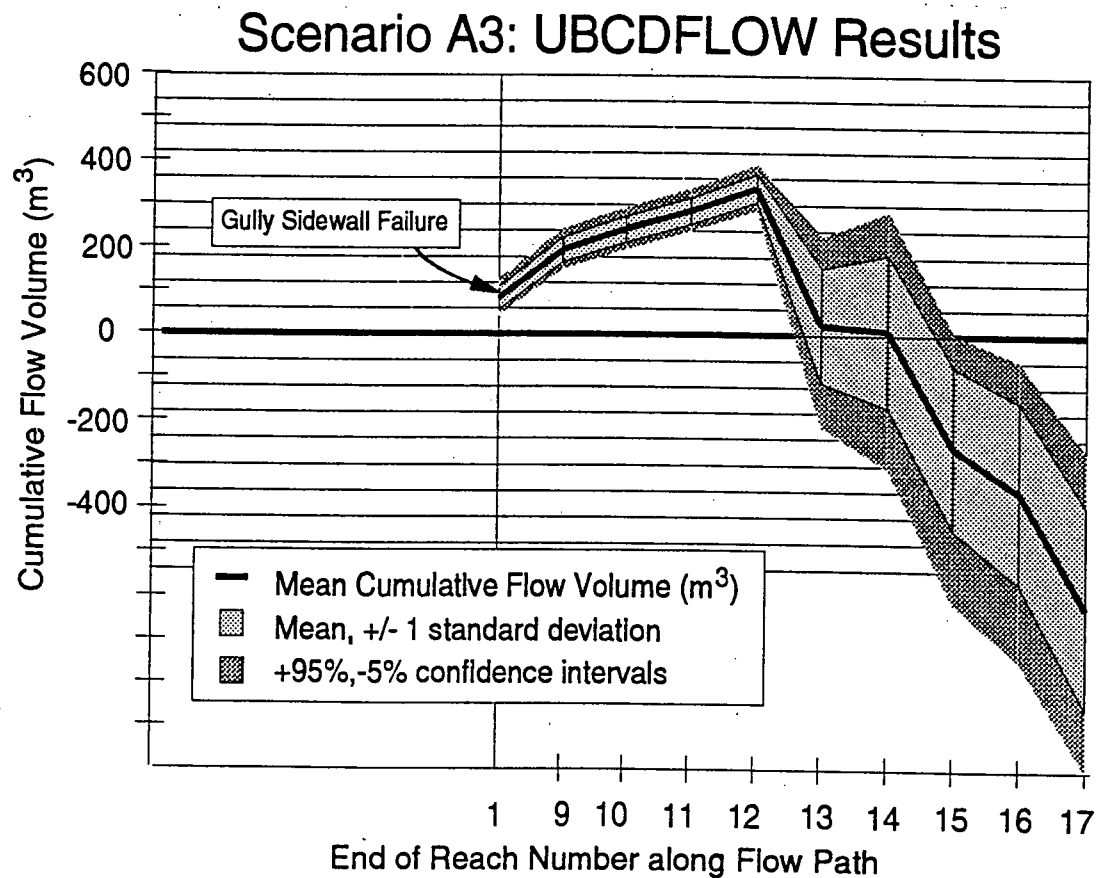


Figure 7.9(a): Input data and results for Scenario A3

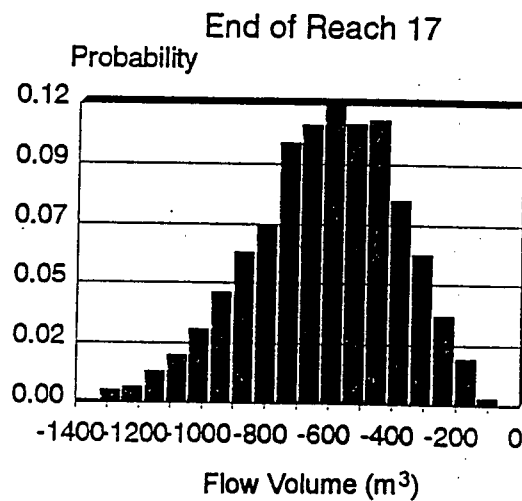
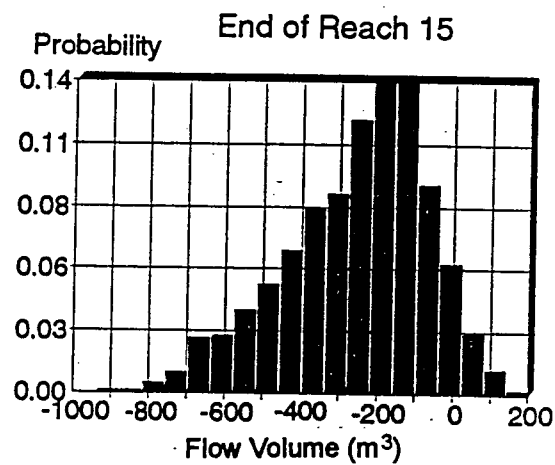
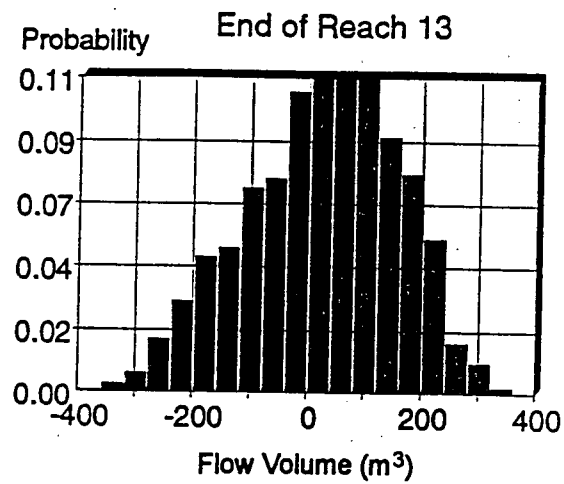


Figure 7.9(b): Flow volumes at the ends of selected reaches, Scenario A3

UBCDFLOW Results for Scenarios A1, A2, and A3

			Scenario A1 Figure 7.7(a)			Scenario A2 Figure 7.8(a)			Scenario A3 Figure 7.9(a)		
Reach	SM	Path Length	#T	$\Sigma T/n$	P(Ex)	#T	$\Sigma T/n$	P(Ex)			
1	U	13	0	0.0	1.0	0	0.0	1.0	#T	$\Sigma T/n$	P(Ex)
2	U	27	0	0.0	1.0	0	0.0	1.0			
3	U	34	0	0.0	1.0	0	0.0	1.0			
4	C	49	0	0.0	1.0	0	0.0	1.0			
5	C	79	0	0.0	1.0	0	0.0	1.0			
6	C	92	0	0.0	1.0	0	0.0	1.0			
7	C	113	0	0.0	1.0	0	0.0	1.0			
8	C	161	0	0.0	1.0	0	0.0	1.0			
9	C	201	0	0.0	1.0	0	0.0	1.0			
10	C	227	0	0.0	1.0	0	0.0	1.0			
11	C	247	0	0.0	1.0	0	0.0	1.0			
12	C	274	0	0.0	1.0	0	0.0	1.0			
13	U	286	0	0.0	1.0	0	0.0	1.0			
14	U	296	4	0.002	0.998	1	0.0005	0.9995			
15	U	331	350	0.177	0.823	267	0.134	0.866			
16	U	347	334	0.344	0.656	344	0.306	0.694			
17	U	374	991	0.840	0.161	938	0.775	0.225			
			321*			450*			0*		

T = the number of simulated events which terminate in a given reach
n = the total number of simulations for a scenario (2000 used for these analyses)
*number of events exceeding surveyed geometry

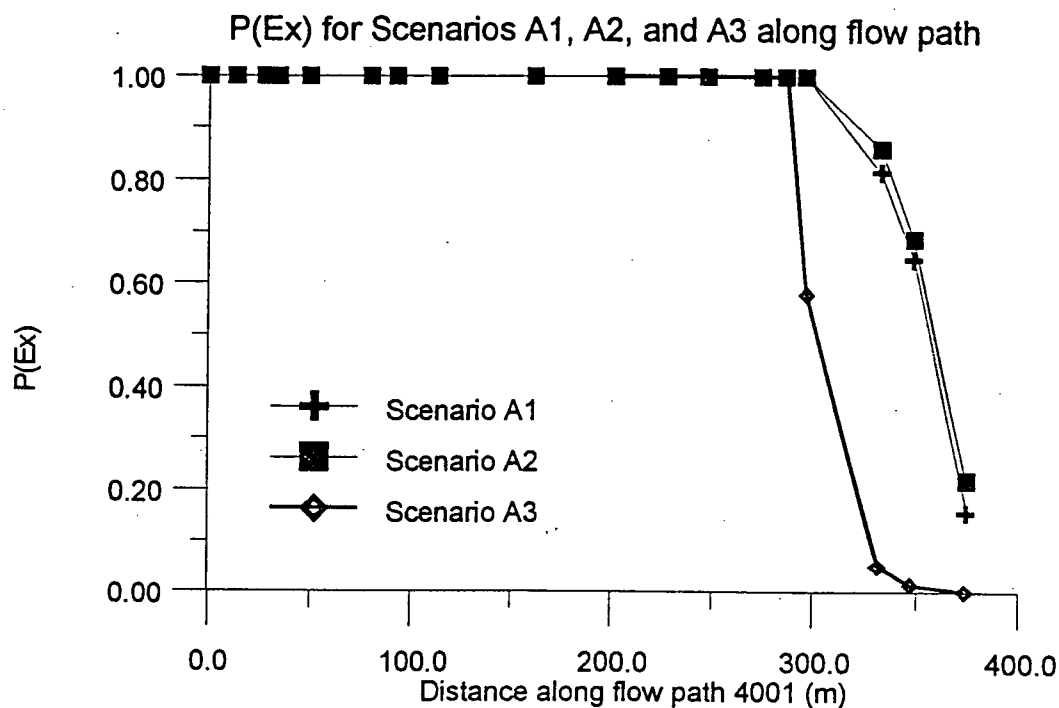


Figure 7.10: Tabulated results and P(Ex) along flow path for Scenarios A1, A2, and A3

INPUT DATA FOR SCENARIO B1, EVENT 3202, Constant Initial Volume
Initiation Volume: constant 400 m³

Reach	SM	Path Length	Reach Length	W_f	W_e	W_d	TH	dTH	dAZ
1	U	26	26	n/a	n/a	n/a	35	n/a	n/a
2	U	49	23	(2,5,10)	$W_e(27)$	0	27	-8	8
3	U	99	50	(2,5,10)	$W_f-W_d(21)$	$W_d(21)$	21	-6	-10
4	U	171	72	(2,5,10)	0	$W_d(17)$	17	-4	17
5	U	213	42	(2,5,10)	0	$W_d(17)$	17	0	10
6	U	234	21	(2,5,10)	0	W_f	8	-9	3
7	U	250	16	(2,5,10)	0	W_f	5	-3	-10
8	U	266	16	(2,5,10)	0	W_f	0.5	-4.5	19

Scenario B1: UBCDFLOW Results

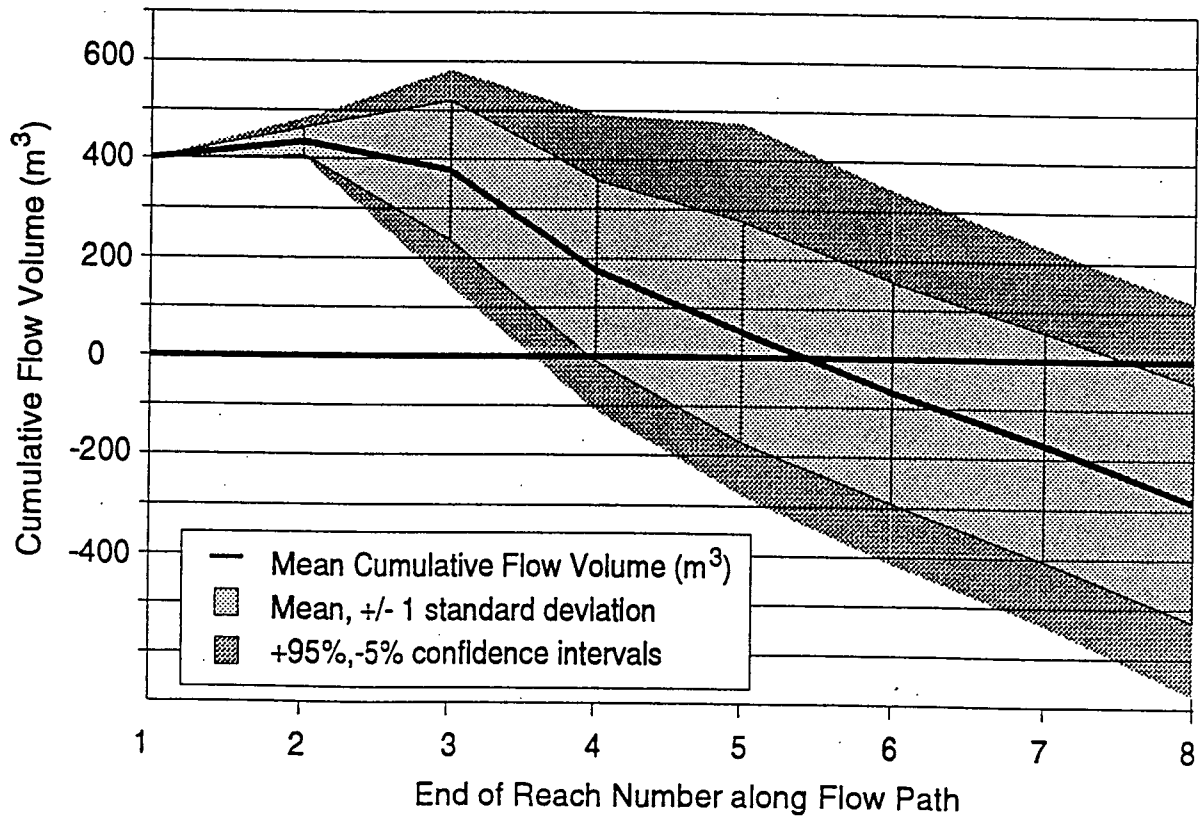


Figure 7.11(a): Input data and results for Scenario B1

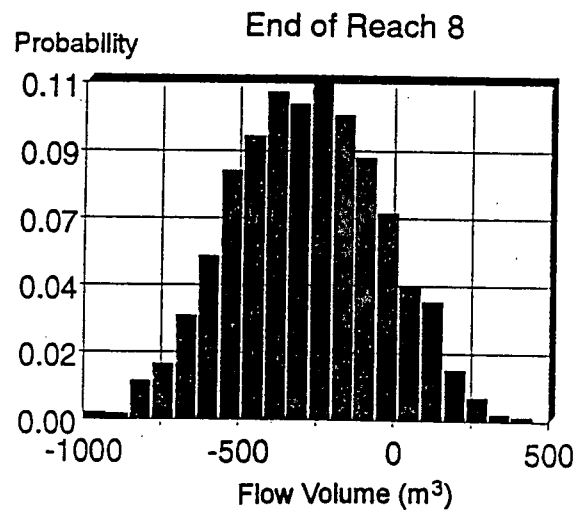
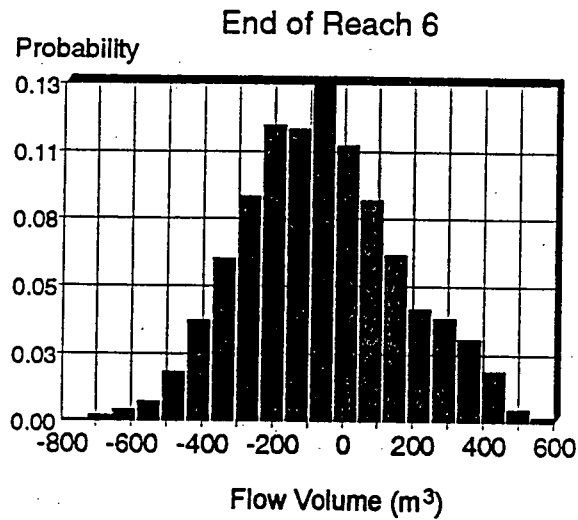
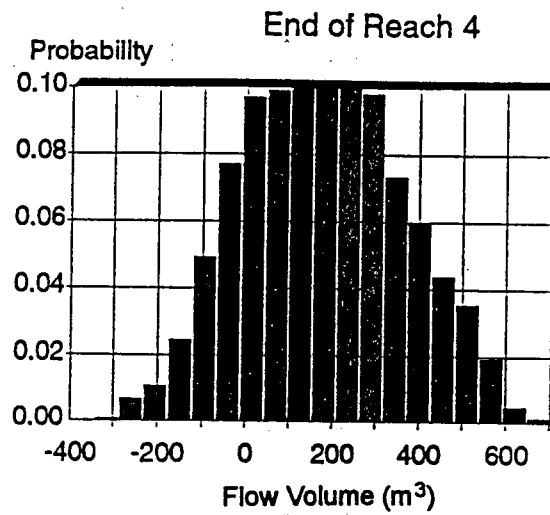


Figure 7.11(b): Flow volumes at the ends of selected reaches, Scenario B1

INPUT DATA FOR SCENARIO B2, EVENT 3202, Variable Initial Volume
Initiation Volume: triangular distribution of (75,150,400 m³)

Reach	SM	Path Length	Reach Length	W_f	W_e	W_d	TH	dTH	dAZ
1	U	26	26	n/a	n/a	n/a	35	n/a	n/a
2	U	49	23	(2,5,10)	$W_e(27)$	0	27	-8	8
3	U	99	50	(2,5,10)	$W_f - W_d(21)$	$W_d(21)$	21	-6	-10
4	U	171	72	(2,5,10)	0	$W_d(17)$	17	-4	17
5	U	213	42	(2,5,10)	0	$W_d(17)$	17	0	10
6	U	234	21	(2,5,10)	0	W_f	8	-9	3
7	U	250	16	(2,5,10)	0	W_f	5	-3	-10
8	U	266	16	(2,5,10)	0	W_f	0.5	-4.5	19

Scenario B2: UBCDFLOW Results

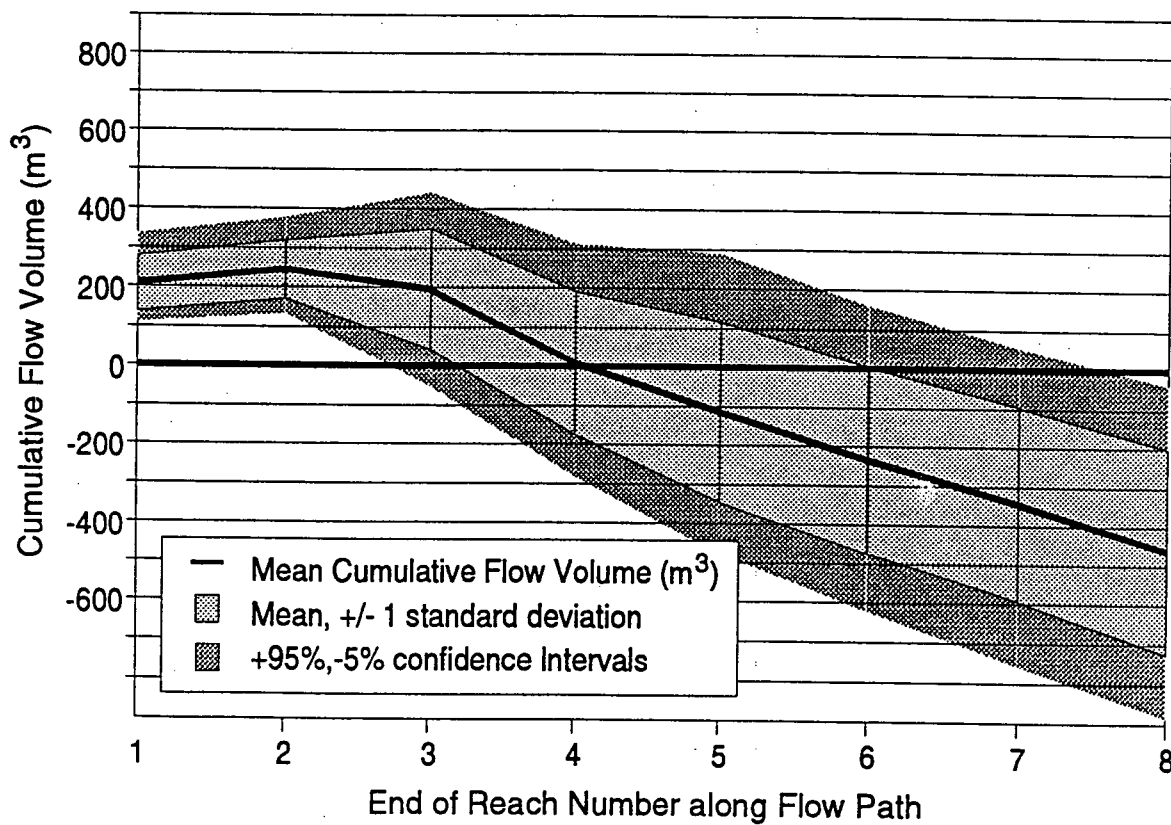


Figure 7.12(a): Input data and results for Scenario B2

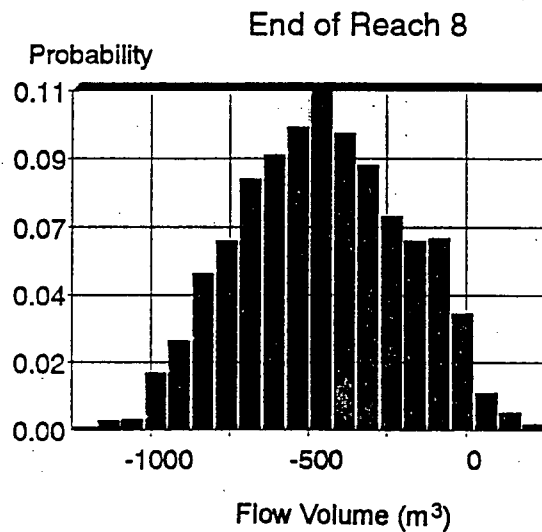
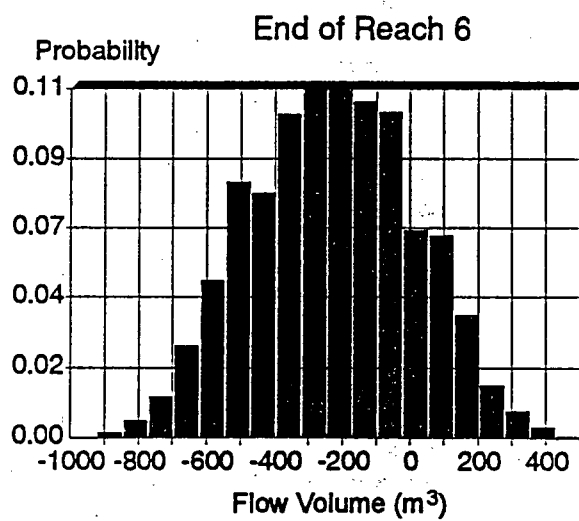
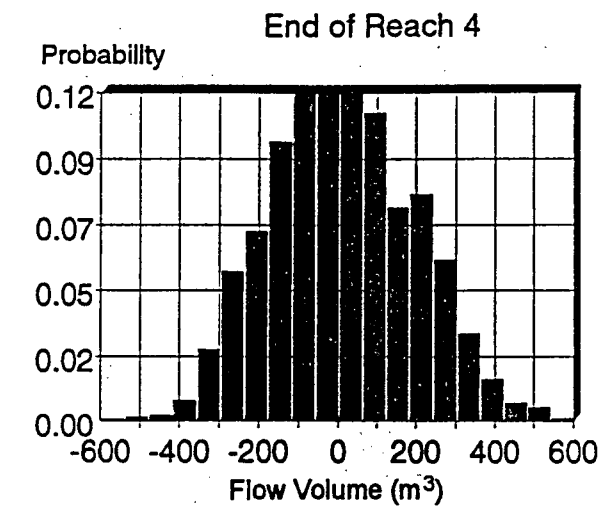


Figure 7.12(b): Flow volumes at the ends of selected reaches, Scenario B2

INPUT DATA FOR SCENARIO B3, EVENT 3202, Variable Initial Volume
Initiation Volume: triangular distribution of (250,500,1000 m³)

Reach	SM	Path Length	Reach Length	W_f	W_e	W_d	TH	dTH	dAZ
1	U	26	26	n/a	n/a	n/a	35	n/a	n/a
2	U	49	23	(2,5,10)	$W_e(27)$	0	27	-8	8
3	U	99	50	(2,5,10)	$W_f - W_d(21)$	$W_d(21)$	21	-6	-10
4	U	171	72	(2,5,10)	0	$W_d(17)$	17	-4	17
5	U	213	42	(2,5,10)	0	$W_d(17)$	17	0	10
6	U	234	21	(2,5,10)	0	W_f	8	-9	3
7	U	250	16	(2,5,10)	0	W_f	5	-3	-10
8	U	266	16	(2,5,10)	0	W_f	0.5	-4.5	19

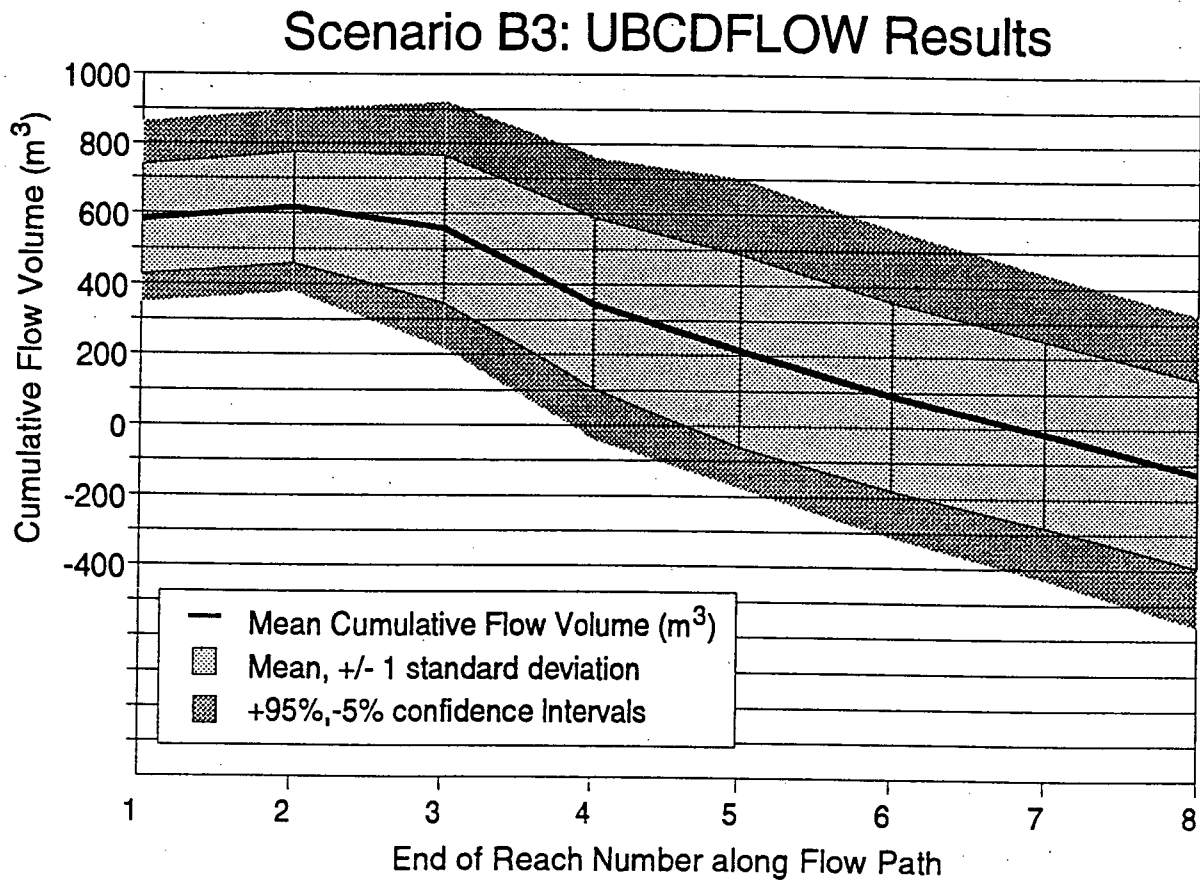


Figure 7.13(a): Input data and results for Scenario A1

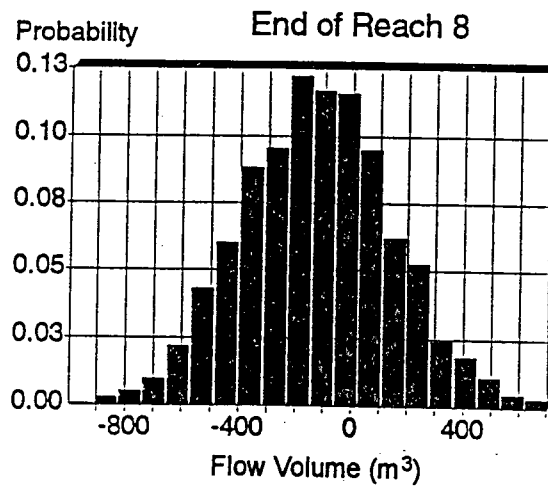
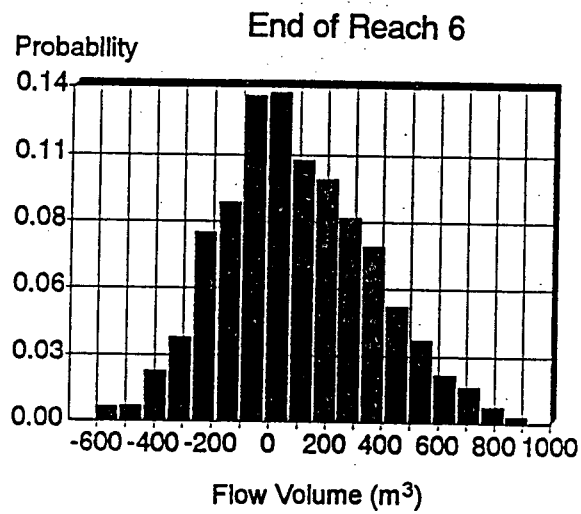
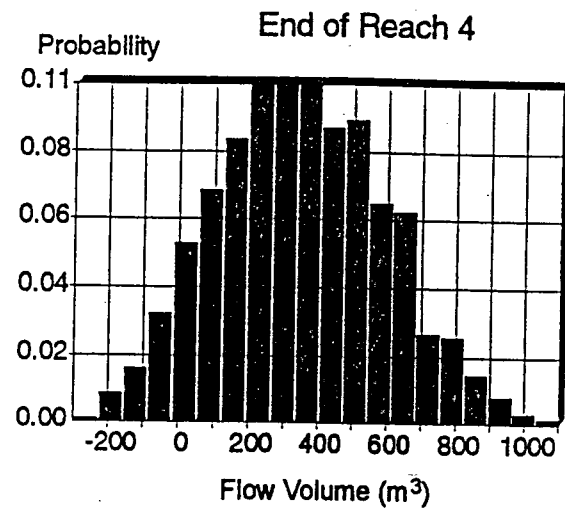


Figure 7.13(b): Flow volumes at the ends of selected reaches, Scenario B3

UBCDFLOW Results for Scenarios B1, B2, and B3

Reach	SM	Path Length	Scenario B1 Figure 7.11(a)			Scenario B2 Figure 7.12(a)			Scenario B3 Figure 7.13(a)		
			#T	$\Sigma T/n$	P(Ex)	#T	$\Sigma T/n$	P(Ex)	#T	$\Sigma T/n$	P(Ex)
1	U	26	0	0.0	1.0	0	0.0	1.0	0	0.0	1.0
2	U	49	0	0.0	1.0	0	0.0	1.0	0	0.0	1.0
3	U	99	0	0.0	1.0	235	0.118	0.883	0	0.0	1.0
4	U	171	355	0.178	0.823	781	0.508	0.492	162	0.081	0.919
5	U	213	551	0.453	0.547	401	0.709	0.292	319	0.241	0.760
6	U	234	370	0.638	0.362	259	0.838	0.162	313	0.397	0.603
7	U	250	286	0.781	0.219	163	0.920	0.081	271	0.533	0.468
8	U	266	200	0.881	0.119	100	0.970	0.031	313	0.689	0.311
			238*			61*			611*		

T = the number of simulated events which terminate in a given reach

n = the total number of simulations for a scenario (2000 used for these analyses)

*number of events exceeding surveyed geometry

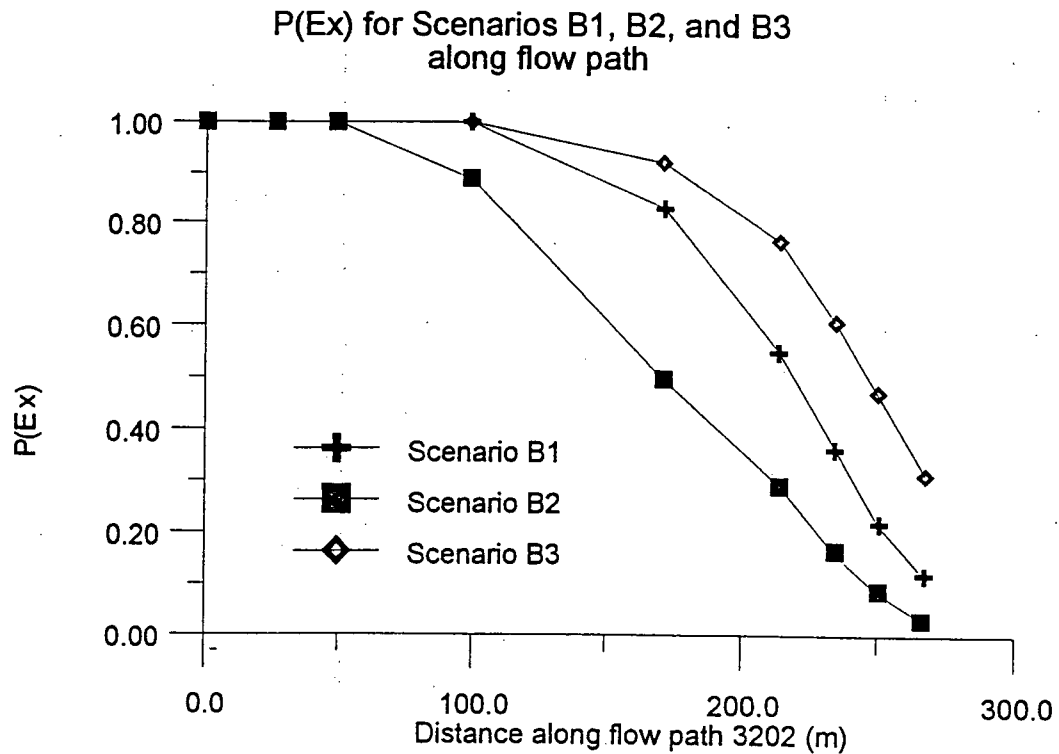


Figure 7.14: Tabulated results and P(Ex) along flow path for Scenarios B1, B2, and B3

Chapter 8 CONCLUSIONS AND RECOMMENDATIONS

The objective of this research project was to develop a model which can be used to determine the likelihood of direct impact for potential debris slides, debris avalanches, and debris torrents for hillslopes in coastal British Columbia which have been affected by clearcut logging. Work activities have included the characterization of the debris flow data, mapped from actual debris flow events; the development of regression equations to predict volume change behaviour, and the incorporation of probability using the observed variability in flow events. Repeated simulations in *UBCDFLOW* are used to determine the probability of exceedance, $P(Ex)$, at a point of interest along a potential debris flow path. The probability of impact at a point of interest is then the product of the probability of initiation and the probability of exceedance.

8.1 Volumetric Model

The Volumetric Model is a deterministic method which can be used to back-analyze the travel distance of a debris flow using empirical volumetric relationships. The model accounts for volume changes along the event path; flow is deemed to have terminated when the flow volume decreases to less than zero. The model, in addition to determining the travel distance of potential debris flow events, also provides the cumulative flow volume at the endpoints of the reaches of the surveyed path. These results can be used to determine the potential severity of an event, which is often directly related to the volume of the flow at impact. This is

particularly useful in the forestry applications, where the risk management decisions relating to logging on unstable terrain should take into account both the probability of initiation, the probability of exceedance to a point of concern, and the severity of potential downslope impacts.

8.1.1 Debris Flow Data

Debris flow data from the Queen Charlotte Islands in coastal British Columbia have been used for the development of empirical regression equations to predict the volumetric behaviour of debris flows. The data are from the forensic observations of debris flow events which have occurred after logging. Statistical characterization of the event type, peak flow volume, and travel distance for events from the Queen Charlotte Islands and the Mamquam River, Eve River, and Nootka Island areas of coastal British Columbia show a number of similarities. These similarities may be due to the similarities in the gradation of material involved (Fannin and Wilkinson, 1995) as well as several feedback mechanisms which occur during debris flow movement to limit the flow velocity (Jordan, 1994).

Data for each debris flow event consists of the geometry, slope morphology, and volume change behaviour for each distinct reach of the travel path. The several types of slope morphology recorded in the study were grouped into unconfined flow, confined flow, and transitional flow on the basis of lateral confinement of the flow in the reach. Transitional flow reaches, taken as the first unconfined reach downslope of a gully channel, were separated from other unconfined reaches since the sudden lack of confinement very often leads to deposition

of debris flow material.

8.1.2 Regression Analyses

The volume changes of a debris flow as it travels along the event path are related to the attributes of each reach (geometry and slope morphology) as well as the size of the incoming flow volume and the availability of material for entrainment. Regression analyses were carried out on selected debris flow event data from the Queen Charlotte Islands. The original data from the Queen Charlotte Islands were tested for internal accuracy, by determining the volumetric error of the event. Events with a volumetric error of 40% or less were selected for use in regression analyses. A survey correction was applied to correct the observed flow volumes by equating total entrainment and deposition volumes along the travel path of each event. Subsequently, the data were partitioned into unconfined flow, confined flow, and transition flow reaches for development of the regression equations.

For the Volumetric Model, the entrainment and deposition volumes within each reach must be calculated. Thus, the entrainment and deposition volume were chosen as the response variables for the regression analyses. Possible predictors for the regression equations included the length, widths of entrainment and deposition, slope angle, as well as the incoming flow volume and the Bend Angle Function. The Bend Angle Function was developed to determine the effects of changes in path direction on deposition.

Preliminary analyses of the data yielded only weak correlations between the potential predictor variables and the response variables. These correlations were strengthened by logarithmic transformation of both the response variables and the predictor variables. Due to the non-linear relationship between entrainment volume and slope angle for unconfined flow reaches, these data were partitioned prior to regression analyses to strengthen the relationships between the predictor and response variables.

Separate regression equations were developed to calculate entrainment and deposition, since the factors which control each process differ and should not be grouped together as a single equation which would predict the net volume change of the debris flow. Statistical interpretation and cross-validation of the results showed the regression equations are valid for predicting entrainment and deposition volumes along the path on a reach-by-reach basis. Since these data are based on forensic observations, the hydrologic conditions as well as the quantity, gradation, and composition of materials prior to the event are unknown. In the context of the regression equations, it is assumed that these factors cause an "observed variability" when the results of the regression equations are compared to data from actual flow events.

For predictor variables, the length and width of the reaches along the flow path proved to be strong predictors in the regression equations. Slope angle, incoming flow volume, as well as changes in azimuth angle and slope angle along the path, proved to be weaker, but nonetheless beneficial, predictors of entrainment and/or deposition. Confinement was also shown to have a strong influence on flow behaviour, and this fact led to the separation of reach data on the basis

of flow confinement. These results imply that the slope morphology along the path, which influences the width of the event and the confinement of the flow, heavily influences the cumulative flow volume and travel distance of the event.

8.1.3 Testing of Volumetric Model

Cross-validation was carried out to determine validity of the regression equations. The data were divided into a construction set and a validation set, on an event basis, from the Q.C.I. (Selected) Data. Regression equations, similar in format to the equations developed from the entire Q.C.I. (Selected) Data set, were developed. These equations were then tested using data in the validation set, with the predicted entrainment and deposition values from the construction set regression equations showing good agreement with the actual values from the validation set.

The model was used, with the regression equations from the Queen Charlotte Islands, to back-analyze debris flow events from the Mamquam River, Eve River, and Nootka Island areas of coastal British Columbia. The results were generally in agreement with the observed data, however the observed variability of flow behaviour was determined to be a significant factor in cases where the model results differed from the observed data. A large amount of variability was observed for unconfined flow conditions, which is likely the result of more variable moisture contents in the flows as compared to confined flow conditions.

Results of the Volumetric Model have not been compared with other numerical analysis models for debris flow movement. These models, which generally use either finite element or finite difference methods, are difficult to apply using the types of forensic parameters from the Q.C.I. (Original) data.

8.2 Incorporation of Probability

Probability was incorporated into the model to create *UBCDFLOW*. Using probability density functions for the input variables to represent the initial flow volume and the width of the flow within each reach, as well as a sampling technique to determine the proportion of deposition on unconfined reaches, repeated simulations are carried out to determine the travel distance of potential debris flows. An evaluation of these simulations can be carried out to determine the probability of exceedance, $P(Ex)$, for the endpoints of the reaches of the potential debris flow path. The cumulative flow volumes at the endpoints of the reaches are also calculated to provide information on the potential severity of debris flow impacts.

The testing of *UBCDFLOW* has shown some site factors are important for determining the travel distance of potential debris flow events. For events with an unconfined flow path, the size of the initiation volume is important to determine the travel distance. This conclusion is based on the observation that for unconfined (open slope) events with a large initial volume will travel farther than events with a small initial volume. For events along a confined flow path, the location of the initiation point was shown to be important: events from the upper part

of the gully system entraining more material, and consequently travelling to the apex of the fan with a larger volume, travel farther than events which initiate in the lower portions of the gully system.

8.3 Recommendations for Future Research

This section discusses the conclusions based on the development of *UBCDFLOW* as well as the recommendations for future research to further validate *UBCDFLOW* for probabilistic assessment. Also, several recommendations can be made regarding the future research on the probabilistic assessment of debris flow travel distance. The following comments are made to guide future research activities.

Several regression equations were developed from a limited range of slope angle due to the limited amount of data in the Q.C.I. (Selected) Data set. While a large number of data points for entrainment and deposition of unconfined and confined flow exist, there are relatively few data points for deposition of transition flow. Thus, there is not as much confidence in predicting deposition in transition flow reaches. Moreover, the lack of data for deposition in gully channels and entrainment on transition reaches precludes development of regression equations to predict deposition/entrainment for these cases.

The regression equations which have been developed are based on forensic data, and thus only a limited number of field parameters could be measured. However, a link must be firmly

established between the entrainment and deposition equations and the pre-event conditions on the slope before the regression equations can be used with confidence. Thus, establishing study sites to develop these links for both gully systems and open slopes should be undertaken. A study of this nature should include an inventory of the soil, rock, and organic debris on slopes and in gullies where a debris flow event may occur, and how these components change over time, both before logging and after logging. The content of the fine soil is particularly important, since the rheology of the flow is determined by the amount of fine soil in the flow (Jordan, 1994). Aspects of this research are currently being undertaken by the Geography Department at the University of British Columbia, among others.

The moisture conditions present in the flow are particularly important in determining the flow behaviour for unconfined flow conditions. A research study to link the antecedent moisture conditions/climatic factors to debris flow occurrence would also strengthen aspects of the research, and possibly provide a valuable tool for the prediction of debris flow initiation. Such a study should also incorporate the effects of snowmelt in applicable areas.

Although the regression equations developed from the Q.C.I. (Selected) Data have been tested in three other areas of coastal British Columbia, the applicability of these equations to other parts of the Pacific Northwest (including interior British Columbia) should be investigated through forensic studies of debris flow sites. Such a study may lead to the development of other regression equations for use in probabilistic modelling of debris flow travel distance, which may in turn improve the capability of the Volumetric Model to back-analyze debris flow

events and provide more confidence in the predictive nature of *UBCDFLOW*. Also, further regression analyses could be carried out to extend the slope ranges over which the regression equations are applied in *UBCDFLOW*, improving the capability of the model to simulate dual mode flow behaviour. Such studies should also consider the differences in climate, surficial geology, and forestry practices relative to coastal British Columbia.

Finally, the probability of deposition of a debris flow at a particular point along the flow path can be viewed as a combination of conditional probabilities, with $P(Ex)$ being one of several which must be assessed for a true probabilistic approach to modelling potential debris flow impact. Other conditional probabilities include the meteorological and hydrological factors which influence the probability of initiation, as well as the influence of logging on the quantity and composition of debris material stored in the gully channels and on open hillslopes. Further research studies can be carried out to determine these conditional probabilities and facilitate a true probabilistic approach to modelling debris flow impact.

Chapter 9 REFERENCES

- Bagnold, R.A. 1954. Experiments on a gravity-free dispersion of large spheres in a Newtonian fluid under shear. *Proceedings of the Royal Society of London, Series A*, **225**: 49-63.
- Benda, L.E. and Cundy, T.W. 1990. Predicting deposition of debris flows in mountain channels. *Canadian Geotechnical Journal*, **27**: 409-417.
- Bovis, M.J. and Dagg, B.R. 1992. Debris flow triggering by impulsive loading: mechanical modelling and case studies. *Canadian Geotechnical Journal*, **29**: 345-352.
- Bovis, M.J. and Dagg, B.R. 1988. A model for debris accumulation and mobilization in steep mountain channels. *Hydrological Sciences Journal*, **33**: 589-604.
- British Columbia Ministry of Forests and Ministry of Environment. 1995a. Gully Assessment Procedure. *Forest Practices Code Guidebook*, Government of British Columbia. Crown Publications Inc., 546 Yates St., Victoria, B.C. V8W 1K8.
- British Columbia Ministry of Forests and Ministry of Environment, 1995b. Mapping and Assessing Terrain Stability. *Forest Practices Code Guidebook*, Government of British Columbia. Crown Publications Inc., 546 Yates St., Victoria, B.C. V8W 1K8.
- Cannon, 1993. An empirical model to predict debris flow travel distance. *Proceedings, ASCE Hydraulic Engineering '93*. Edited by Shen, H.W. and Wen, F. pp 1768-1773.
- Chatwin, S.C., Howes, D.E., Schwab, J.W., and Swanston, D.N. 1994. A guide for management of landslide-prone terrain in the Pacific Northwest. *Ministry of Forests, Land Management Handbook No. 18 (Second Edition)*. Crown Publications Inc., 546 Yates St., Victoria, B.C. V8W 1K8.
- Chen, C.L. 1987. Comprehensive review of debris flow modelling concepts in Japan. *In Debris Flows/Avalanches: Process, Recognition, and Mitigation*. Geological Society of America, *Reviews in Engineering Geology*, Volume VII: 13-29.
- Craig, R.F. 1992. *Soil Mechanics*, Fifth Edition. Chapman and Hall, London, U.K.

- Evans, S.G., Hungr, O., and Eneqren, R. 1993. The Avalanche Lake rock avalanche, Mackenzie Mountains, Northwest Territories, Canada: description, dating, and dynamics. Canadian Geotechnical Journal, (in press).
- Fannin, R.J., and Rollerson, T.P. 1993. Debris Flows: some physical characteristics and behaviour. Canadian Geotechnical Journal, **30**: 71-81.
- Fannin, R.J. and Wilkinson, J.M.T. 1995. An analysis of the Jamieson Creek landslide. Proceedings of the 48th Canadian Geotechnical Conference, Vancouver, Canada, September, 1995 p 635-642.
- Hammond, C., Hall, D., and Miller, S. and Swetik, P. 1992. Level I Stability Analysis (LISA). Documentation for Version 2.0. United States Department of Agriculture, Forest Service, Intermountain Research Station, General Technical Report, INT-000.
- Hungr, 1995. A model for the runout analysis of flow slides, debris flows, and avalanches. Canadian Geotechnical Journal, **32**: 115-126.
- Hungr, O., Morgan, G.C., and Kellerhals, R. 1984. Quantitative analysis of debris torrent hazards for design of remedial measures. Canadian Geotechnical Journal, **21**: 663-677.
- Jordan, R. P. 1994. Debris Flows in the Southern Coast Mountains, British Columbia: Dynamic Behaviour and Physical Properties. P.h.D. Thesis., University of British Columbia, Vancouver.
- Karanka, E.J. 1986. Trends and fluctuations in precipitation and stream runoff in the Queen Charlotte Islands. British Columbia, Ministry of Forests Land Management Report, No. 46, Government of British Columbia.
- Kennedy, J.B. and Neville, A.M. 1976. Basic Statistical Methods for Engineers and Scientists, Second Edition. Harper and Row, New York.
- Kozak, A. and Kozak, R.A. 1995. Notes on regression through the origin. The Forestry Chronicle, **71**: No. 3, 326-330.
- Media Cybernetics, Inc. 1991. Minitab Reference Manual, Release 8 PC Version. State College, Pennsylvania, USA.
- Millard, T.H. 1993. Sediment in Forested and Logged Gullies, Coastal British Columbia. M.Sc. Thesis, Department of Geography, University of British Columbia.

Morgan, G.C., Rawlings, G.E., and Sobkowicz, J.C. 1992. Evaluating total risk to communities from large debris flows. Proceedings, Geohazards'92, BiTech Publishing, Vancouver British Columbia.

Muller, J.E. 1977. Geology of Vancouver Island. Open File 463, Geological Association of Canada.

O'Loughlin, C.L. 1972. An investigation of the stability of steep land forest soils in the coast mountains, southwest British Columbia. Ph.D. Thesis, University of British Columbia, Vancouver.

Pallisade, 1995. @Risk Analysis for Spreadsheets. Documentation for Release 3.0, March 1, 1994. Pallisade Corporation, Newfield, New York, U.S.A.

Pierson, T.C. 1986. Flow behaviour of channelized debris flows, Mount St. Helens, Washington. *In Hillslope Processes. Edited by Abrams, A.D. and Allen and Unwin, Boston, p 269-297.*

Pierson, T.C. and Costa, J.E. 1987. A rheologic classification of subareal sediment-water flows. *In Debris Flows/Avalanches: Process, Recognition, and Mitigation. Edited by Costa, J.E. and Weiczorek, G.F. Geological Society of America, Reviews in Engineering Geology, VII: 1-12.*

Rollerson, T.P. 1992. Relationships between landscape attributes and landslide frequencies after logging: Skidegate Plateau, Queen Charlotte Islands. Land Management Report No. 76. Research Branch, Ministry of Forests, 31 Bastion Square, Victoria, B.C. V8W 1K8

Sidle, R.C. 1992. A theoretical model of the effects of timber harvesting on slope stability. *Water Resources Research, 28(7): 1879-1910.*

Sutherland-Brown, A. 1968. Geology of the Queen Charlotte Islands, British Columbia. British Columbia Department of Mines and Petroleum Resources, Bulletin 54.

Takahashi, T. 1978. Mechanical characteristics of debris flow. *ASCE Journal of the Hydraulics Division, 104: 1153-1169.*

Takahashi, T. 1980. Debris flow on open prismatic channel. *ASCE Journal of Hydraulics Engineering, 106(3): 381-396.*

Takahashi, T. 1991.. Debris Flow. IAHR Monograph Series, A.A. Balkema, Rotterdam, The Netherlands. 165 pp.

Takahashi, T., Nakagawa, H., Harada, T., Yamashiki, Y. 1992. Routing debris flows with particle segregation. *ASCE Journal of Hydraulic Engineering*, **118**(11): 1490-1507.

Takahashi, T. and Yoshida, H. 1979. Study on the deposition of debris flows, Part 1 - Deposition due to abrupt change of bed slope. *Annuals, Disaster Prevention Research Institute, Kyoto University, Japan*, 22 B-2. (In Japanese).

VanDine, D.F. 1985. Debris flows and debris torrents in the southern Canadian Cordillera. *Canadian Geotechnical Journal*, **22**: 44-68.

Varnes, 1978. Slope movement types and processes. *In Landslides, Analysis and Control. Edited by Schuster, R.L. and Krizek, R.J.* Transportation Research Board, National Academy of Sciences, Washington, D.C., Special Report 176, pp 12-33.

Weisburg, 1985. *Applied Regression Analysis*. John Wiley and Sons, Inc.

Wilkinson, J.M.T. 1996. *Landslide Initiation: A Unified Geostatistical and Probabilistic Modelling Technique*. M.A.Sc. Thesis, University of British Columbia, Vancouver.

Appendix A

Q.C.I. (Selected) Data

**Data used by permission of
Terry Rollerson, P.Geo.
Ministry of Forests, Vancouver Forest Region**

Notes:

E# = event number
R# = reach number
ELEN = length of entrainment in reach (m)
EWID = average width of entrainment in reach (m)
EDEP = average depth of entrainment in reach (m)
DLEN = length of deposition in reach (m)
DWID = average width of deposition in reach (m)
DDEP = average depth of deposition in reach (m)
TH = average slope angle of reach (degrees)
PAZ = average change in azimuth angle relative to upslope reach (degrees)
SM = slope morphology
FDEP = flow depth (m); not used as part of this study
%REV = % revegetation in reach (not used as part of this study)

Q.C.I. (Selected) Data - Appendix A

E#	R#	ELEN	EWID	EDEP	DLEN	DWID	DDEP	TH	PAZ	SM	FDEP	%REV
101	1	25	30	1	0	0	0	35	80	OS	1	70
101	2	26	25	0.6	2	10	1	26	80	OS	1	80
101	3	24	10	0.3	24	10	0.3	18	90	OS	1	100
101	4	72	20	0.2	72	5	1	22	90	OS	1	80
101	5	23	17	0.2	23	1.5	0.5	27	90	OS	1	70
101	6	0	0	0	16	20	1	5	90	RD	1	100
101	7	0	0	0	40	11	2	17	125	OS	2	100
102	1	19	10	1	0	0	0	35	265	OS	1	5
102	2	31	10	1.5	5	2	0.5	22	280	OS	1.3	20
102	3	39	10	0.2	20	2	0.2	19	280	OS	1.3	60
102	4	21	10	0.4	0	0	0	28	287	OS	0.7	50
102	5	38	12	0.2	0	0	0	20	290	BE	1.3	90
102	6	27	4	0.2	27	8	1.5	22	280	OS	1.5	95
102	7	0	0	0	20	8	2	16	288	OS	2	95
102	8	0	0	0	22	8	1.5	13	320	OS	1.5	100
103	1	14	10	1	0	0	0	40	300	OS	1	20
103	2	20	11	0.5	5	1	0.5	25	300	OS	1	20
103	3	33	6	0.3	33	6	0.5	23	310	OS	1	30
103	4	0	0	0	10	8	1.5	24	290	OS	1.5	50
105	1	17	10	1	0	0	0	38	270	OS	1	1
105	2	24	14	0.5	0	0	0	35	270	OS	1	5
105	3	14	14	0.2	0	0	0	25	280	OS	1	10
105	4	0	0	0	25	14	0.5	22	300	OS	1	60
210	1	12	42	1	0	0	0	39	230	OS	1	10
210	2	17	42	0.5	0	0	0	27	230	OS	0.5	10
210	3	31	7	1	31	30	1	25	230	OS	1	25
210	4	15	7	0.5	0	0	0	27	230	OS	0.5	20
210	5	0	0	0	17	7	1.5	25	230	OS	1.5	60
210	6	14	8	0.7	0	0	0	25	230	OS	0.7	25
210	7	0	0	0	37	7	0.3	26	230	OS	0.3	25
210	8	0	0	0	30	9	1	22	230	BE	1	25
210	9	0	0	0	22	18	1.5	12	230	BE	1.5	30
212	1	25	9	0.3	0	0	0	28	100	GC	2	40
212	2	15	8	0.3	0	0	0	30	75	GC	3	40
212	3	55	9	0.5	0	0	0	19	100	GC	3	30
212	4	25	12	0.3	0	0	0	40	100	GS	1	20
212	5	0	0	0	50	8	2	13	150	GC	1	95
214	1	20	15	0.5	0	0	0	40	320	GH	1	0
214	2	100	9	0.3	0	0	0	38	290	G	2.5	5
214	3	45	9	0.3	0	0	0	33	285	G	3	5
214	4	60	14	0.5	0	0	0	21	260	G	5	5
214	5	0	0	0	15	20	2	2	260	RD	3	0
214	6	30	20	0.3	0	0	0	25	270	G	5	0
214	7	20	20	0.3	0	0	0	30	285	G	5	0
214	8	25	8	0.3	25	7	-1	14	285	G	5	2
214	9	35	6	0.3	35	9	-1	21	300	G	6	2
214	10	80	20	0.3	0	0	0	29	260	G	6	5
214	11	85	20	0.3	0	0	0	23	290	G	5	20
214	12	55	20	0.5	0	0	0	12	300	G	5	20
214	13	35	20	0.5	0	0	0	25	305	GC	5	30
214	14	0	0	0	35	11	5	10	330	GC	5	0
214	15	0	0	110	15	5	5	5	100	SC	5	40
217	1	15	7	0.5	0	0	0	30	120	OS	0.8	20
217	2	20	7	0.5	0	0	0	30	90	OS	1	5
217	3	25	9	0.5	0	0	0	32	90	GH	1	5
217	4	0	0	0	15	9	1.5	21	75	GC	1.5	95
301	1	14	23	0.5	0	0	0	35	160	OS	0	0
301	2	44	20	1	0	0	0	26	160	OS	0	0
301	3	9	20	0.1	9	20	0.1	0	160	RD	0	0

E#	R#	ELEN	EWID	EDEP	DLEN	DWID	DDEP	TH	PAZ	SM	FDEP	%REV
301	4	19	5	0.2	0	0	0	30	160	OS	0	0
301	5	0	0	0	22	18	2	20	160	OS	0	0
302	1	4	16	1	0	0	0	29	150	OS	0	0
302	2	34	18	0.7	0	0	0	28	150	OS	0	0
302	3	7	13	0.2	0	0	0	38	150	OS	0	0
302	4	0	0	0	15	30	1	0	150	RD	0	0
303	1	34	14	0.5	0	0	0	23	120	OS	0	0
303	2	17	7	0.5	0	0	0	40	120	G	0	0
303	3	67	4	0.5	67	1	0.2	29	120	G	2	0
303	4	28	4	0.5	28	3	1	20	150	G	2	0
303	5	30	4	0.5	30	4	0.5	18	110	G	3	0
303	6	0	0	0	43	12	1.5	18	140	OS	2	0
303	7	0	0	0	10	12	1	0	140	RD	1	0
307	1	15	17	0.3	0	0	0	40	310	GH	0.5	0
307	2	25	13	0.3	0	0	0	26	310	G	4	5
307	3	39	11	0.3	0	0	0	22	290	G	4	10
307	4	41	12	0.3	0	0	0	16	270	G	5	5
307	5	55	12	0.3	30	2	0.5	19	290	G	5	10
307	6	60	12	0.3	60	3	0.5	18	265	G	5	20
307	7	45	14	0.3	25	7	0.5	32	270	G	6	5
307	8	25	10	0.5	0	0	0	20	270	G	5	1
307	9	35	10	0.5	35	2	1	17	305	G	5	20
307	10	35	27	0.5	35	10	1	22	260	OS	4	5
307	11	60	32	0.3	60	5	0.5	35	280	G	5	10
307	12	15	15	0.3	0	0	0	50	270	G	8	20
307	13	35	15	0.3	0	0	0	18	270	G	6	30
307	14	0	0	0	30	20	2.5	10	325	OS	2.5	40
307	15	0	0	0	20	32	2	10	325	OS	2	50
307	16	0	0	0	21	45	1	0	325	SC	1	20
409	1	25	4	0.5	0	0	0	30	260	G	2	50
409	2	21	6	0.5	0	1	0.5	25	250	G	1.5	50
409	3	30	7	0.5	0	0	0	28	220	G	2	50
409	4	44	4	0.5	0	0	0	30	240	G	1.5	50
409	5	40	9	0.5	10	1	0.3	32	255	OS	1	40
409	6	60	2	0.5	60	4	1	23	240	G	2	80
417	1	11	11	1	0	0	0	27	260	OS	1	-1
417	2	28	10	0.5	0	0	0	23	260	OS	0.5	-1
417	3	0	0	0	20	10	1.5	0	270	OS	1.5	-1
420	1	61	20	1	0	0	0	34	290	OS	1	5
420	2	39	6	1	0	0	0	33	310	G	3	5
420	3	60	10	0.5	0	0	0	28	310	G	4	5
420	4	95	10	0.5	0	0	0	27	290	G	5	10
420	5	42	10	0.5	0	0	0	22	320	G	5	50
420	6	65	12	0.5	0	0	0	21	335	G	5	40
420	7	36	12	0.5	1	1	1	14	320	G	6	40
420	8	52	2	0.5	52	16	2.5	10	330	G	4	90
420	9	0	0	0	90	20	2.5	6	20	FL	2.5	90
423	1	21	12	1	0	0	0	31	290	OS	1	5
423	2	60	22	0.5	60	2	0.5	21	290	OS	1	75
423	3	82	13	0.5	60	2	0.5	21	270	G	4	0
423	4	0	0	0	19	12	2.5	3	300	FL	2.5	0
427	1	29	20	0.8	0	0	0	19	290	OS	1	60
427	2	33	14	0.5	33	2	0.5	17	300	OS	2	80
427	3	54	10	0.2	54	4	0.5	16	300	OS	2	95
427	4	42	13	0.4	0	0	0	24	300	G	3	25
427	5	0	0	0	16	27	1	2	290	FL	1	100
428	1	20	10	1	0	0	0	25	160	OS	-1	60
428	2	12	10	0.5	5	8	-1	15	160	OS	-1	80
428	3	15	6	0.8	0	0	0	28	120	OS	1	50
428	4	0	0	0	13	14	1	0	130	RD	1	80
451	1	11	8	0.8	0	0	0	32	100	GH	-1	20

E#	R#	ELEN	EWID	EDEP	DLEN	DWID	DDEP	TH	PAZ	SM	FDEP	%REV
451	2	43	8	0.5	0	0	0	24	100	G	2.5	40
451	3	0	0	0	10	7	1.5	5	100	FL	1.5	90
451	4	0	0	0	12	6	1	5	180	FL	1	10
461	1	40	19	0.8	0	0	0	20	340	OS	1	90
461	2	10	5	0.8	10	7	1	18	340	OS	1.5	100
461	3	0	0	0	50	15	2	14	340	OS	2	100
462	1	25	10	0.8	0	0	0	25	330	OS	-1	10
462	2	25	5	0.5	25	10	0.5	19	330	OS	-1	90
462	3	117	7	0.5	117	1	0.5	18	310	G	3	50
462	4	20	8	0.5	20	1	0.5	18	350	G	4	20
462	5	33	7	0.5	33	1	0.5	15	270	G	4	10
462	6	24	8	0.5	24	1	0.5	14	310	G	3	10
462	7	31	8	0.2	31	1	0.5	20	310	G	3	5
462	8	36	9	0.2	36	6	1	12	290	G	3	5
462	9	35	5	0.5	35	5	1	12	340	G	4	10
462	10	0	0	0	15	10	2	7	360	F	2.5	30
462	11	0	0	0	15	5	1	7	360	F	1	80
463	1	31	9	1	0	0	0	27	130	GH	1	5
463	2	46	7	0.5	46	1	0.5	26	120	G	2.5	5
463	3	33	10	0.5	0	0	0	27	130	G	3	5
463	4	0	0	0	22	12	2	0	110	RD	2	20
465	1	13	24	2	0	0	0	25	10	OS	2	0
465	2	14	24	1	0	0	0	24	10	OS	1	0
465	3	30	20	1.5	0	0	0	29	10	OS	1.5	5
465	4	45	13	1.5	0	0	0	30	10	OS	1.5	0
465	5	0	0	0	26	13	1	31	10	OS	1	10
465	6	22	7	0.3	22	5	1	13	20	G	0	30
465	7	52	6	0.3	52	4	0.5	24	20	G	0.5	10
465	8	50	10	0.2	50	10	1.5	11	120	G	0	25
505	1	14	12	1	0	0	0	30	310	GH	1	1
505	2	26	8	1	10	8	1.5	23	310	G	2	10
505	3	0	0	0	19	8	2	20	310	OS	2	90
601	1	10	21	1	0	0	0	24	250	OS	0.8	60
601	2	15	21	0.5	0	0	0	17	250	OS	0.5	80
601	3	0	0	0	35	15	1	11	250	OS	1	80
603	1	28	8	1	0	0	0	22	340	OS	1	0
603	2	35	7	0.5	0	0	0	19	340	OS	0.5	5
603	3	0	0	0	15	8	1.5	13	340	OS	1.2	0
604	1	39	23	1	0	0	0	23	260	OS	1	10
604	2	53	23	0.4	53	3	1	17	270	OS	1.5	30
604	3	33	11	0.5	33	4	0.5	24	280	GC	4	10
604	4	0	0	0	50	12	2.5	3	320	FL	3	30
604	5	0	0	0	37	14	2.5	5	330	FL	3	30
605	1	26	19	0.5	0	0	0	27	290	OS	1	30
605	2	17	10	0.5	17	11	1	20	300	OS	1	90
605	3	20	9	0.2	20	2	0.5	15	290	OS	1	95
605	4	0	0	0	18	13	1	12	290	OS	1	100
701	1	28	7	1.5	0	0	0	25	-1	OS	-1	-1
701	2	25	4	1	25	6	0.5	20	-1	OS	-1	-1
701	3	0	0	0	15	12	2	20	-1	OS	-1	-1
702	1	10	22	0.8	0	0	0	28	280	OS	1	5
702	2	39	17	1	0	0	0	22	280	OS	1	10
702	3	81	11	0.5	81	2	0.5	23	270	G	3	20
702	4	83	8	0.5	83	7	0.5	25	300	G	5	20
702	5	0	0	0	44	27	2	12	300	OS	0.4	95
702	6	0	0	0	10	0	0	0	300	RD	4	0
702	7	0	0	0	18	12	2	10	300	OS	2	80
703	1	41	17	1	0	0	0	25	90	OS	1.5	5
703	2	82	15	0.5	82	2	0.5	21	110	OS	4	20
703	3	48	12	0.5	48	2	0.5	20	135	OS	5	10

E#	R#	ELEN	EWID	EDEP	DLEN	DWID	DDEP	TH	PAZ	SM	FDEP	%REV
703	4	0	0	0	62	23	1.5	14	120	OS	2.5	95
703	5	0	0	0	10	20	1	0	120	RD	0	0
703	6	0	0	0	23	13	2.5	7	120	OS	2.5	100
704	1	23	7	0.5	0	0	0	22	130	OS	0.5	0
704	2	11	5	0.8	11	3	1	15	110	OS	2	0
704	3	18	4	0.7	18	4	0.5	11	120	OS	1.5	30
704	4	17	3	1	17	2	0.5	15	90	OS	2	30
704	5	0	0	0	14	12	1.5	11	90	OS	1.5	60
706	1	16	10	1	0	0	0	19	290	GH	1	20
706	2	79	10	0.5	79	2	0.5	17	300	G	3	30
706	3	0	0	0	14	8	1	14	300	G	3	50
706	4	0	0	0	14	17	2	12	300	F	2	90
801	1	16	6	0.7	0	0	0	32	150	OS	0.7	2
801	2	24	5	1	0	0	0	26	150	OS	1	2
801	3	24	5	0.5	0	0	0	26	160	G	1	2
801	4	0	0	0	30	9	1.5	22	160	RD	0	25
801	5	65	4	0.2	0	0	0	21	160	G	0.5	75
801	6	0	0	0	13	5	1	9	160	FL	0	60
802	1	20	10	1.5	0	0	0	32	280	OS	1.5	80
802	2	10	12	0.7	0	0	0	31	280	OS	0.7	100
802	3	0	0	0	17	12	1.5	11	280	OS	1.5	100
803	1	22	12	1	0	0	0	27	280	OS	1	60
803	2	18	14	1	18	4	0.5	24	280	OS	0.5	80
803	3	0	0	0	35	5	1.3	17	280	OS	1.5	100
804	1	18	8	1.5	0	0	0	26	130	G	1.5	60
804	2	30	7	0.5	0	0	0	25	170	G	0.7	50
804	3	20	6	0.5	0	0	0	18	150	G	0.7	50
804	4	0	0	0	50	8	0.7	20	150	OS	1	100
804	5	0	0	0	30	8	1	10	150	OS	1	100
805	1	20	5	1	0	0	0	25	160	G	1	30
805	2	25	5	1	0	0	0	21	160	OS	1	50
805	3	0	0	0	10	10	1	20	160	OS	1	100
805	4	0	0	0	10	10	1.3	6	160	OS	1	100
901	1	18	18	0.4	0	0	0	23	350	OS	0.5	30
901	2	17	14	1	0	0	0	28	350	OS	1	20
901	3	35	5	0.3	0	0	0	27	350	G	0.5	70
901	4	20	5	0.3	0	0	0	27	350	G	0.3	50
901	5	0	0	0	25	8	1	6	60	SC	1.5	100
1001	1	15	28	1	0	0	0	35	310	OS	1	5
1001	2	40	23	0.4	20	2	0.5	24	300	OS	1	60
1001	3	25	10	0.4	25	20	0.5	18	310	OS	1.5	70
1001	4	0	0	0	50	15	0.8	11	320	OS	1.5	0
1002	1	25	11	1	0	0	0	38	300	OS	1	5
1002	2	25	7	0.3	25	2	0.5	28	295	OS	1	10
1002	3	0	0	0	20	8	1	19	295	OS	1.5	80
1003	1	30	15	1	0	0	0	38	305	OS	1.5	0
1003	2	28	9	0.3	28	4	0.5	28	300	OS	1.5	2
1003	3	0	0	0	20	12	1	13	295	OS	1.5	2
1003	4	0	0	0	22	11	1	11	350	OS	-1	1
1004	1	30	8	1	0	0	0	19	125	OS	-1	95
1004	2	18	4	0.1	18	6	0.5	10	120	OS	-1	99
1004	3	7	11	0.1	0	0	0	35	130	OS	-1	10
1004	4	0	0	0	27	16	1	10	70	RD	1	100
1005	1	30	9	0.5	0	0	0	23	295	OS	1	80
1005	2	19	7	0.2	0	0	0	32	310	RD	1	10
1005	3	0	0	0	24	7	0.5	12	240	RD	1.5	80
1010	1	15	17	-1	0	0	0	25	280	OS	1	40
1010	2	30	11	0.3	30	8	0.5	14	260	OS	1	99
1010	3	38	11	0.3	38	7	0.5	19	290	OS	1	99
1010	4	0	0	0	24	16	1	9	305	OS	1	100

E#	R#	ELEN	EWID	EDEP	DLEN	DWID	DDEP	TH	PAZ	SM	FDEP	%REV
1014	1	17	21	1	0	0	0	30	270	OS	1	15
1014	2	14	23	0.3	0	0	0	20	270	OS	1	5
1014	3	0	0	0	28	22	1.5	15	300	OS	1.5	95
1018	1	15	18	1	0	0	0	37	260	OS	1	50
1018	2	18	8	0.5	0	0	0	21	250	OS	1.5	60
1018	3	10	5	0.5	0	0	0	25	250	G	2	80
1018	4	47	4	0.5	0	0	0	28	250	G	2	75
1018	5	0	0	0	14	10	2	14	250	OS	2	95
1018	6	7	12	0.5	0	0	0	10	250	OS	2	60
1018	7	23	12	0.1	0	0	0	90	250	OS	0	0
1018	8	0	0	0	27	15	2	0	230	RD	0	0
1019	1	17	10	0.5	0	0	0	45	260	GH	1	1
1019	2	33	13	1.5	0	0	0	24	280	GH	2	2
1019	3	47	7	0.5	0	0	0	23	250	GC	3	30
1019	4	35	8	0.5	35	2	0.5	22	230	GC	3.5	30
1019	5	21	9	0.5	21	4	0.5	18	270	GC	3.5	60
1019	6	0	0	0	55	20	1	12	255	OS	2	40
1026	1	9	15	0.5	0	0	0	35	290	OS	1	20
1026	2	15	14	0.8	0	0	0	33	290	OS	1	10
1026	3	0	0	0	9	14	1	1	290	RD	1	0
1027	1	23	15	0.5	0	0	0	43	230	OS	1	0
1027	2	11	3	0.5	1	20	0.5	30	230	OS	1	5
1027	3	0	0	0	16	20	1	27	230	OS	1	80
1028	1	7	32	0.5	0	0	0	44	80	OS	1	5
1028	2	33	35	0.8	0	0	0	27	80	OS	1	20
1028	3	0	0	0	7	38	0.5	18	80	OS	1	100
1028	4	0	0	0	20	30	1	3	80	OS	1	100
1102	1	15	20	0.5	0	0	0	33	15	OS	0.5	0
1102	2	45	26	0.4	0	0	0	28	15	OS	1	0
1102	3	15	10	0.7	0	0	0	32	20	OS	2	0
1102	4	52	7	0.5	0	0	0	24	20	G	3	0
1102	5	27	6	0.3	0	0	0	22	2	G	3	0
1102	6	29	7	0.3	0	0	0	28	30	G	3	0
1102	7	0	0	0	14	7	1	3	20	RD	0	0
1102	8	38	7	0.5	0	0	0	20	20	G	3	0
1102	9	21	7	0.4	0	0	0	27	30	G	2.5	0
1102	10	39	4	0.2	0	0	0	0	355	G	3	0
1102	11	0	0	0	24	8	2.5	5	360	G	3	0
1102	12	0	0	0	9	10	1	0	360	RD	0	0
1102	13	0	0	0	12	10	3	25	350	G	3	0
1201	1	21	20	0.1	0	0	0	45	320	GH	0.7	1
1201	2	60	11	0.4	0	0	0	42	320	G	1.5	1
1201	3	90	15	0.4	0	0	0	30	335	G	2.5	1
1201	4	40	20	0.4	0	0	0	38	360	G	3	5
1201	5	45	20	0.5	0	0	0	25	345	G	3	1
1201	6	35	20	0.6	0	0	0	22	330	G	4	5
1201	7	50	25	0.7	0	0	0	15	320	G	4	5
1201	8	40	10	0.3	40	10	1	14	335	G	4	5
1201	9	48	15	0.7	0	0	0	16	330	G	5	5
1201	10	75	17	1	45	5	0.6	10	310	G	3.5	30
1201	11	0	0	0	72	20	2	8	285	G	3	40
1201	12	0	0	0	255	15	0.3	14	310	OS	0.3	100
1201	13	0	0	0	220	20	0.2	5	285	OS	0.2	100
1202	1	10	12	0.3	0	0	0	48	5	OS	0.3	0
1202	2	33	17	0.4	0	0	0	43	5	OS	0.6	1
1202	3	25	18	0.2	0	0	0	51	5	OS	0.5	1
1202	4	75	13	0.1	75	13	0.5	37	5	OS	0.6	2
1203	1	32	23	0.5	0	0	0	44	190	OS	0.5	1
1203	2	23	5	0.5	5	4	1	42	190	OS	0.8	1
1203	3	20	5	0.2	80	11	0.4	36	190	OS	0.8	10

E#	R#	ELEN	EWID	EDEP	DLEN	DWID	DDEP	TH	PAZ	SM	FDEP	%REV
1204	1	50	22	0.3	0	0	0	48	140	OS	0.3	0
1204	2	18	18	0.5	0	0	0	42	140	OS	0.5	1
1204	3	52	18	0.2	0	0	0	46	140	OS	0.7	0
1204	4	115	20	0.3	0	0	0	39	140	OS	1	30
1204	5	32	10	0.1	32	10	1	26	140	OS	1.5	50
1204	6	40	11	0.2	0	0	0	34	140	OS	1	70
1204	7	0	0	0	41	14	1.5	11	105	OS	1	95
1205	1	23	11	0.4	0	0	0	49	110	OS	0.5	1
1205	2	19	5	0.4	0	0	0	49	115	OS	1.2	1
1205	3	18	8	0.3	0	0	0	44	105	OS	0.8	15
1205	4	0	0	0	24	10	0.7	33	110	OS	1	30
1206	1	38	21	0.2	0	0	0	47	295	GH	0.2	10
1206	2	93	16	0.4	0	0	0	39	290	G	1.2	15
1206	3	24	9	0.3	0	0	0	34	310	G	1.5	30
1206	4	21	10	0.4	0	0	0	39	290	G	1.5	30
1206	5	23	12	0.5	0	0	0	22	290	G	1.5	40
1206	6	17	13	0.2	0	0	0	43	290	G	1.5	10
1206	7	11	12	0.3	0	0	0	15	290	G	1.5	25
1206	8	19	10	0.4	0	0	0	31	265	G	1	15
1206	9	18	10	0.5	0	0	0	18	245	OS	1	75
1206	10	32	7	0.5	32	5	2	16	245	OS	2	95
1206	11	52	11	0.4	52	12	0.8	15	280	OS	1.5	95
1206	12	0	0	0	11	24	1.3	4	270	OS	1.5	95
1206	13	0	0	0	21	10	1.5	14	270	OS	1.5	90
1208	1	20	10	0.5	0	0	0	42	70	OS	-1	5
1208	2	25	9	0.5	10	3	1	37	80	OS	1.5	20
1208	3	19	5	0.2	19	7	0.5	33	85	OS	1.5	30
1208	4	0	0	0	16	15	1.5	29	80	OS	1.5	60
1209	1	17	6	0.5	0	0	0	30	150	G	2	30
1209	2	19	7	0.5	0	0	0	31	165	G	2	30
1209	3	6	5	0.3	6	2	0.5	23	180	G	2	40
1209	4	0	0	0	12	11	2	15	180	G	2	100
1210	1	17	6	0.8	0	0	0	35	110	GS	0.8	5
1210	2	15	5	0.5	0	0	0	30	40	G	0.5	30
1210	3	47	6	0.5	0	0	0	29	60	G	2	20
1210	4	29	1	1	29	6	1.5	21	60	G	2	40
1210	5	0	0	0	17	10	2	15	30	G	20	60
1211	1	46	25	0.3	0	0	0	41	100	OS	0.5	0
1211	2	39	20	0.8	0	0	0	42	110	OS	1	0
1211	3	35	22	1	0	0	0	38	110	OS	1.5	0
1211	4	50	35	0.3	0	0	0	44	110	OS	1	0
1211	5	49	25	0.4	0	0	0	33	110	OS	1	20
1211	6	14	23	0.3	0	0	0	45	115	OS	1.5	40
1211	7	0	0	0	28	23	1.5	25	110	OS	2	80
1211	8	0	0	0	27	16	2	17	110	OS	2	80
1212	1	36	20	1	0	0	0	36	355	OS	1	1
1212	2	31	7	0.5	31	14	0.5	22	355	OS	1	10
1212	3	38	15	0.2	38	5	0.5	19	350	OS	1	5
1212	4	37	16	0.3	37	6	0.5	22	350	OS	1.5	10
1212	5	0	0	0	20	16	1.5	10	350	OS	1.5	20
1302	1	29	6	0.5	0	0	0	40	80	GH	0.5	0
1302	2	24	3	0.2	0	0	0	39	80	G	1	1
1302	3	25	5	0.3	0	0	0	39	80	G	0.7	0
1302	4	19	6	0.3	0	0	0	34	80	G	1	1
1302	5	31	5	0.4	13	1	1	33	75	G	0.7	1
1302	6	10	5	0.7	0	0	0	29	50	G	1.3	10
1302	7	29	5	0.7	0	0	0	28	70	G	1.3	10
1302	8	36	5	1	0	0	0	29	95	G	1.5	10
1302	9	37	5	1.3	0	0	0	26	75	G	2	10
1302	10	0	0	0	39	8	2	16	130	OS	2	95

E#	R#	ELEN	EWID	EDEP	DLEN	DWID	DDEP	TH	PAZ	SM	FDEP	%REV
1302	11	0	0	0	29	8	2	16	130	OS	2	95
1402	1	81	10	0.2	0	0	0	27	20	OS	0.3	90
1402	2	30	13	0.3	0	0	0	36	10	OS	0.7	80
1402	3	42	13	0.3	0	0	0	42	10	OS	0.7	80
1402	4	56	13	0.3	0	0	0	31	10	OS	0.8	100
1402	5	29	17	0.3	0	0	0	41	10	G	1.3	100
1402	6	74	15	0.3	0	0	0	35	10	G	1.3	100
1402	7	25	15	0.3	0	0	0	34	360	G	1.3	100
1402	8	32	20	0.3	0	0	0	38	360	OS	1.5	100
1402	9	28	24	0.3	0	0	0	25	360	OS	1.5	100
1402	10	14	16	0.2	0	0	0	41	360	OS	1.5	100
1402	11	0	0	0	24	30	1.5	4	360	SC	1.5	100
1403	1	15	11	0.7	0	0	0	35	175	OS	0.7	10
1403	2	35	7	0.5	0	0	0	25	175	OS	0.7	25
1403	3	50	8	0.3	0	0	0	25	185	OS	0.7	25
1403	4	70	10	0.1	0	0	0	40	185	OS	0.5	5
1403	5	18	10	0.1	0	0	0	35	175	OS	0.5	5
1403	6	33	10	0.1	0	0	0	42	175	OS	0.6	5
1403	7	115	12	0.1	0	0	0	30	160	OS	0.8	2
1403	8	70	12	0.1	0	0	0	45	160	OS	0.9	1
1403	9	0	0	0	20	9	2	7	160	OS	2	1
1501	1	15	25	0.2	0	0	0	42	210	OS	0.2	5
1501	2	18	30	0.1	0	0	0	32	210	OS	0.2	70
1501	3	10	30	0.1	0	0	0	1	201	RD	0.3	1
1501	4	33	36	0.2	0	0	0	28	201	OS	0.3	0
1501	5	26	45	0.2	0	0	0	25	201	OS	0.4	50
1501	6	50	42	0.2	0	0	0	25	198	OS	0.5	40
1501	7	33	60	0.4	0	0	0	25	196	OS	0.8	40
1501	8	30	60	0.5	0	0	0	29	200	OS	1	10
1501	9	22	85	0.7	0	0	0	22	200	OS	1	1
1501	10	0	0	0	4	11	1	3	205	RD	1	0
1501	11	90	28	0.1	90	17	1	9	220	OS	1	0
1501	12	0	0	0	52	22	1	8	220	OS	1	45
1610	1	14	4	1	0	0	0	33	230	GH	1	5
1610	2	16	9	0.5	0	0	0	33	250	GH	0.5	2
1610	3	8	15	2	0	0	0	48	250	GH	1	1
1610	4	21	15	1	0	0	0	33	230	G	2	2
1610	5	19	9	0.2	0	0	0	38	230	G	2	1
1610	6	32	8	0.5	0	0	0	32	230	G	4	1
1610	7	25	8	0.5	0	0	0	27	220	G	2	5
1610	8	21	10	0.2	0	0	0	40	210	OS	1	1
1610	9	0	0	0	12	15	1	4	210	RD	1	10
1610	10	16	12	1	16	15	2	33	240	RD	2	5
1610	11	0	0	0	36	10	4	25	250	G	4	10
1611	1	34	16	1	0	0	0	32	300	OS	1	10
1611	2	12	23	0.5	12	3	0.5	22	300	OS	1	5
1611	3	20	12	0.5	20	12	1	28	300	OS	2	40
1611	4	34	12	0.5	34	18	1	30	300	OS	1.5	20
1611	5	0	0	0	15	30	1	0	300	RD	1.5	0
1612	1	25	30	0.5	0	0	0	35	320	OS	0.5	80
1612	2	9	22	0.5	0	0	0	38	320	OS	0.5	60
1612	3	9	18	0.5	0	0	0	45	320	OS	0.5	50
1612	4	0	0	0	23	12	1	26	320	OS	1	95
1612	5	0	0	0	17	8	2	26	350	OS	2	100
1613	1	7	6	0.5	0	0	0	22	70	OS	0.5	0
1613	2	20	8	0.5	0	0	0	33	80	OS	1	1
1613	3	13	8	0.5	0	0	0	22	80	OS	2	5
1613	4	14	6	0.5	14	2	0.5	23	20	OS	2	10
1613	5	13	5	1	13	2	0.5	37	60	G	3	2
1613	6	16	4	0.5	16	2	0.5	28	50	G	3	5

E#	R#	ELEN	EWID	EDEP	DLEN	DWID	DDEP	TH	PAZ	SM	FDEP	%REV
1613	7	16	4	0.5	16	2	1	27	70	OS	2	5
1613	8	0	0	0	7	10	2	26	80	OS	2	10
1613	9	22	4	1	22	5	0.5	32	60	G	2	25
1613	10	14	2	0.2	14	3	0.5	22	80	OS	2	10
1613	11	12	4	0.1	12	5	0.2	23	70	OS	1	15
1613	12	10	1	0.5	10	7	1.5	22	80	OS	3	10
1613	13	12	4	1	12	4	0.5	25	80	G	2	5
1613	14	16	5	1	16	1	0.2	28	60	G	2	2
1613	15	17	5	0.1	0	0	0	70	60	OS	2	0
1613	16	0	0	0	16	7	1	2	40	RD	2	1
1613	17	0	0	0	4	18	2	2	40	RD	2	5
1614	1	12	10	1	0	0	0	40	290	OS	1	0
1614	2	18	6	2	18	2	1	18	280	OS	3	2
1614	3	10	6	0.2	0	0	0	21	280	OS	1	10
1614	4	10	6	0.2	10	2	1	32	280	OS	2	10
1614	5	6	3	0.2	6	3	2	22	310	OS	2	50
1614	6	20	3	0.3	0	0	0	35	280	OS	2	0
1614	7	42	3	0.2	42	5	1	25	250	OS	2	10
1614	8	0	0	0	12	9	3	20	250	OS	3	10
1614	9	6	4	0.1	6	4	0.2	22	270	OS	0.5	60
1614	10	7	6	0.1	0	0	0	35	270	OS	0.5	60
1614	11	0	0	0	17	4	2	15	250	G	2	25
1619	1	67	50	2	0	0	0	40	310	OS	2	2
1619	2	30	19	1	30	8	1	25	310	OS	2	5
1619	3	43	7	1	43	7	2	18	310	G	3	30
1619	4	54	6	1	54	23	2	15	310	G	3	70
1619	5	0	0	0	23	23	2	13	310	OS	3	60
1619	6	0	0	0	72	30	2	9	310	OS	3	80
1619	7	0	0	0	23	46	2	5	290	OS	2	80
1621	1	27	26	1	0	0	0	38	290	OS	1	1
1621	2	9	10	0.5	0	0	0	35	290	OS	3	5
1621	3	8	16	0.2	0	0	0	46	290	OS	2	10
1621	4	20	9	1	0	0	0	26	290	OS	2	10
1621	5	0	0	0	23	16	1	18	290	OS	2	50
1621	6	0	0	0	18	20	2	8	290	OS	2	50
1623	1	15	12	2	0	0	0	45	140	OS	2	15
1623	2	28	20	0.5	0	0	0	35	130	OS	2	50
1623	3	0	0	0	19	15	2	12	100	OS	2	40
1704	1	5	15	1	0	0	0	33	280	OS	1	5
1704	2	15	15	1	0	0	0	24	315	OS	2	5
1704	3	0	0	0	13	11	2	17	340	OS	2	50
1704	4	0	0	0	22	16	1	12	340	OS	1	90
1705	1	7	6	1	0	0	0	32	290	OS	1	5
1705	2	9	6	1	0	0	0	18	290	OS	1	10
1705	3	18	8	0.2	0	0	0	19	330	OS	1	95
1705	4	0	0	0	10	8	2	15	4	OS	2	90
1707	1	8	15	2	0	0	0	35	240	GH	2	25
1707	2	17	20	1	0	0	0	18	250	G	2	10
1707	3	18	9	1	18	11	1	10	270	G	2	50
1707	4	26	10	1	0	0	0	18	260	G	2	2
1707	5	11	3	1	11	5	1	10	260	G	2	50
1707	6	7	9	0.5	0	0	0	7	310	G	2	5
1707	7	13	10	0.5	0	0	0	21	310	G	2	10
1707	8	42	10	0.5	0	0	0	8	320	G	2	40
1707	9	24	5	2	24	5	3	6	320	G	3	30
1707	10	22	5	0.5	22	2	0.5	6	310	G	2	40
1707	11	21	9	0.5	0	0	0	5	260	G	2	10
1707	12	0	0	0	5	5	1	5	260	G	2	10
1707	13	0	0	0	35	3	1	7	340	G	2	15
1707	14	0	0	0	22	8	2	4	260	G	2	25

E#	R#	ELEN	EWID	EDEP	DLEN	DWID	DDEP	TH	PAZ	SM	FDEP	%REV
1707	15	0	0	0	21	15	3	4	320	G	3	20
1807	1	4	15	1	0	0	0	34	160	OS	1	5
1807	2	29	9	0.2	0	0	0	34	160	OS	0.5	5
1807	3	0	0	0	17	4	2	12	110	OS	2	10
1808	1	17	12	2	0	0	0	31	170	OS	2	5
1808	2	0	0	0	14	15	2	26	150	OS	2	5
1808	3	10	2	0.5	0	0	0	30	180	OS	1	0
1808	4	0	0	0	12	3	1	23	170	OS	1	2
1809	1	25	5	0.5	0	0	0	25	220	GC	2	0
1809	2	40	8	0.1	0	0	0	55	200	GC	2	0
1809	3	120	8	0.5	0	0	0	30	200	GC	3	5
1809	4	30	6	0.5	30	3	1	15	220	GC	2	5
1809	5	20	5	0.5	20	2	1	25	180	GC	2.5	5
1809	6	25	4	0.5	25	6	1.5	15	160	GC	3	40
1809	7	30	4	0.5	30	4	1	17	160	GC	3	40
1809	8	20	6	0.5	20	1	1	19	145	GC	2	20
1809	9	40	7	0.5	0	0	0	18	170	GC	2	60
1809	10	25	7	0.2	0	0	0	37	155	GC	3	60
1809	11	0	0	0	15	8	1	15	170	GC	2	85
1809	12	0	0	0	40	10	1	15	170	F	1	90
1810	1	35	10	0.5	0	0	0	25	20	OS	1	5
1810	2	10	10	0.3	0	0	0	36	20	GH	1	40
1810	3	45	6	0.5	0	0	0	32	30	G	1.5	5
1810	4	40	6	0.5	0	0	0	32	40	G	1.5	5
1810	5	75	6	0.5	0	0	0	32	360	G	1	5
1810	6	65	7	0.2	0	0	0	37	360	G	2.5	5
1810	7	35	8	0.5	0	0	0	26	340	G	3.5	5
1810	8	30	8	0.5	0	0	0	25	10	G	3	0
1810	9	15	8	0.5	0	0	0	25	340	G	3	5
1810	10	45	9	0.2	45	4	0.5	26	10	G	3	10
1810	11	50	12	0.2	50	12	0.2	22	30	G	3	10
1810	12	45	18	0.5	45	10	0.2	24	350	G	3	10
1810	13	25	10	0.5	0	0	0	33	350	G	5	10
1810	14	60	7	0.5	0	0	0	15	340	G	3	10
1810	15	0	0	0	28	13	2	9	10	F	3	20
1810	16	20	5	1	20	8	1	13	340	GF	5	20
1810	17	17	3	0.5	17	6	1	8	360	GF	2	10
1810	18	26	4	0.5	26	4	1	10	315	GF	2	10
1810	19	21	7	1	21	1	1	8	260	SC	1.5	0
1810	20	0	0	0	38	10	1.5	3	260	SC	1.5	0
1815	1	22	12	0.5	0	0	0	42	10	GH	0.5	20
1815	2	19	7	0.3	0	0	0	40	10	G	1	25
1815	3	9	8	0.2	0	0	0	34	10	G	1	40
1815	4	15	10	0.5	15	7	1	42	20	G	2	50
1815	5	11	5	1	0	0	0	30	10	G	2	2
1815	6	0	0	0	3	5	1	28	40	OS	1	20
1815	7	7	3	0.5	0	0	0	35	20	OS	1	50
1815	8	0	0	0	15	8	2	28	360	OS	2	80
1901	1	14	8	1.7	0	0	0	35	200	GH	1.8	10
1901	2	35	11	3	0	0	0	22	220	G	2.5	40
1901	3	26	6	1.7	0	0	0	15	170	G	1.5	70
1901	4	0	0	0	12	10	1	0	170	RD	0	0
1901	5	0	0	0	55	15	1	18	190	OS	0	90
1901	6	0	0	0	35	12	1.5	11	190	OS	0	90
1903	1	20	20	1	0	0	0	28	190	OS	1	35
1903	2	0	0	0	19	10	1.2	24	190	OS	1	75
1903	3	0	0	0	15	11	1.5	16	190	OS	1	90
1903	4	0	0	0	16	9	1	16	190	OS	1	100
1905	1	10	10	0.9	0	0	0	33	220	OS	0.9	30
1905	2	17	8	0.5	0	0	0	22	190	OS	0.5	80

E#	R#	ELEN	EWID	EDEP	DLEN	DWID	DDEP	TH	PAZ	SM	FDEP	%REV
1905	3	29	11	0.3	0	0	0	18	160	OS	0.5	100
1905	4	0	0	0	34	11	0.7	18	150	OS	0.7	100
1907	1	38	12	0.8	0	0	0	36	190	OS	0.5	15
1907	2	27	11	0.9	0	0	0	39	190	OS	0.7	50
1907	3	18	7	0.3	0	0	0	22	190	G	1	70
1907	4	15	4	0.3	0	0	0	21	190	G	1	90
1907	5	0	0	0	27	12	1	10	190	OS	1	90
1909	1	14	7	1.1	0	0	0	48	165	GS	1	2
1908	1	25	10	0.2	0	0	0	33	110	OS	0.2	20
1908	2	30	11	0.3	0	0	0	32	110	OS	0.3	20
1908	3	0	0	0	26	5	1	17	170	OS	1	90
1909	2	13	8	1.5	13	3	0.5	36	165	GS	0	5
1909	3	8	5	0.5	0	0	0	30	135	G	0	10
1909	4	20	4	0.5	0	0	0	33	135	G	0	30
1909	5	20	2	0.5	0	0	0	28	135	G	0	10
1909	6	0	0	0.4	18	3	1.2	21	135	G	0	40
1909	7	0	0	0.3	20	3	0.8	13	135	G	0	40
1909	8	0	0	0.2	60	8	1.3	10	135	G	0	0
1912	1	25	15	2.7	0	0	0	35	100	GH	2	0
1912	2	16	9	1.5	0	0	0	30	100	GH	1.5	20
1912	3	35	3	0.5	0	0	0	15	200	G	1	35
1912	4	49	3	0.3	0	0	0	19	200	G	1	35
1912	5	45	2	0.3	0	0	0	17	200	G	1.5	20
1912	6	0	0	0	110	12	1.5	10	200	OS	0	95
1914	1	14	8	1.3	0	0	0	33	160	OS	1.3	0
1914	2	50	17	1.3	0	0	0	24	160	OS	1.3	30
1914	3	51	10	1	0	0	0	22	160	OS	1	30
1914	4	0	0	0	84	15	1.3	13	160	OS	0	80
1915	1	80	22	1.3	0	0	0	37	150	OS	1.3	10
1915	2	43	15	2	0	0	0	30	150	OS	1.5	60
1915	3	0	0	0	125	33	1.5	15	150	OS	1.5	100
1916	1	53	15	0.3	0	0	0	42	145	OS	0.3	45
1916	2	30	12	0.3	0	0	0	40	145	OS	0.4	60
1916	3	0	0	0	35	15	0.7	33	145	OS	0.7	75
1917	1	35	21	1	0	0	0	37	140	OS	1	2
1917	2	30	20	1.3	0	0	0	37	140	OS	1	5
1917	3	20	11	1.5	0	0	0	33	140	OS	1.3	5
1917	4	17	16	0.8	0	0	0	38	140	OS	0.8	5
1917	5	0	0	0	28	12	1.3	0	140	OS	0	0
1917	6	0	0	0	46	21	1.5	30	140	OS	0	70
1918	1	4	22	0.8	0	0	0	32	110	OS	0.8	-1
1918	2	21	22	1.3	0	0	0	25	110	OS	1.2	5
1918	3	0	0	0	22	28	1	17	110	OS	1	80
1919	1	10	14	1.2	0	0	0	30	170	OS	1.2	2
1919	2	19	12	0.9	0	0	0	16	170	OS	0.9	5
1919	3	0	0	0	21	14	1.4	9	170	OS	1.4	30
1925	1	20	9	1.5	0	0	0	24	150	OS	1.5	30
1925	2	47	10	0.3	47	4	1	22	140	OS	1	100
1925	3	0	0	0	11	10	1.5	15	140	OS	1.5	100
1925	4	20	15	0.5	0	0	0	20	170	OS	1	100
1925	5	20	10	0.5	5	10	1.5	18	170	OS	1	100
1925	6	0	0	0	32	10	1	7	170	OS	1	100
1928	1	20	20	1.5	0	0	0	43	180	OS	1.2	25
1928	2	24	20	0.8	0	0	0	32	180	OS	0.7	25
1928	3	0	0	0	36	24	1.2	16	180	OS	1.2	100
1929	1	10	14	2	0	0	0	35	110	OS	2	30
1929	2	0	0	0	23	14	1.5	27	110	OS	0	60
1929	3	36	8	1	0	0	0	22	110	OS	1	40
1929	4	25	6	0.5	0	0	0	22	150	G	2	50
1929	5	28	6	0.5	7	4	1.5	23	160	G	2	100

E#	R#	ELEN	EWID	EDEP	DLEN	DWID	DDEP	TH	PAZ	SM	FDEP	%REV
1929	6	0	0	0	53	6	1.2	12	160	OS	0	100
1930	1	10	13	1.5	0	0	0	35	165	OS	1.5	25
1930	2	18	12	1	0	0	0	21	165	OS	1	70
1930	3	22	7	0.3	0	0	0	22	165	OS	0	100
1930	4	0	0	0	22	10	1.3	14	165	OS	0	80
1934	1	50	24	0.5	0	0	0	40	340	GH	4	10
1932	1	16	40	0.4	0	0	0	31	95	OS	0.3	75
1932	2	36	7	0.5	36	14	0.5	21	95	OS	0.5	80
1932	3	0	0	0	40	4	0.3	21	95	OS	0.3	100
1934	2	28	5	0.3	0	0	0	33	340	G	1.5	10
1934	3	27	4	0.3	0	0	0	25	340	G	1	15
1934	4	20	2	0.3	20	5	1.5	15	340	G	1.5	20
1934	5	0	0	0	25	7	1.5	12	340	G	1.5	30
1936	1	11	15	1	0	0	0	25	140	GH	1	70
1936	2	40	10	0.5	0	0	0	19	140	GC	1.5	100
1936	3	21	12	0.5	0	0	0	15	170	GC	1.5	95
1936	4	0	0	0	15	8	1	10	140	RD	1	0
1936	5	23	10	0.5	0	0	0	35	150	RD	1	100
1936	6	120	10	0.5	0	0	0	17	160	GC	1.5	95
1936	7	20	10	0.5	0	0	0	27	155	GC	2	75
1936	8	15	4	0.5	60	11	1.5	5	110	GC	2	95
1940	1	17	22	0.5	0	0	0	30	140	OS	0.5	95
1940	2	35	14	0.2	0	0	0	18	140	OS	1	100
1940	3	0	0	0	30	20	1	13	140	OS	1	100
1941	1	26	15	1	0	0	0	19	110	OS	1	85
1941	2	21	5	1	21	10	1	11	110	OS	1	95
1941	3	15	10	0.5	15	2	1	20	130	OS	1	100
1941	4	0	0	0	13	10	1	15	130	OS	1	100
1941	5	0	0	0	5	5	1	0	130	RD	1	100
2002	1	20	16	2.5	0	0	0	40	140	OS	2.5	0
2002	2	0	0	0	38	15	0.8	21	140	OS	0.8	100
2002	3	26	8	0.3	0	0	0	23	140	OS	0.3	100
2002	4	0	0	0	30	9	0.5	14	140	OS	0.5	100
2004	1	10	40	1	0	0	0	30	300	OS	1	5
2004	2	60	30	0.5	60	5	1	17	295	OS	1	40
2004	3	0	0	0	45	26	1.5	5	310	OS	1.5	95
2004	4	0	0	0	10	21	1.5	0	310	RD	1.5	0
2006	1	30	12	0.5	0	0	0	20	100	OS	0.5	10
2006	2	30	11	0.5	0	0	0	18	150	GC	2	15
2006	3	20	4	0.5	0	0	0	16	110	GC	3	20
2006	4	25	8	0.5	25	2	0.5	16	140	OS	2	40
2006	5	0	0	0	25	11	1.5	12	140	OS	2	95
2006	6	0	0	0	40	7	0.5	17	140	OS	1	95
2007	1	17	7	2	0	0	0	31	215	OS	2	0
2007	2	0	0	0	17	4	1.2	24	215	OS	0	30
2007	3	30	2	0.3	0	0	0	26	215	OS	0.5	15
2007	4	0	0	0	19	4	1	21	215	OS	1	50
2008	1	25	8	2.5	0	0	0	32	180	OS	2	10
2008	2	26	8	0.5	0	0	0	18	180	G	1.5	40
2008	3	11	5	0.7	0	0	0	20	160	OS	0.7	70
2008	4	0	0	0	20	14	1.5	13	160	OS	1.5	100
2009	1	20	11	0.5	0	0	0	40	180	OS	0.5	50
2009	2	26	4	1.5	0	0	0	19	180	G	1.5	90
2009	3	34	5	2	0	0	0	25	180	G	2	80
2009	4	0	0	0	40	17	1.5	15	180	OS	1.5	100
2010	1	17	13	1	0	0	0	22	210	OS	1	15
2010	2	25	11	0.8	25	11	0.5	16	210	OS	0.5	20
2010	3	0	0	0	46	5	1.2	20	210	OS	1.2	80
2016	1	16	12	1	0	0	0	27	170	OS	1	5
2016	2	0	0	0	10	12	1	3	170	OS	1	80

E#	R#	ELEN	EWID	EDEP	DLEN	DWID	DDEP	TH	PAZ	SM	FDEP	%REV
2016	3	0	0	0	12	9	0.5	28	170	OS	0.5	80
2016	4	10	7	5	0	0	0	24	170	OS	0.5	50
2016	5	0	0	0	16	9	0.5	17	170	G	0.5	100
2204	1	9	8	0.5	0	0	0	29	40	OS	0.5	20
2204	2	12	24	0.5	0	0	0	18	45	OS	0.5	95
2204	3	69	24	0.5	0	0	0	20	45	OS	1	95
2204	4	27	35	0.5	27	5	2	24	45	OS	2	95
2204	5	16	12	1.5	0	0	0	11	100	G	3	85
2204	6	42	3	0.5	42	12	4	11	100	G	0	90
2204	7	0	0	0	10	12	1	0	100	RD	0	0
2204	8	0	0	0	15	12	4	12	100	RD	4	95
2230	1	12	8	1	0	0	0	39	40	GH	1	15
2230	2	9	5	1.5	0	0	0	33	40	G	1.5	30
2230	3	33	5	1.5	0	0	0	23	40	G	2	30
2230	4	18	5	1	18	6	1	18	10	G	2	70
2230	5	13	3	0.5	13	8	0.5	19	40	OS	2	95
2230	6	23	4	0.2	23	11	1	19	0	OS	1.5	95
2230	7	28	5	1	0	0	0	23	40	G	2	70
2230	8	19	3	0.5	19	5	0.2	18	60	G	2	95
2230	9	0	0	0	23	11	3	8	90	G	3	95
2257	1	4	17	1	0	0	0	29	315	OS	1	2
2257	2	40	18	1	0	0	0	25	315	OS	2	20
2257	3	0	0	0	20	15	3	12	315	OS	3	100
2262	1	15	33	1.5	0	0	0	26	265	OS	1.5	5
2262	2	13	16	0.5	13	17	1	18	265	OS	1	50
2262	3	0	0	0	22	27	1	13	265	OS	1	25
2262	4	0	0	0	40	27	1	2	265	OS	1	40
2265	1	12	28	0.3	0	0	0	40	320	OS	0.3	30
2265	2	13	28	0.5	0	0	0	28	320	OS	2	60
2265	3	47	6	0.5	47	8	2	17	320	OS	3	95
2265	4	33	4	0.5	33	4	1	21	345	G	2	90
2265	5	40	6	0.5	0	0	0	18	345	G	2	100
2265	6	37	3	1	37	1	0.5	12	20	G	2	100
2265	7	0	0	0	10	10	2	8	20	F	2	100
2268	1	19	18	1	0	0	0	33	195	E	1	60
2268	2	16	8	0.5	0	0	0	28	195	G	1.5	40
2268	3	16	3	0.5	16	4	0.5	20	195	G	1.5	80
2268	4	0	0	0	18	18	3	11	195	SC	3	90
2281	1	9	9	1.5	0	0	0	30	210	OS	1.5	5
2281	2	8	7	1	0	0	0	20	210	OS	1.5	5
2281	3	0	0	0	9	13	3	15	210	OS	3	5
2510	1	40	10	1	0	0	0	40	10	OS	2	5
2510	2	20	10	0.5	25	2	0.5	34	10	OS	2	20
2510	3	0	0	0	25	10	0.5	31	10	OS	1	20
2510	4	0	0	0	25	4	0.2	35	10	OS	0.5	20
2510	5	0	0	0	30	6	0.4	24	20	OS	0.5	20
2510	6	0	0	0	20	8	0.4	30	340	OS	0.5	20
2517	1	40	12	0.5	0	0	0	42	200	OS	2	0
2517	2	70	18	0.5	0	0	0	38	200	OS	3	10
2517	3	95	10	0.2	95	6	0.5	29	180	OS	2	50
2517	4	35	19	0.4	0	0	0	35	195	OS	2	60
2517	5	60	15	0.5	0	0	0	28	190	OS	2	60
2517	6	55	9	0.5	55	6	0.5	25	190	OS	2	60
2517	7	45	20	0.2	0	0	0	25	195	OS	2	80
2517	8	0	0	0	10	22	1	13	160	OS	2	80
2517	9	0	0	0	10	20	1	30	160	RD	2	90
2517	10	0	0	0	25	8	0.5	10	90	RD	1.5	90
2605	1	22	9	0.8	0	0	0	26	270	OS	1	-1
2605	2	16	10	0.2	0	0	0	33	270	OS	1	40
2605	3	0	0	0	17	10	1	10	280	OS	1	95

E#	R#	ELEN	EWID	EDEP	DLEN	DWID	DDEP	TH	PAZ	SM	FDEP	%REV
2701	1	23	13	2	0	0	0	24	250	GH	2	10
2701	2	27	7	0.5	0	0	0	26	260	G	2	20
2701	3	40	7	0.5	0	0	0	28	280	G	2	10
2701	4	35	6	0.5	0	0	0	25	245	G	2	5
2701	5	34	7	0.5	0	0	0	27	270	G	2.5	5
2701	6	15	5	0.5	15	4	0.5	15	280	G	3	40
2701	7	0	0	0	40	16	2	9	290	OS	3	95
2701	8	0	0	0	25	15	1	8	300	OS	1	95
2702	1	13	9	0.8	0	0	0	23	70	OS	1	20
2702	2	28	9	0.2	28	4	0.2	27	70	OS	1	40
2702	3	0	0	0	23	10	0.2	30	70	OS	1	30
2702	4	0	0	0	27	10	0.5	27	80	OS	1	40
2802	1	22	10	1	0	0	0	33	50	OS	2	5
2802	2	29	10	0.5	0	0	0	30	30	OS	2	15
2802	3	20	7	0.3	20	3	1	32	40	OS	2	30
2802	4	15	9	0.3	0	0	0	32	40	OS	2	20
2802	5	6	6	0.2	0	0	0	40	40	OS	1	0
2802	6	25	14	0.5	0	0	0	40	40	OS	1	2
2802	7	0	0	0	35	16	1	40	40	OS	2	20
2802	8	0	0	0	20	12	1	30	40	OS	2	20
2802	9	0	0	0	6	12	2	30	40	OS	2	5
22103	1	10	8	1.5	0	0	0	35	180	OS	1.5	2
22103	2	48	14	1	0	0	0	30	180	OS	2	2
22103	3	0	0	0	20	36	2	0	180	OS	2	1
22106	1	41	27	1	0	0	0	32	200	OS	1	10
22106	2	15	3	0.2	15	8	1	27	200	OS	2	50
22106	3	24	12	0.2	0	0	0	34	180	OS	2	5
22106	4	0	0	0	37	9	2	26	190	OS	3	25
22113	1	20	9	0.5	0	0	0	40	10	OS	0.5	1
22113	2	20	9	0.5	0	0	0	35	10	OS	1	5
22113	3	0	0	0	15	10	1	27	10	OS	1	95
22114	1	50	90	0.5	0	0	0	36	320	OS	1	30
22114	2	65	70	0.5	0	0	0	38	320	OS	1	60
22114	3	35	60	0.5	0	0	0	27	330	OS	2	60
22114	4	30	10	0.2	30	10	1	20	330	OS	2	80
22114	5	90	50	0.3	0	0	0	29	340	OS	2	90
22114	6	45	50	0.5	0	0	0	36	360	OS	2	20
22114	7	0	0	0	10	50	2	0	360	RD	2	0
22114	8	0	0	0	40	60	2	12	360	OS	2	95
22114	9	0	0	0	55	70	2	5	360	OS	2	95
22115	1	50	65	0.4	0	0	0	38	330	OS	1	5
22115	2	40	60	0.4	0	0	0	30	320	OS	1	80
22115	3	60	60	0.4	0	0	0	37	315	OS	1	90
22115	4	60	10	0.4	30	50	1	20	315	OS	1	95
22115	5	150	50	0.4	15	12	1	25	310	OS	2	95
22115	6	50	50	0.4	0	0	0	32	325	OS	2	95
22115	7	0	0	0	65	50	1	13	320	OS	2	95
22115	8	50	40	0.4	50	3	1	27	315	OS	2	95
22115	9	0	0	0	45	50	2	15	315	OS	2	95
22115	10	0	0	0	10	60	1	0	315	RD	2	0
22115	11	0	0	0	20	60	1	10	300	OS	1	95

Appendix B

Supplementary Data

Notes:

E# = event number
R# = reach number
ELEN = length of entrainment in reach (m)
EWID = average width of entrainment in reach (m)
EDEP = average depth of entrainment in reach (m)
DLEN = length of deposition in reach (m)
DWID = average width of deposition in reach (m)
DDEP = average depth of deposition in reach (m)
TH = average slope angle of reach (degrees)
PAZ = average change in azimuth angle relative to upslope reach (degrees)
SM = slope morphology
FDEP = flow depth (m); not used as part of this study
%REV = % revegetation in reach (not used as part of this study)

SUPPLEMENTARY Data - Appendix B													
E#	R#	ELEN	EWID	EDEP	DLEN	DWID	DDEP	TH	PAZ	SM	FDEP	%REV	
3001	1	11	2	1	0	0	0	29	212	G	-1	0	
3001	2	21	2	1	0	0	0	25	272	G	-1	0	
3001	3	13	4	1.5	0	0	0	30	250	G	-1	0	
3001	4	19	7	1.5	0	0	0	40	226	G	-1	0	
3001	5	42	4	2	0	0	0	30	216	G	-1	0	
3001	6	12	2	2	0	0	0	30	216	G	-1	0	
3001	7	20	3	3	0	0	0	30	242	G	-1	0	
3001	8	19	3	3	0	0	0	34	256	G	-1	5	
3001	9	4	2	1.5	16	4	4	14	242	G	-1	5	
3001	10	0	0	0	40	8	1.5	17	251	OS	-1	5	
3002	1	9	15	1	0	0	0	46	308	GH	-1	0	
3002	2	35	12	1	0	0	0	32	300	G	-1	0	
3002	3	61	6	2	6	4	1	31	280	G	-1	0	
3002	4	30	8	2	0	0	0	30	278	G	-1	0	
3002	5	14	9	0.5	14	9	1	2	262	RD	-1	0	
3002	6	20	10	2	0	0	0	37	270	OS	-1	0	
3002	7	49	5	2	0	0	0	25	278	G	-1	0	
3002	8	84	5	1	0	0	0	26	268	G	-1	0	
3002	9	65	4	1	0	0	0	22	290	G	-1	0	
3002	10	24	4	1	0	0	0	40	319	G	-1	0	
3002	11	27	4	1	27	8	2	27	263	G	-1	0	
3002	12	0	0	0	0	0	0	28	222	G	-1	0	
3002	13	0	0	0	68	3	1	21	272	G	-1	0	
3002	14	0	0	0	24	6	4	16	272	G	-1	0	
3002	15	0	0	0	24	3	1	27	285	G	-1	0	
3002	16	0	0	0	23	2	1	26	268	G	-1	0	
3002	17	0	0	0	40	2	1	13	299	G	-1	0	
3003	1	19	9	1	0	0	0	37	186	OS	-1	0	
3003	2	56	4	1	0	0	0	28	152	G	-1	0	
point of entry of Event 3004													
3003	3	16	2	2	0	0	0	26	170	G	-1	0	
3003	4	26	2	2	0	0	0	26	148	G	-1	0	
3003	5	15	3	2	0	0	0	25	142	G	-1	0	
3003	6	0	0	0	24	5	2	7	147	OS	-1	0	
3004	1	28	1	1	0	0	0	27	148	G	-1	0	
3004	2	13	2	1	0	0	0	32	130	G	-1	0	
3005	1	10	1.5	3	0	0	0	25	148	GH	-1	0	
3005	2	21	3	3	0	0	0	26	166	G	-1	0	
3005	3	16	2	4	0	0	0	33	162	G	-1	0	
3005	4	18	2	3	18	1	1	23	156	G	-1	0	
3005	5	40	2	3	15	1	1	25	168	G	-1	0	
3005	6	36	2	2	0	0	0	24	163	G	-1	0	
3005	7	18	2	1	18	2	2	15	145	G	-1	0	
3005	8	0	0	0	0	0	0	90	145	G	-1	0	
3005	9	0	0	0	28	3	1	18	151	G	-1	0	
3005	10	0	0	0	29	1	1	18	188	G	-1	0	
3005	11	0	0	0	28	1	0.5	20	162	G	-1	0	
3005	12	0	0	0	38	3	1	10	171	G	-1	0	
3005	13	0	0	0	28	4	1	7	169	F	-1	0	
3005	14	0	0	0	28	5	1	2	168	F	-1	0	
3006	1	104	24	1	0	0	0	32	238	OS	-1	0	
3006	2	35	30	1	0	0	0	36	238	OS	-1	0	
3006	3	44	30	1	0	0	0	34	238	OS	-1	0	
3006	4	40	35	2	0	0	0	28	238	OS	-1	0	
3006	5	66	40	5	0	0	0	20	238	OS	-1	0	
3006	6	19	60	4	0	0	0	20	238	OS	-1	0	
3006	7	5	80	3	0	0	0	29	238	OS	-1	0	
3006	8	9	110	5	0	0	0	0	238	RD	-1	0	

E#	R#	ELEN	EWID	EDEP	DLEN	DWID	DDEP	TH	PAZ	SM	FDEP	%REV
3006	9	0	0	0	51	110	3	26	238	OS	-1	0
3006	10	0	0	0	44	120	4	13	238	OS	-1	0
3006	11	0	0	0	44	100	2	7	238	OS	-1	0
event travelled 17m into standing timber												
4103	1	42	4	1	0	0	0	24	301	OS	1	0
4103	2	12	4	1.5	0	0	0	10	280	RD	1.5	0
4103	3	26	9	1	0	0	0	28	268	OS	1.5	0
4103	4	97	6	1.5	0	0	0	22	210	G	1.5	0
4103	5	0	0	0	8	8	2	5	210	RD	2	0
4103	6	41	1	0.2	0	0	0	29	292	OS	0.3	0
4103	7	110	2	0.2	50	1	0.1	20	308	OS	-1	0
4103	8	95	0	0	95	1	0.3	16	308	OS	-1	0
5001	1	5	17	1	0	0	0	40	308	OS	-1	0
5001	2	14	3	1	0	0	0	36	304	OS	-1	0
5001	3	16	2.5	1.5	0	0	0	34	304	OS	1	0
5001	4	23	2	1.5	0	0	0	26	300	OS	1	0
5001	5	16	3.5	1.5	0	0	0	42	260	OS	1	0
5001	6	15	4	1	0	0	0	18	260	OS	1	0
5001	7	10	2	0.5	10	4	1	12	250	OS	1	0
5001	8	10	2	0.5	0	0	0	18	248	OS	1	0
5001	9	0	0	0	13	20	2	0.5	246	RD	1.5	0
5002	1	71	16	0.5	0	0	0	44	315	OS	0.5	0
5002	2	52	12	0.5	0	0	0	40	315	OS	0.5	0
5002	3	58	8	0.5	58	1	1	36	320	G	1	0
5002	4	68	6	1	0	0	0	31	310	G	1.5	0
5002	5	20	4	1	0	0	0	29	305	G	1.5	0
5002	6	25	4	1	0	0	0	22	313	G	1.5	0
5002	7	0	0	0	15	14	0.5	23	320	OS	1	0
5002	8	0	0	0	8	14	0.5	0.5	320	RD	1	0
5002	9	0	0	0	33	11	1	14	320	F	1	0
5002	10	0	0	0	9	10	1	7	320	F	1	0
5002	11	0	0	0	25	12	0.5	7	320	F	0.5	0
5003	1	18	8	1	0	0	0	33	285	OS	1	0
5003	2	15	7	1.6	0	0	0	34	318	GH	1.5	0
5003	3	54	5	1.5	0	0	0	33	300	G	1.5	0
5003	4	58	5	1.5	0	0	0	23	300	G	1.5	0
5003	5	28	6	0.5	0	0	0	25	288	G	1	0
5003	6	30	3	0.5	0	0	0	25	288	G	1.5	0
5003	7	0	0	0	32	10	0.5	15	288	G	1.5	0
5003	8	0	0	0	9	12	1	0.5	288	RD	1.5	0
5003	9	0	0	0	24	14	0.5	3	288	F	1	0
5003	10	0	0	0	42	22	1	3	256	F	1	0
5101	1	53	18	0.5	0	0	0	30	291	GS	0.5	0
5101	2	42	3	0.5	0	0	0	23	326	G	1	0
5101	3	31	4	0.5	0	0	0	33	344	G	1	0
5101	4	54	4	0.5	0	0	0	23	344	G	1	0
5101	5	0	0	0	22	16	1	15	325	F	1.5	0
5101	6	0	0	0	16	14	1.5	10	318	F	1.5	0
5102	1	38	12	1	0	0	0	40	59	OS	1	0
5102	2	55	14	1	0	0	0	25	60	OS	1	0
5102	3	28	10	1	6	8	2	19	60	OS	2.5	0
5102	4	45	6	1	5	4	0.5	22	60	OS	2	0
5102	5	64	4	1.5	0	0	0	24	62	OS	2	0
5102	6	33	4	1	0	0	0	17	32	OS	2	0
5102	7	0	0	0	18	12	1.5	3	20	RD	1.5	0
5102	8	0	0	0	31	12	0.5	7	52	RD	0.5	0
5103	1	21	18	1	0	0	0	35	333	ESC	1	0
5103	2	36	9	0.5	0	0	0	32	335	OS	0.5	70
5103	3	21	4	0.5	21	3	0.5	27	332	OS	0.5	80
5103	4	23	3	0.5	0	0	0	30	330	OS	-1	70
5103	5	0	0	0	10	16	1.5	0.5	325	RD	-1	0

E#	R#	ELEN	EWID	EDEP	DLEN	DWID	DDEP	TH	PAZ	SM	FDEP	%REV
5104	1	27	5	0.5	0	0	0	31	327	OS	1	0
5104	2	42	10	0.5	0	0	0	29	326	OS	1	0
5104	3	21	6	0.5	0	0	0	29	334	GS	1	0
5104	4	23	4	0.5	0	0	0	25	328	G	1	0
5104	5	36	3	0.5	0	0	0	26	287	G	1	0
5104	6	21	4	0.5	0	0	0	23	230	G	1	0
5104	7	0	0	0	42	20	1.5	15	287	F	1.5	0
5201	1	13	19	1	0	0	0	39	75	OS	1.5	0
5201	2	91	18	1	0	0	0	33	74	OS	1.5	0
5201	3	24	20	1	0	0	0	28	78	OS	1.5	0
5201	4	31	3	1	31	3	1.5	25	74	OS	1.5	0
5201	5	0	0	0	17	8	2	12	74	OS	2	0
5201	6	0	0	0	37	12	1	8	140	RD	1	0
5202	1	61	10	0.5	0	0	0	44	245	GH	1	0
5202	2	58	6	0.5	0	0	0	34	247	GH	1	0
5202	3	68	3	1	0	0	0	27	238	G	1	0
5202	4	30	5	1	0	0	0	26	235	G	1	0
5202	5	27	4	0.5	27	15	1	14	230	G	-1	0
point of entry of Event 5203												
5202	6	0	0	0	24	4	1	9	235	RD	1	25
5202	7	33	6	1	33	1	1	26	246	G	1	0
5202	8	63	5	0.5	0	0	0	15	247	G	1.5	35
5202	9	29	6	0.5	0	0	0	16	243	G	1.5	35
5202	10	97	6	0.5	0	0	0	14	239	G	1.5	25
5202	11	0	0	0	53	14	0.5	11	230	G	1.5	15
5202	12	0	0	0	45	18	1.5	8	234	F	1.5	15
5202	13	10	1	0.5	10	25	2.5	5	213	F	2.5	15
5202	14	0	0	0	105	12	2	3	148	SC	2	25
5202	15	0	0	0	45	10	1.5	2	148	SC	1.5	25
5203	1	20	16	1	0	0	0	34	230	OS	1	10
5203	2	11	3	0.5	0	0	0	35	230	GH	1	15
5203	3	37	3	0.5	0	0	0	33	234	G	1	15
5203	4	18	3	1	0	0	0	30	237	G	1	0
5203	5	87	3	1	0	0	0	23	221	G	1	0
5203	6	66	3	1	0	0	0	24	208	G	1	0
5204	1	25	4	0.3	0	0	0	36	270	OS	0.5	0
5204	2	20	2	0.3	0	0	0	38	260	G	0.5	0
5204	3	0	0	0	10	2	0.5	31	260	G	0.5	0
5204	4	24	2	0.3	0	0	0	31	240	G	0.5	0
5204	5	35	2	0.3	0	0	0	32	256	G	0.5	0
5204	6	0	0	0	15	15	1	10	254	RD	-1	0
5301	1	32	12	1.5	0	0	0	35	123	GH	1.5	5
5301	2	70	4	1	0	0	0	33	136	G	1.5	0
5301	3	44	4	0.5	0	0	0	35	122	G	1.5	0
5301	4	35	3	1	0	0	0	30	132	G	1.5	0
5301	5	40	4	1	5	4	0.5	31	129	G	1	0
5301	6	69	15	1	89	15	0.5	27	124	OS	1	65
5301	7	64	10	0.5	64	20	0.3	25	124	OS	1	90
5301	8	0	0	0	83	30	1	17	122	F	1	90
5302	1	12	11	1	0	0	0	38	136	OS	1.5	0
5302	2	22	3	1	0	0	0	45	128	GH	1	0
5302	3	35	3	0.5	35	2	0.5	32	115	G	1.5	0
5302	4	35	2	0.5	36	1.5	0.5	30	138	G	1	0
5302	5	30	1	0.5	39	1.5	0.5	28	147	G	1	0
5302	6	0	0	0	24	5	0.5	25	150	G	1	0
5302	7	0	0	0	20	30	1	2	150	RD	1	0
5303	1	3	15	0.3	0	0	0	45	70	GS	0.3	0
5303	2	16	3	0.5	0	0	0	32	132	G	0.5	0
5303	3	77	2	0.5	0	0	0	29	93	G	0.5	0
5303	4	37	2	0.5	0	0	0	24	110	G	0.5	0
5303	5	0	0	0	20	4	0.5	30	118	F	0.5	0

E#	R#	ELEN	EWID	EDEP	DLEN	DWID	DDEP	TH	PAZ	SM	FDEP	%REV
5303	6	0	0	0	35	2	1	11	77	SC	1	0
5303	7	0	0	0	41	33	0.5	5	51	RD	1	0
5401	1	88	25	1	0	0	0	45	124	OS	1.5	0
5401	2	0	0	0	12	27	0.5	5	124	RD	1.5	0
5401	3	25	28	1	0	0	0	42	122	OS	1	0
5401	4	76	33	1	0	0	0	31	118	OS	1	0
5401	5	22	35	1	0	0	0	28	108	OS	1	0
5401	6	37	35	1	0	0	0	21	85	OS	1	20
5401	7	0	0	0	24	40	2	10	90	OS	2.5	0
5401	8	0	0	0	19	40	0.5	4	88	OS	0.5	40
5401	9	0	0	0	35	35	0.5	11	74	OS	0.5	40
5402	1	75	8	1.5	0	0	0	31	338	GH	1	0
5402	2	121	10	1	0	0	0	29	355	G	1.5	0
5402	3	70	12	2	70	12	2	27	2	OS	2.5	0
5402	4	29	8	0.5	0	0	0	24	35	G	-1	0
5402	5	88	4	1	0	0	0	26	356	G	2	0
5402	6	46	5	1	0	0	0	28	342	G	2	0
5402	7	64	10	1	0	0	0	27	22	G	1.5	0
5402	8	55	10	1	20	2	0.5	24	16	G	1.5	30
5402	9	51	15	0.5	0	0	0	27	48	G	1.5	0
5402	10	60	20	0.5	0	0	0	25	48	G	-1	0
5402	11	30	25	0.5	0	0	0	25	30	G	-1	0
5402	12	49	35	0.5	0	0	0	22	24	G	-1	0
5402	13	66	28	0.5	66	10	0.5	20	30	OS	1.5	30
5402	14	0	0	0	13	20	0.5	1	30	RD	1.5	15
5402	15	64	20	0.5	0	0	0	20	30	OS	1.5	60
5402	16	0	0	0	35	20	1	8	26	F	1.5	60
5402	17	0	0	0	39	80	1	9	33	F	1.5	80
5402	18	0	0	0	40	35	1.5	6	111	SC	1.5	60
5402	19	0	0	0	34	30	1	7	98	SC	1	85
5501	1	14	10	1.5	0	0	0	30	78	OS	1.5	0
5501	2	20	10	0.5	20	10	1	18	75	OS	1	0
5501	3	0	0	0	25	10	0.5	28	75	OS	0.5	0
5501	4	0	0	0	16	10	1	8	70	RD	0.5	0
5501	5	0	0	0	24	4	0.5	25	100	OS	0.5	0

Appendix C

Correlation Tables for Regression Analyses

- Correlation Tables: Q.C.I. (Selected Data)
- Correlation Tables for Predictors,
Unconfined Flow, Q.C.I. (Selected) Data
- Correlation Tables for Predictors,
Confined Flow, Q.C.I. (Selected) Data
- Correlation Tables for Predictors,
Transition Flow, Q.C.I. (Selected) Data
- Correlation Tables for Predictors,
Unconfined Flow, Subset Data
- Correlation Tables for Predictors,
Confined Flow, Subset Data
- Correlation Tables for Predictors,
Transition Flow, Subset Data

MTB > Retrieve 'C:\MINITAB\QCI\MTW\UFWIDTH2.WK1';

SUBC> Lotus.

Converting Lotus 1-2-3 v2/v3 to MINITAB

LOTUS 1-2-3 file: C:\MINITAB\QCI\MTW\UFWIDTH2.WK1

MTB > CORRELATION '+dV' '-dV' 'L' 'We' 'Wd' 'Wf' 'TH' 'dTH' 'dAZ' 'sigV' 'BAF'

	+dV	-dV	L	We	Wd	Wf	TH	dTH	dAZ	sigV
-dV	0.153									
L	0.477	-0.307								
We	0.738	0.251	0.294							
Wd	-0.241	-0.747	0.044	-0.408						
Wf	0.514	-0.389	0.324	0.627	0.455					
TH	0.233	0.333	0.121	0.376	-0.538	-0.092				
dTH	0.164	0.196	0.106	0.221	-0.345	-0.063	0.530			
dAZ	0.012	0.008	-0.005	0.005	-0.019	-0.012	0.082	0.110		
sigV	0.332	-0.499	0.307	0.254	0.412	0.599	-0.078	-0.070	0.009	
BAF	0.315	-0.390	0.383	0.266	0.349	0.555	0.014	0.207	-0.002	0.693

MTB > Retrieve 'C:\MINITAB\QCI\MTW\CF040GTH.WK1';

SUBC> Lotus.

Converting Lotus 1-2-3 v2/v3 to MINITAB

LOTUS 1-2-3 file: C:\MINITAB\QCI\MTW\CF040GTH.WK1

MTB > CORRELATION '+dV' '-dV' 'LEN' 'WIDS' 'WIDd' 'WIDE' 'TH' 'dTH' 'dAZ' 'sigV' 'BAF'

	+dV	-dV	LEN	WIDS	WIDd	WIDE	TH	dTH	dAZ	sigV
-dV	0.075									
LEN	0.592	-0.075								
WIDS	0.616	0.234	0.309							
WIDd	-0.133	-0.719	-0.041	-0.303						
WIDE	0.492	-0.268	0.260	0.742	0.408					
TH	-0.049	0.320	-0.008	0.207	-0.433	-0.107				
dTH	-0.084	0.118	-0.088	0.142	-0.099	0.068	0.466			
dAZ	0.059	-0.020	0.043	0.050	-0.003	0.045	-0.175	-0.013		
sigV	0.589	0.850	0.252	0.515	-0.652	0.043	0.233	0.051	0.015	
BAF	0.050	-0.235	-0.025	-0.090	0.175	0.033	-0.242	0.004	-0.123	-0.161

MTB > NOOUTFILE

MTB > Retrieve 'C:\MINITAB\QCI\MTW\UFW1929.WK1';

SUBC> Lotus.

Converting Lotus 1-2-3 v2/v3 to MINITAB

LOTUS 1-2-3 file: C:\MINITAB\QCI\MTW\UFW1929.WK1

MTB > CORRELATION 'F+dV' 'F-dV' 'LEN' 'WIDS' 'WIDD' 'WIDE' 'TH' 'dTH' 'dAZ' 'FsigV' 'BAF'

	F+dV	F-dV	LEN	WIDS	WIDD	WIDE	TH	dTH	dAZ	FsigV
F-dV	-0.215									
LEN	0.525	-0.220								
WIDS	0.636	0.230	0.323							
WIDD	-0.053	-0.673	0.086	-0.331						
WIDE	0.598	-0.288	0.382	0.870	0.178					
TH	0.195	-0.015	0.029	0.223	-0.126	0.166				
dTH	-0.090	0.187	0.127	0.089	-0.230	-0.030	0.049			
dAZ	-0.213	0.063	-0.058	-0.136	-0.066	-0.177	-0.011	0.065		
FsigV	0.265	-0.454	0.366	0.338	0.337	0.529	0.050	-0.034	-0.129	
BAF	0.235	-0.463	0.365	0.339	0.323	0.525	0.047	0.032	-0.127	0.997

MTB > Retrieve 'C:\MINITAB\QCI\MTW\UFW3055.WK1';

SUBC> Lotus.

Converting Lotus 1-2-3 v2/v3 to MINITAB

LOTUS 1-2-3 file: C:\MINITAB\QCI\MTW\UFW3055.WK1

MTB > CORRELATION 'F+dV' 'F-dV' 'LEN' 'WIDS' 'WIDD' 'WIDE' 'TH' 'dTH' 'dAZ' 'FsigV' 'BAF'

	F+dV	F-dV	LEN	WIDS	WIDD	WIDE	TH	dTH	dAZ	FsigV
F-dV	-0.368									
LEN	0.466	-0.483								
WIDS	0.687	0.094	0.329							
WIDD	-0.083	-0.825	-0.013	-0.388						
WIDE	0.666	-0.664	0.350	0.902	0.047					
TH	-0.021	0.204	0.045	0.183	-0.320	0.049				
dTH	-0.088	0.218	-0.240	0.110	-0.263	0.014	0.266			
dAZ	-0.050	0.061	-0.072	-0.009	-0.037	-0.027	-0.244	0.216		
FsigV	0.453	-0.608	0.247	0.479	0.103	0.567	0.037	0.098	-0.143	
BAF	0.587	-0.549	0.300	0.532	0.026	0.592	0.017	0.113	-0.189	0.999

MTB > Retrieve 'C:\MINITAB\QCI\MTW\CF040GTH.WK1';
SUBC> Lotus.

Converting Lotus 1-2-3 v2/v3 to MINITAB

LOTUS 1-2-3 file: C:\MINITAB\QCI\MTW\CF040GTH.WK1

MTB > CORRELATION 'F+dV' 'F-dV' 'LEN' 'WIDS' 'WIDD' 'WIDE' 'TH' 'dTH' 'dAZ' 'FsigV' 'BAF'

F-dV	F+dV	F-dV	LEN	WIDS	WIDD	WIDE	TH	dTH	dAZ	FsigV
-0.116	-0.208									
LEN	0.627	0.188	0.309							
WIDS	0.597	-0.782	-0.041	-0.303						
WIDD	-0.023	-0.374	0.260	0.742	0.408					
WIDE	0.506	0.354	-0.008	0.207	-0.433	-0.107				
TH	-0.126	0.186	-0.088	0.142	-0.099	0.068	0.466			
dTH	-0.109	0.091	0.043	0.050	-0.003	0.045	-0.175	-0.013		
dAZ	0.116	-0.347	0.631	0.592	-0.007	0.550	-0.179	-0.172	0.060	
FsigV	0.946	-0.229	-0.025	-0.090	0.175	0.033	-0.242	0.004	-0.123	-0.030
BAF	-0.008									

MTB > Retrieve 'C:\MINITAB\QCI\MTW\CFUF040.WK1';
SUBC> Lotus.

Converting Lotus 1-2-3 v2/v3 to MINITAB

LOTUS 1-2-3 file: C:\MINITAB\QCI\MTW\CFUF040.WK1

MTB > CORRELATION 'F+dV' 'F-dV' 'LEN' 'WIDS' 'WIDD' 'WIDE' 'TH' 'dTH' 'dAZ' 'FsigV' 'BAF'

F-dV	F+dV	F-dV	LEN	WIDS	WIDD	WIDE	TH	dTH	dAZ	FsigV
-0.433	-0.402									
LEN	0.773	0.209	-0.072							
WIDS	0.746	-0.795	0.232	-0.452						
WIDD	0.191	-0.594	0.189	0.322	0.699					
WIDE	0.673	0.466	-0.030	0.513	-0.578	-0.202				
TH	-0.278	0.194	0.142	0.431	-0.419	-0.099	0.856			
dTH	-0.164	-0.088	0.172	0.116	0.054	0.150	-0.080	-0.054		
dAZ	0.206	-0.687	0.365	0.063	0.550	0.634	-0.224	-0.113	0.345	
FsigV	0.434	-0.417	0.235	-0.024	0.405	0.411	-0.201	-0.106	-0.406	0.626
BAF	0.316									

MTB > Retrieve 'C:\MINITAB\QCI\MTW\CFUF040.WK1';

SUBC> Lotus.

Converting Lotus 1-2-3 v2/v3 to MINITAB

LOTUS 1-2-3 file: C:\MINITAB\QCI\MTW\CFUF040.WK1

MTB > CORRELATION '+dV' '-dV' 'LEN' 'WIDS' 'WIDD' 'WIDE' 'TH' 'dTH' 'dAZ' 'sigV' 'BAF'

	+dV	-dV	LEN	WIDS	WIDD	WIDE	TH	dTH	dAZ	sigV
-dV	0.195									
LEN	-0.023	-0.501								
WIDS	0.879	0.302	-0.072							
WIDD	-0.255	-0.697	0.232	-0.452						
WIDE	0.435	-0.498	0.189	0.322	0.699					
TH	0.283	0.341	-0.030	0.513	-0.578	-0.202				
dTH	0.270	0.197	0.142	0.431	-0.419	-0.099	0.856			
dAZ	0.217	-0.310	0.172	0.116	0.054	0.150	-0.080	-0.054		
sigV	0.010	-0.594	0.283	-0.024	0.523	0.536	-0.169	-0.046	0.230	
BAF	-0.104	-0.253	0.235	-0.024	0.405	0.411	-0.201	-0.106	-0.406	0.522

MTB > NOOUTFILE

MTB > Retrieve 'C:\MINITAB\QCI\MTW\UFW024.WK1';

SUBC> Lotus.

Converting Lotus 1-2-3 v2/v3 to MINITAB

LOTUS 1-2-3 file: C:\MINITAB\QCI\MTW\UFW024.WK1

MTB > CORRELATION 'F+dV' 'F-dV' 'LEN' 'FWIDS' 'FWIDD' 'FWIDE' 'TH' 'dTH' 'dAZ' 'FsigV' 'BAF'

	F+dV	F-dV	LEN	FWIDS	FWIDD	FWIDE	TH	dTH	dAZ	FsigV
F-dV	-0.302									
LEN	0.582	-0.447								
FWIDS	0.651	-0.183	0.343							
FWIDD	-0.124	-0.807	0.061	0.042						
FWIDE	0.432	-0.514	0.292	0.748	0.680					
TH	0.336	0.318	0.167	-0.027	-0.489	-0.271				
dTH	-0.103	0.206	0.125	-0.180	-0.290	-0.160	0.501			
dAZ	-0.140	0.137	-0.037	-0.188	-0.222	-0.213	0.015	-0.041		
FsigV	0.206	-0.634	0.442	0.241	0.566	0.667	-0.207	-0.135	-0.176	
BAF	0.207	-0.492	0.446	0.213	0.416	0.572	-0.001	0.277	-0.195	0.877

MTB > RETRIEVE 'C:\MINITAB\QCI\MTW\D024.MTW'
WORKSHEET SAVED 1/ 1/1996

Unconfined Flow:
Deposition $0^\circ < \theta \leq 24^\circ$.

Worksheet retrieved from file: C:\MINITAB\QCI\MTW\D024.MTW
MTB > CORRELATION '-dV' 'F-dV' 'FL' 'FWe' 'FWd' 'FWf' 'FsigV' 'L' 'We' 'Wd' 'Wf'
> 'dWf' 'TH' 'dTH' 'dAZ'

	-dV	F-dV	FL	FWe	FWd	FWf	FsigV	L
F-dV	0.737							
FL	-0.458	-0.506						
FWe	-0.291	-0.288	0.559					
FWd	-0.583	-0.829	0.107	0.088				
FWf	-0.552	-0.626	0.273	0.778	0.746			
FsigV	-0.654	-0.700	0.392	0.416	0.631	0.750		
L	-0.578	-0.520	0.906	0.570	0.147	0.328	0.467	
We	0.114	0.258	0.283	0.911	-0.367	0.272	0.114	0.321
Wd	-0.713	-0.724	0.127	0.108	0.885	0.789	0.676	0.180
Wf	-0.669	-0.615	0.256	0.651	0.729	0.921	0.735	0.327
dWf	-0.462	-0.469	0.301	0.148	0.350	0.276	0.131	0.271
TH	0.172	0.304	0.230	-0.014	-0.454	-0.266	-0.147	0.162
dTH	0.020	0.152	0.080	-0.157	-0.205	-0.113	-0.123	0.061
dAZ	-0.039	-0.061	0.122	0.160	0.038	0.097	0.116	0.110

	We	Wd	Wf	dWf	TH	dTH
Wd	-0.248					
Wf	0.202	0.899				
dWf	0.077	0.255	0.218			
TH	0.326	-0.386	-0.243	0.092		
dTH	0.148	-0.154	-0.095	-0.010	0.474	
dAZ	0.084	0.027	0.066	0.297	0.047	0.101

MTB > RETRIEVE 'C:\MINITAB\QCI\MTW\UFLOG040.MTW'
 WORKSHEET SAVED 1/ 1/1996

*Unconfined Flow:
 Entrainment 19° TH ≤ 29°*

Worksheet retrieved from file: C:\MINITAB\QCI\MTW\UFLOG040.MTW

MTB > DELETE 250:343 C1-C26

MTB > DELETE 1:123 C1-C26

MTB > Correlation '+dV' 'F+dV' 'FL' 'FWe' 'FWd' 'FWf' 'FsigV' 'L' 'We' 'Wd' 'Wf'
 > 'dWf' 'TH' 'dTH' 'dAZ'

	+dV	F+dV	FL	FWe	FWd	FWf	FsigV	L
F+dV	0.734							
FL	0.510	0.586						
FWe	0.587	0.783	0.357					
FWd	-0.040	0.056	0.033	-0.127				
FWf	0.551	0.657	0.392	0.833	0.351			
FsigV	0.329	0.265	0.341	0.311	0.294	0.523		
L	0.675	0.525	0.906	0.325	0.014	0.378	0.366	
We	0.677	0.636	0.301	0.881	-0.281	0.764	0.338	0.323
Wd	-0.152	-0.053	0.087	-0.184	0.857	0.211	0.337	0.086
Wf	0.627	0.598	0.359	0.779	0.369	0.907	0.529	0.382
dWf	0.094	0.195	0.158	0.055	0.060	0.057	-0.357	0.086
TH	0.148	0.195	0.025	0.282	0.030	0.163	0.050	0.029
dTH	0.082	-0.056	0.020	0.074	-0.220	-0.034	-0.022	0.086
dAZ	-0.036	-0.031	-0.109	0.007	-0.014	-0.067	-0.058	-0.090
	We	Wd	Wf	dWf	TH	dTH		
Wd	-0.331							
Wf	0.870	0.178						
dWf	0.073	-0.040	0.034					
TH	0.223	-0.126	0.166	-0.297				
dTH	0.123	-0.214	0.016	-0.049	0.170			
dAZ	-0.068	0.009	-0.067	-0.136	0.037	-0.012		

MTB > RETRIEVE 'C:\MINITAB\QCI\MTW\UFLOG040.MTW' *Unconfined Flow:*
 WORKSHEET SAVED 12/29/1995 *Entrainment 30° < TH < 55°*

Worksheet retrieved from file: C:\MINITAB\QCI\MTW\UFLOG040.MTW

MTB > DELETE 1:249 C1-C26

MTB > Correlation '+dV' 'F+dV' 'FL' 'FWe' 'FWD' 'FWf' 'FsigV' 'L' 'We' 'Wd' 'Wf'
 > 'dWf' 'TH' 'dTH' 'dAZ'

	+dV	F+dV	FL	FWe	FWD	FWf	FsigV	L
F+dV	0.768							
FL	0.413	0.592						
FWe	0.648	0.745	0.384					
FWD	-0.041	0.222	0.141	0.002				
FWf	0.606	0.706	0.382	0.873	0.662			
FsigV	0.501	0.453	0.241	0.520	0.356	0.569		
L	0.387	0.466	0.913	0.337	0.212	0.367	0.247	
We	0.802	0.687	0.339	0.885	-0.288	0.764	0.479	0.329
Wd	-0.203	-0.083	-0.004	-0.268	0.954	0.138	0.103	-0.013
Wf	0.775	0.666	0.365	0.809	0.645	0.893	0.567	0.350
dWf	0.593	0.400	-0.292	0.710	0.335	0.584	0.481	-0.235
TH	-0.043	-0.072	0.003	0.118	-0.324	0.063	0.054	0.006
dTH	-0.109	-0.270	-0.227	-0.077	0.139	-0.114	0.145	-0.212
dAZ	-0.034	0.048	-0.057	0.021	-0.032	-0.068	-0.124	-0.076
	We	Wd	Wf	dWf	TH	dTH		
Wd	-0.388							
Wf	0.902	0.047						
dWf	0.703	0.450	0.573					
TH	0.115	-0.253	0.006	-0.663				
dTH	-0.053	-0.022	-0.068	0.693	0.565			
dAZ	-0.094	0.124	-0.044	0.628	-0.083	0.063		

Confined Flow: Entrainment 10° < TH

MTB > CORRELATION '+dV' 'F+dV' 'FL' 'FWe' 'FWd' 'FWf' 'FsigV' 'L' 'We' 'Wf' 'TH'
> 'dTH' 'dAZ' 'BAF'

	+dV	F+dV	FL	FWe	FWd	FWf	FsigV	L
F+dV	0.857							
FL	0.546	0.631						
FWe	0.530	0.603	0.244					
FWd	0.024	-0.049	0.064	-0.087				
FWf	0.464	0.507	0.268	0.753	0.625			
FsigV	0.263	0.254	0.179	0.214	0.500	0.391		
L	0.580	0.607	0.932	0.253	0.002	0.260	0.105	
We	0.582	0.595	0.268	0.930	0.020	0.774	0.254	0.267
Wf	0.495	0.497	0.285	0.701	0.592	0.943	0.411	0.265
TH	-0.077	-0.064	-0.054	0.147	-0.168	-0.107	-0.345	-0.014
dTH	-0.112	-0.065	-0.072	0.104	-0.173	0.048	-0.017	-0.117
dAZ	0.004	0.040	0.005	0.030	0.137	0.070	0.060	-0.025
BAF	0.237	0.204	0.131	0.159	0.317	0.282	0.635	0.089
	We	Wf	TH	dTH	dAZ			
Wf	0.796							
TH	0.126	-0.098						
dTH	0.098	0.056	0.478					
dAZ	0.033	0.084	-0.070	-0.041				
BAF	0.201	0.281	-0.030	0.095	-0.110			

TRANSITION FLOW: $0^\circ \leq \text{TH} \leq 22^\circ$

MTB > CORRELATION '-dV' 'F-dV' 'FL' 'FWe' 'FWd' 'FWf' 'FsigV' 'L' 'We' 'Wf'
'TH'
> 'sigV' 'dTH' 'dAZ' 'BAF'

	-dV	F-dV	FL	FWe	FWd	FWf	FsigV	L
F-dV	0.770							
FL	-0.633	-0.583						
FWe	-0.860	-0.713	0.659					
FWd	-0.607	-0.842	0.354	0.411				
FWf	-0.573	-0.746	0.363	0.851	0.788			
FsigV	-0.676	-0.687	0.499	0.835	0.619	0.716		
L	-0.492	-0.402	0.816	0.604	0.243	0.218	0.382	
We	0.172	0.209	0.056	0.953	-0.231	0.253	0.058	-0.030
Wf	-0.495	-0.594	0.306	0.890	0.674	0.951	0.631	0.164
TH	0.240	0.466	0.104	-0.186	-0.453	-0.328	-0.252	0.083
sigV	-0.600	-0.521	0.357	0.871	0.501	0.554	0.830	0.275
dTH	0.041	0.194	0.272	0.725	-0.174	-0.017	-0.017	0.331
dAZ	-0.307	-0.047	0.160	-0.814	-0.111	-0.175	0.180	0.185
BAF	-0.287	-0.417	0.271	0.049	0.509	0.478	0.579	0.250
	We	Wf	TH	sigV	dTH	dAZ		
Wf	0.446							
TH	0.354	-0.168						
sigV	0.008	0.529	-0.142					
dTH	0.354	0.032	0.676	0.072				
dAZ	-0.302	-0.258	0.140	0.179	0.132			
BAF	-0.173	0.377	-0.207	0.516	0.028	-0.308		

MTB > RETRIEVE 'C:\MINITAB\QCI\MTW\DH024.MTW'
 WORKSHEET SAVED 1/1/1996

Unconfined Flow
 Deposition

$0^\circ \leq TH \leq 24^\circ$
 Subset Regression

Worksheet retrieved from file: C:\MINITAB\QCI\MTW\DH024.MTW

MTB > CORRELATION '-dV' 'F-dV' 'FL' 'FWe' 'FWD' 'FWf' 'FsigV' 'L' 'We' 'Wd' 'Wf'
 > 'TH' 'dTH' 'dAZ'

	-dV	F-dV	FL	FWe	FWD	FWf	FsigV	L
F-dV	0.688							
FL	-0.414	-0.345						
FWe	0.046	-0.327	0.462					
FWD	-0.463	-0.761	-0.173	-0.159				
FWf	-0.335	-0.448	0.175	0.698	0.592			
FsigV	-0.592	-0.667	0.437	0.182	0.400	0.568		
L	-0.660	-0.415	0.902	0.451	-0.082	0.284	0.489	
We	0.277	0.385	0.229	0.915	-0.531	0.311	-0.147	0.229
Wd	-0.570	-0.655	-0.048	-0.315	0.907	0.568	0.575	0.075
Wf	-0.398	-0.421	0.155	0.693	0.593	0.948	0.534	0.298
TH	0.230	0.367	0.270	0.262	-0.513	-0.228	-0.253	0.219
dTH	0.243	0.422	0.113	-0.040	-0.412	-0.163	-0.211	0.116
dAZ	-0.032	-0.091	0.157	0.137	0.035	0.159	0.143	0.114
	We	Wd	Wf	TH	dTH			
Wd	-0.561							
Wf	0.267	0.648						
TH	0.508	-0.586	-0.215					
dTH	0.286	-0.397	-0.199	0.540				
dAZ	0.124	0.013	0.129	0.043	0.028			

MTB > retrieve 'c:\minitab\qci\mtw\sh1929a.mtw'
 WORKSHEET SAVED 1/18/1996

Unconfined Flow: Subset Regression
 Entrainment 19° ≤ TH ≤ 29°

Worksheet retrieved from file: c:\minitab\qci\mtw\sh1929a.mtw

MTB > note retrieve 'c:\minitab\qci\mtw\sh1929B.mtw'

MTB > Correlation '+dV' 'F+dV' 'FL' 'FWe' 'FWd' 'FWf' 'FsigV' 'L' 'We' 'Wd' 'Wf'
 > 'TH' 'dTH' 'dAZ'

	+dV	F+dV	FL	FWe	FWd	FWf	FsigV	L
F+dV	0.842							
FL	0.503	0.527						
FWe	0.604	0.813	0.356					
FWd	-0.279	-0.156	-0.151	-0.304				
FWf	0.553	0.627	0.296	0.733	0.236			
FsigV	0.038	0.067	0.175	0.177	0.077	0.405		
L	0.567	0.514	0.953	0.327	-0.217	0.293	0.206	
We	0.701	0.708	0.282	0.894	-0.337	0.745	0.118	0.286
Wd	-0.291	-0.123	-0.015	-0.251	0.875	0.215	0.353	-0.048
Wf	0.561	0.596	0.291	0.693	0.289	0.934	0.355	0.274
TH	-0.012	0.048	-0.190	0.184	0.056	0.061	0.074	-0.235
dTH	0.015	-0.086	0.054	-0.148	-0.196	-0.203	0.106	0.129
dAZ	-0.065	0.037	-0.117	-0.038	0.013	-0.091	-0.016	-0.084
	We	Wd	Wf	TH	dTH			
Wd	-0.404							
Wf	0.806	0.215						
TH	0.157	-0.059	0.130					
dTH	-0.104	-0.139	-0.201	-0.015				
dAZ	-0.131	0.049	-0.109	0.154	-0.027			

MTB > RETRIEVE 'C:\MINITAB\QCI\MTW\SH3055.MTW'
 WORKSHEET SAVED 12/29/1995

*Unconfined Flow:
 Entrainment*

30° ≤ TH ≤ 55°

Subset Regression

Worksheet retrieved from file: C:\MINITAB\QCI\MTW\SH3055.MTW
 UH3055WT.LIS

MTB > Correlation '+dV' 'F+dV' 'FL' 'FWe' 'FWd' 'FWf' 'FsigV' 'L' 'We' 'Wd' 'Wf'
 > 'TH' 'dTH' 'dAZ'

	+dV	F+dV	FL	FWe	FWd	FWf	FsigV	L
F+dV	0.792							
FL	0.254	0.332						
FWe	0.438	0.631	0.181					
FWd	-0.240	-0.052	0.134	-0.101				
FWf	0.327	0.561	0.259	0.668	0.572			
FsigV	0.310	0.244	0.137	0.286	0.518	0.457		
L	0.223	0.235	0.906	0.184	0.245	0.269	0.139	
We	0.485	0.634	0.167	0.976	-0.525	0.425	0.110	0.219
Wd	-0.257	-0.107	0.000	-0.409	0.960	0.279	0.233	-0.039
Wf	0.322	0.521	0.230	0.614	0.588	0.962	0.466	0.249
TH	-0.123	-0.151	-0.009	0.223	-0.326	0.163	0.001	0.046
dTH	-0.243	-0.331	-0.352	-0.078	-0.093	-0.351	-0.023	-0.400
dAZ	-0.078	0.042	-0.096	-0.193	0.001	-0.162	-0.228	-0.116
	We	Wd	Wf	TH	dTH			
Wd	-0.731							
Wf	0.392	0.342						
TH	0.410	-0.297	0.164					
dTH	-0.031	-0.188	-0.317	0.269				
dAZ	-0.253	0.162	-0.130	-0.164	0.201			

MTB > RETRIEVE 'C:\MINITAB\QCI\MTW\CFHGS.MTW'
 WORKSHEET SAVED 12/29/1995

Confined Flow: 10° STH
Entrainment
Subset Regression

Worksheet retrieved from file: C:\MINITAB\QCI\MTW\CFHGS.MTW

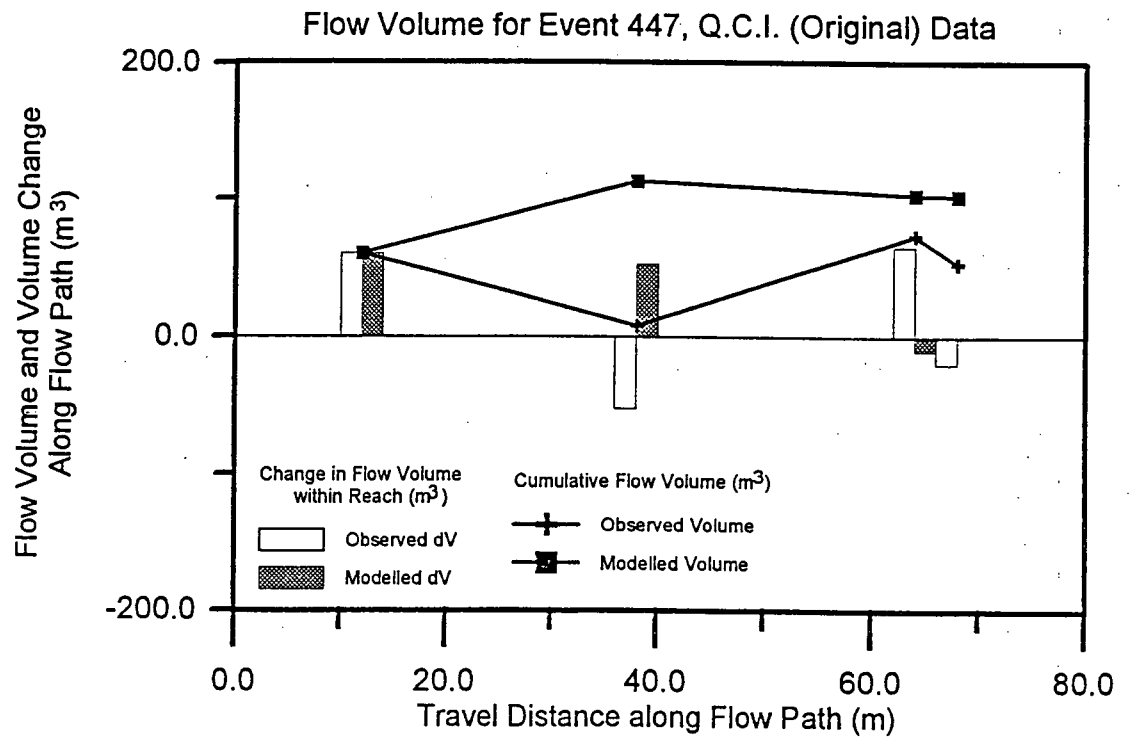
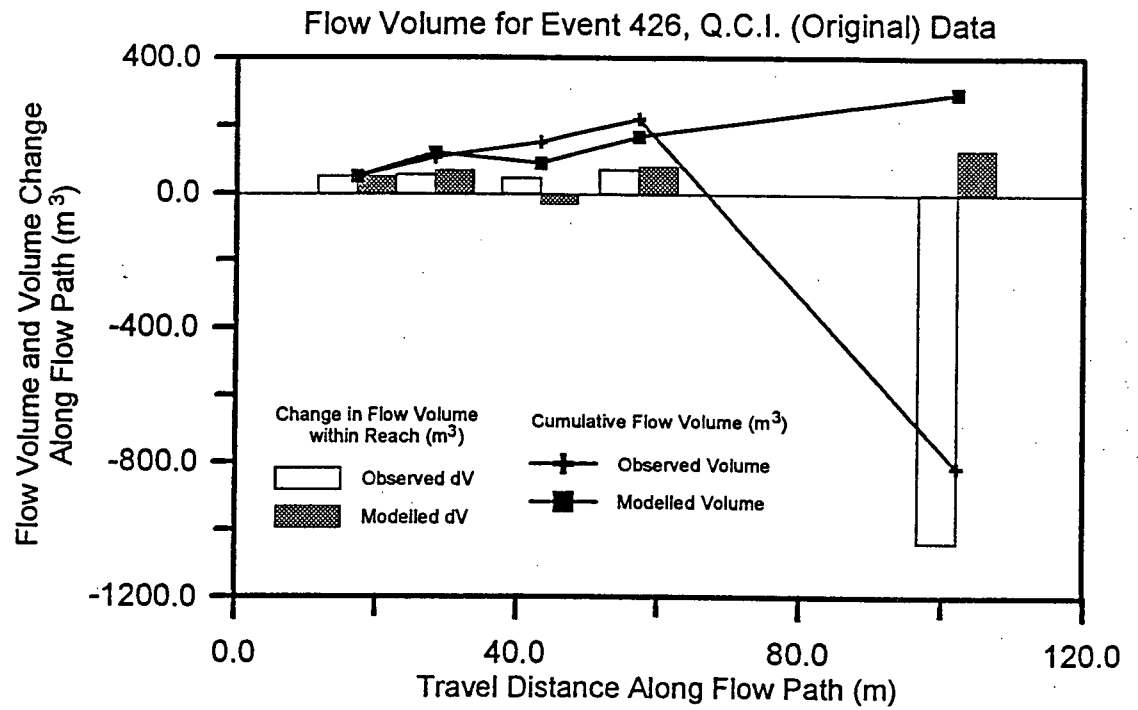
MTB > CORRELATION '+dV' 'F+dV' 'FL' 'FWe' 'FWd' 'FWf' 'FsigV' 'L' 'We'
 'Wf' 'TH'
 > 'dTH' 'dAZ' 'BAF'

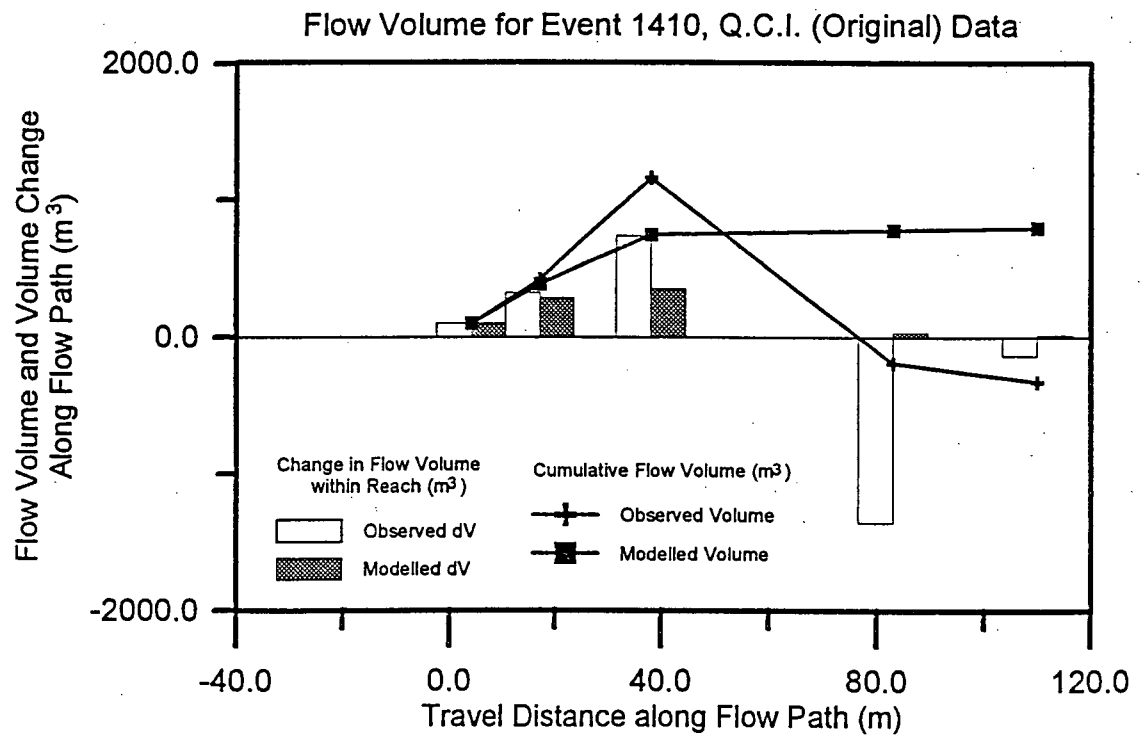
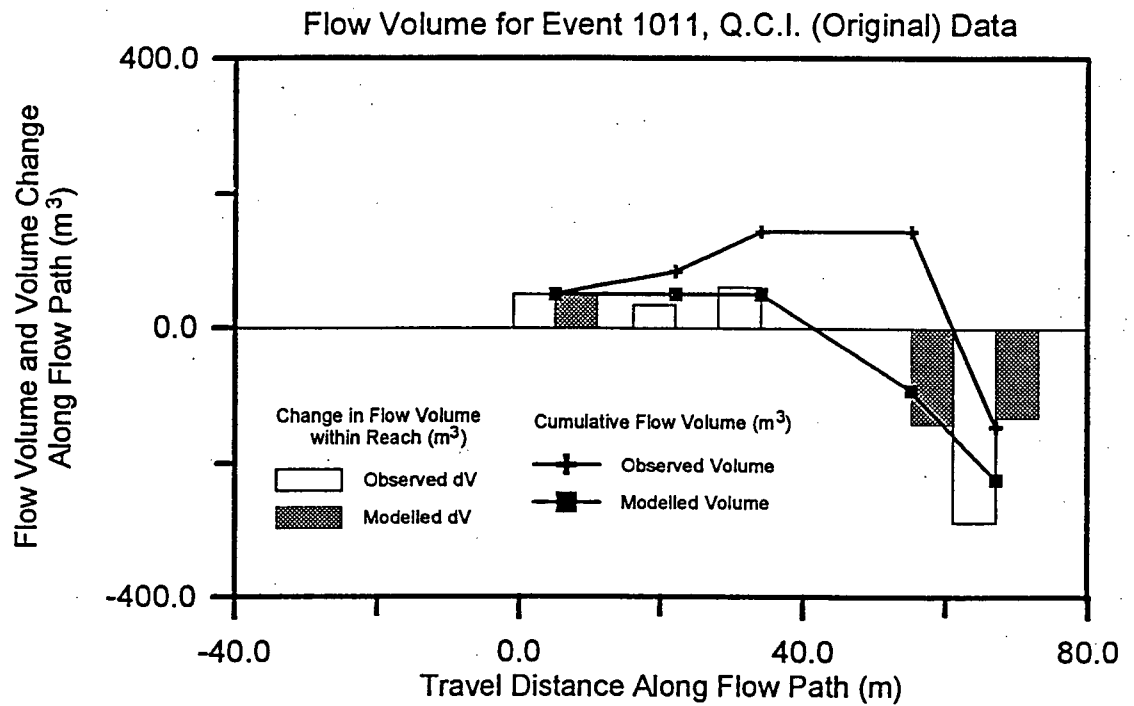
	+dV	F+dV	FL	FWe	FWd	FWf	FsigV
L							
F+dV	0.888						
FL	0.480	0.468					
FWe	0.472	0.552	0.041				
FWd	-0.118	-0.141	-0.049	-0.185			
FWf	0.370	0.403	0.058	0.693	0.647		
FsigV	0.099	0.084	0.205	0.041	0.469	0.223	
L	0.582	0.480	0.920	0.074	-0.116	0.096	0.126
We	0.483	0.530	0.059	0.952	-0.119	0.702	0.082
0.081							
Wf	0.355	0.378	0.091	0.635	0.632	0.946	0.251
0.111							
TH	-0.074	-0.047	-0.163	0.108	-0.302	-0.170	-0.471
-0.151							
dTH	-0.109	0.041	-0.093	0.114	-0.297	-0.003	-0.066
-0.131							
dAZ	0.050	0.075	-0.034	0.110	0.120	0.097	0.115
-0.024							
BAF	0.103	0.052	0.046	0.014	0.117	0.074	0.339
0.039							
	We	Wf	TH	dTH	dAZ		
Wf	0.686						
TH	0.097	-0.182					
dTH	0.046	-0.068	0.410				
dAZ	0.109	0.145	-0.053	-0.002			
BAF	0.045	0.032	0.088	0.202	-0.340		

Appendix D

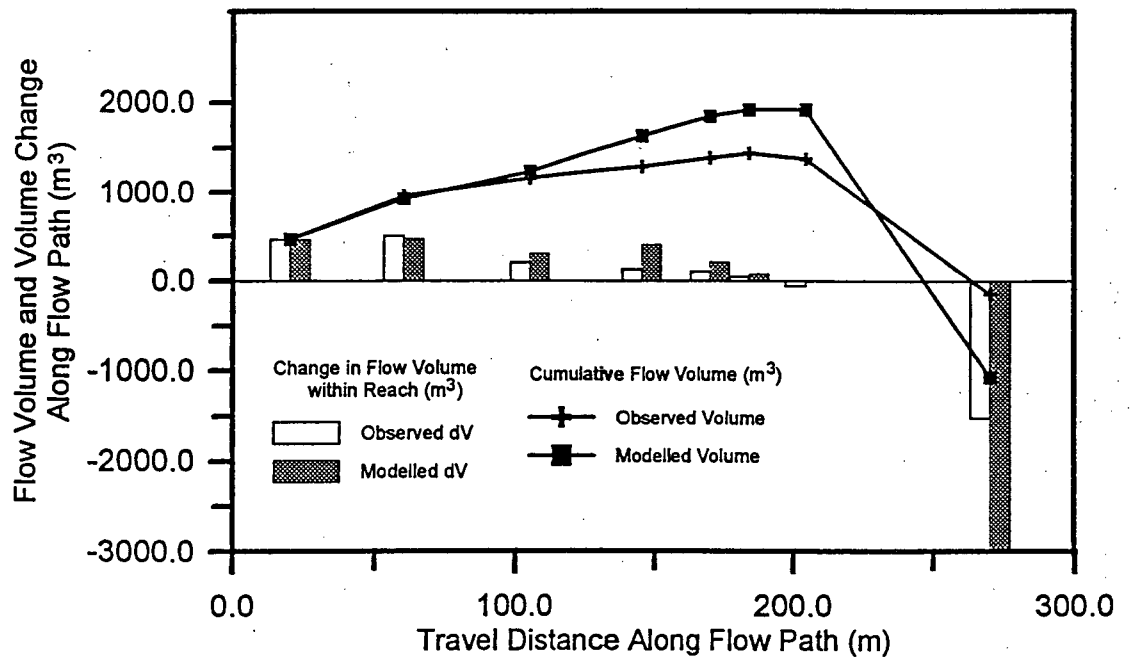
Results of Back-Analyses

- Type 7 Events - Volume Plots
- Supplementary Events - Volume Plots
- Tabulated Input Data - Type 7 Events
- Tabulated Results -
Type 7 Events and Supplementary Events

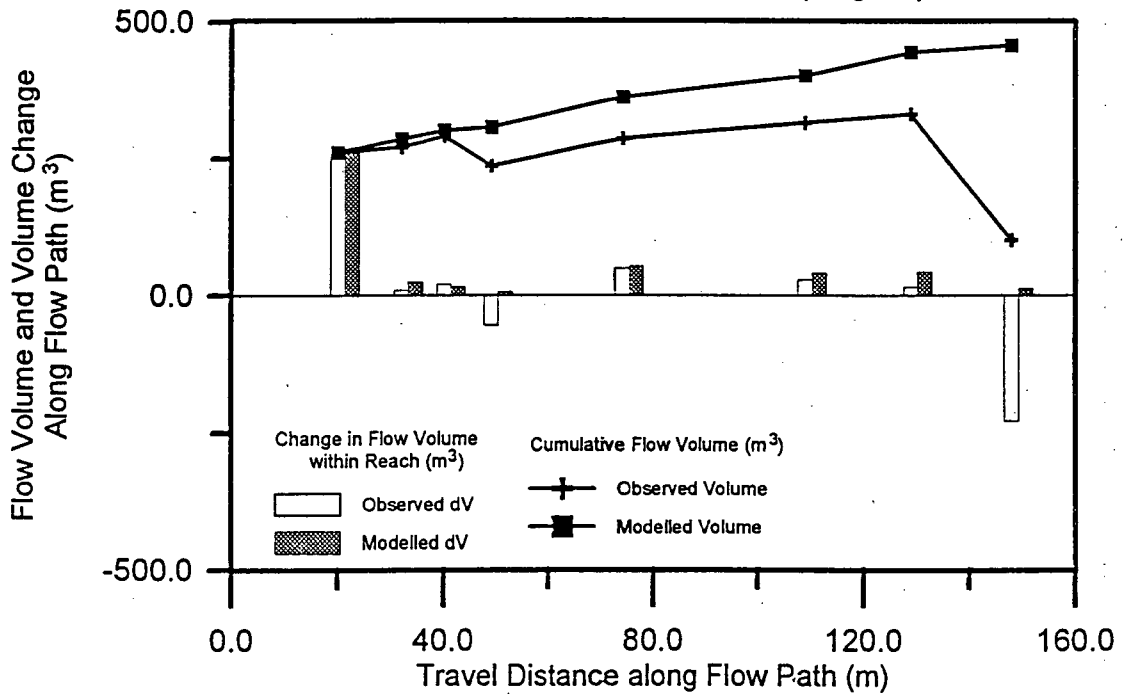


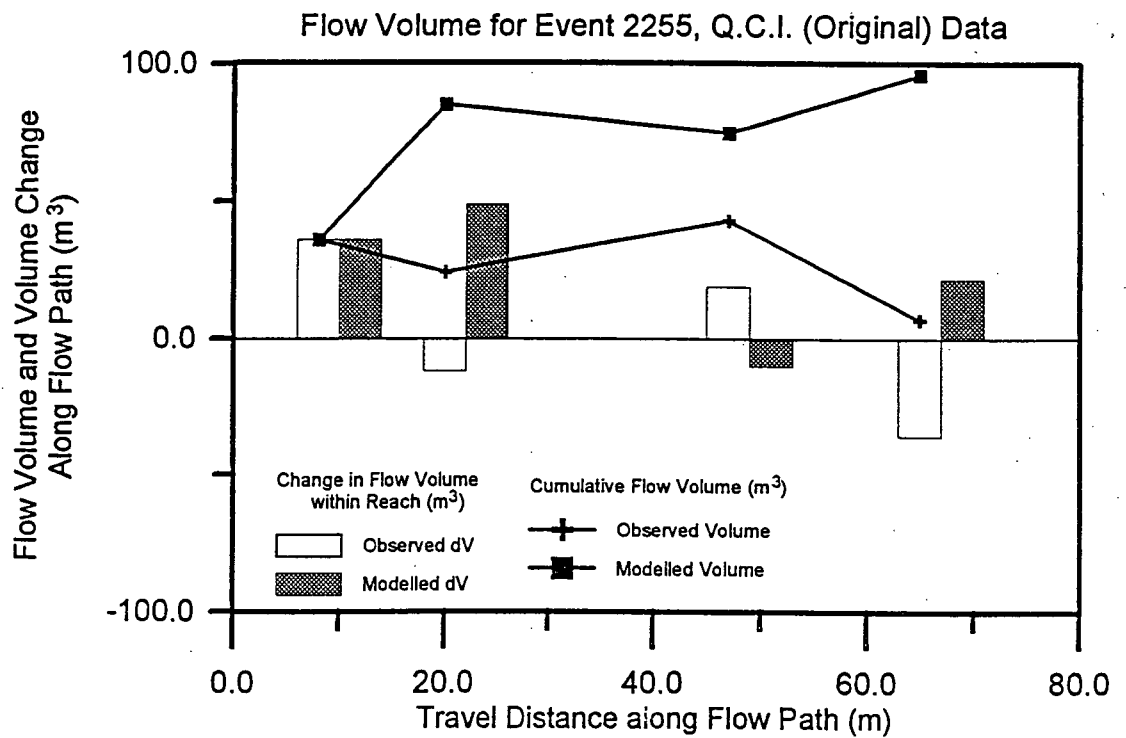
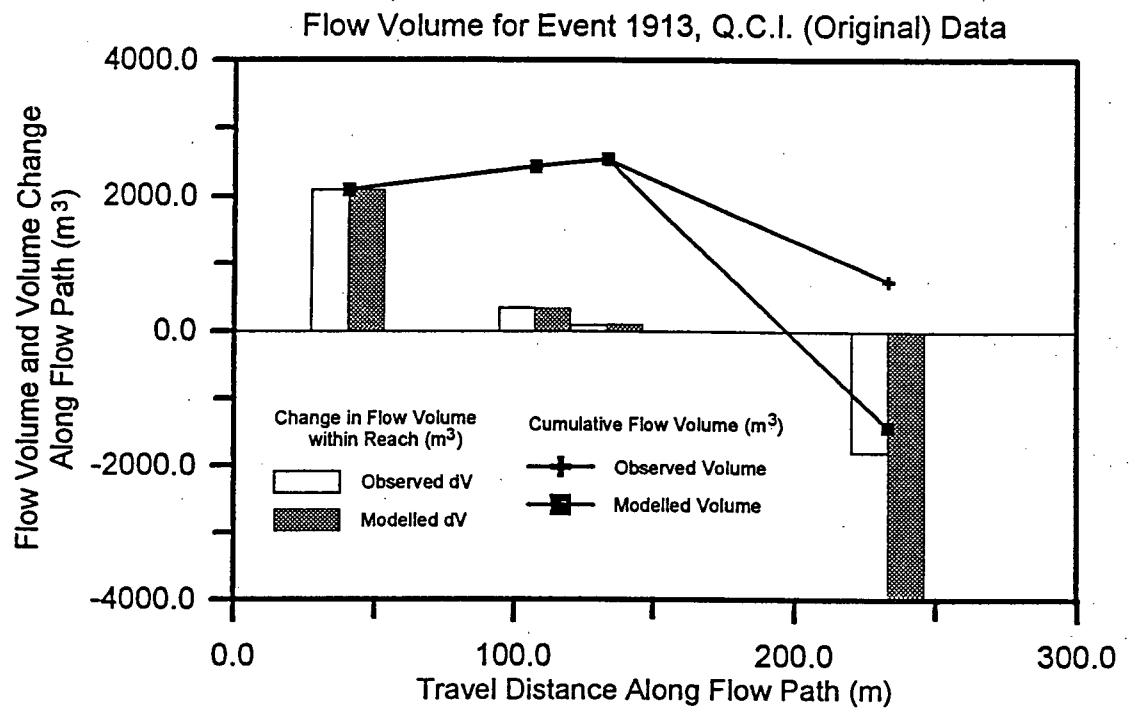


Flow Volume for Event 1417, Q.C.I. (Original) Data

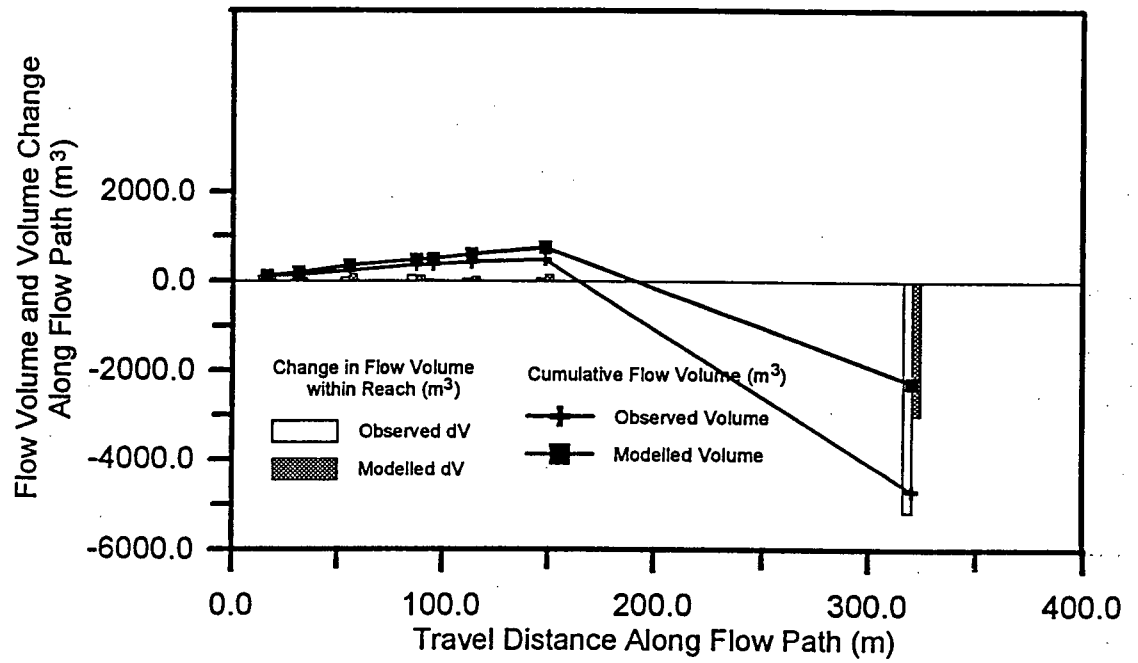


Flow Volume for Event 1804, Q.C.I. (Original) Data

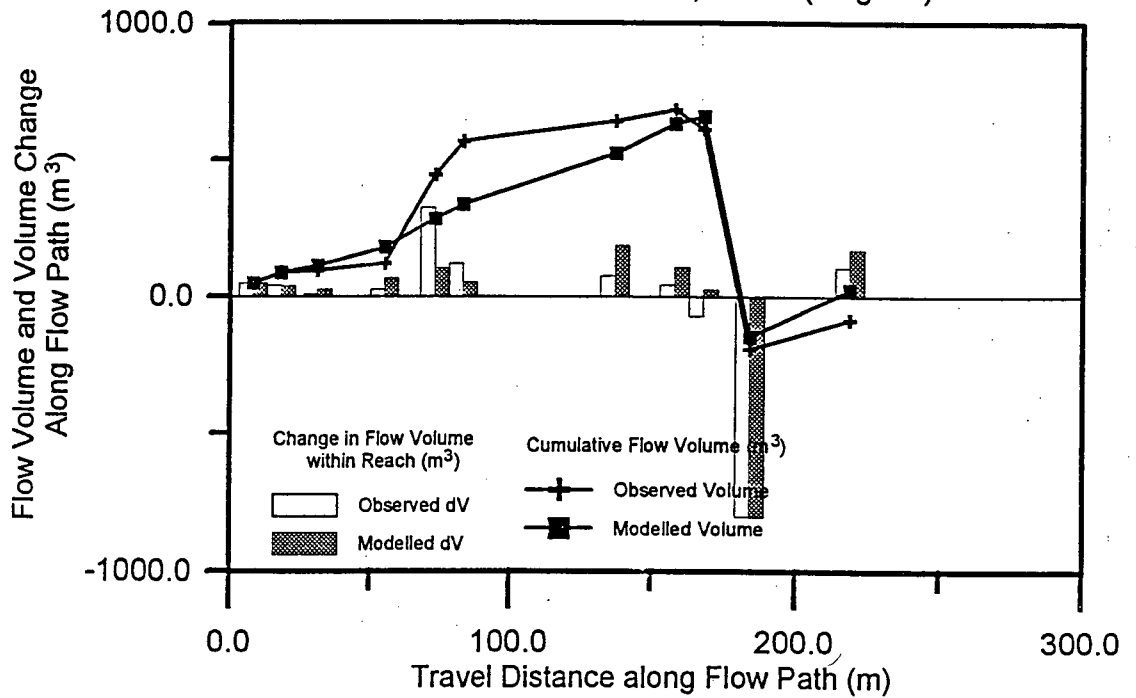


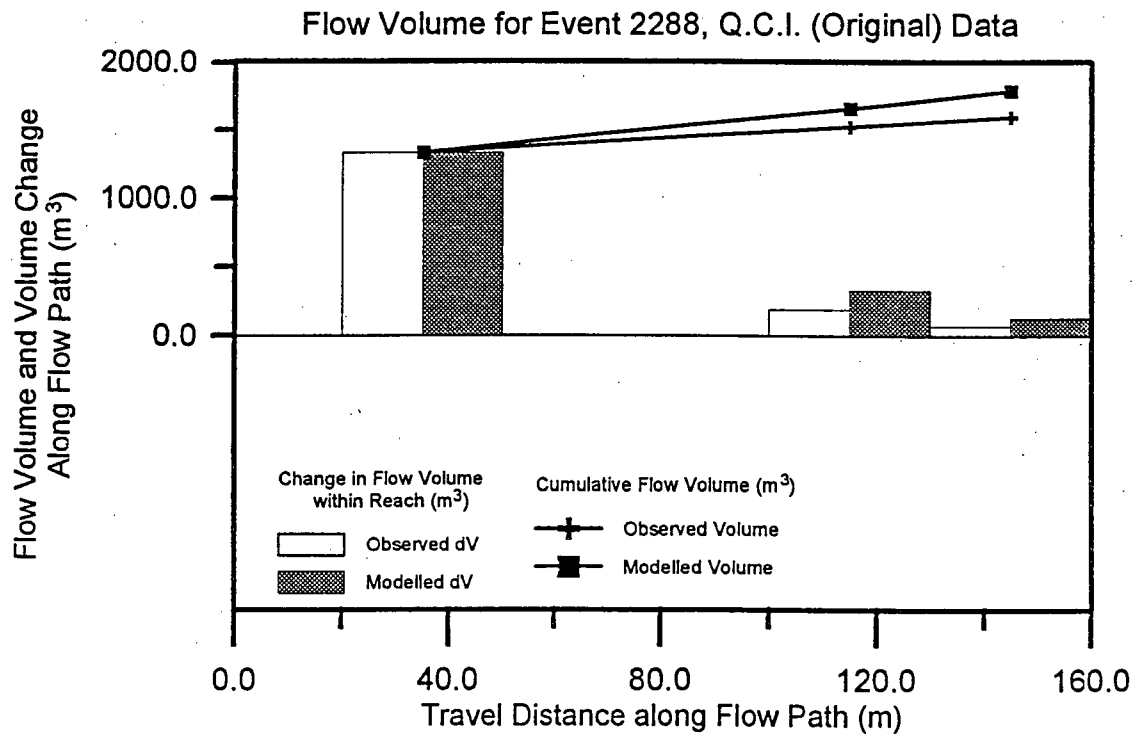
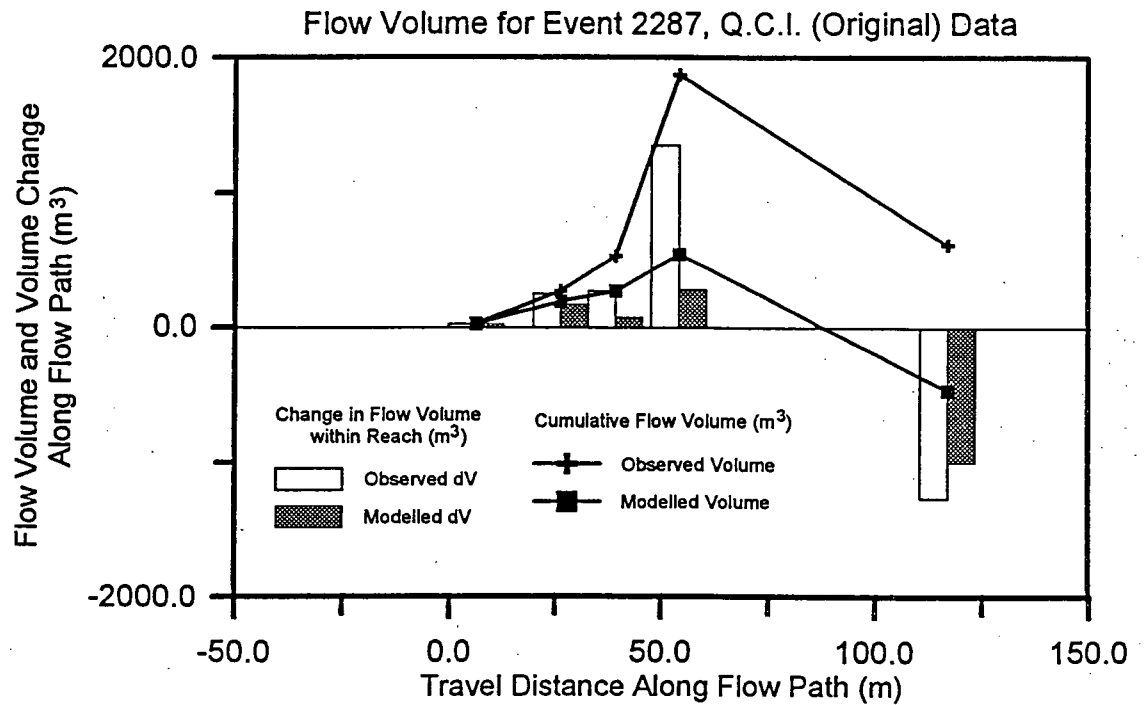


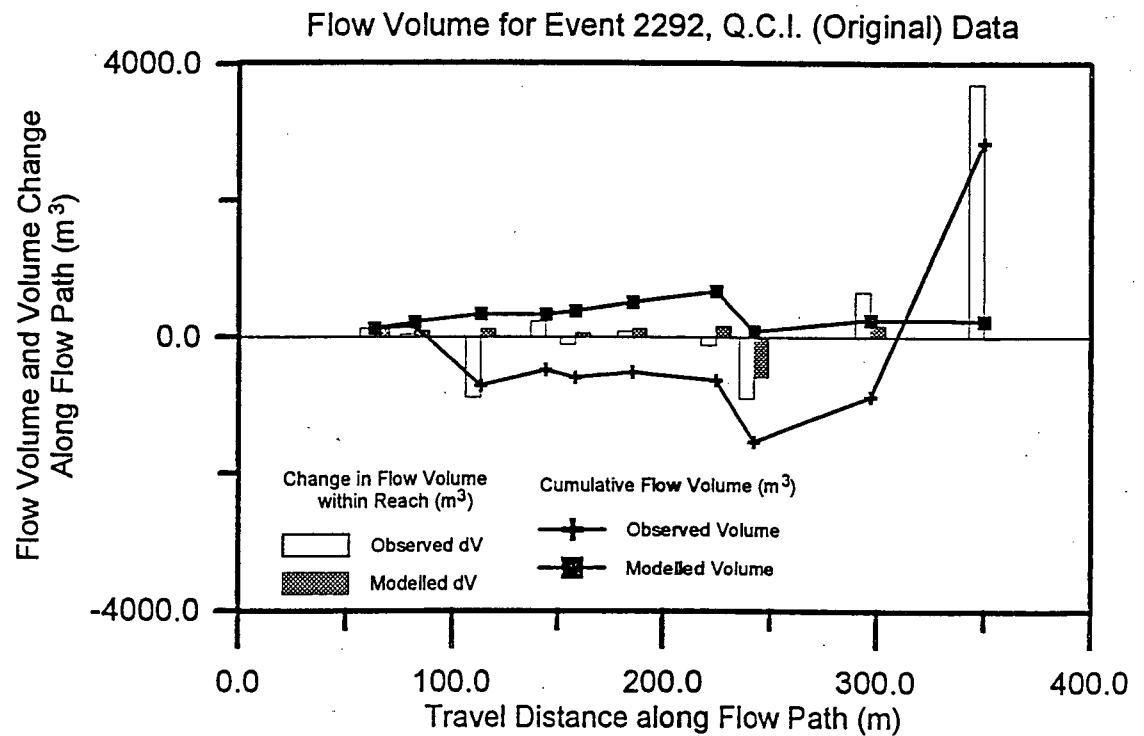
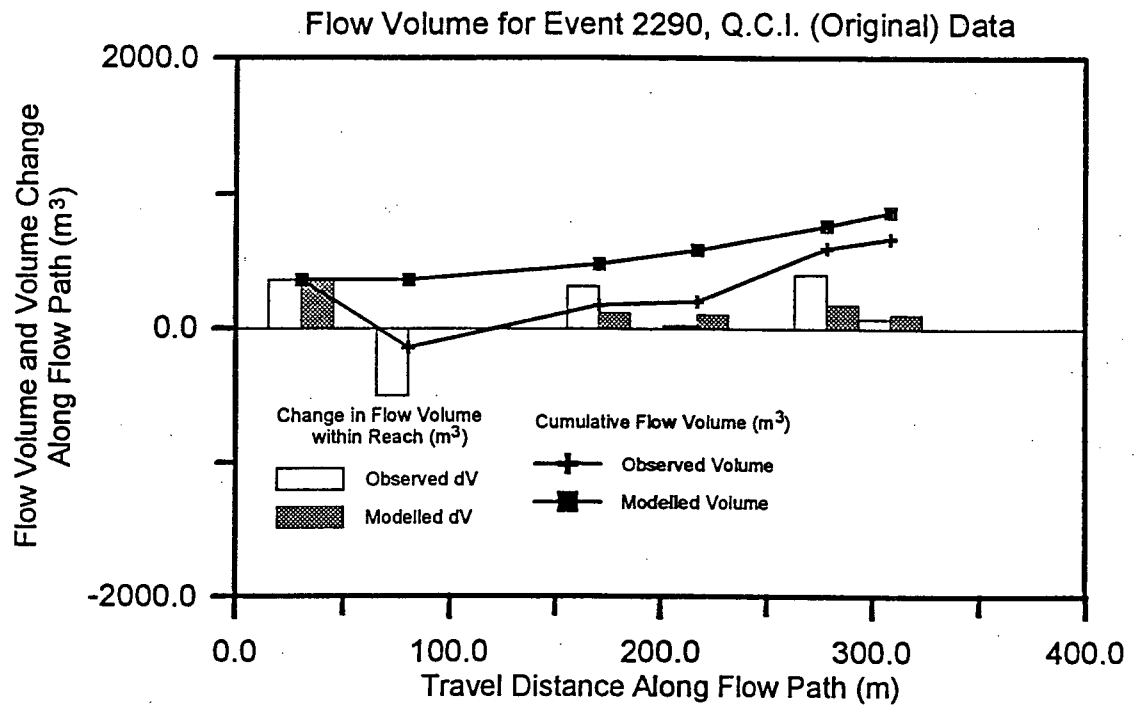
Flow Volume for Event 2259, Q.C.I. (Original) Data

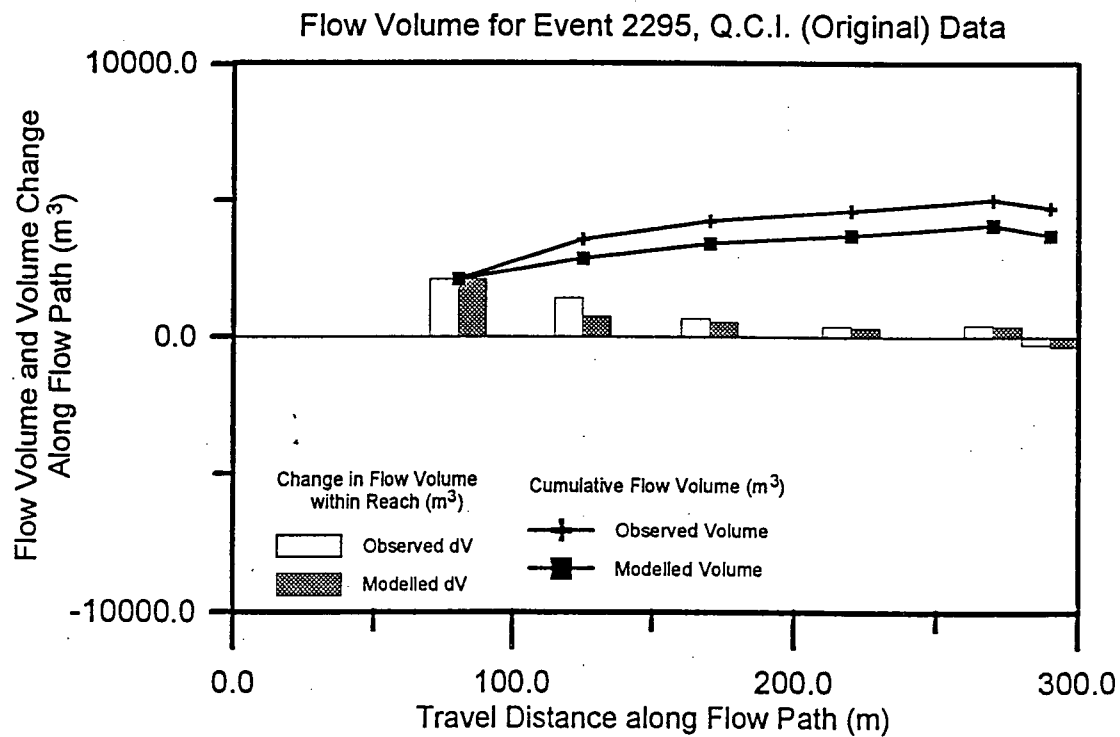
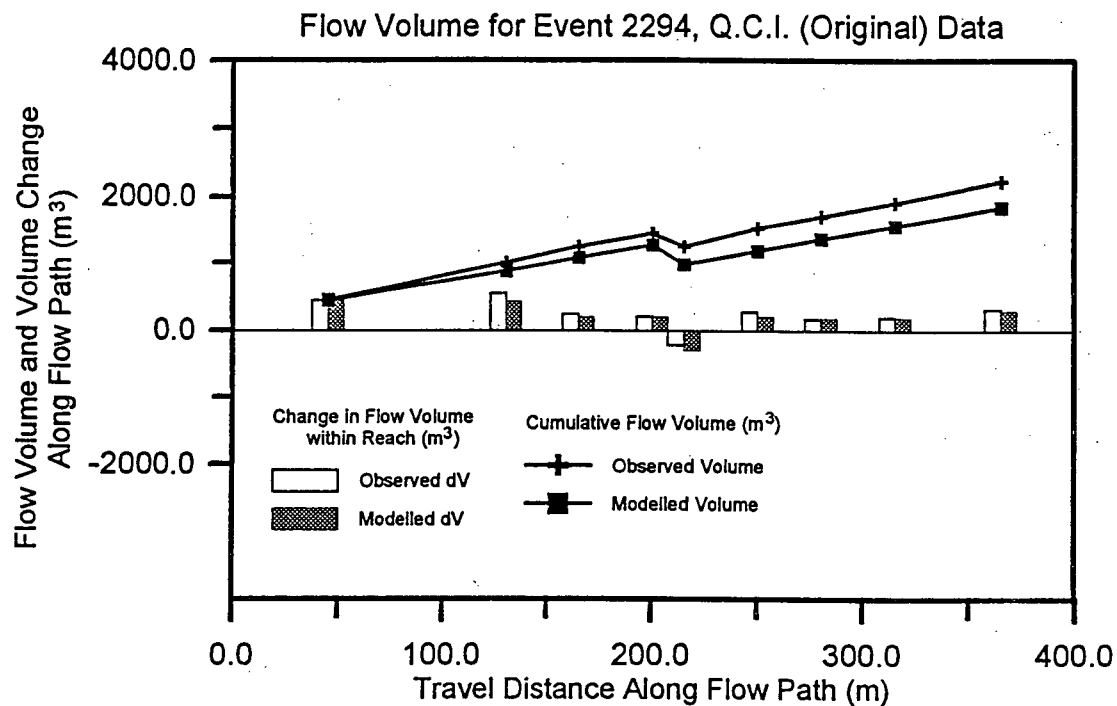


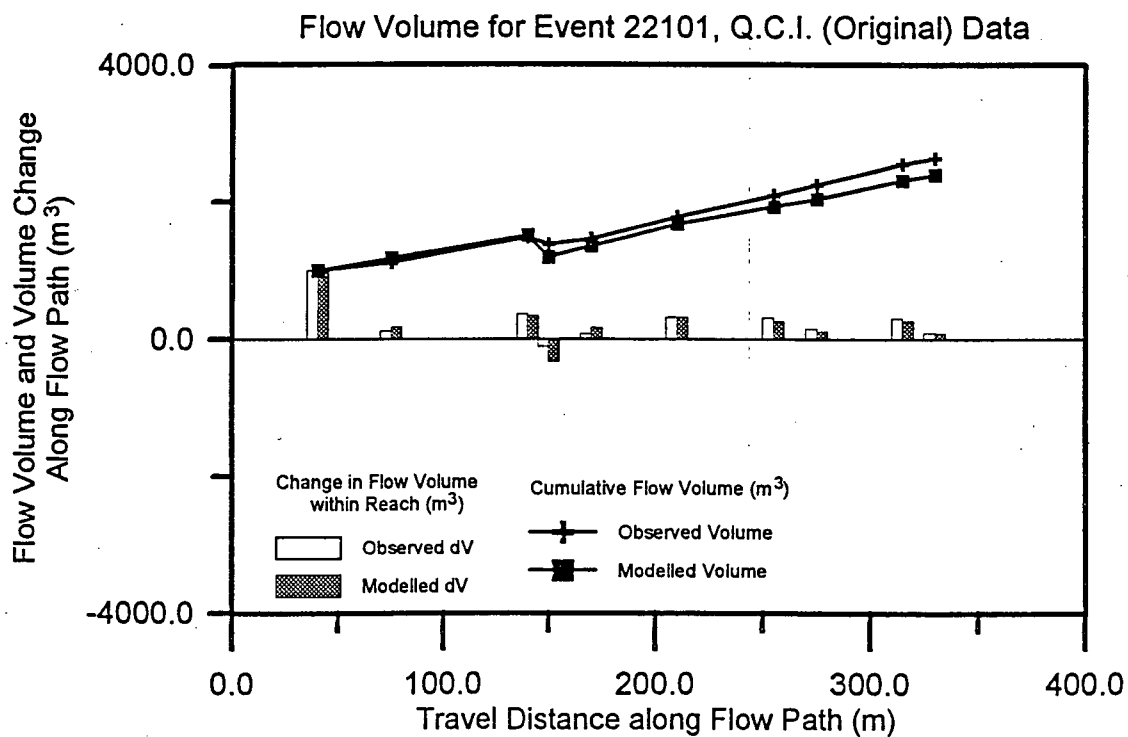
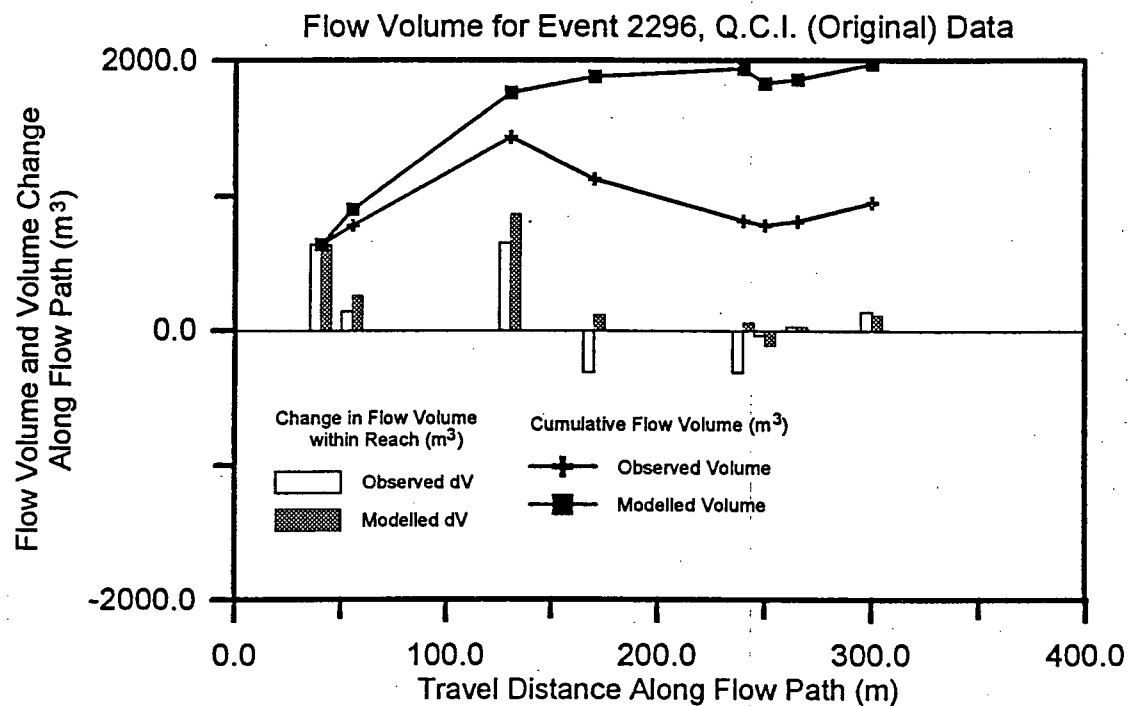
Flow Volume for Event 2274, Q.C.I. (Original) Data

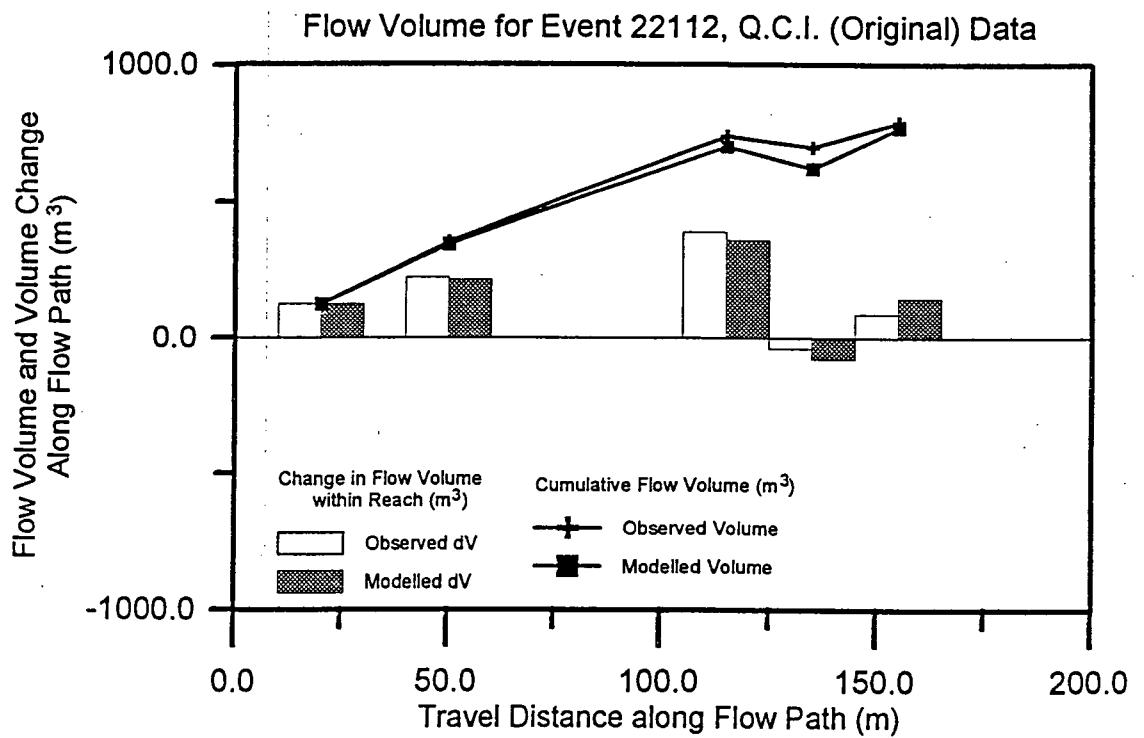
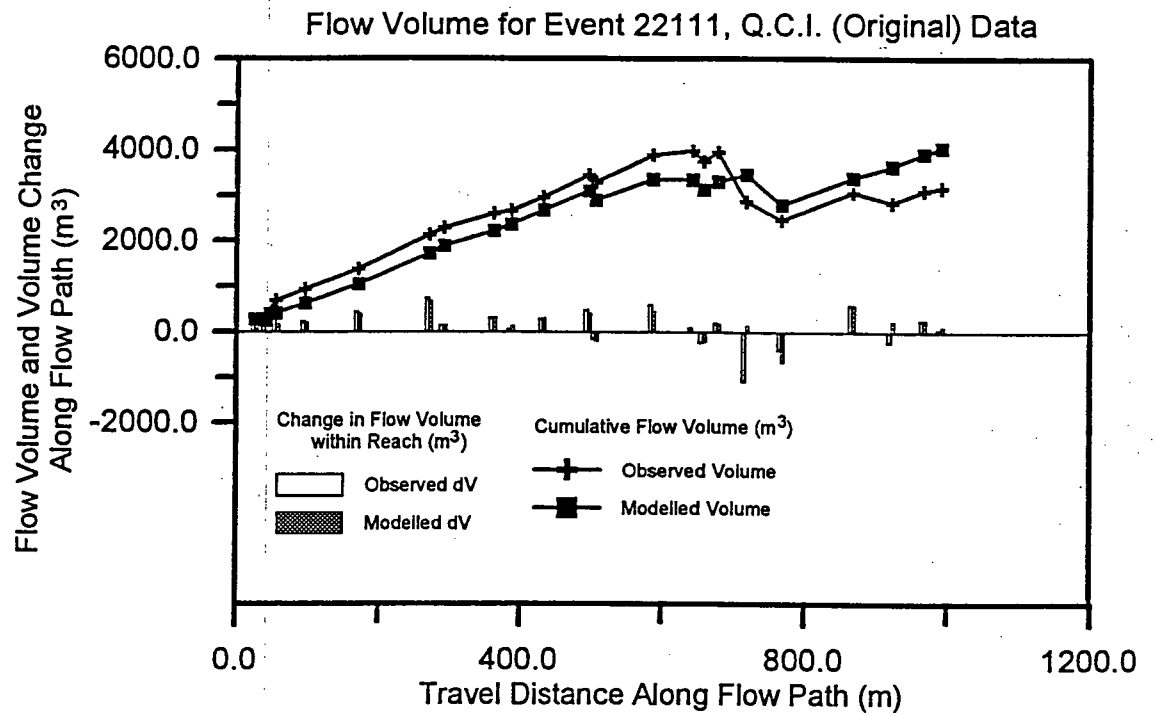


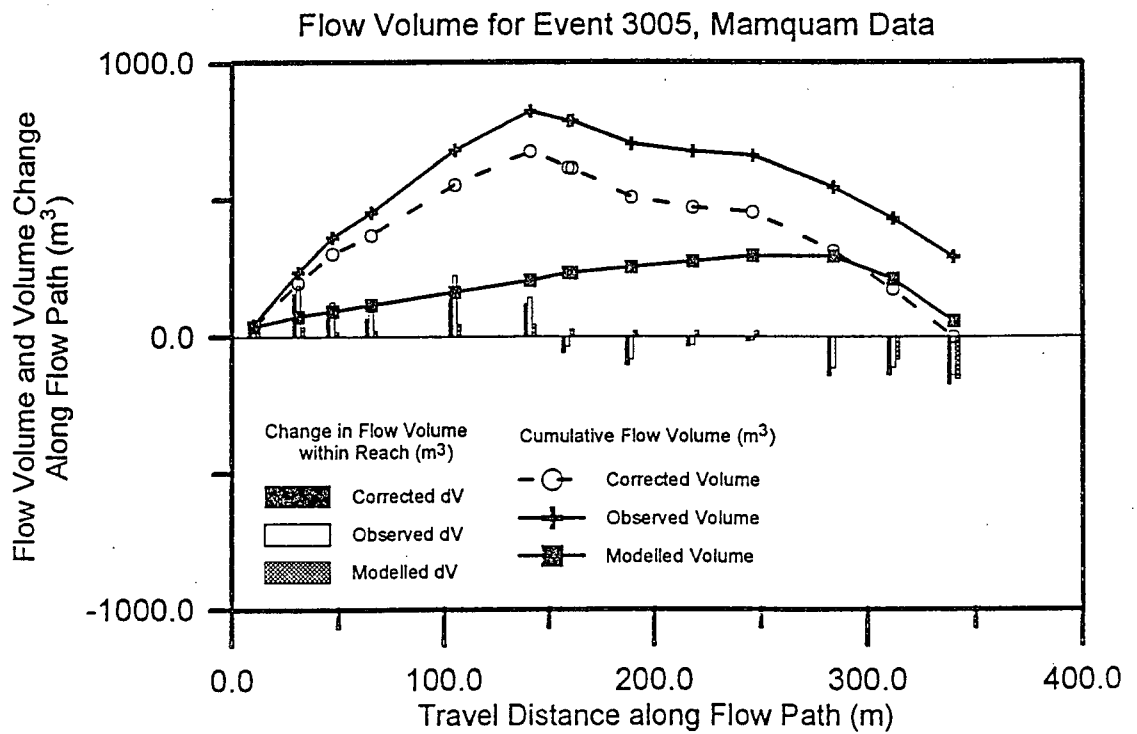
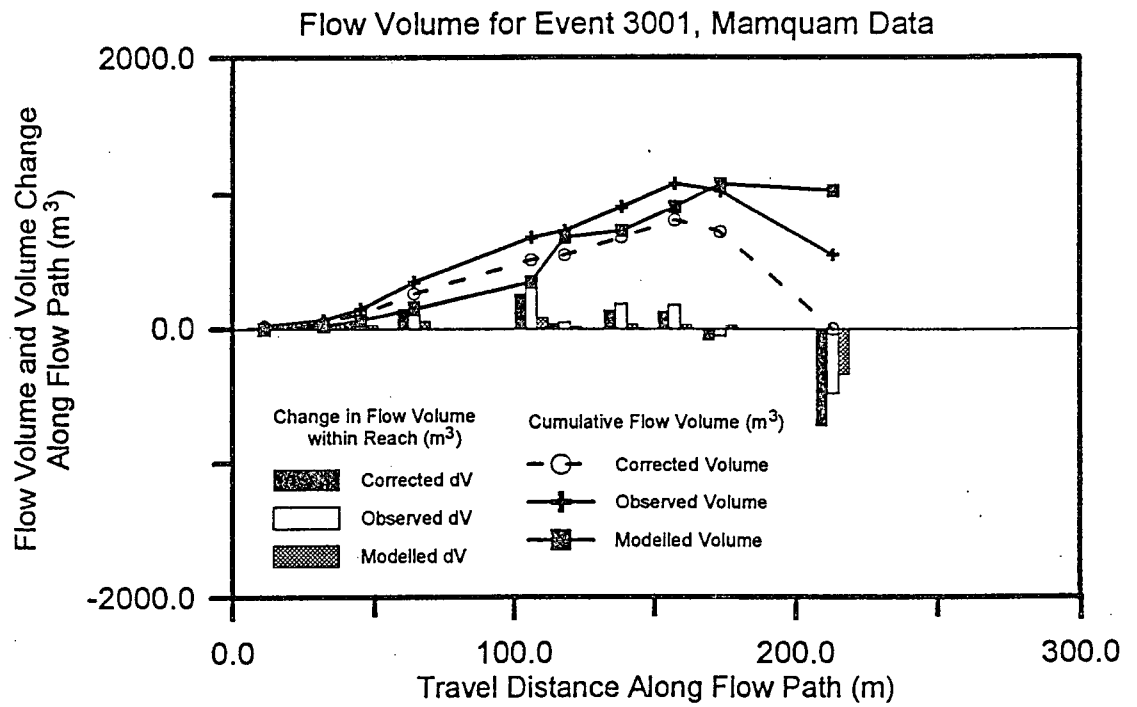


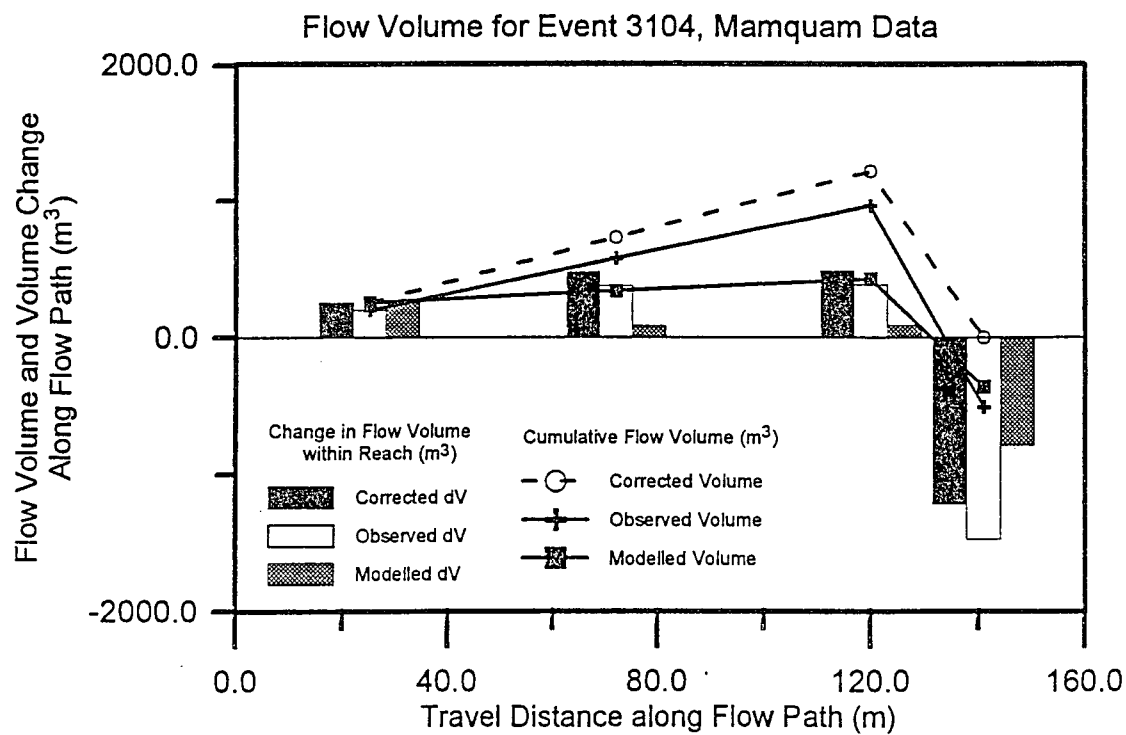
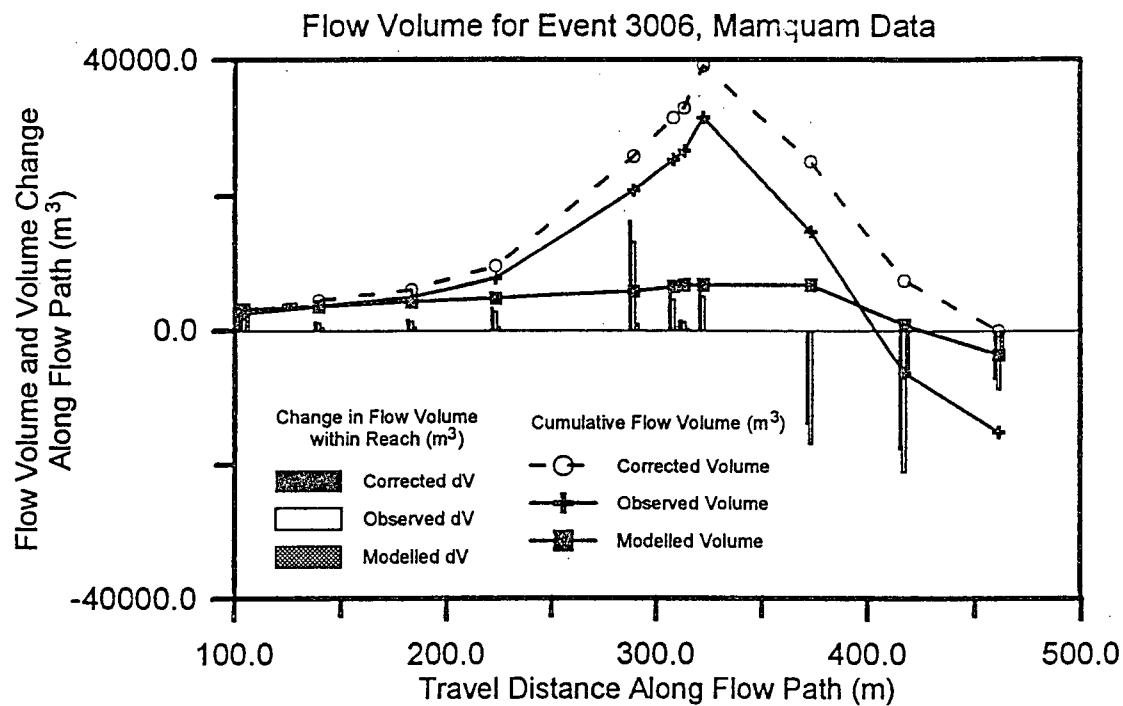


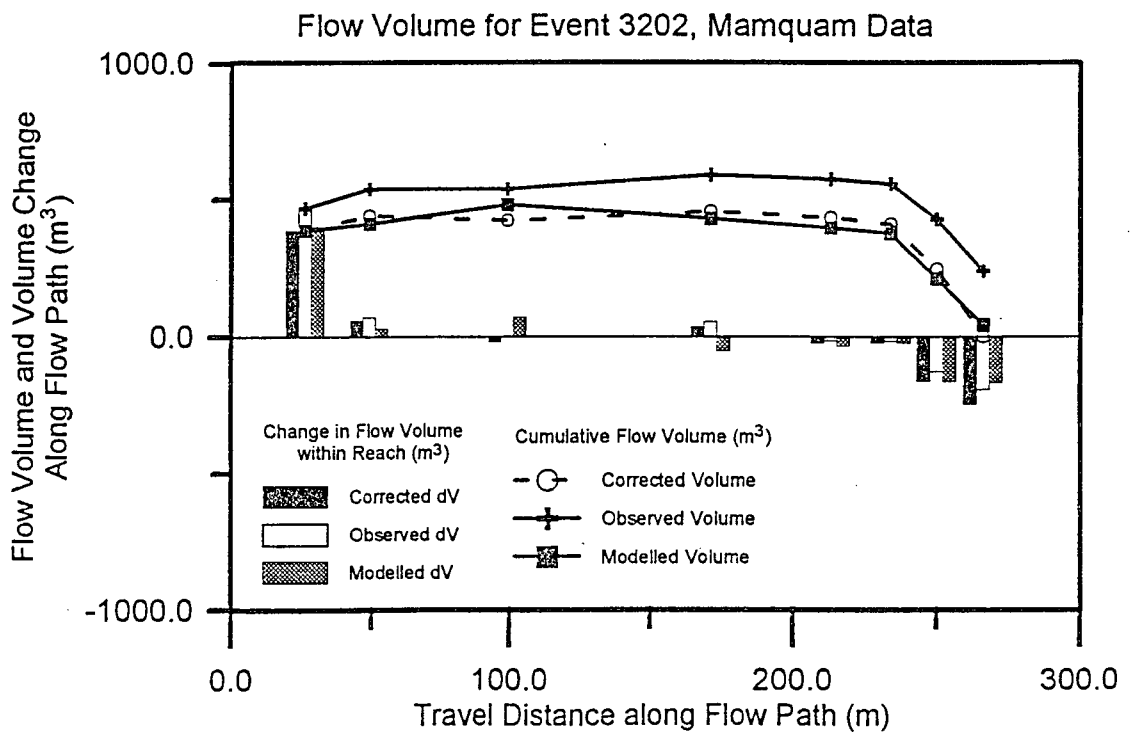
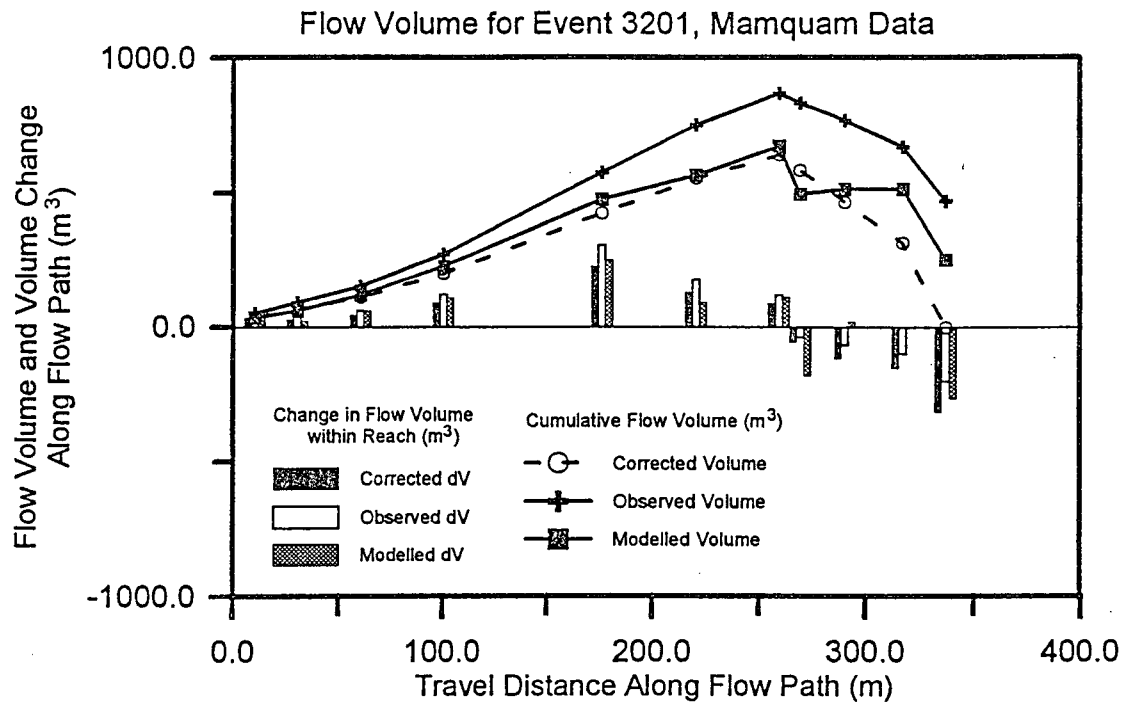


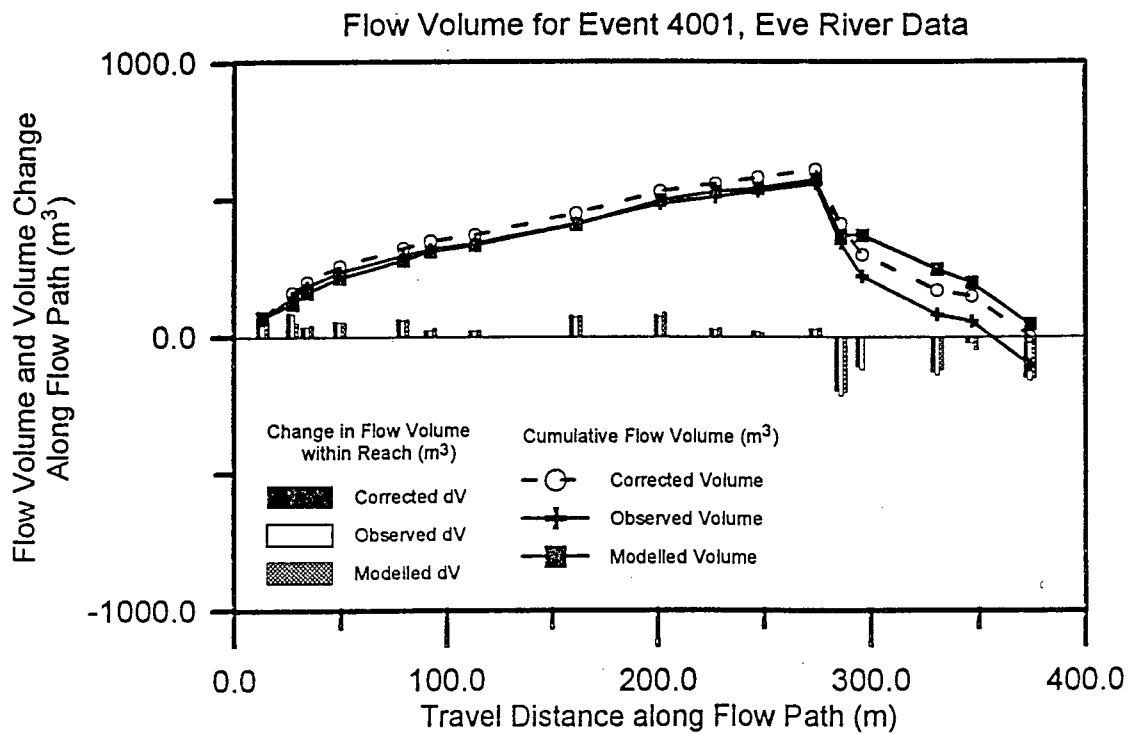
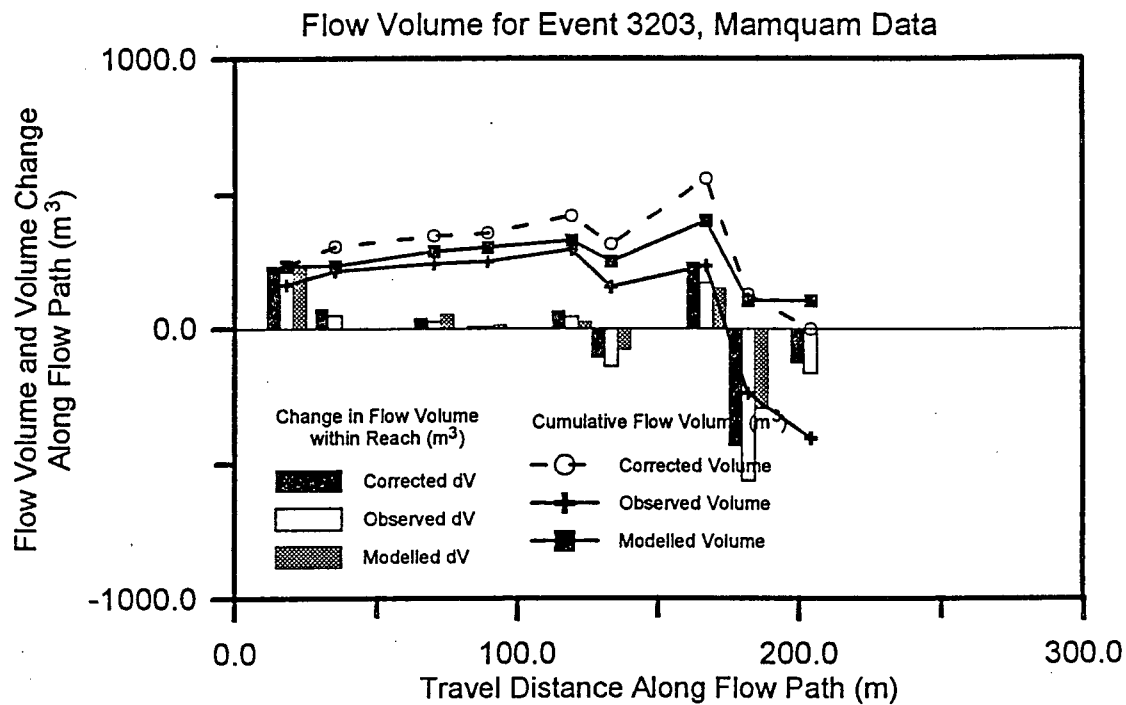


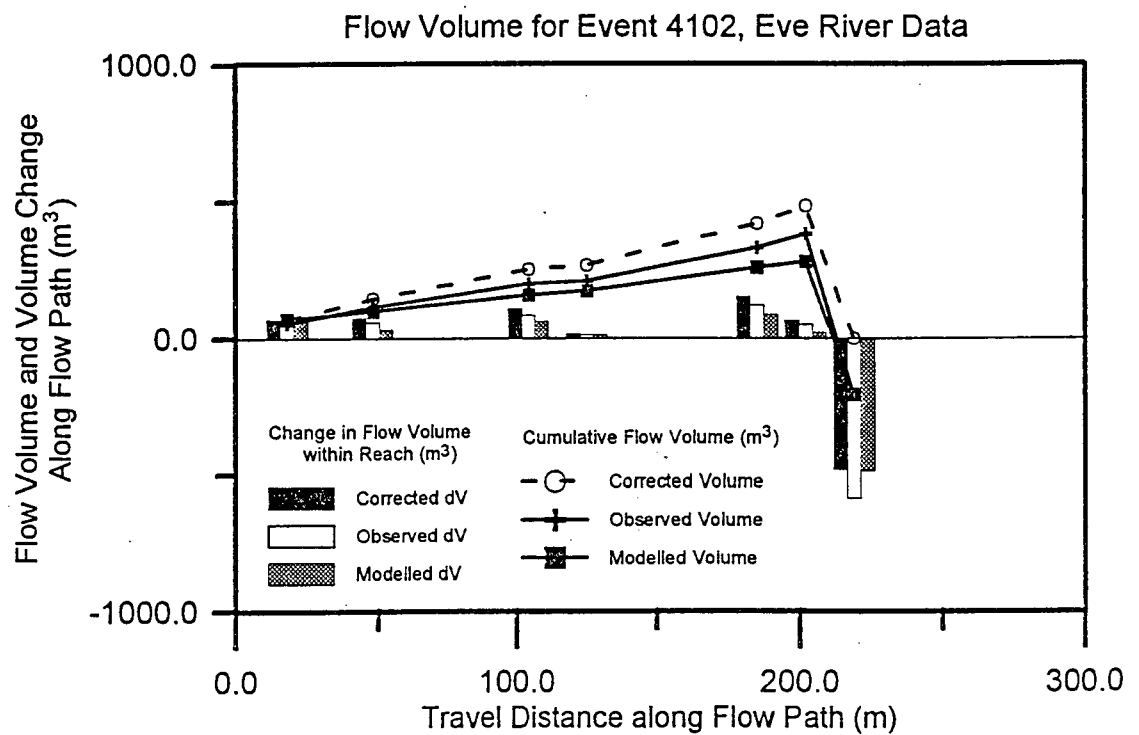
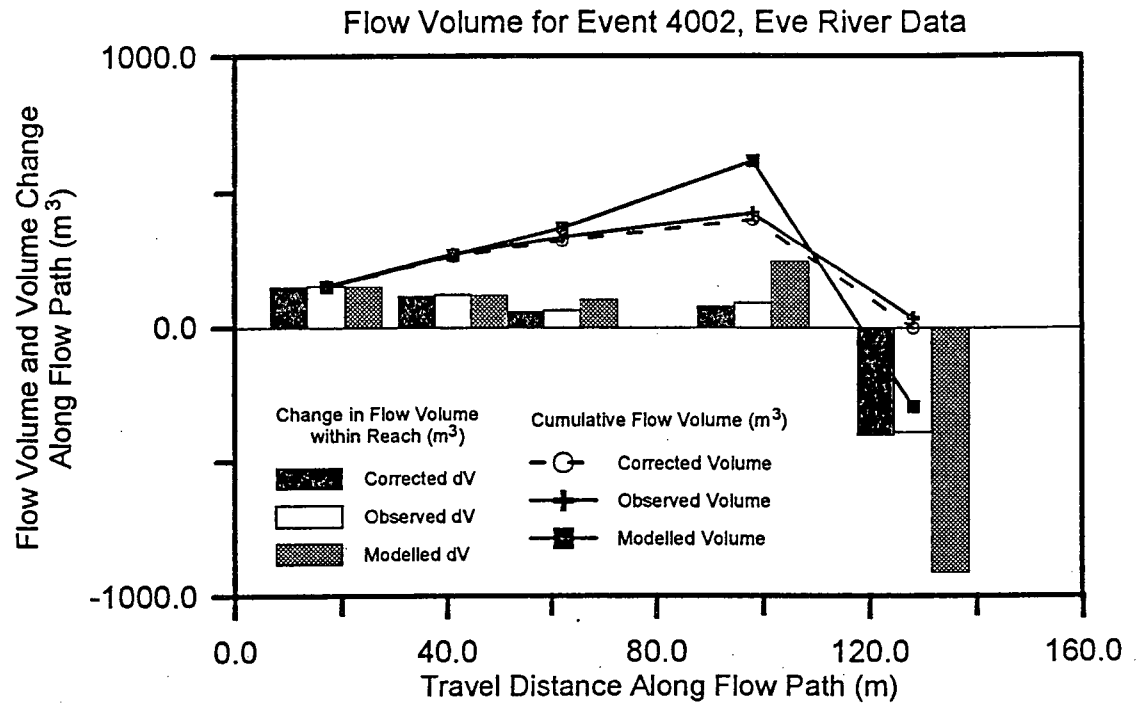


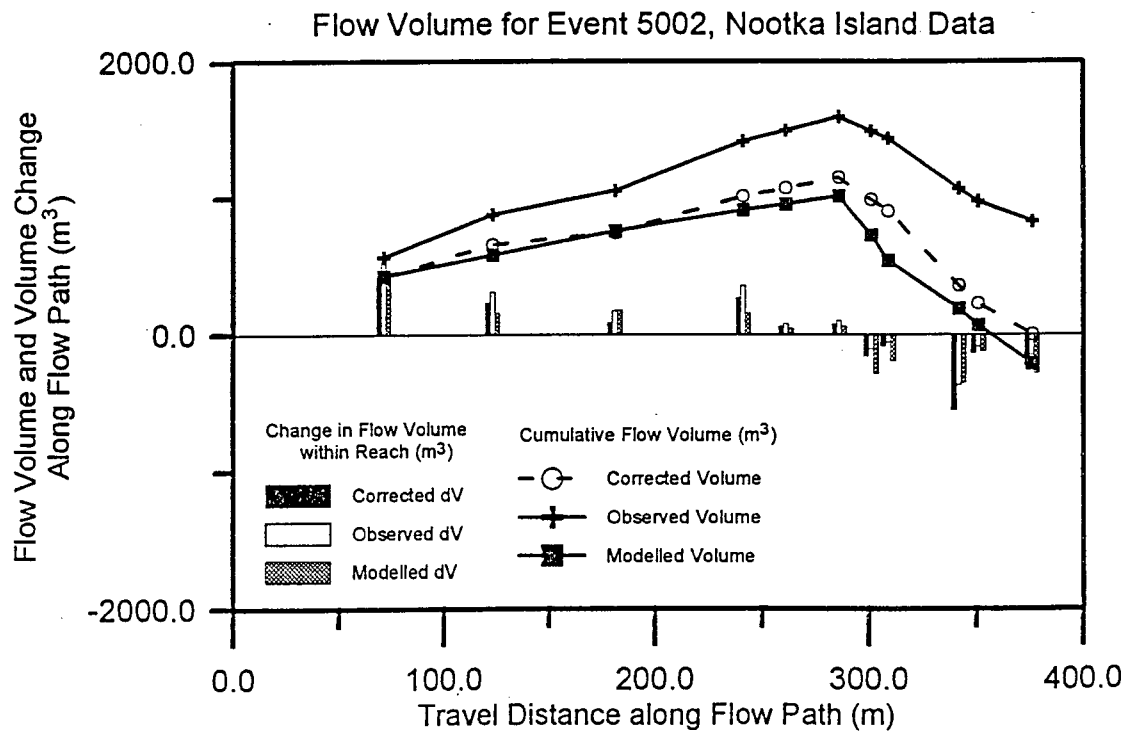
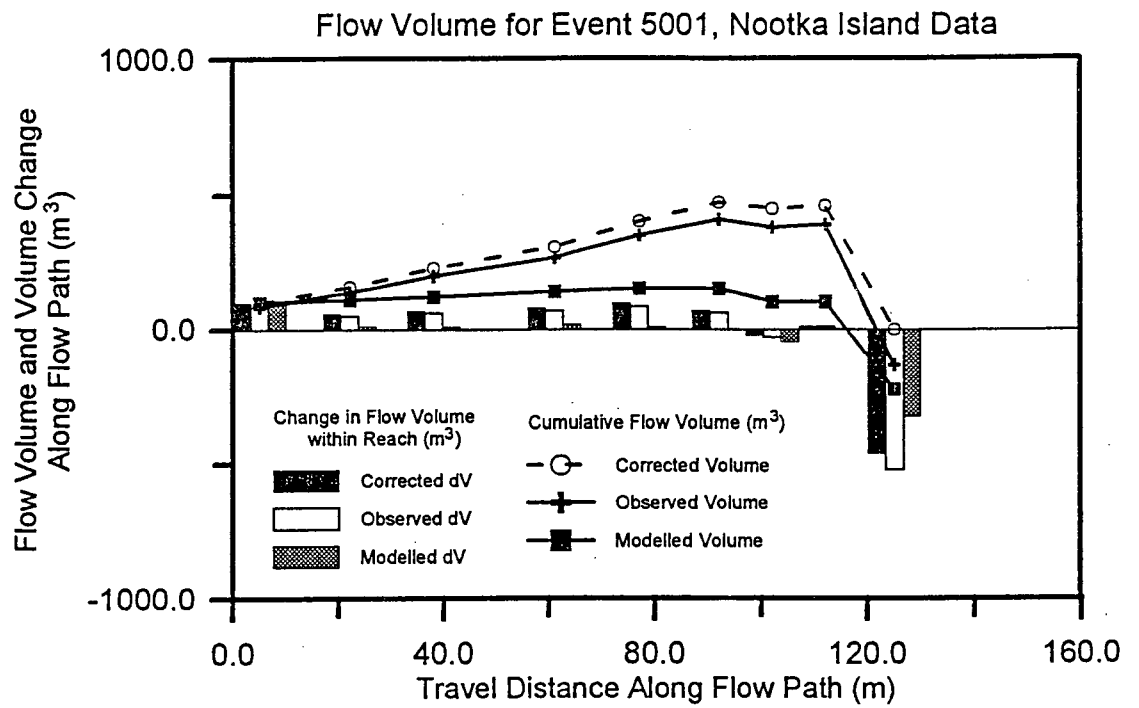


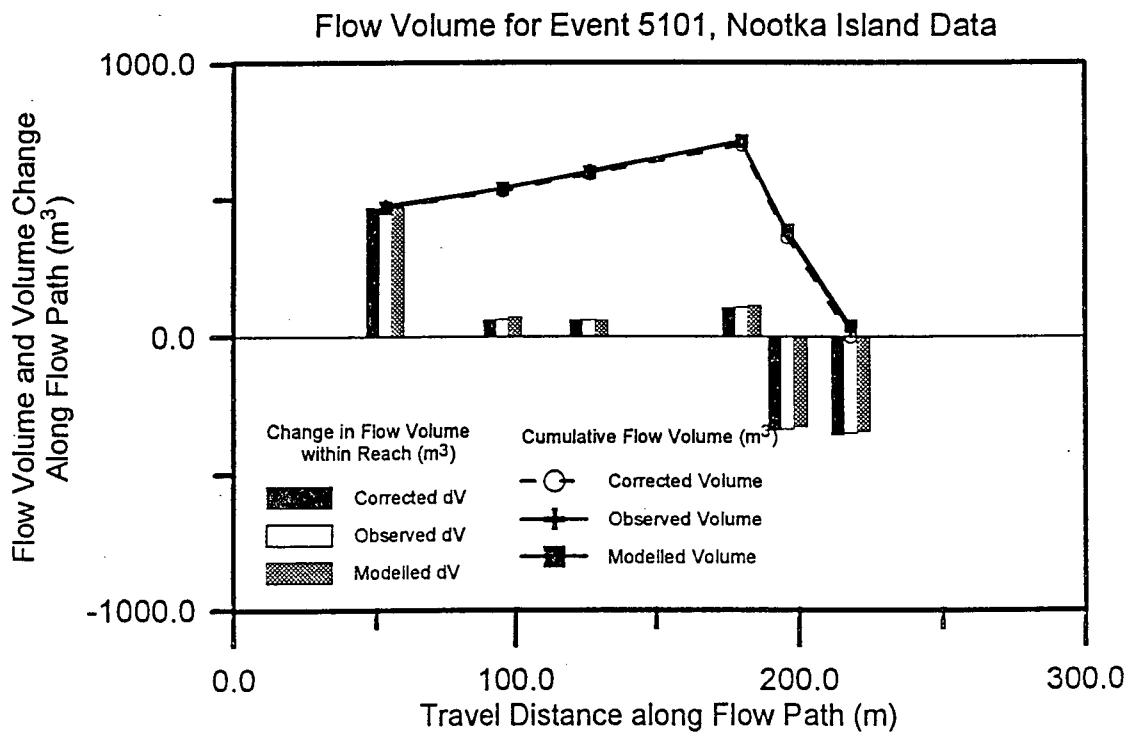
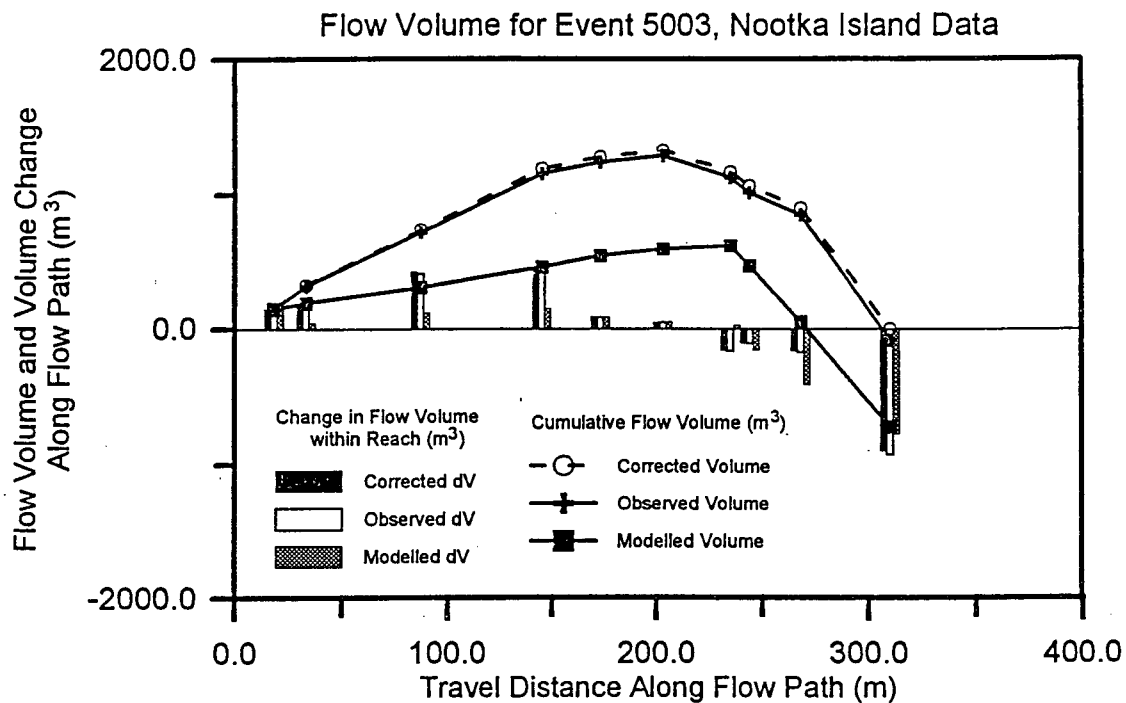


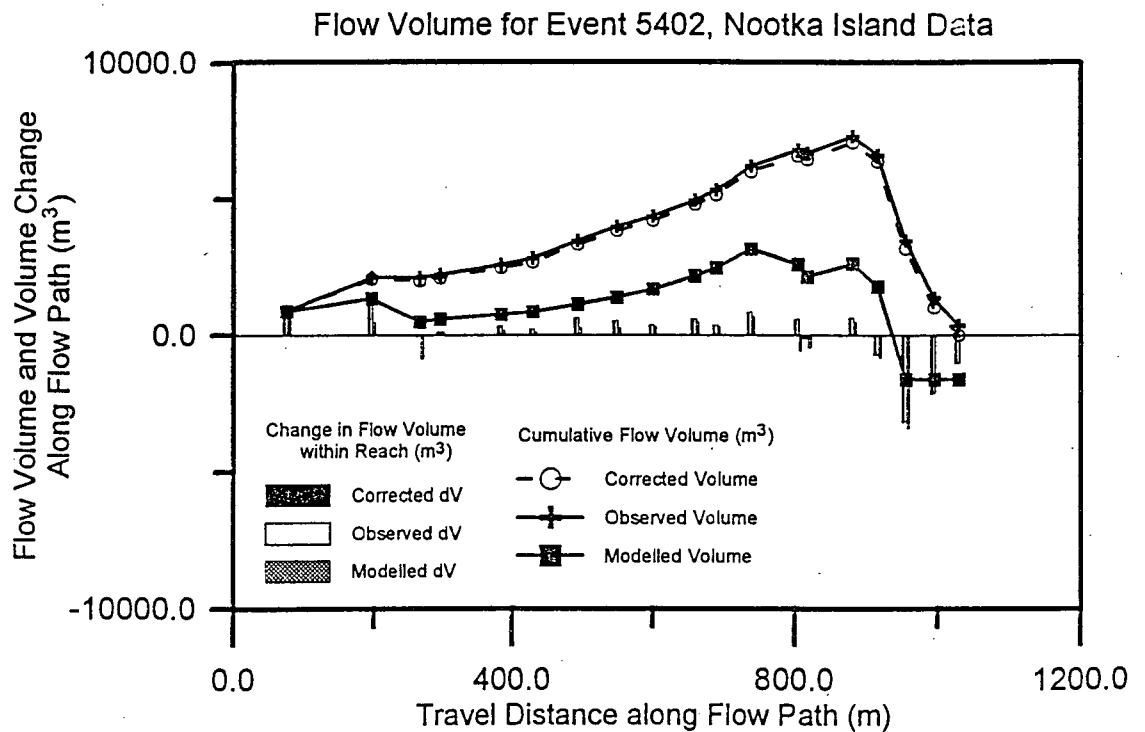
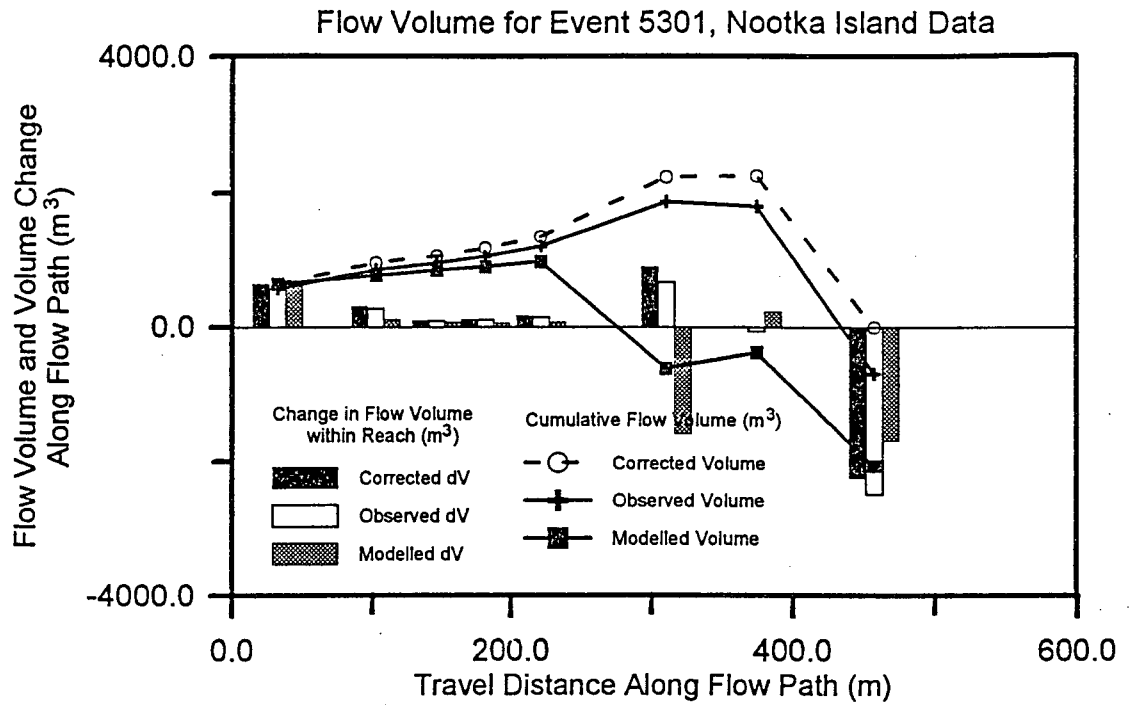


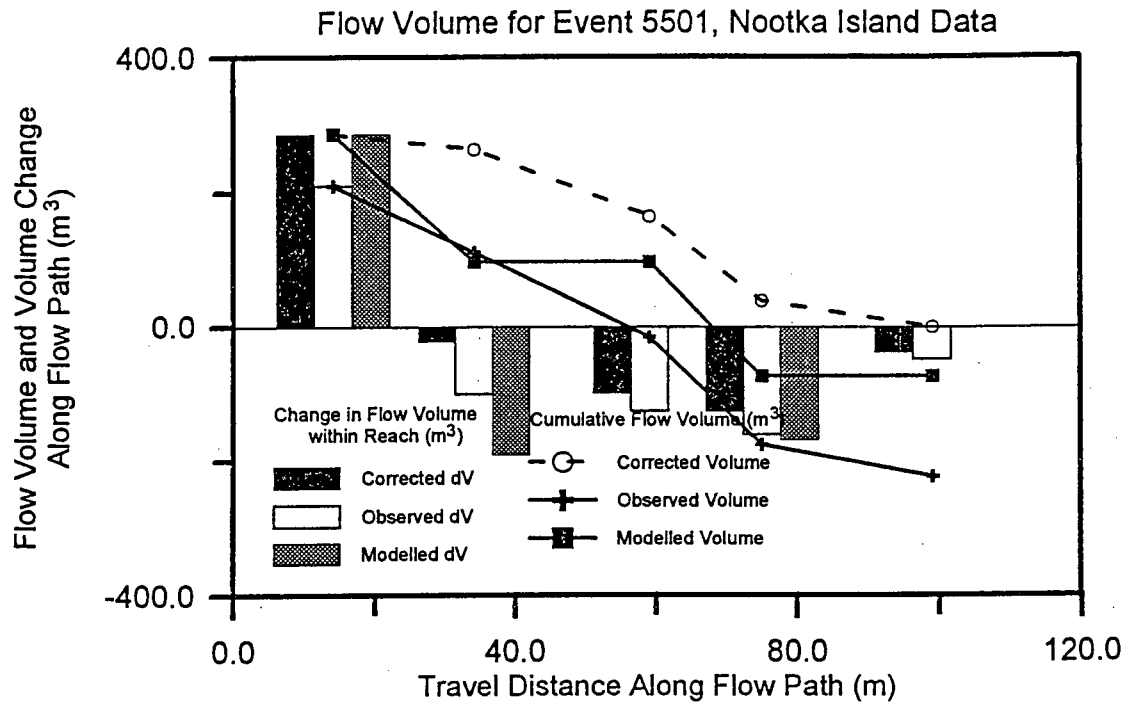












Tabulated Data for Type 7 Events

E#	S#	M	XLEN	L	Wf	We	Wd	TH	OBSERVED DATA				sigv+dv	dV	sigv+dv	dTH	dAZ
									sigv	+dv	-dv						
426	1	U	17	17	6	6	0	29	0	51	0		51	51		*	*
426	2	U	28	11	10	10	0	27	51	55	0		55	106		-2	-20
426	3	U	43	15	10	8	2	12	106	60	-15		45	151		-15	0
426	4	U	57	14	10	10	0	22	151	70	0		70	221		10	0
426	5	U	102	45	10	7	3	19	221	315	-1350		-1035	-814		-3	-20
447	1	U	12	12	10	10	0	25	0	60	0		60	60		*	*
447	2	C	38	26	7	4	3	30	60	104	-156		-52	8		5	-10
447	3	U	64	26	5	5	0	40	8	65	0		65	73		10	0
447	4	C	68	4	5	0	5	8	73	0	-20		-20	53		-32	0
1011	1	U	5	5	10	10	0	35	0	50	0		50	50		*	*
1011	2	U	22	17	10	10	0	13	50	34	0		34	84		-22	0
1011	3	U	34	12	5	5	0	13	84	60	0		60	144		0	0
1011	4	U	55	21	12	4	8	9	144	0	0		0	144		-4	5
1011	5	U	67	12	12	0	12	9	144	0	-288		-288	-144		0	40
1410	1	U	4	4	50	50	0	38	0	100	0		100	100		*	*
1410	2	U	17	13	50	50	0	45	100	325	0		325	425		7	0
1410	3	C	38	21	50	50	0	33	425	735	0		735	1160		-12	0
1410	4	C	83	45	20	0	20	15	1160	0	-1350		-1350	-190		-18	0
1410	5	C	110	27	5	0	5	32	-190	0	-135		-135	-325		17	0
1417	1	U	20	20	23	23	0	35	0	460	0		460	460		*	*
1417	2	U	60	40	25	25	0	25	460	500	0		500	960		-10	0
1417	3	C	105	45	15	15	0	22	960	203	0		203	1163		-3	20
1417	4	C	145	40	26	23	3	20	1163	184	-60		124	1287		-2	-20
1417	5	C	170	25	20	16	4	15	1287	120	-20		100	1387		-5	-10
1417	6	C	184	14	8	8	0	11	1387	45	0		45	1431		-4	20
1417	7	C	204	20	12	6	6	10	1431	60	-120		-60	1371		-1	-10

Tabulated Data for Type 7 Events

E#	S#	M	XLEN	OBSERVED DATA												
				L	Wf	We	Wd	TH	sigV	+dV	-dV	dV	sigV+dV	dTH	dAZ	
1417	8	U	270	66	23	0	23	7	1371	0	-1518	-1518	-147	-3	50	
1804	1	U	20	20	13	13	0	27	0	260	0	260	260	*	*	
1804	2	C	32	12	4	4	0	35	260	10	0	10	270	8	20	
1804	3	C	40	8	4	3	1	26	270	24	-4	20	290	-9	-50	
1804	4	C	49	9	3	0	3	26	290	0	-54	-54	236	0	0	
1804	5	C	74	25	4	4	0	26	236	50	0	50	286	0	10	
1804	6	C	109	35	3	2	1	26	286	35	-7	28	314	0	0	
1804	7	C	129	20	4	4	0	27	314	16	0	16	330	1	20	
1804	8	C	148	19	4	0	4	28	330	0	-228	-228	102	1	0	
1913	1	U	40	40	35	35	0	36	0	2100	0	2100	2100	*	*	
1913	2	C	107	67	13	13	0	30	2100	348	0	348	2448	-6	0	
1913	3	C	133	26	9	9	0	27	2448	94	0	94	2542	-3	0	
1913	4	U	233	100	12	0	12	10	2542	0	-1800	-1800	742	-17	110	
2255	1	U	8	8	9	9	0	31	0	36	0	36	36	*	*	
2255	2	C	20	12	10	7	3	21	36	17	-29	-12	24	-10	-20	
2255	3	U	47	27	6	5	1	24	24	27	-8	19	43	3	-10	
2255	4	C	65	18	5	2	3	28	43	18	-54	-36	7	4	30	
2259	1	U	16	16	14	14	0	40	0	112	0	112	112	*	*	
2259	2	C	31	15	11	11	0	28	112	33	0	33	145	-12	-5	
2259	3	C	55	24	16	16	0	32	145	77	0	77	222	4	25	
2259	4	C	87	32	8	8	0	25	222	128	0	128	350	-7	-10	
2259	5	C	95	8	6	6	0	32	350	24	0	24	374	7	0	
2259	6	C	113	18	13	13	0	28	374	47	0	47	421	-4	0	
2259	7	C	148	35	8	8	0	20	421	56	0	56	477	-8	0	
2259	8	U	320	172	15	0	15	8	477	0	-5160	-5160	-4683	-12	0	
2274	1	U	8	8	12	12	0	48	0	48	0	48	48	*	*	
2274	2	U	18	10	8	8	0	32	48	40	0	40	88	-16	0	
2274	3	C	31	13	7	3	4	22	88	8	0	8	96	-10	0	
2274	4	C	55	24	5	5	0	22	96	24	0	24	120	0	10	
2274	5	C	73	18	12	12	0	25	120	324	0	324	444	3	-30	
2274	6	C	83	10	12	12	0	34	444	120	0	120	564	9	0	

Tabulated Data for Type 7 Events

E#	S#	M	XLEN	L	Wf	We	Wd	TH	OBSERVED DATA				dV	sigV+dV	dTH	dAZ
									+dV	-dV	sigV	+dV				
2274	7	C	137	54	7	7	0	22	564	76	0	76	76	639	-12	20
2274	8	C	158	21	10	10	0	22	639	42	0	42	42	681	0	0
2274	9	C	168	10	8	4	4	22	681	8	-80	8	-72	609	0	0
2274	10	U	184	16	25	0	25	5	609	0	-800	0	-800	-191	-17	0
2274	11	U	219	35	15	15	0	38	-191	105	0	105	105	-86	33	20
2287	1	U	6	6	8	8	0	30	0	24	0	24	24	24	*	*
2287	2	U	26	20	15	15	0	30	24	240	0	240	240	264	0	0
2287	3	U	39	13	10	10	0	25	264	260	0	260	260	524	-5	-10
2287	4	U	54	15	30	30	0	22	524	1350	0	1350	1350	1874	-3	20
2287	5	U	117	63	30	10	20	12	1874	2520	-3780	2520	-1260	614	-10	20
2288	1	U	35	35	19	19	0	24	0	1330	0	1330	1330	1330	*	*
2288	2	U	115	80	12	12	0	24	1330	192	0	192	192	1522	0	0
2288	3	U	145	30	12	12	0	35	1522	72	0	72	72	1594	11	40
2290	1	U	30	30	12	12	0	38	0	360	0	360	360	360	*	*
2290	2	U	80	50	10	0	10	29	360	0	-500	0	-500	-140	-9	0
2290	3	U	170	90	8	5	3	30	-140	450	-135	450	315	175	1	0
2290	4	U	216	46	10	7	3	31	175	161	-138	161	23	198	1	10
2290	5	U	278	62	8	8	0	24	198	397	0	397	397	595	-7	30
2290	6	U	308	30	12	12	0	40	595	72	0	72	72	667	16	10
2292	1	U	63	63	10	10	0	36	0	126	0	126	126	126	*	*
2292	2	C	82	19	10	10	0	25	126	38	0	38	38	164	-11	10
2292	3	C	113	31	18	8	10	28	164	50	-930	50	-880	-716	3	0
2292	4	U	144	31	15	15	0	30	-716	233	0	233	233	-484	2	10
2292	5	U	158	14	16	8	8	26	-484	56	-168	56	-112	-596	-4	0
2292	6	U	185	27	15	15	0	40	-596	81	0	81	81	-515	14	0
2292	7	U	224	39	18	10	8	30	-515	195	-312	195	-117	-632	-10	0
2292	8	U	242	18	25	0	25	0	-632	0	-900	0	-900	-1532	-30	0
2292	9	C	297	55	16	8	8	35	-1532	880	-220	880	660	-872	35	10
2292	10	U	350	53	35	35	0	38	-872	3710	0	3710	3710	2838	3	0
2294	1	U	45	45	20	20	0	33	0	450	0	450	450	450	*	*
2294	2	C	130	85	13	13	0	28	450	553	0	553	553	1003	-5	-10

Tabulated Data for Type 7 Events

E#	S#	M	XLEN	L	Wf	We	Wd	TH	OBSERVED DATA				sigV+dv	dTH	dAZ
									+dv	-dv	dv	sigV+dv			
2294	3	C	165	35	14	14	0	30	1003	245	0	245	1248	2	-20
2294	4	C	200	35	12	12	0	22	1248	210	0	210	1458	-8	-10
2294	5	U	215	15	14	0	14	0	1458	0	-210	-210	1248	-22	10
2294	6	C	250	35	16	16	0	35	1248	280	0	280	1528	35	0
2294	7	C	280	30	12	12	0	18	1528	180	0	180	1708	-17	-30
2294	8	C	315	35	13	12	0.5	25	1708	210	-9	201	1909	7	10
2294	9	C	365	50	14	13	1	22	1909	325	0	325	2234	-3	30
2295	1	U	80	80	33	33	0	32	0	2112	0	2112	2112	*	*
2295	2	U	125	45	40	40	0	38	2112	1440	0	1440	3552	6	0
2295	3	U	170	45	30	30	0	37	3552	675	0	675	4227	-1	0
2295	4	C	220	50	15	15	0	27	4227	375	0	375	4602	-10	-10
2295	5	C	270	50	17	17	0	22	4602	425	0	425	5027	-5	20
2295	6	U	290	20	15	0	15	0	5027	0	-300	-300	4727	-22	10
2296	1	U	40	40	20	20	0	30	0	640	0	640	640	*	*
2296	2	U	55	15	35	30	5	27	640	180	-38	143	783	-3	0
2296	3	U	130	75	33	28	5	33	783	840	-188	653	1435	6	0
2296	4	U	170	40	30	8	22	27	1435	128	-440	-312	1123	-6	20
2296	5	U	240	70	8	3	5	27	1123	42	-350	-308	815	0	10
2296	6	U	250	10	8	1	7	0	815	1	-35	-34	781	-27	-30
2296	7	U	265	15	5	5	0	32	781	30	0	30	811	32	40
2296	8	C	300	35	8	8	0	35	811	140	0	140	951	3	0
22101	1	U	40	40	25	25	0	25	0	1000	0	1000	1000	*	*
22101	2	U	75	35	15	12	3	20	1000	168	-53	116	1116	-5	0
22101	3	U	140	65	14	14	0	27	1116	364	0	364	1480	7	10
22101	4	U	150	10	20	0	20	0	1480	0	-100	-100	1380	-27	20
22101	5	U	170	20	20	20	0	38	1380	80	0	80	1460	38	180
22101	6	U	210	40	20	20	0	35	1460	320	0	320	1780	-3	-180
22101	7	C	255	45	14	14	0	28	1780	315	0	315	2095	-7	0
22101	8	C	275	20	15	15	0	38	2095	150	0	150	2245	10	0
22101	9	C	315	40	15	15	0	22	2245	300	0	300	2545	-16	20
22101	10	C	330	15	12	12	0	30	2545	90	0	90	2635	8	10
22111	1	U	25	25	22	22	0	33	0	275	0	275	275	*	*

E#	S#	M	XLEN	OBSERVED DATA												dV	sigV+dV	dTH	dAZ
				L	Wf	We	Wd	TH	sigV	+dV	-dV								
22111	2	U	40	15	22	20	2	18	275	150	-30	120	395	-15	0				
22111	3	U	55	15	20	20	0	28	395	300	0	300	695	10	0				
22111	4	C	95	40	12	12	0	23	695	240	0	240	935	-5	0				
22111	5	C	170	75	12	12	0	20	935	450	0	450	1385	-3	20				
22111	6	C	270	100	15	15	0	16	1385	750	0	750	2135	-4	-30				
22111	7	C	290	20	15	15	0	15	2135	150	0	150	2285	-1	20				
22111	8	C	360	70	9	9	0	14	2285	315	0	315	2600	-1	40				
22111	9	C	385	25	12	12	0	25	2600	60	0	60	2660	11	-30				
22111	10	C	430	45	13	13	0	12	2660	293	0	293	2953	-13	40				
22111	11	C	495	65	15	15	0	22	2953	488	0	488	3440	10	30				
22111	12	U	505	10	15	0	15	0	3440	0	-150	-150	3290	-22	0				
22111	13	C	585	80	15	15	0	28	3290	600	0	600	3890	28	0				
22111	14	U	640	55	15	15	0	70	3890	83	0	83	3973	42	-20				
22111	15	U	655	15	15	0	15	0	3973	0	-225	-225	3748	-70	30				
22111	16	U	675	20	20	20	0	35	3748	200	0	200	3948	35	0				
22111	17	U	715	40	26	10	16	24	3948	200	-1280	-1080	2868	-11	0				
22111	18	U	765	50	20	8	12	8	2868	200	-600	-400	2468	-16	0				
22111	19	C	865	100	13	12	1	12	2468	600	-1	599	3067	4	0				
22111	20	C	920	55	16	8	8	11	3067	220	-440	-220	2847	-1	40				
22111	21	C	965	45	12	12	0	15	2847	270	0	270	3117	4	10				
22111	22	C	990	25	12	12	0	33	3117	60	0	60	3177	18	-20				
22112	1	U	20	20	16	16	0	26	0	128	0	128	128	*	*				
22112	2	C	50	30	15	15	0	20	128	225	0	225	353	-6	10				
22112	3	C	115	65	12	12	0	20	353	390	0	390	743	0	-20				
22112	4	U	135	20	15	10	5	16	743	60	-100	-40	703	-4	-10				
22112	5	U	155	20	15	15	0	20	703	90	0	90	793	4	-20				

MODELLED RESULTS - TYPE 7 EVENTS AND SUPPLEMENTARY EVENTS

E#	R#	M	TH	OBSERVED DATA			MODELLED RESULTS			sigv +dv
				sigv	+dv	-dv	dv	sigv	+dv	
426	1	U	29	0	51	0	51	0	51	51
426	2	U	27	51	55	0	55	51	68	119
426	3	U	12	106	60	-15	45	119	-31	89
426	4	U	22	151	70	0	70	89	80	168
426	5	U	19	221	315	-1350	-1035	168	129	298
447	1	U	25	0	60	0	60	0	60	60
447	2	C	30	60	104	-156	-52	60	53	113
447	3	U	40	8	65	0	65	113	-10	103
447	4	C	8	73	0	-20	-20	103	-1	102
1011	1	U	35	0	50	0	50	0	50	50
1011	2	U	13	50	34	0	34	50	0	50
1011	3	U	13	84	60	0	60	50	0	50
1011	4	U	9	144	0	0	0	50	-155	-105
1011	5	U	9	144	0	-288	-288	-105	-148	-253
1410	1	U	38	0	100	0	100	0	100	100
1410	2	U	45	100	325	0	325	100	288	388
1410	3	C	33	425	735	0	735	388	355	744
1410	4	C	15	1160	0	-1350	-1350	744	34	777
1410	5	C	32	-190	0	-135	-135	777	16	794
1417	1	U	35	0	460	0	460	0	460	460
1417	2	U	25	460	500	0	500	460	468	928
1417	3	C	22	960	203	0	203	928	302	1230
1417	4	C	20	1163	184	-60	124	1230	404	1634
1417	5	C	15	1287	120	-20	100	1634	211	1845
1417	6	C	11	1387	45	0	45	1845	74	1919
1417	7	C	10	1431	60	-120	-60	1919	-1	1918
1417	8	U	7	1371	0	-1518	-1518	1918	-2987	-1070
1804	1	U	27	0	260	0	260	0	260	260
1804	2	C	35	260	10	0	10	260	24	284
1804	3	C	26	270	24	-4	20	284	15	300

E#	R#	M	TH	OBSERVED DATA			MODELLED RESULTS			sigV +dV	sigV +dV
				sigV	+dV	-dV	dV	+dV	-dV		
2274	11	U	38	-191	105	0	105	-86	-147	172	25
2287	1	U	30	0	24	0	24	24	0	24	24
2287	2	U	30	24	240	0	240	264	24	164	188
2287	3	U	25	264	260	0	260	524	188	72	260
2287	4	U	22	524	1350	0	1350	1874	260	275	535
2287	5	U	12	1874	2520	-3780	-1260	614	535	-995	-460
2288	1	U	24	0	1330	0	1330	1330	0	1330	1330
2288	2	U	24	1330	192	0	192	1522	1330	329	1659
2288	3	U	35	1522	72	0	72	1594	1659	131	1790
2290	1	U	38	0	360	0	360	360	0	360	360
2290	2	U	29	360	0	-500	-500	-140	360	0	360
2290	3	U	30	-140	450	-135	315	175	360	118	478
2290	4	U	31	175	161	-138	23	198	478	107	585
2290	5	U	24	198	397	0	397	595	585	179	764
2290	6	U	40	595	72	0	72	667	764	104	868
2292	1	U	36	0	126	0	126	126	0	126	126
2292	2	C	25	126	38	0	38	164	126	94	220
2292	3	C	28	164	50	-930	-880	-716	220	115	335
2292	4	U	30	-716	233	0	233	-484	335	-10	325
2292	5	U	26	-484	56	-168	-112	-596	325	57	382
2292	6	U	40	-596	81	0	81	-515	382	129	511
2292	7	U	30	-515	195	-312	-117	-632	511	158	669
2292	8	U	0	-632	0	-900	-900	-1532	669	-587	82
2292	9	C	35	-1532	880	-220	660	-872	82	172	254
2292	10	U	38	-872	3710	0	3710	2838	254	-17	237
2294	1	U	33	0	450	0	450	450	0	450	450
2294	2	C	28	450	553	0	553	1003	450	430	880
2294	3	C	30	1003	245	0	245	1248	880	200	1079
2294	4	C	22	1248	210	0	210	1458	1079	199	1278
2294	5	U	0	1458	0	-210	-210	1248	1278	-297	981
2294	6	C	35	1248	280	0	280	1528	981	206	1187

E#	R#	M	TH	OBSERVED DATA		MODELLED RESULTS		sigv +dv	sigv +dv
				+dv	-dv	dV	dV		
2294	7	C	18	1528	180	0	180	1708	1187
2294	8	C	25	1708	210	-9	201	1909	1373
2294	9	C	22	1909	325	0	325	2234	1563
2295	1	U	32	0	2112	0	2112	2112	0
2295	2	U	38	2112	1440	0	1440	3552	2112
2295	3	U	37	3552	675	0	675	4227	2862
2295	4	C	27	4227	375	0	375	4602	3401
2295	5	C	22	4602	425	0	425	5027	3707
2295	6	U	0	5027	0	-300	-300	4727	4077
2296	1	U	30	0	640	0	640	640	0
2296	2	U	27	640	180	-38	143	783	640
2296	3	U	33	783	840	-188	653	1435	900
2296	4	U	27	1435	128	-440	-312	1123	1766
2296	5	U	27	1123	42	-350	-308	815	1884
2296	6	U	0	815	1	-35	-34	781	60
2296	7	U	32	781	30	0	30	811	1944
2296	8	C	35	811	140	0	140	951	1834
22101	1	U	25	0	1000	0	1000	1000	1861
22101	2	U	20	1000	168	-53	116	1116	0
22101	3	U	27	1116	364	0	364	1480	1000
22101	4	U	0	1480	0	-100	-100	1380	174
22101	5	U	38	1380	80	0	80	1460	335
22101	6	U	35	1460	320	0	320	1780	-321
22101	7	C	28	1780	315	0	315	2095	1510
22101	8	C	38	2095	150	0	150	2245	1188
22101	9	C	22	2245	300	0	300	2545	1353
22101	10	C	30	2545	90	0	90	2635	165
22111	1	U	33	0	275	0	275	275	318
22111	2	U	18	275	150	-30	120	395	258
22111	3	U	28	395	300	0	300	695	113
22111	4	C	23	695	240	0	240	935	272

OBSERVED DATA				MODELLED RESULTS			
E#	R#	M	TH	sigV	+dV	-dV	sigV
22111	5	C	20	935	450	0	1385
22111	6	C	16	1385	750	0	2135
22111	7	C	15	2135	150	0	2285
22111	8	C	14	2285	315	0	2600
22111	9	C	25	2600	60	0	2660
22111	10	C	12	2660	293	0	2953
22111	11	C	22	2953	488	0	3440
22111	12	U	0	3440	0	-150	3290
22111	13	C	28	3290	600	0	3890
22111	14	U	70	3890	83	0	3973
22111	15	U	0	3973	0	-225	3748
22111	16	U	35	3748	200	0	3948
22111	17	U	24	3948	200	-1280	2868
22111	18	U	8	2868	200	-600	2468
22111	19	C	12	2468	600	-1	3067
22111	20	C	11	3067	220	-440	2847
22111	21	C	15	2847	270	0	3117
22111	22	C	33	3117	60	0	3177
22112	1	U	26	0	128	0	128
22112	2	C	20	128	225	0	353
22112	3	C	20	353	390	0	743
22112	4	U	16	743	60	-100	703
22112	5	U	20	703	90	0	793
CORRECTED DATA				MODELLED RESULTS			
E#	R#	M	TH	sigV	+dV	-dV	sigV
3001	1	C	29	0	16	0	16
3001	2	C	25	16	31	0	48
3001	3	C	30	48	58	0	106
3001	4	C	40	106	150	0	256
3001	5	C	30	256	252	0	508
3001	6	C	30	508	36	0	544

E#	R#	M	TH	CORRECTED DATA				MODELLED RESULTS				sigv +dv	sigv +dv
				sigv	+dv	-dv	dV	sigv	dV				
3001	7	C	30	544	135	0	135	679	221	33	253		
3001	8	C	34	679	128	0	128	807	253	29	283		
3001	9	C	14	807	9	-96	-87	720	283	24	307		
3001	10	U	17	720	0	-720	-720	0	307	-339	-32		
3005	1	U	25	0	38	0	38	38	0	38	38		
3005	2	C	26	38	158	0	158	196	38	36	74		
3005	3	C	33	196	107	0	107	303	74	18	92		
3005	4	C	23	303	90	-22	68	371	92	23	115		
3005	5	C	25	371	201	-19	182	553	115	47	162		
3005	6	C	24	553	120	0	120	674	162	43	205		
3005	7	C	15	674	30	-89	-59	614	205	27	232		
3005	8	C	90	614	3	-5	-2	613	232	1	233		
3005	9	C	18	613	0	-104	-104	508	233	21	254		
3005	10	C	18	508	0	-36	-36	472	254	22	276		
3005	11	C	20	472	0	-17	-17	455	276	20	296		
3005	12	C	10	455	0	-142	-142	313	296	-1	295		
3005	13	U	7	313	0	-139	-139	174	295	-83	212		
3005	14	U	2	174	0	-174	-174	0	212	-155	57		
3006	1	U	32	0	3096	0	3096	3096	0	3096	3096		
3006	2	U	36	3096	1302	0	1302	4398	3096	468	3564		
3006	3	U	34	4398	1637	0	1637	6035	3564	609	4173		
3006	4	U	28	6035	3473	0	3473	9508	4173	595	4768		
3006	5	U	20	9508	16372	0	16372	25880	4768	1018	5787		
3006	6	U	20	25880	5656	0	5656	31535	5787	597	6383		
3006	7	U	29	31535	1488	0	1488	33024	6383	286	6670		
3006	8	U	0	33024	6139	0	6139	39163	6670	0	6670		
3006	9	U	26	39163	0	-14099	-14099	25064	6670	0	6670		
3006	10	U	13	25064	0	-17692	-17692	7372	6670	-5856	814		
3006	11	U	7	7372	0	-7372	-7372	0	814	-4423	-3609		
3104	1	U	60	0	253	0	253	253	0	253	253		
3104	2	C	34	253	476	0	476	729	253	84	337		

285

E#	R#	M	TH	CORRECTED DATA			MODELLED RESULTS			sigv +dv	sigv +dv
				sigv	+dv	-dv	dv	sigv	dv		
3104	3	C	32	729	486	0	486	1215	337	88	425
3104	4	U	10	1215	0	-1215	-1215	0	425	-787	-362
3201	1	U	46	0	37	0	37	37	0	37	37
3201	2	U	34	37	29	0	29	66	37	23	60
3201	3	C	32	66	44	0	44	110	60	58	118
3201	4	C	31	110	88	0	88	199	118	108	226
3201	5	C	30	199	224	0	224	422	226	249	474
3201	6	C	27	422	129	0	129	552	474	89	563
3201	7	C	29	552	86	0	86	638	563	109	672
3201	8	U	0	638	0	-56	-56	581	672	-180	492
3201	9	U	30	581	14	-131	-117	464	492	20	512
3201	10	U	20	464	0	-152	-152	312	512	0	512
3201	11	U	0	312	0	-312	-312	0	512	-262	250
3202	1	U	26	0	384	0	384	384	0	384	384
3202	2	U	27	384	57	0	57	441	384	27	411
3202	3	U	21	441	33	-51	-18	422	411	70	481
3202	4	U	17	422	59	-26	33	456	481	-51	430
3202	5	U	17	456	4	-27	-23	433	430	-34	396
3202	6	U	8	433	3	-27	-23	410	396	-23	373
3202	7	U	5	410	0	-164	-164	246	373	-164	210
3202	8	U	0.5	246	0	-246	-246	0	210	-167	42
3203	1	U	28	0	233	0	233	233	0	233	233
3203	2	U	18	233	73	0	73	306	233	0	233
3203	3	U	24	306	40	0	40	346	233	55	287
3203	4	U	21	346	11	0	11	357	287	14	302
3203	5	U	30	357	65	0	65	421	302	26	328
3203	6	U	15	421	0	-107	-107	314	328	-78	250
3203	7	U	28	314	244	0	244	558	250	151	402
3203	8	U	0.5	558	0	-432	-432	127	402	-297	104
3203	9	U	19	127	0	-127	-127	0	104	0	104
4001	1	U	35	0	71	0	286	71	0	71	71

E#	R#	M	TH	CORRECTED DATA		dv	sigv		MODELLED RESULTS		sigv
				+dv	-dv		+dv	dv	+dv	dv	
4001	2	U	43	71	92	0	163	92	71	51	122
4001	3	U	31	163	38	0	201	38	122	42	163
4001	4	C	28	201	57	0	258	57	163	53	217
4001	5	C	27	258	66	0	324	66	217	63	279
4001	6	C	25	324	28	-4	349	25	279	31	310
4001	7	C	30	349	23	0	371	23	310	24	334
4001	8	C	27	371	79	0	450	79	334	75	409
4001	9	C	22	450	87	-6	531	81	409	88	497
4001	10	C	26	531	28	0	559	28	497	31	529
4001	11	C	24	559	22	0	581	22	529	14	543
4001	12	C	27	581	29	0	611	29	543	32	574
4001	13	U	8	611	0	-199	411	-199	574	-204	370
4001	14	U	23	411	0	-111	301	-111	370	0	370
4001	15	U	15	301	0	-129	172	-129	370	-122	248
4001	16	U	18	172	0	-22	149	-22	248	-48	200
4001	17	U	12	149	13	-162	0	-149	200	-153	47
4002	1	U	32	0	149	0	149	149	0	149	149
4002	2	U	27	149	117	0	265	117	149	119	267
4002	3	U	23	265	102	-43	324	59	267	103	370
4002	4	U	22	324	263	-185	401	77	370	245	615
4002	5	U	0.5	401	0	-401	0	-401	615	-910	-295
4102	1	U	38	0	68	0	68	68	0	68	68
4102	2	U	35	68	76	0	145	76	68	30	99
4102	3	U	19	145	107	0	251	107	99	60	159
4102	4	U	38	251	16	0	267	16	159	13	173
4102	5	U	25	267	152	0	419	152	173	86	258
4102	6	U	27	419	65	0	484	65	258	22	280
4102	7	U	0	484	0	-484	0	-484	280	-487	-207
5001	1	U	40	0	98	0	98	98	0	98	98
5001	2	U	36	98	59	0	157	59	98	12	110
5001	3	U	34	157	69	0	226	69	110	10	121

E#	R#	M	TH	CORRECTED DATA		sigV	MODELLED RESULTS		sigv	+dv	sigv	+dv
				+dv	-dv		dV	dV				
5001	4	U	26	226	80	0	80	121	305	121	18	139
5001	5	U	42	305	97	0	97	139	402	139	11	149
5001	6	U	18	402	69	0	69	149	471	149	0	149
5001	7	U	12	471	12	-35	-24	149	448	149	-47	102
5001	8	U	18	448	12	0	12	102	459	102	0	102
5001	9	U	0.5	459	0	-459	-459	102	0	102	-325	-223
5002	1	U	44	0	425	0	425	0	425	0	425	425
5002	2	U	40	425	234	0	234	425	659	425	156	582
5002	3	C	36	659	174	-87	86	582	745	582	177	759
5002	4	C	31	745	270	0	270	759	1015	759	155	914
5002	5	C	29	1015	60	0	60	914	1075	914	42	956
5002	6	C	22	1075	75	0	75	956	1150	956	58	1014
5002	7	U	23	1150	0	-158	-158	1014	992	1014	-285	729
5002	8	U	0.5	992	0	-84	-84	729	907	729	-189	539
5002	9	U	14	907	0	-546	-546	539	361	539	-349	191
5002	10	U	7	361	0	-135	-135	191	226	191	-122	69
5002	11	U	7	226	0	-226	-226	69	0	69	-281	-212
5003	1	U	33	0	148	0	148	0	148	0	148	148
5003	2	U	34	148	173	0	173	148	322	148	40	188
5003	3	C	33	322	417	0	417	188	739	188	117	305
5003	4	C	23	739	448	0	448	305	1188	305	147	452
5003	5	C	25	1188	87	0	87	452	1274	452	86	538
5003	6	C	25	1274	46	0	46	538	1321	538	51	589
5003	7	C	15	1321	0	-155	-155	589	1165	589	25	613
5003	8	U	0.5	1165	0	-105	-105	613	1060	613	-153	460
5003	9	U	3	1060	0	-163	-163	460	897	460	-409	51
5003	10	U	3	897	0	-897	-897	51	0	51	-772	-721
5101	1	U	30	0	470	0	470	0	470	0	470	470
5101	2	C	23	470	62	0	62	470	532	470	71	541
5101	3	C	33	532	61	0	61	541	593	541	59	599
5101	4	C	23	593	106	0	106	599	699	599	114	713

CORRECTED DATA											
E#	R#	M	TH	CORRECTED DATA			MODELLED RESULTS				
				sigV	+dV	-dV	dV	sigV	+dV	sigV	dV
5101	5	U	15	699	0	-341	-341	358	713	-329	384
5101	6	U	10	358	0	-358	-358	0	384	-346	39
5301	1	U	35	0	645	0	645	645	0	645	645
5301	2	C	33	645	314	0	314	959	645	122	767
5301	3	C	35	959	99	0	99	1057	767	78	845
5301	4	C	30	1057	118	0	118	1175	845	54	899
5301	5	C	31	1175	179	-9	170	1345	899	76	975
5301	6	U	27	1345	1495	-603	892	2237	975	-1585	-610
5301	7	U	25	2237	358	-347	12	2249	-610	236	-374
5301	8	U	17	2249	0	-2249	-2249	0	-374	-1690	-2064
5402	1	U	31	0	883	0	883	883	0	883	883
5402	2	C	29	883	1187	0	1187	2070	883	464	1347
5402	3	U	27	2070	1648	-1713	-65	2006	1347	-871	476
5402	4	C	24	2006	114	0	114	2119	476	115	591
5402	5	C	26	2119	345	0	345	2465	591	168	759
5402	6	C	28	2465	226	0	226	2690	759	110	869
5402	7	C	27	2690	628	0	628	3318	869	271	1139
5402	8	C	24	3318	540	-20	519	3837	1139	248	1387
5402	9	C	27	3837	375	0	375	4213	1387	312	1699
5402	10	C	25	4213	589	0	589	4801	1699	476	2175
5402	11	C	25	4801	368	0	368	5169	2175	309	2484
5402	12	C	22	5169	841	0	841	6011	2484	671	3154
5402	13	U	20	6011	907	-336	570	6581	3154	-561	2593
5402	14	U	1	6581	0	-133	-133	6448	2593	-438	2155
5402	15	U	20	6448	628	0	628	7076	2155	477	2633
5402	16	U	8	7076	0	-714	-714	6362	2633	-832	1801
5402	17	U	9	6362	-61	-3120	-3181	3181	1801	-3405	-1604
5402	18	C	6	3181	-41	-2100	-2141	1040	-1604	-1	-1605
5402	19	C	7	1040	-20	-1020	-1040	0	-1605	-1	-1606
5501	1	U	30	0	286	0	286	286	0	286	286
5501	2	U	18	286	136	-158	-22	263	286	-190	95

E#	R#	M	TH	CORRECTED DATA		MODELLED RESULTS		sigv	
				+dv	-dv	+dv	dv	+dv	dv
5501	3	U	23	263	-99	164	95	95	0
5501	4	U	8	164	-127	38	95	-74	-169
5501	5	U	25	38	-38	0	-74	-74	0